NOVEL EMULSION-BASED DELIVERY SYSTEMS

A DISSERTATION
SUBMITTED TO THE FACULTY OF THE GRADUATE SCHOOL OF THE
UNIVERSITY OF MINNESOTA
BY

Jian Zhang

IN PARTIAL FULFILLMENT OF THE REQUIREMENTS
FOR THE DEGREE OF
DOCTOR OF PHILOSOPHY

Advisor: Gary A. Reineccius

September 2011

ACKNOWLEDGEMENTS

I would like to express my deepest gratitude and appreciation to my advisor, Dr. Gary Reineccius, for his inspiration, patience and encouragement through the last 5 years. What I have learned from him is not just about research. His philosophy and positive thinking enriched me and helped me reach my goal successfully.

I would like to thank Robertet Flavors, Inc. for the financial support of my Ph.D. study and also for the great opportunity of one-year internship. The intern experience at Robertet prepared me well for my future career. I would like to give a special thank to Dr. Terry Peppard, who served on my committee, for his great hospitality, friendliness, and valuable suggestions.

I would like to express my appreciation to my committee, Dr. David Smith and Dr. Mirko Bunzel for their valuable advice and kind help. I would like to thank Dr. Steven Severtson for his friendliness and discussions on my projects. I enjoyed his class of colloid and surface chemistry.

I want to thank the past and current lab mates in the flavor lab for their support and sharing their knowledge. I enjoyed talking with them and learning from them. The diverse culture in the lab broadened my views and perspective of the world. I will miss the coffee break and the chocolate.

I am especially grateful to my wife, Lu Bing, for her love, understanding and encouragement. She always cheers me up when I am in difficulty. Finally, I would like to thank my parents for their support in every ways.

Abstract

Novel emulsions with useful attributes such as improved stability, clarity and label friendliness were investigated in this thesis. Overall, this thesis has three parts: the first part systematically studied the formation and optical properties of nanoemulsions; the second part focused on formation and beverage cloud application of multilayer emulsions; and the third part evaluated the formation, stability and beverage cloud application of multiple phase emulsions.

In part 1, nanoemulsions were prepared using four different food grade biopolymers (different concentrations) and high pressure homogenization (Microfluidizer®, different pressures, temperature and number of passes). It was found that increasing number of passes through the microfluidizer led to a wider particle size distribution. The effect of oil types on mean droplet diameter (MDD) was complex being dependent on the emulsifier, homogenization pressure, phase viscosity and number of passes. It was also found that interface composition, relative refractive index, volume fraction of dispersed phase and droplet size influenced the turbidity. A polynomial relationship was found between MDD and turbidity within the MDD range of 80 to 400 nm. The effects of lipid phase and interface composition on turbidity were droplet size dependent. A linear relationship between volume fraction of dispersed phase and turbidity was established. Experiment results demonstrated that matching refractive indices between phases led to clear emulsions. Finally the primary destabilization

mechanism of MCT nanoemulsions emulsified with modified starch was identified as coalescence from a two-week shelf life study.

In part 2 of this thesis, the ability to prepare secondary and tertiary beverage cloud emulsions using a layer-by-layer deposition technique was developed. Proteins, β-lactoglobulin (L) and sodium caseinate (S), were selected to stabilize the primary emulsions. Biopolymers of sodium alginate (S), ι-carrageenan (C), gum Arabic (G), pectin (P), chitosan (Ch) and gelatin (Ge) were evaluated as secondary and tertiary layers. Biopolymer concentration and pH were found critical to the formation of stable multilayer emulsions. Protein and polysaccharide type also impacted droplet size and ζ-potential of multilayer emulsions. Interestingly, β-lactoglobulin was found better than sodium caseinate in forming protein-polysaccharide interfacial complexes as demonstrated by smaller MDD of LA, LP and LC than those of SA, SP and SC. It was also found biopolymer concentration has to be above a critical value (0.2 ~ 0.5% w/w) to prevent multilayer emulsions from bridging flocculation. Our data showed that both secondary (LA, LC, LG) and tertiary (LGC) emulsions formed by electrostatic deposition could provide the same performance as traditional emulsifiers of gum Arabic (G) and modified starch (M). After four weeks of storage at room temperature, beverage clouds stabilized with G, M, LA, LC, LG and LGCh showed MDDs of 0.68, 0.67, 0.90, 0.82, 0.65 and 2.2 μm, respectively, and turbidity losses of 18, 28, 22, 19, 25 and 17%, respectively.

In part 3 of this thesis, water-in-oil-in-water emulsions (W/O/W, also called double emulsions) were studied using a concentrated sucrose solution as a natural weighing agent to increase the density of the oil phase. The results indicated that MDD of W/O emulsions decreased with increasing emulsifier (polyglycerol polyricinoleate, PGPR) concentration. Homogenization pressure and number of passes through a microfluidizer affected MDD, size distribution and encapsulation efficiency (EE) of yellow #6 (included in the water phase as a marker to measure EE). The hydrophilic emulsifier type and oil phase showed great impacts on EE and stability of the W/O/W emulsions. A high EE (>85%) was achieved in gum acacia (GA) stabilized double emulsions whereas Tween 20 and modified starch (MS) stabilized double emulsions showed low EE (< 50%) demonstrating that the type of hydrophilic emulsifier is a critical factor governing stability of double emulsions. Gelling the inner aqueous phase proved to be ineffective in improving EE and stabilizing double emulsion in this study.

Results on beverage cloud applications of W/O/W emulsions indicated that GA stabilized emulsions are more stable to turbidity loss and ring formation than those stabilized by MS. Beverage clouds containing OT-based W/O/W emulsions without gelling the inner phase showed low turbidity loss during shelf-life without ring formation demonstrating potential commercial value of these emulsions.

Table of Contents

List of Tables

List of Figures

Thesis Flow Chart

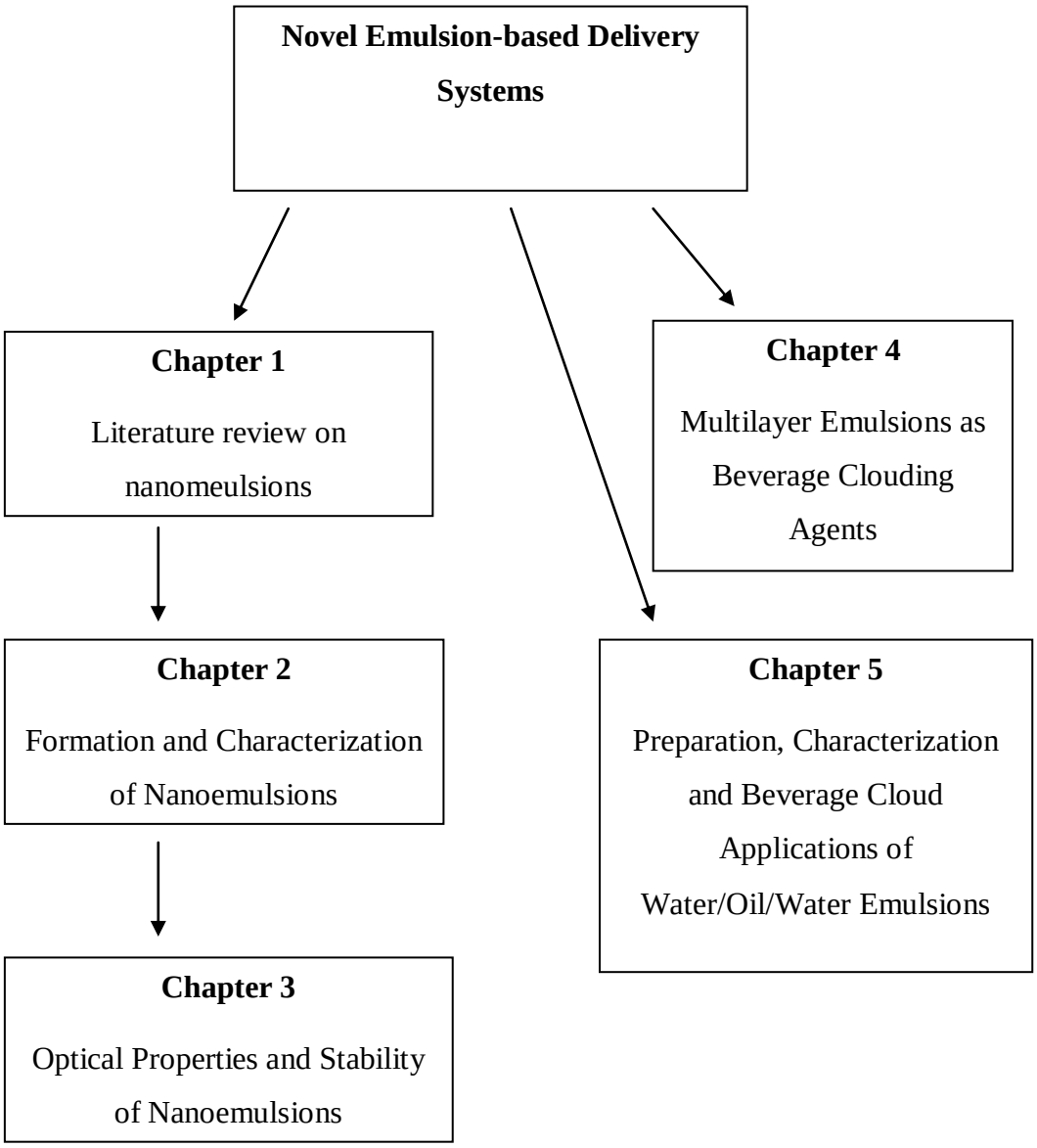

Chapter 1

Literature Review of Nanoemulsions

1 .1 Introduction

Nanoemulsions are gaining increasing attention in food industry as a novel delivery system for lipophilic materials (e.g., fatty acids, polyphenols, natural colors, and flavors) (1-6). The potential benefits of food nanoemulsions include optical clarity, good stability to gravitational separation, flocculation and coalescence, and improved absorption and bioavailability of functional components (7-10). A deeper understanding of the basic physiochemical properties of food nanoemulsions would, therefore, provide key information to better guide formulation and application of nanoemulsion to food products. Considering the significant commercial applications of food nanoemulsions, elucidating mechanisms that govern the formation and stability of flavor nanoemulsions would be useful.

The aim of this review is to discuss the formation and physical properties of nanoemulsions. The review will start with the basic theories of nanoemulsion formation, characterization, and stability and then discuss potential applications of them.

1.2. Classification of emulsions

Generally, an emulsion consists of two immiscible liquids with one of the liquid being dispersed as small droplets in the other (11-12). A number of different terms are commonly used to describe different types of emulsions and it is important to clarify

these terms (Table 1.1) (13-16). The range of droplet size for each type of emulsion is quite arbitrary and is defined in terms of the physical and thermodynamic properties of emulsions. A conventional emulsion, also known as a macroemulsion, typically has a mean droplet diameter (MDD) between 100 nm and 100 μm. Macroemulsions are the most common form of emulsions used in food industry and are found in a variety of products, including milk, beverages, dressings, mayonnaises, dips, sauces, and desserts. Macroemulsions are prone to physical instability (e.g., gravitational separation, flocculation, and coalescence), especially when exposed to environmental stresses (17-20).

Table 1.1 Properties of different types of emulsions (Reprinted from Ref. 13)

Emulsion type	**Diameter**	**Thermodynamic Stability**	**Surface-to-mass ratio (m^2/g)**	**Appearance**
Macroemulsion	0.1-100 μm	Unstable	0.07-70	Turbid
Nanoemulsion	20-100 nm	Unstable	70-330	transparent
Microemulsion	5-100 nm	Stable	330-1300	Transparent

In general, nanoemulsions are dispersions of nanoscale droplets with a MDD between 20-100 nm. It is worth noting that in old days "miniemulsion" was also used to refer to emulsions comprised of submicron droplets (21-23). In contrast to nanoemulsions, miniemulsions have droplets in the range from 100 nm to 1 μm. Because miniemulsions

and macroemulsions have similar thermodynamic and physical properties, it is reasonable to put them in the same category, macroemulsions. Both nanoemulsions and macroemulsions are thermodynamically unstable.

A microemulsion is a thermodynamically stable system and forms spontaneously with droplet size between 5 to 50 nm (13). Researchers commonly believe that nanoemulsions are the same as microemulsions since they both typically contain oil, water, and surfactant and also have similar MDD. However, the two systems are very different since nanoemulsions are formed by mechanical shear and microemulsions are formed by self-assembly. A mixture of the right amount of water, surfactants and oil may spontaneously form a microemulsion (24-28). The main difference between microemulsions and microscale emulsions is not composition but rather thermodynamics (15, 29). Although extensive research on microemulsions has been conducted, the formation mechanism is still not well understood (30).

1.3 Formation of nanoemulsions

Compared to microemulsions, relatively little is known about creating and controlling nanoemulsions. This is primarily because extreme shear has to be applied to overcome the effects of surface tension to rupture the droplets into a nanoscale regime, which is beyond the capability of ordinary mixing devices (15). Fortunately, the development of high pressure homogenizers in the past 10 years makes it possible to

explore nanoemulsions. Nanoemulsions show interesting delivery properties ranging from lipophilic materials to flavors and optical properties ranging from opaque to nearly transparent, which drives increasing research activity in nanoemulsion (31-34).

Nanoemulsions are non-equilibrium systems and cannot form spontaneously (35, 36). Consequently, energy input, generally from a mechanical device or from the chemical potential of the components, is required. As with conventional emulsions, nanoemulsions are usually prepared by homogenizing an oil phase and an aqueous phase together in the presence of water soluble emulsifier(s). Under mechanical energy, the interface between the two phases is deformed to such an extent that droplets form and they are subsequently broken up or disrupted into smaller ones. The formation of conventional emulsions and the role of emulsifiers have been well documented (12, 37-40). However, a number of special factors must be taken into account to produce stable nanoemulsions.

1.3.1 Homogenization devices

Emulsions are dispersions of one liquid phase in another immiscible phase that are made using mechanical shear. Figure 1 shows the process of emulsion formation. Due to differences in attractive interactions between the molecules of the two phases, an interfacial tension, σ, exists between the two liquids everywhere they are in contact shown in Figure 1.1 (a). Surfactants tend to deposit onto the oil-water interface due to

their amphiphilic structure and reduce interfacial tension shown in Figure 1.1 (b). In Figure 1.1 (c) mechanical shear is applied to homogenize the two phases. The energy required to create interfacial area, *A*, between the two liquids is σA. The relationship between interfacial area and droplet radius is given in equation 1.1.

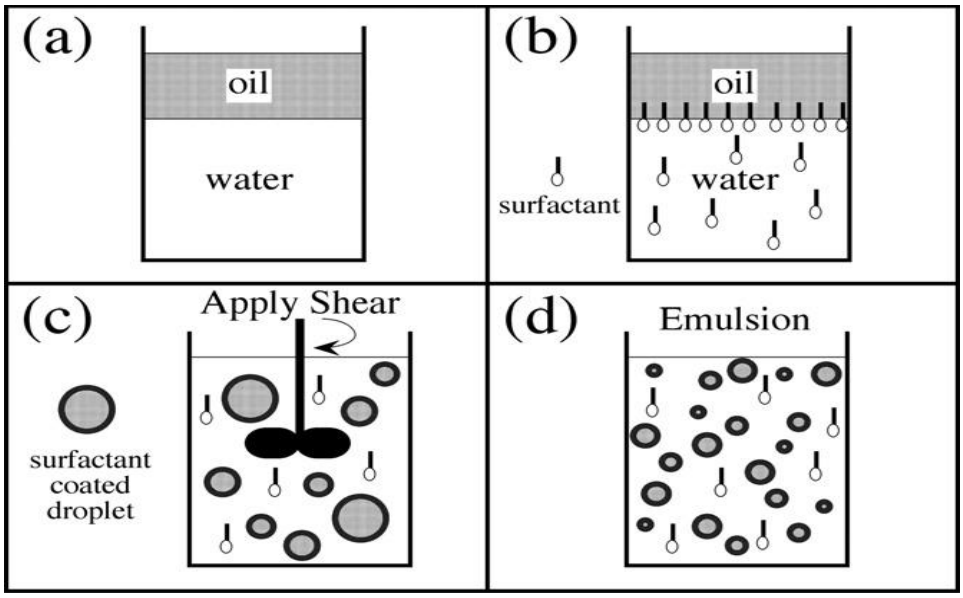

Figure 1.1 Formation of oil-in-water emulsions. (a) Two separate phases, oil and water. (b) A surfactant soluble in water phase and adsorb on the interface. (c) Shear is applied to form oil droplets. (d) Emulsion is formed. Reprinted from Ref. (15).

$$A = \frac{6m}{\rho d} \qquad \textbf{[1.1]}$$

Where *A* is interfacial area, m is the mass of oil phase, ρ is the density of oil phase, and d is the droplet diameter. With a fixed volume fraction of oil phase, *A* is inversely

proportional to d. In order to better understand the effect of droplet diameter on interfacial area, Figure 1.2 shows the plot of *A* vs. d with orange oil as an example. *A* increases seven times from 5 to 35 m^2/g when d decreases from 500 to 100 nm. Considering such a large *A* for extreme small droplet, intense energy and high shear rate are needed during homogenization to create nanoemulsions.

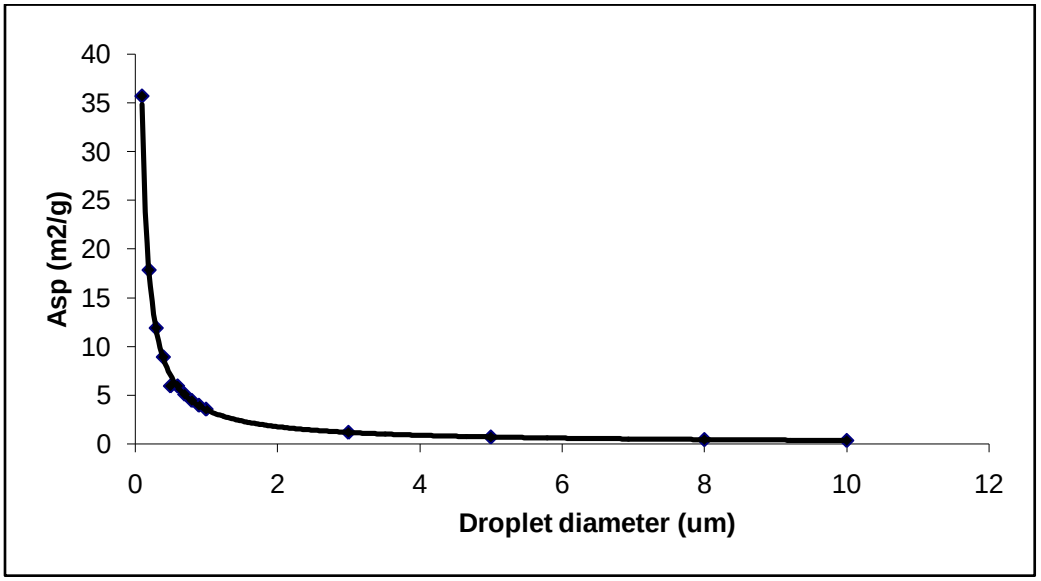

Figure 1.2 Relationship between droplet diameter and specific surface area of oil droplets. Calculation based on orange oil emulsion; A_{sp} stands for specific surface area with the unit m^2/g.

In a simplest case where the dispersed phase viscosity, $\eta_{d,}$ can be ignored, the diameter, d, of ruptured droplet is determined by Taylor's formula (41).

$$d \approx \frac{\sigma}{\eta_C \gamma} \qquad \textbf{[1.2]}$$

Where η_c is viscosity of continuous phase, γ is the shear rate and σ is the interfacial tension. Based on the Taylor estimate, it is possible to predict the shear rate required to form nanoemulsions. Assuming the interfacial tension is $\sigma = 10$ dyn cm^{-1} and continuous phase viscosity is $\eta_c = 1.0$ mPa.s for an oil-in-water emulsions, a shear rate of $\gamma = 1 \times 10^8$ s^{-1} is required for producing nanoemulsions with d = 100 nm. This shear rate is generally out of the range of most common mixing devices (e.g., overhead mixer 10^{3-4} s^{-1} (42), rotor stator mixer 10^{4-5} s^{-1} (43, 44) and sonicator 10^{6-7} s^{-1} (44, 45)). Considering the practical difficulty in obtaining such extreme shear rates, only three methods are commonly used for high-throughput production of nanoemulsions: high frequency ultrasonication, homogenization by high pressure valve homogenizer, and microfludization.

1.3.1.1 Ultrasonication

One of the first applications of ultrasound was to make emulsions and the first patent on this technology is more than fifty years ago (46). Since then, different types of ultrasonic devices have been developed for emulsion applications. Cavitation is the main phenomenon of ultrasonically induced effects, which is the formation and collapse of vapor cavities in a flowing liquid (47, 48). Two mechanisms are proposed for ultrasonic emulsification. First, the application of an acoustic field produces interfacial waves resulting in the dispersion of the oil phase in the continuous phase in the form of droplets

(49). Secondly, the application of ultrasound causes acoustic cavitation causing the formation and subsequent collapse of microbubbles by the pressure fluctuations of a simple sound wave, which creates extreme levels of highly localized turbulence. Therefore, the turbulent micro-implosions break up primary droplets into sub-micron size (50). Since the emitted sound field is typically inhomogeneous in most ultrasonic devices, it is necessary to recirculate the emulsions through the region of high power so that all droplets experience the highest shear rate.

The preparation of nanoemulsions by ultrasonics is well documented by Kentish et al. (51). The results showed that flaxseed oil MDD as low as 135 nm were achieved in the presence of Tween 40 as surfactant. As an emerging technology for nanoemulsion production, ultrasonics is comprehensively compared with microfluidization by Jafari et al. (47, 48). The general conclusion is that nanoemulsions produced by ultrasonication show wider and bimodal size distributions and greater dependence on coarse emulsion preparation methods than do those prepared using microfluidization. It is worth noting that all these researchers use small lab scale ultrasonic experimental set-ups. Commercial ultrasonic devices for nanoemulsion applications are not directly available since there are some design issues to be solved (33, 51).

1.3.1.2 Homogenization by high pressure valve homogenizer

High pressure valve homogenizers are the most commonly used devices to produce fine emulsions in the food industry. The oldest application is for milk processing to reduce the size of fat globules. A coarse emulsion is usually produced using a high speed mixer and is then fed into the input of a high pressure valve homogenizer. As it enters the gap between the valve and the valve seat (Figure 1.3), the flow velocity is increased rapidly. Homogenization is completed in the area between the valve and the seat, where the emulsion experiences a combination of intense disruptive forces that cause the larger droplets to be broken down to smaller ones. The combination of two theories, turbulence and cavitation, explain the droplet size reduction during the homogenization process (52-54). The high velocity gives the liquid high energy in the homogenizer valve and generates intense turbulent eddies of the same size as the MDD. Droplets are thus torn apart by these eddie currents resulting in a reduction in droplet size. Simultaneously, due to considerable pressure drop across the valve, cavitation occurs and generates further eddies disrupting droplets. Decreasing the gap size increases the pressure drop, which causes a greater degree of cavitation. Emulsion droplet diameters as small as 100 nm can be produced using this method if there is sufficient emulsifier present to completely cover the oil-water interface formed and the adsorption kinetics is high enough to prevent droplet coalescence (12).

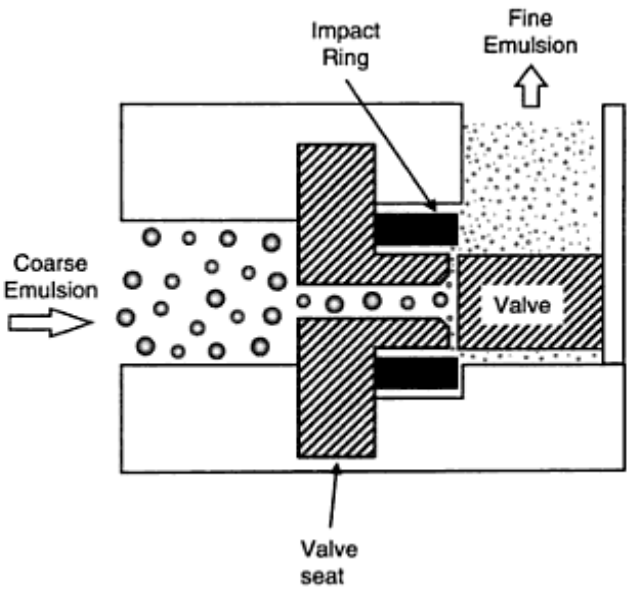

Figure 1.3 Schematic of high pressure valve homogenizer. Reprinted from Ref. 12.

In the last ten years homogenization technology has advanced so much that high pressure homogenization devices are available from lab, pilot to production scales. This technological progress is reflected by an increasing number of publications on food nanoemulsions in the past two years (55-62). Recent literature shows that lab-scale nanoemulsions can be prepared using different types of high pressure valve homogenizers. An APV lab unit was reported to be able to make milk fat fraction nanoemulsions (55) and palm-based lipid nanodispersions with MDD as small as 98 nm (56). Mao et al. (57, 58) and Yuan et al. (59, 60) reported the preparation of β-carotene nanoemulsions using a Niro-Soavi Panda homogenizer. At optimal conditions, β-carotene nanoemulsions prepared had a MDD of 121 nm. A lab unit of EmulsiFlex also could be used to prepare orange oil nanoemulsions (61) and curcumin nanodispersions (62). This

research demonstrates that it is feasible to prepare nanoemulsions by using high pressure valve homogenizer.

1.3.1.3 Microfluidization

Microfluidization is most commonly used in the pharmaceutical industry for the production of fine emulsions (63, 64). Recently it has been used to produce flavor emulsions and homogenize dairy products (65-67). In the microfluidizer processor shown in Figure 1.4, a coarse emulsion is pumped under high pressure (up to 40,000 psi/270 MPa) through a patented interaction chamber with microchannels of fixed geometry. Two jets of crude emulsions are accelerated at high velocities from two opposite channels collide with one another creating tremendous shearing action (69). In general, inertial forces in turbulent flow along with cavitation are predominantly responsible for droplet disruption (47, 48). These extreme shear rates and impact effects create exceptionally fine emulsions.

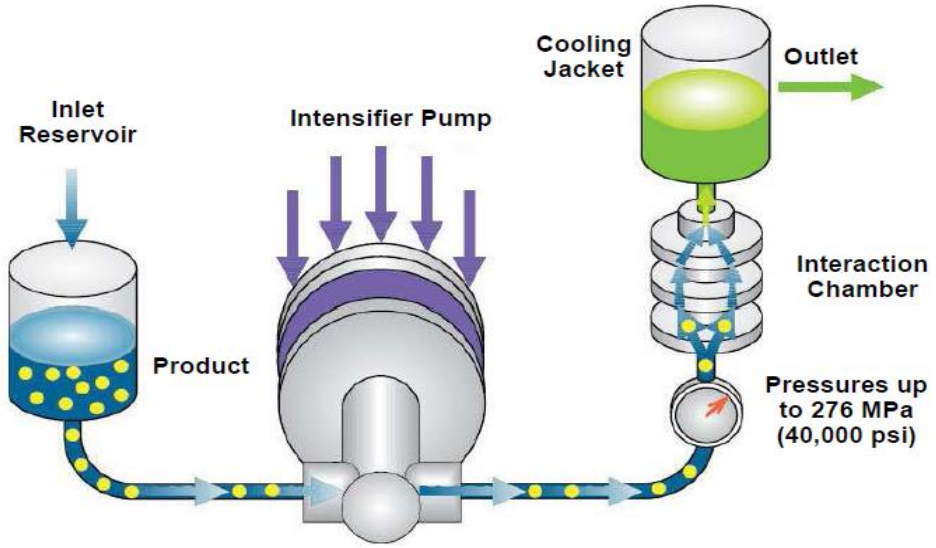

Figure 1.4 Schematic of microfluidizer processor configuration. Reprinted from Ref. 68.

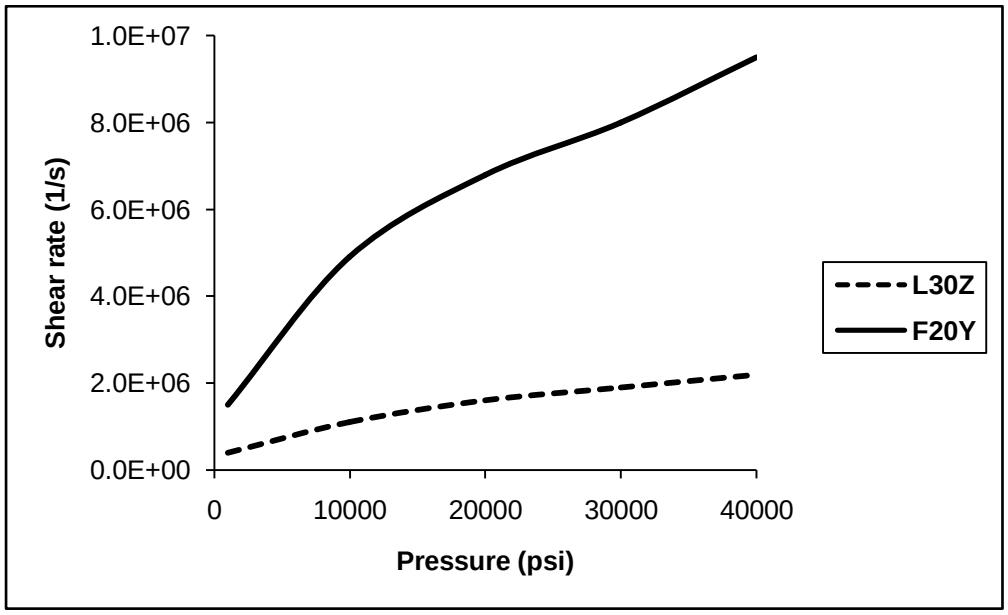

Figure 1.5 Shear rate of a microfluidizer as a function of pressure and chamber diameter. L30Z and F20Y have chamber dimensions of 300 and 75 μm, respectively. Data from Ref. 68.

The key component of a microfluidizer is the fixed geometry interaction chamber where the size reduction operation takes place. Various interaction chamber types and sizes are available for different applications. Y-type chambers are commonly used in emulsion applications. The fluid channels have typical dimensions in the range of 50 - 300 μm where sample velocities reach over 400 m/s. Shear rates inside the chamber can be as high as 10^7 s^{-1}. Figure 1.5 (68) shows shear rate of a Microfluidizer as a function of pressure and chamber diameter. Shear rate increases with a decrease in channel dimensions or increases in pressure. The extremely high shear generated under high pressure makes it possible to produce nanoemulsions.

There are numerous studies regarding the application of a Microfluidizer in milk and dairy model emulsions (70-72). Research results have shown that the droplet size distribution appeared to be narrower and smaller in Microfluidized emulsions than in conventional homogenization devices (47, 71, 73). Due to the high efficiency of droplet disruption, Microfluidizers are being used to prepare nanoemulsions. Jafari et al. (47) reported the production of d-limonene nanoemulsions with the size range D_{32} (surface weighted) of 150-700 nm using a microfluidizer at the pressure range of 35 ~ 105 MPa. Mason et al. (74) and Meleson et al. (36) demonstrated that silicone oil nanoemulsions as small as 50 nm stabilized by sodium dodecylsulfate (SDS) can be formed by using a Microfluidizer. Very recently, Yuan et al. (59, 60) showed that β-carotene nanoemulsions with MCT (medium chain triglyceride) as carrier could be formed using Tween 20 as emulsifier at homogenization pressures ranging from 80 ~ 130 MPa. Clearly, these

publications provide evidence that microfluidization is a powerful tool to manufacture nanoemulsions.

1.3.2 Emulsifier

Emulsifiers are amphiphilic molecules with both hydrophilic and lipophilic portions, which help stabilize emulsions by adsorbing at the particle interface. The hydrophilic portions align themselves within the lipid phase, while the lipophilic portions align in the water phase. Extensive information on food emulsifiers and their applications is provided by Hasenhuettl and Hartel (75).

An effective emulsifier should have three general characteristics: 1) rapidly adsorb to the oil/water interface of newly formed droplets during homogenization; 2) substantially reduce the interfacial tension; and 3) form an interfacial membrane to stabilize the emulsion by steric or electrostatic interactions between droplets. A number of food components exhibit these characteristics and can be used as emulsifier (e.g.; lecithin, proteins, gums, modified starches, phospholipids, etc.). However, these emulsifiers vary considerably in their molecular structure, which influences their ability to form and stabilize emulsions, as well as to withstand environmental stresses, such as variations in ionic strength, pH, and temperature. It is disappointing that little research was conducted to systematically evaluate performance of different types of emulsifiers and no standard criteria has been established to assess their efficiency for specific

applications. Emulsifier performance is one of the most important factors determining the formation and stability of nanoemulsions and several special emulsifier characteristics have to be considered in selecting emulsifiers for producing nanoemulsions which is discussed below.

1.3.2.1 Adsorption kinetics

The physiochemical properties of an emulsifier play a key role in the formation of nanoemulsions. One of the most important characteristics is fast adsorption kinetics to the oil-water interface. The emulsification process involves both the creation of new droplets and frequent collisions between droplets. The MDD of an emulsion is the result of competition between the two oppositely directed processes: 1) breaking of droplets into smaller ones by shear; and 2) coalescence of the newly formed droplets into larger ones upon collision. During homogenization, emulsifiers tend to adsorb at the droplet interface and thus to protect them against coalescence. The rate of emulsifier adsorption should be large enough to guarantee obtaining a sufficiently high coverage of the oil-water interface during the extremely short period between droplet formation and subsequent collisions where coalescence may occur. Unfortunately, experiments on the rate of adsorption of surfactant molecules or macromolecules at the oil-water interface during homogenization are scare. This is due to the experimental difficulties encountered in monitoring interfacial changes at short time intervals (37).

Emulsifier adsorption kinetics is directly related to the characteristic time of diffusion (τ_D) of an emulsifier to the interface (76, 77). As τ_D decreases, the mobility of emulsifier in the bulk phase increases and consequently the rates of adsorption at the oil-water interface increases. Figure 1.6 provides a good example demonstrating effect of molecular weight of methylcellulose molecules on their τ_D to a water-sunflower oil interface. Obviously methylcellulose with lower molecular weight showed faster adsorption kinetics compared to that with high molecular weight. Though τ_D is determined by many factors (e.g., emulsifier structure, temperature and bulk viscosity, etc.), generally small emulsifiers have faster adsorption kinetics and helps to form nanoemulsions, which is supported by the fact that most research on food nanoemulsions used Tweens, instead of food biopolymers, as emulsifier.

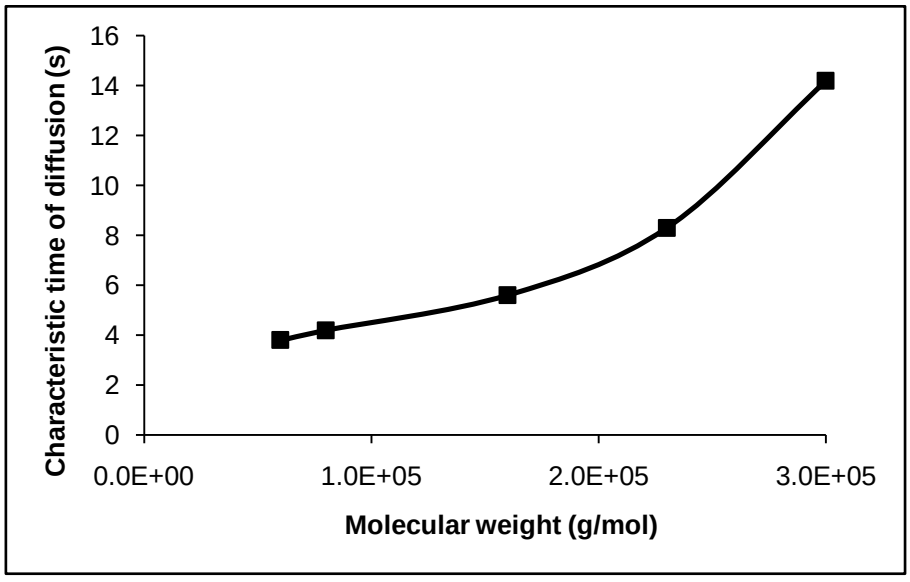

Figure 1.6 Average molecular weight and characteristic time of diffusion of methylcellulose molecules to a water-sunflower oil interface. Data from Ref. 76.

1.3.2.2 Reduction of interfacial tension

Another important role of emulsifier during homogenization is a reduction of interfacial tension. Emulsifier molecules diffuse to the interface of newly formed droplet and lower the interfacial tension to facilitate further rupture of droplet. According to Taylor's formula, the typical size of a ruptured drop is proportional to the interfacial tension, σ. The greater the reduction of interfacial tension, the smaller the droplets that can be produced during homogenization at a certain energy input. The presence of emulsifier lowers the interfacial tension of triglyceride-water interface from about 30 mN/m to 1~ 20 mN/m depending on emulsifier type and concentration (78). Figure 1.7 demonstrates how the concentrations of Tween 20 and β-lactoglobulin affect interfacial tension of corn oil-water system with an oil volume fraction of 0.4. Interfacial tension of β-lactoglobulin surrounded droplets is three times that of Tween 20. From this point of view, Tween 20 is more effective to prepare nanoemulsions than β-lactoglobulin because less energy is required to disrupt the droplets. Therefore, an evaluation of dynamic interfacial tension could be used to screen emulsifier candidates for nanoemulsions.

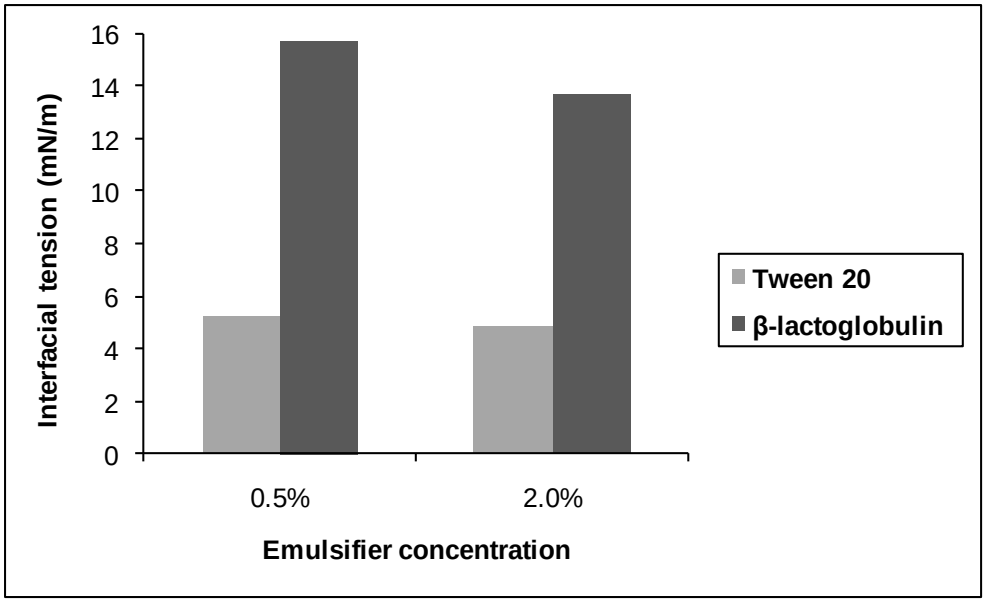

Figure 1.7 Effect of concentration of Tween 20 and β-lactoglobulin on dynamic interfacial tension of corn oil/water interfaces. Data from Ref. 79; interfacial tension was measured using a drop shape analysis method.

1.3.2.3 Formation of interfacial membrane

The formation of a strong interfacial membrane is also an important factor for producing nanoemulsions. During high pressure homogenization, droplet collisions occur more frequently than under low pressure emulsification methods. The droplet coalescence rate was found to be higher at higher homogenization pressure due to larger turbulent squeezing force (80). Therefore, the formation of a robust interfacial membrane is critical for producing nanoemulsions.

A number of mechanisms have been suggested for coalescence hindering during homogenization. Surface coverage is the first factor to prevent droplet coalescence. The timescale of high pressure homogenization is so small that the interface is not at

equilibrium. A special term, Γ, is used to describe the interfacial loading of emulsifiers: Γ = n/*A*, where n is the number of emulsifier molecules and *A* is the interfacial area. Larger Γ means better interfacial coverage. To a large extent, Γ is determined by adsorption kinetics and the concentration of emulsifier molecules before droplet collision. Therefore, the use of a higher concentration of emulsifiers with fast adsorption kinetics contributes to higher interfacial load of emulsifiers and thus a reduction in droplet coalescence.

Another mechanism, albeit controversial, to minimize coalescence during homogenization is electrostatic forces. Generally it is accepted that strong electrostatic force provides a wall like repulsion to prevent coalescence (81, 82). Hakansson et al. (81) showed that coalescence could be hindered by electrostatic repulsion in a high pressure homogenizer by using a dynamic simulation model. However, Walstra (83) stated that electrostatic forces can never be sufficiently strong to prevent drop coalescence because the stabilizing force is in the order of 100 times weaker than aggregating pressure under turbulent conditions in a high pressure homogenizer. The controversy on the role of electrostatic repulsion might be attributed to the difference in process conditions, homogenization devices, and emulsion systems. Overall, a highly charged emulsifier with fast adsorption kinetics might be beneficial to minimize coalescence during nanoemulsion formation.

1.3.3 Viscosity of phases

The experimental difficulty of considering all parameters involved in the emulsification process makes it hard, if not impossible, to create a universal mathematical model for predicting droplet size during high pressure homogenization (81, 82). However, the simplified equation developed by Taylor provides valuable information that emulsification relies not only on shear rate but also rheological properties of the phases (84). Taylor's equation has particular significance for producing nanoemulsions because in practice, it is much easier to alter phase viscosity than produce extreme shear. Experiments have shown that it is very important to ensure that the ratio of disperse/continuous phase viscosity (η_d/η_c) is in an optimal range to facilitate droplet disruption and form small particles (12, 85, 86). It was proposed that when η_d/η_c is too high, droplets are more resistant to disruption as there is insufficient time to deform before the flow field causes the droplet to rotate (12).

In practice, η_d/η_c can be controlled by altering the composition of either the oil phase (e.g., by mixing low- and high- viscosity oils) or the aqueous phase (e.g., by mixing emulsifier and viscous cosolvents with water). Alternatively, η_d/η_c can be tailored by controlling homogenization temperature because phase viscosities decrease rapidly with increasing temperature.

1.4 Stability of nanoemulsions

Emulsions are thermodynamically unstable due to their large interfacial energy. However, they can be kinetically stable for considerable periods of time. The stability of emulsions is determined by their resistance to changes in physicochemical properties over time. Physically, emulsions can be destabilized by creaming, flocculation, coalescence, and Ostwald ripening. Oxidation and degradation of emulsion components are major causes of chemical destabilization of emulsions, which is beyond the scope of this review. Compared to macroemulsions, nanoemulsions are more resistant to creaming, flocculation and coalescence due to the small droplet size. In contrast, Ostwald ripening is the main stability problem for nanoemulsions due to the difference in free energy among droplets of different size. In the following section, nanoemulsion stability is discussed in detail.

1.4.1 Creaming

Creaming is the separation of oil droplets as a layer at the top of emulsion due to the density difference between the continuous and dispersed phases (12, 87, 88). The rate of creaming in dilute emulsions can be predicted using Stokes' law (12).

$$v = \frac{2gr^2(\rho_w - \rho_o)}{9\eta_c} \qquad \textbf{[1.3]}$$

Where ν is the creaming velocity of the droplet, ρ_w is the aqueous phase density, ρ_0 is oil phase density, r is radius of the droplet, η_c is viscosity of continuous phase, and g is the acceleration due to gravity. Stokes' law captures the essence of creaming phenomenon of emulsions and also provides solutions to prevent creaming by reducing droplet size, and phase density contrasts, and increase continuous phase viscosity. The very small droplet size of nanoemulsions causes a large reduction in the gravity force and Brownian motion may be sufficient to overcome gravity, which means that nanoemulsions are stable against creaming or sedimentation during storage (13, 89, 90).

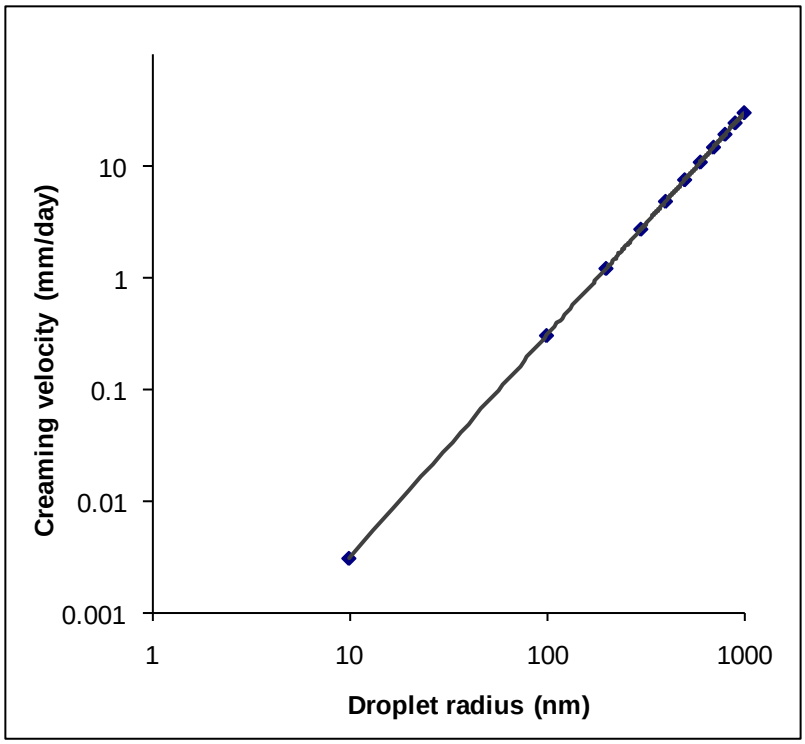

Figure 1.8 Creaming velocity of emulsions. Calculation is based on Stokes' law and assumptions of ρ_w=1.0 g/ml, ρ_0=0.84 g/ml, and η_c=1.0 mPa **s**.

Generally a low value of v (e.g., < 1 mm/day) would be adequate to provide a stable emulsion (91, 92). Figure 1.8 shows calculated creaming velocity as a function of droplet radius based on Stokes' law. Clearly, nanoemulsions with a MDD around 100 nm have a creaming velocity far below 1 mm/day while the creaming velocity will be above 1 mm/day for emulsions with radius about 200 nm. Therefore, nanoemulsions with a small fraction of droplets with large radius (e.g., > 200 nm) may have creaming issues. This demonstrates how important a narrow droplet size distribution is to prevent creaming of nanoemulsions.

1.4.2 Flocculation and Coalescence

When two drops collide, different results can occur depending on the intermolecular forces between two drops (12, 90): 1) they can flocculate if the intermolecular repulsive forces are sufficiently strong to keep the droplets separated at a small equilibrium distance; or 2) they can coalescence if the interfacial membrane ruptures. It was shown that the drop-drop interactions depend on both droplet size and interfacial properties. In food applications, electrostatic interactions between droplets are influenced by many factors (e.g., emulsifier type, charge density, pH and salt concentration), so it is more practical to consider steric interactions induced by an adsorbed interfacial membrane (89, 90).

When two droplets with interfacial membrane thickness of δ approach to a distance h, total energy of interactions G is determined by three forces (90): 1) repulsive force due to osmotic interaction driven by unfavorable mixing of adsorbed layer on the interface; 2) repulsive force from reduction in configuration entropy of emulsifier chains; and 3) attractive force due to van der Waals. Combining the three forces, the magnitude of G to a large extent depends on particle radius r and interfacial thickness δ, which is illustrated in equation 4. The high value of G is due to small droplet size resulting in high kinetic stability of nanoemulsions against flocculation and coalescence.

$$G \propto \frac{\delta}{r} \qquad \textbf{[1.4]}$$

Another explanation for improved kinetic stability of nanoemulsions is that nanoscale droplets are non-deformable (90, 93, 94). Recently, research in fundamental structure, mechanical and physical properties of nanoemulsions is an emerging field and frontier in physics (15). It is proposed that the very small size of droplets relative to the dense interfacial layers ensures the interface is non-deformable, which enhances the interface resistance to film thinning and disruption between droplets (90, 93). Hence flocculation and coalescence are reduced or prevented in nanoemulsions.

1.4.3 Oswald ripening

Ostwald ripening in emulsions is the phenomenon that large droplets grow over time at the expense of small droplets (95-97). The physical basis of Ostwald ripening is due to the Laplace's Law effect on the solubility of the dispersed phase in the continuous phase (98, 99). The pressure difference between the inside and outside of a drop is described by equation 5.

$$\Delta P = \frac{2\sigma}{r} \qquad \textbf{[1.5]}$$

Where ΔP is pressure contrast, σ is interfacial tension, and r is droplet radius. The solubility, S, of the dispersed phase in the continuous phase just at the boundary of the drop of radius r is predicted by the Kelvin equation (100-102).

$$S(r) = S_0 \exp(2\sigma v_m / rRT) \qquad \textbf{[1.6]}$$

Where S_0 is the solubility of the dispersed phase in the bulk of continuous phase, v_m is the molar volume of continuous phase. R is gas constant, and T is the absolute temperature. The Kelvin effect originates from the difference in chemical potential between small and large droplets as a result of the different Laplace pressure. This effect is limited to small droplets and has minimal effect on large droplets.

From the Kelvin equation, obviously the smaller the droplet, the higher the solubility of emulsified oil. The difference in solubility generates a concentration gradient

from the surroundings of a small drop to the surroundings of a large one, which drives a mass transfer by diffusion from small to large drop. As a consequence the small droplets tend to shink and the large droplets tend to grow. This process slows down as the droplets grow.

The phenomenon of Ostwald ripening is described by the Lisfshitz-Slesov-Wagner (LSW) theory.

$$r^3 = \frac{8}{9}\left[\frac{S_0 \sigma v_m D}{\rho RT}\right]t \qquad \textbf{[1.7]}$$

Where D is the diffusion coefficient of the dispersed phase in the continuous phase, ρ is the density of the dispersed phase, and t is the time. LSW captures the key of Ostwald ripening, which is the dispersed phase solubility in the continuous phase.

Ostwald ripening is the major destabilization mechanism of most nanoemulsions, and thus is the biggest challenge in producing stable nanoemulsions for practical applications. A number of factors have to be considered to slow down the Ostwald ripening rate. Obviously decreasing oil solubility in the aqueous phase is the most effective method to retard or prevent Ostwald ripening in O/W nanoemulsions. The Ostwald ripening rate could be reduced by using a less polar oils (e.g., medium or long chain triglycerides). Molecular weight (MW) of oil phase is also critical to Ostwald ripening because the diffusion coefficient, D, largely depends on MW and higher MW oil would reduce Ostwald ripening rate (3, 97).

The effect of emulsifier on Ostwald ripening is complex because emulsifier type, concentration, and interfacial structure affect Ostwald ripening in different ways. Generally, emulsifiers with greater reduction in interfacial tension help reduce Ostwald ripening, which is obvious from the Kelvin equation. However, emulsifier concentration also has to be considered. Below the critical micelle concentration (CMC), an increase in emulsifier concentration results in lower interfacial tension and hence a lower Ostwald ripening rate. Above the CMC the interfacial tension stays constant, but the micelles can transport oil molecules between drops in a faster way than diffusion and hence increase Ostwald ripening rate (103-107). The structure of deposited emulsifier on the interface acts as a diffusion barrier and thus is also relevant to Ostwald ripening rate. Deposition of an insoluble layer (e.g., polymeric substances) on the interface could greatly reduce mass transfer and hence Ostwald ripening rate (99, 108).

The fundamental cause of Ostwald ripening is the chemical potential difference between different sizes of droplets. The smaller the difference in droplet size the lower the driving force for Ostwald ripening (96). So one would expect if the initial distribution of droplets is narrow (e.g., monodisperse) Ostwald ripening will be retarded. In contrast, if the initial distribution of droplets is wide, bimodal distribution will be achieved during the storage of nanoemulsions.

1.5 Droplet size characterization of nanoemulsions

The size and size distribution of nanoemulsions have a strong influence on their physicochemical properties (e.g., stability, appearance and rheology). Monodisperse nanoemulsions are rare, but sometimes are prepared by ultracentrifugation of polydisperse nanoemulsions for use in fundamental studies because the interpretation of experimental measurements is usually simpler (15). Most nanoemulsions are polydisperse and can be characterized according to the shape of size distributions as being monomodal, bimodal, or multimodal depending on whether there are one, two, or more peaks in the distribution.

1.5.1 Mean droplet diameter

There are a number of expressions of MDD charactering different physical aspect of the distribution. In the case where the number of particles is important, a number-based MDD, d_N , is described as equation 8. Where N_i is the number of particles with diameter d_i. In the case where the surface area of particles is of interest, a surface-based MDD, d_S, can be used to characterize the particles. If one is interested in the mass of particles, a volume-based MDD, d_V, is always used. Equations 8 to 10 describe the mathematical formulas for different expressions of MDD.

$$d_N = \frac{\sum N_i d_i}{\sum N_i} \qquad \textbf{[1.8]}$$

$$d_S = \frac{\sum N_i d_i^3}{\sum N_i d_i^2} \qquad \textbf{[1.9]}$$

$$d_V = \frac{\sum N_i d_i^4}{\sum N_i d_i^3} \qquad \textbf{[1.10]}$$

For monodisperse nanoemulsions, d_N, d_S, and d_V have the same value. For polydisperse nanoemulsions, $d_N < d_S < d_V$. Since monodisperse emulsions do not exist in the real world, it is important to specify which MDD has been determined in an experiment when comparing or quoting droplet size data. Generally for food nanoemulsions, d_V is commonly used to represent MDD since it provides more information on large droplets which is particularly important for the stability of nanoemulsion.

1.5.2 Size characterization by light scattering

When a beam of light passes through a colloidal dispersion, the particles or droplets scatter some of the light in all directions. When the particles are very small compared with the wavelength of the light, the intensity of the scattered light is uniform

in all directions (Rayleigh scattering); for larger particles above approximately 250nm diameter, the intensity is angle dependent (Mie scattering) (109).

Dynamic light scattering (DLS), also known as photon correlation spectroscopy (PCS), is the basis of a common particle sizing measurement covering the range of nanometers to microns (1 nm – 6 μm). This technique is based on analyzing time-dependent fluctuations in the scattered intensity. These fluctuations arise from the fact that the particles are small enough to undergo random thermal (Brownian) motion and the distance between particles is therefore constantly varying. Constructive and destructive interference of light scattered by neighboring particles within the illuminated zone gives rise to the intensity fluctuation at the detector plane which contains information about this motion. Analysis of the time dependence of the intensity fluctuation can therefore yield the diffusion coefficient of the particles.

The Stokes-Einstein theory of Brownian motion describes the relationship between particle size and diffusion coefficient of particles in a known medium, which is the basis of particle size measurement by DLS.

$$d_H = \frac{kT}{3\pi\eta D} \qquad \textbf{[1.11]}$$

Where d_H is the droplet diameter, k is the Boltzmann's constant, T is the absolute temperature (Kelvin), η is the viscosity of continuous phase, and D is the diffusion coefficient of droplet.

While DLS is a powerful technique to measure particle size and size distribution, the results are always mathematical model dependent and special caution is needed to interpret data. Sometimes, a large error can occur for inhomogeneous or polydisperse nanoemulsion with a wide particle size distribution. Electron microscopy always serves as a supplemental tool to characterize the size and size distribution of nanoemulsions. Cryogenic transmission electron microscopy (Cryo-TEM) and cryogenic scanning electron microscopy (Cryo-SEM) are commonly used techniques to confirm droplet size measurement obtained by DLS.

1.6 Properties of nanoemulsions

1.6.1 Optical properties

For monodisperse particles, the general expression for optical transmission is described in equation 12.

$$T = \exp(-\tau L) \quad \textbf{[1.12]}$$

Where τ is the turbidity and L is the optical path length (110). The specific turbidity for a light scattering cross section is given by equation 13.

$$\frac{\tau}{c} = \frac{3\pi}{4\rho_c} \frac{Q_{av}}{r_{vs}} \qquad \textbf{[1.13]}$$

Where c is the volume concentration of particles, ρ_c is the density of the continuous phase, Q_{av} is the mean light scattering efficiency, r_{vs} is the volume mean radius. Q_{av} is determined by particles size, refractive indices of dispersed and continuous phases, and wavelength of light scattered. Figure 1.9 shows the calculated relationship between specific turbidity and particle size for different wavelengths of light. The curves show strong oscillatory behavior, particularly at low wavelengths. The maximum specific turbidity increases as wavelength decreases. The specific turbidity at light wavelengths similar to the radius of particles reaches maximum. For nanoemulsions, the droplet dimensions are much smaller than the wavelength of light ($r << \lambda$), causing weak light scattering and hence low turbidity. Therefore, nanoemulsions tend to be transparent in appearance.

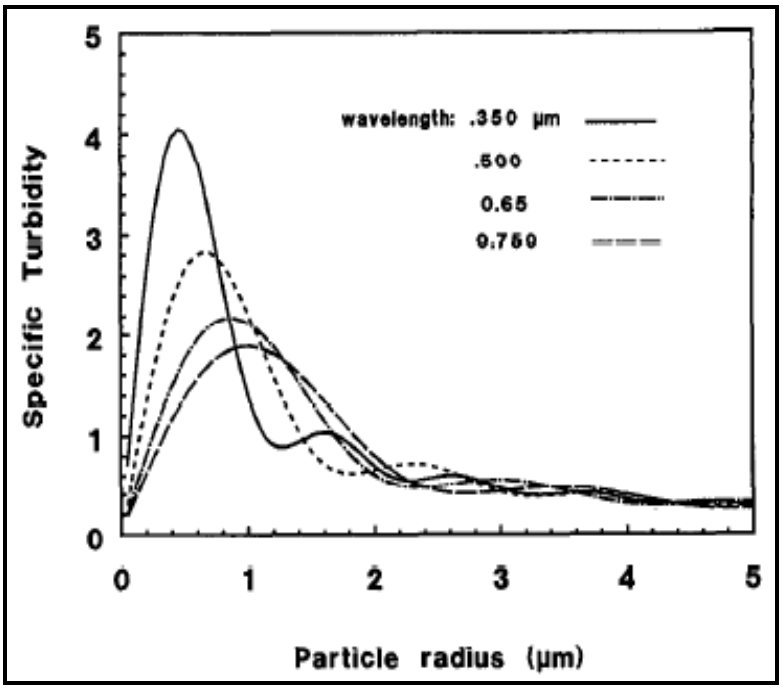

Figure 1.9 Relationship between specific turbidity and particle size. Calculation is based on monodisperse particles and fixed refractive of 1.506. Reprinted from Ref. 111.

1.6.2 Physical stability

As discussed in Section 1.4.1, nanoemulsions are highly stable against creaming because the relatively small droplet size means that Browning motion effects dominate gravitational forces. Moreover, the viscosities of nanoemulsions are appreciably higher than those of macroemulsions at the same lipid concentration if they contain a thick or electrically charged interfacial layer which increases droplet-droplet repulsion. This increase in viscosity also contributes to improved stability against creaming. As discussed in Section 1.4.2, nanoemulsions also have good stability against droplet aggregation

because the strength of the net attractive forces acting between droplets decreases with decreasing droplet size. Overall, nanoemulsions show better physical stability compared to macroemulsions due to the reduction in droplet size.

1.6.3 Improved bioavailability of lipophilic actives

The health promoting benefits of food bioactive components (e.g.; catechins, phytosterols, curcumin, lycopene, ω-3 fatty acids, and carotenes) have attracted more attention in recent years because their biological and pharmacological effects including antioxidation, anticancer, and chronic disease prevention properties have been demonstrated in numerous studies (4,7, 112, 113). However, one of the major challenges of these actives is their poor solubility and low bioavailability. Nanoemulsions were reported to improve the solubility, stability and bioactivity of various oil-soluble phytochemicals due to their small droplet size and high kinetic stability (7, 31, 32, 114).

Considerable research has been conducted to evaluate nanoemulsions as a vehicle for lipophilic drug delivery and a number of drug nanoemulsions are commercially available in the market (114). In food and nutraceutical industries, nanoemulsions also show potential commercial applications. Nanoemulsions have been found to markedly increase the solubility of curcumin to 1 wt%, while it is almost insoluble in water (4). Analytical data (4, 7) suggested epigallocatechin gallate (EGCG) encapsulated in nanoemulsions resulted in less oxidation than that of EGCG in aqueous solution (15 wt%

vs. 60 wt%). It was reported that nanoemulsions could improve stability and oral bioavailability of EGCG and curcumin in a mouse model. The bioactivity was further enhanced when the MDD of nanoemulsions were further reduced to below 100 nm (4). Recent research also has shown that nanoemulsions loaded with coenzyme Q10 (CoQ10) significantly enhanced the bioavailability (114). There is no question that nanoemulsions as delivery carrier for lipophilic food components will continue to be one of the frontiers of food nanotechnology due to potential commercial applications and health benefits.

1.7 Potential applications of nanoemulsions in food industry

The pharmaceutical industry is the dominant field where most applications of nanoemulsions are proposed. Extensive research has been conducted on a variety of drug delivery systems with enhanced solubilization of poorly soluble drugs and improved bioavailability following incorporation into nanoemulsions (114, 115). In the food industry, many food-derived bioactive compounds demonstrate significant health benefits when consumed in relatively high concentrations (25, 31). Unfortunately, most of these compounds exhibit poor solubility and bioavailability in aqueous-based foods. Recently the development of nanoemulsions loaded with lipophilic food components has demonstrated the potential of nanoemulsions as a carrier to deliver lipophilic actives in food applications (31, 32).

Emulsions are widely used in beverage products as it is frequently necessary to incorporate water-insoluble flavors into an aqueous beverage. However, it is often desired that the beverage be clear in appearance. The current solution for this particular need is to use a cosolvent, most commonly alcohol, in the system (often introduced as the flavor carrier or solvent). However, alcohol-based flavors have transportation issues due to their low flash point. The use of alcohol also disqualifies the product from obtaining a Halal certificate, which is desirable in many regions of the world. Nanoemulsions can solve these problems since emulsions with MDD below 100 nm have the potential to provide transparent appearance that can be incorporated into beverages without loss of clarity (116-117).

Another unique application of nanoemulsions is non-weighted flavor emulsions. For conventional flavor emulsions, weighing agents (e.g., ester gum and brominated vegetable oil) are commonly used to weigh the oil phase and reduce density contrast between oil and aqueous phases. These weighing agents significantly reduce the creaming velocity of droplets, but they have strict usage limits due to their toxicity. Weighing agents can be removed in nanoemulsions due to their high stability against creaming, which provides a cleaner label.

1.8 Current status of nanoemulsions

Mason and coworkers (15, 36, 74) conducted studies on the formation of SDS stabilized silicone oil-in-water nanoemulsions by using a Microfluidizer. The mechanical and interfacial rheology properties of concentrated nanoemulsions with a dispersed phase volume fraction, Φ, up to 0.7 were of the interest. The MDD of nanoemulsions was evaluated as functions of the number of passes through the Microfludizer, homogenization pressure, droplet volume fraction, and surfactant concentration. The results showed that MDD decreased with an increase in SDS concentration, homogenization pressure, and number of passes, while MDD increased with Φ. Nanoemulsions were obtained with smallest MDD being 18 nm. Mason et al. (15) also provided a thorough review on the formation, structure, and physical properties of nanoemulsions. In this review, the fundamental differences between nanoemulsions and microemulsions were emphasized and emulsification parameters were thoroughly discussed based on the Taylor's estimate of ruptured droplet radius.

Jafari et al. (47, 48, 69) reported on *d*-limonene nanoemulsions by using Microfluidization and ultrasonication. Whey protein concentrate (WPI) and modified starch (HI-Cap®) were evaluated as emulsifiers. The results indicated that both Microfludization and ultrasonication were capable of producing nanoemulsions with a MDD range of 150 ~ 700 nm. The MDD decreased initially with increasing pressure and number of passes through Microfluidizer; however, the emulsions become over-processed when the pressure was above a critical point. The optimum pressure and process cycles were about 70 MPa with 2 passes for nanoemulsions with 20% w/w *d*-

limonene as dispersed phase stabilized by HI-Cap® or WPI. The smallest surface-weighted MDD obtained was 150 nm.

Chen and Wagner (2) reported vitamin E nanoemulsions stabilized by modified starch prepared using a Microfludizer. Vitamin E was homogenized at 70 and 150 MPa for up to 12 passes and then the prepared nanoemulsions were spray dried to yield a powder. The results showed that higher pressure and a greater number of passes produced smaller droplets. Particle size did not significantly increase upon rehydration in water. Apple juice fortified with *ca*. 62 ppm vitamin E with nanoemulsions as carrier had a turbidity of 14 NTU. Moreover, during a 6-month storage study of the fortified juice, no ringing or creaming occurred, and the turbidity of juice was highly stable with an increase of only 2 NTU. To our knowledge, this is the first report to prepare true nanoemulsions with a MDD < 100 nm by using food grade ingredients.

Very recently, Mao et al. (57, 58) and Yuan et al. (59, 60) investigated the formation of β-carotene nanoemulsions by using high pressure homogenization. In the studies, modified starches, why protein isolate (WPI), Tween 20 and blend of Tween 20 and WPI were tested to stabilize nanoemulsions. MCT was used as the solvent to dissolve β-carotene. The results showed that nanoemulsions stabilized with Tween 20 had the smallest MDD of 132 nm, while nanoemulsions stabilized with a blend of WPI and Tween 20 were most stable. Furthermore, response surface methodology was employed to optimize the formation of nanoemulsions. In the experiment, 10% w/w MCT was used as a carrier and Tween 20 as surfactant. The optimum preparation conditions were

suggested to be: pressure 129 MPa, homogenization temperature 47 ℃, load of β-carotene 0.82%, and Tween 20 8.2%.

In the past two years, considerable research on curcumin nanoemulsions was conducted in Huang's research group (4, 7, 62, 118) with an interest in enhanced bioavailability of curcumin. Nanoemulsions with medium chain triglyceride (MCT) as oil and Tween 20 as emulsifier were successfully prepared with MDD ranging from 618 nm to 79.5 nm. MCT, Tween 20, and water were mixed at a ratio *ca*. 10/10/80 and homogenized under a pressure ranging from 500 bar to 1500 bar. The results showed that multiple passes and higher pressures generated smaller MDD of nanoemulsions and thus higher bioavailability of curcumin in *in-vitro* study.

Wooster et al. (3) reported on Ostwald ripening of nanoemulsions stabilized by SDS and Tween 80 under high pressure homogenization. They found that the physical properties of the oil phase and the nature of the surfactant layer had considerable impact on nanoemulsion formation and stability. Nanoemulsions made with high viscosity oils, such as long chain triglycerides (LCT), had larger MDD (120 nm) than those prepared with low viscosity oils such as hexadecane (80 nm). The optimization of the viscosity ratio between phases led to formation of smallest nanoemulsions (*ca.* 40 nm). The author also identified Ostwald ripening as the main destabilization mechanism of prepared nanoemulsions and the use of high molecular weight oils like LCT significantly reduced the rate of Ostwald ripening.

Overall, these references provide clear information that high pressure homogenization is a relatively simple and effective method of producing nanoemulsions under the proper conditions. Most studies used small molecule surfactants, such as Tweens and SDS, to stabilize model nanoemulsions. The primary focus of previous studies has been the formation of nanoemulsions, while research on the long term stability of nanoemulsions is rare due to the difficulty of preventing Ostwald ripening. The primary application of nanoemulsions has been to improve the bioavailability of encapsulated lipophilic actives in nanoemulsions. There has been little work on the physical properties of nanoemulsions (e.g., improved stability and optical transparency).

1.9 Patent review on nanoemulsions

Though nanoemulsion is relatively new in emulsion community, there are an increasing number of patents on nanoemulsions since the first one on producing water/oil nanoemulsions was issued in 1992 (119). However, most of these patents are exclusively for pharmaceutical and cosmetic applications due to the use of non-food grade ingredients, e.g., surfactants, synthesized polymers and organic solvents (119-122). US patent 5,152,923 (119) first described the use of high pressure homogenization to prepare nanoemulsions with MDD below 200 nm as a vehicle for pharmaceutical and cosmetic applications. The patent claimed glycero-phosphatides as preferred emulsifier and optimal homogenization temperature above the phase transition temperature of the

emulsifier. The method of solvent evaporation has been described in particular by Valdivia et al. (123) in US patent 5,698,219 to produce nanoemulsions. In the patent, nanoemulsions were created by emulsifying the aqueous phase containing a non-ionic surfactant with an organic phase containing oil and active substance in a water miscible solvent, and then removing the solvent by evaporation. US patent 6,419,946 (124) described another approach to prepare nanoemulsions by using mixed esters as emulsifiers for cosmetic applications. The emulsifiers are specified as esters of glycerol with α-hydroxy acid, and fatty acid or fatty alcohol and it is required at least one oil has a molecular weight greater than 400. It was claimed the turbidity of prepared nanoemulsions ranged from 60 to 600 NTU.

Due to the limitations in surfactant usage, only a few patents on food grade nanoemulsions were documented. US patent application 20090196972 (125) describes flavor nanoemulsions and their applications which include dressings, marinades, sauces, condiments and beverages. The nanoemulsions are prepared by using food-grade, non-ionic surfactant, e.g., Tween 80 and co-solvents (C2-C8 alcohols). Very recently, food grade nanoemulsions were described by Wooster et al. (126) in US patent application 20100305218. In the patent, nanoemulsions were prepared using hydrophilic non-ionic surfactant (preferably polysorbate), co-surfactant (e.g., lecithin), co-solvent (preferably ethanol) and high pressure homogenization. It was claimed that the oil phase of nanoemulsions contains more than 50 v/v% of long chain triglyceride (C12 or greater, e.g., peanut oil) which greatly reduce Ostwald ripening of nanoemulsion.

Since the term of nanoemulsion and microemulsion are used interchangeably in the literature, patents on microemulsions are also briefly reviewed. Microemulsions were first patented for crude oil recovery in the early 1970 (127-129). Thir et al. (130) first disclosed the microemulsions with broad potential applications including flavors in US patent 4,568,480. The authors discovered that microemulsions can be easily formed using a fatty acid ester of alkoxylated phenol derivatives as emulsifier. In the field of food and beverage applications, the use of microemulsion has been described by Wolf et al. (131) in US patent 4,835,002. The patent discloses microemulsions of edible oils in a matrix of water and certain alcohols, together with food-grade surfactants. Propylene glycol is selected as preferred alcohol in claimed applications including food, beverage, mouthwash, etc.

Ternary phase diagram was used to optimize the formation of microemulsion flavor or fragrance concentrates in several patents issued to International Flavors & Frangrance (132-134). In these patents, the ratio of oil phase, aqueous phase, surfactant and co-surfactant/co-solvent was determined to produce transparent microemulsions using phase diagrams. One recent international patent application WO 2007026271 (135) by Firmenich SA discloses preparation of clear flavor microemulsions using sugar ester of fatty acid and lecithin as surfactant systems, together with propylene glycol as co-solvent. In the patent, the ratio of flavor oil (*ca.* 30 wt%) to surfactants (*ca*. 10 wt%) is relatively low compared to previous patents on microemulsions. Chanamai et al. (136) described a different approach to prepare microemulsions in food and beverage

applications in US patent application 20070087104. In this approach, a ternary food grade emulsifier system was used incorporating low, medium and high HLB emulsifiers without using co-solvent. However, the usage level of emulsifiers is extremely high (*ca*. 90 wt% in total) in microemulsion concentrates. US patent 7,182,950 (137) describes nano-sized self-assembled liquid dilutable vehicles containing water, short chain polyol co-solvent, hydrophilic surfactant, C2-C16 alcohol co-surfactant, and oils. It was claimed this novel structured concentrates can be diluted either in water or oil to any desirable dilutions while maintaining their structure and stability. It was also claimed the structured concentrates greatly enhance the solubility of phytosterol, lycopene, lutein and other active components.

Overall, almost all patents on microemulsions and nanoemulsions used multiple surfactants or single surfactant with co-solvent and co-surfactant. The food grade surfactants used in these patents are exclusively Tweens and esters of fatty acids which may impart undesirable taste and complicate the labeling of nanoemulsion-based products. Clearly there is a need to develop nanoemulsions with simpler emulsifier system and friendly label.

1.10 Conclusions

There is no doubt that emulsion science and technology has advanced so much that manufacturing food nanoemulsions is technically feasible and commercially promising.

However, in practical applications, the use of small surfactants in nanoemulsions is limited due to their legal status and undesirable taste. Little information is available on food biopolymers as emulsifiers to produce nanoemulsions. One would expect a large difference between small surfactants and macromolecules in creating and stabilizing nanoemulsions. Therefore, future research on evaluating food biopolymers and natural emulsifiers in stabilizing nanoemulsions would be of great practical significance. Successful commercial applications of nanoemulsions in the food and flavor industries to a large extent depend on the stability of nanoemulsions, especially for small molecule, flavor nanoemulsions. Flavor oils have considerable solubility in water compared to vegetable oils, which leads to a major challenge of stabilizing flavor nanoemulsions against Ostwald ripening. Thus, more efforts have to be made to develop practical solutions to prevent Ostwald ripening of food nanoemulsions in order to provide a proper shelf life of nanoemulsion-based aqueous food products.

References

[1] Mao, L.; Xu, D.; Yang, J.; Yuan, F.; Gao, Y.; Zhao, J. Effects of small and large molecule emulsifiers on the characteristics of β-carotene nanoemulsions prepared by high pressure homogenization. *Food Technol. Biotechnol.* **2009,** 47, 336-342.

[2] Chen, C.; Wagner, G. Vitamin E nanoparticle for beverage applications. *Chem. Eng. Res. Des.* **2004,** 82, 1432-1437.

[3] Wooster, T.J.; Golding, M.; Sanguansri, P. Impact of oil type on nanoemulsion formation and Ostwald ripening stability. *Langmir.* **2008,** 24, 12758-12765.

[4] Wang, X.Y.; Wang, Y.W; Huang, R. Enhancing stability and oral bioavailability of polyphenols using nanoemulsions. In: *Micro/Nanoencapsulation of Active Food Ingredients.* Q. R. Huang, P. Given and M. Qian (Editors). **2009**. ACS Symposium Series 1007. Washington, DC.

[5] Skiff, R.H.; Baaklini, J.; Vlad, F.J. Clear flavor microemulsions comprising sugar esters of fatty acids. Patent application by Firmenich SA. Publication number **WO2007/026271.**

[6] Seikikawa, K.; Watanabe, M. Transparent emulsified composition for use in beverages. Patent application by Givaudan SA. Publication number **WO2008/055374.**

[7] Wang, X.; Jiang, Y.; Wang, Y.; Huang, M.; Ho, C.T.; Huang, Q. Enhancing anti-inflammation activity of curcumin through O/W nanoemulsions. *Food Chem.* **2008,** 108, 419-424.

[8] Liu, W.; Sun, D.; Li, C.; Liu, Q.; Xu, J. Formation and stability of paraffin oil-in-water nano-emulsions prepared by the emulsion inversion point method. *J. Colloid Interface Sci.* **2006,** 303, 557-563.

[9] Shafiq, S.; Shakeel, F.; Talegaonkar, S.; Ali, J.; Baboota, S.; Ahuja, A.; Khar, R.K.; Ali, M. Formulation development and optimization using nanoemulsion technique: a technical note. *Pharm. Sci. Tech.* **2007,** 8, E1-E6.

[10] Shakeel, F.; Baboota, S.; Ahuja, A.; Ali, J.; Shafiq, S. Accelerated stability testing of celecoxib nanoemulsion containing cremophor-EL. *Afr. J. Pharm. Pharacol.* **2008,** 2, 179-183.

[11] Dickinson, E. An introduction to food colloids. Oxford, UK: *Oxford Univ. Press.* **1992.**

[12] McClements, D.J. Food emulsions: principles, practice, and techniques. Boca Raton, FL: *CRC Press.* **2005.** 2nd ed.

[13] McClements, D.J. Emulsion design to improve the delivery of functional lipophilic components. *Annu. Rev. Food Sci. Technol.* **2010,** 1, 241-69.

[14] Solans, C.; Izquierdo, P.; Nolla, J.; Azemar, N.; Garcia-Celma, M. Nano-emulsions. *Curr. Opin. Colloid Interface Sci.* **2005,** 10, 102-110.

[15] Mason, T.; Wilking, J.; Meleson, K.; Chang, C.; Graves, S. Nanoemulsions: formation, structure, and physical properties. *J. Phys.: Condens. Matter*. **2006,** 18, R635-R666.

[16] Tadros, T.; Izquierdo, P.; Esquena, J.; Solans, C. Formation and stability of nano-emulsions. *Adv. Colloid Interface Sci.* **2004,** 108-10, 303-318.

[17] Peter, G.J. Encapsulation of flavors in emulsions for beverages. *Curr. Opin. Colloid Interface Sci.* **2009,** 14, 43-47.

[18] Djordjevic, D., Cercaci, L.,Alamed, J., McClements, D.J., Decker, E.A. Chemical and physical stability of citral and limonene in sodium dodecyl sulfate-chitosan and gum Arabic-stabilized oil-in-water emulsions, *J. Agric. Food Chem.* **2007,** 55, 3585-3591.

[19] Klinkesorn, U., Sophanodora, P., Chinachoti, P., Decker, E.A., Mcclements, D.J. Encapsulation of emulsified tuna oil in two-layered interfacial membranes prepared using electrostatic layer-by-layer deposition, *Food Hydrocolloid*, **2005,** 19, 1044-1053.

[20] Aoki, T., Decker, E.A., Mcclements, D.J. Influence of environmental stresses on stability of O/W emulsions containing droplets stabilized by multilayered membranes produced by a layer-by-layer electrostatic deposition technique, *Food Hydrocolloid,* **2005,** 19, 209-220

[21] Landfester, K.; Tiarks, F.; Hentze, H.; Antonietti, M. Polyaddition inminiemulsions: a new route to polymer dispersions. *Macromol. Chem. Phys.* **2000,** 201, 1-11.
[22] Choi, Y.T.; El-Aasser, M.S.; Sudol, E.D.; Vanderhoff, J.W. Polymerization of styrene miniemulsions. *J. Polym. Sci. A*, **1985,** 23, 2973-81.
[23] Tang, P.L.; Sudol, E.D.; Silebi, C.A.; El-Aasser, M.S. Miniemulsion polymerization-a comparative study of preparative variables. *J. Appl. Polym. Sci.* **1991,** 43, 1059-71.
[24] Moulik, S.P.; Paul, B.K. Structure, dynamics and transport properties of microemulsions. *Adv. Colloid Interface Sci.* **1998,** 78, 99-105.
[25] Flanagan, J.; Singh, H. Microemulsions: a potential delivery systems for bioactives in food. *Crit. Rev. Food Sci. Nutr.* **2006,** 46, 221-237.
[26] Zhang, H.; Feng, F.; Li, J.; Zhan, X.; Wei, H.; Li, H.; Wang, H.; Zheng, X. Formation of food-grade microemulsions with glycerol monolaurate: effects of short-chain alcohols, polyols, salts and nonionic surfactants. *Eur. Food Res. Technol.* **2008,** 226, 613-619.
[27] Garti, N.; Amar, I.; Spernath, A.; Hoffman, R. Transition and loci of solubilization of nutraceuticals in U-type nonionic microemulsions studied by self-diffusion NMR. *Phys. Chem. Chem. Phys.* **2004,** 6, 2968-76.
[28] Fanun, M. Properties of microemulsions with sugar surfactants and peppermint oil. *Colloid Polym. Sci.* **2009,** 287, 899-910.
[29] Whitesides, G.M.; Grzybowski, B. Self-assembly at all scales. *Science.* **2002,** 295, 2418-26.
[30] Moulik, S.; Rakshit, A. Physicochemistry and applications of microemulsions. *J. Surface Sci. Technol.* **2006,** 22, 159-186.
[31] Garti, N.; Aserin, A.; Spernath, A.; Amar, I. Nano-sized self-assembled structured liquids. U.S. Patent **20030232095.**
[32] Shefer, A.; Shefer, S.D. Multi component controlled release system for oral care, food products, nutraceutical, and beverages. U.S. Patent **20030152629.**

[33] Solan, C.; Izuierdo, P.; Nolla, J.; Azemar, N.; Garcia, M.J. Nanoemulsions. Curr. Opin. *Colloid*. *Interface Sci.* **2005,** 10, 102-110.

[34] Sarker, D.K. Engineering of nanoemulsions for drug delivery. *Current Drug Delivery.* **2005,** 2, 297-310.

[35] Gutierrez, J.; Gonzalez, C.; Maestro, A.; Sole, I.; Pey, C.; Nolla, J. Nano-emulsions: new applications and optimization of their preparation. *Curr. Opin. Colloid Interface Sci.* **2008,** 13, 245-251.

[36] Meleson, K.; Graves, S.; Mason, T. Formation of concentrated nanoemulsions by extreme shear. *Soft Materials,* **2004,** 2, 109-123.

[37] Becher, P. Encyclopedia of emulsion technology-basic theory. New York: *Marcel Dekker.* **1983.**

[38] Sjoblom, J. Enclyopedic handbook of emulsion technology. New York: *Marcel Dekker.* **2001.**

[39] Friberg, S. Food emulsions. New York, NY: *Marcel Dekker.* **1997.** 3rd ed.

[40] Hasenhuettl, G.L. Food emulsifiers and their applications. New York: *Springer.* **2008.** 2rd ed.

[41] Taylor, G.I. The formation of emulsions in definable fields of flow. *Proc. R. Soc. A.* **1934,** 146, 501-507.

[42] Rhoney, I.; Brown S.; Hudson, N.E.; Pethrick, A. Influence of processing method on the exfoliation process for organically modified caly systems. I. Polyurethanes. *J. Appl. Poly. Sci.* **2004,** 91, 1335-1343.

[43] Ouzineb, K.; Lord, C.; Lesauze, N.; Graillat, C.; Tanguy, P.A.; McKenna, T. Homogenization devices for the production of miniemulsions. *Chem. Eng. Sci.* **2006,** 61, 2994-3000.

[44] EI-Jaby, U.; Cunningham, M.; McKenna, T. Comparison of emulsification devices for the production of miniemulsions. *Ind. Eng. Chem. Res.* **2009,** 48, 10147-10151.

[45] Richardson, E.S.; Pitt, W.G.; Woodbury, D.J. The role of cavitation in liposome formation. *Biophys. J.* **2007,** 93, 4100-4107.

[46] Abismail, B.; Canselier, J.P.; Wilhelm, A.M.; Delmas, H.; Gourdon, C. Emulsification by ultrasound: droplet size distribution and stability. *Ultrason. Sonochem.* **1999,** 6, 75-83.

[47] Jafari, S.; He, Y.; Bhandari, B. Nano-emulsion production by sonication and microfluidization- a comparison. *Int. J. Food Prop.* **2006,** 9, 475-485.

[48] Jafari, S.; He, Y.; Bhandari, B. Production of sub-micron emulsions by ultrasound and microfluidization techniques. *J. Food Eng.* **2007,** 82, 478-488.

[49] Li, M.; Fogler, H. Acoustic emulsification. Part 1. The instability of the oil –water interface to form the initial droplets. *J. Fluid Mech.* **1978,** 88, 499-511.

[50] Li, M. and Fogler, H. Acoustic emulsification. Part 2. Break-up of the large primary oil droplets in a water medium. *J. Fluid Mech.* **1978,** 88, 513-528.

[51] Kentish, S.; Wooster, T.; Ashokkumar, M.; Balachandran, S.; Mawson, R.; Simons, L. The use of ultrasonics for nanoemulsion preparation. *Innovat. Food Sci. Emerg. Tech.* **2008,** 9, 170-175.

[52] Schultz, S.; Wagner, G.; Urban, K.; Ulrich, J. High-pressure homogenization as a process for emulsion formation. *Chem. Eng. Technol.* **2004,** 27, 361-368.

[53] Tesch, S.; Freudig, B.; Schubert, H. Production of emulsions in high-pressure homogenizers – part I: disruption and stabilization of droplets. *Chem. Eng. Technol.* **2003,** 26, 569-573.

[54] Narsimhan, G.; Goel, P. Drop coalescence during emulsion formation in a high-pressure homogenizer for tetradecane-in-water emulsion stabilized by sodium dodecyl sulfate. *J. Colloid Interface Sci.* **2001,** 238, 420-432.

[55] Relkin, P.; Yung, J.M.; Kalnin, D.; Ollivon, M. Structureal behaviour of lipid droplets in protein-stabilized nano-emulsions and stability of α-tocopherol. *Food Biophys.* **2008,** 3, 163-168.

[56] Cheong, J.N.; Tan, C.P. Palm-based functional lipid nanodispersions: preparation, characterization and stability evaluation. *Eur. J. Lipid Sci. Technol.* **2010,** 112, 557-564.

[57] Mao, L.; Xu, D.; Yang, J.; Yuan, F.; Gao, Y.; Zhao, J. Effects of small and large molecule emulsifiers on the characteristics of β-carotene nanoemulsions prepared by high pressure homogenization. *Food Technol. Biotechnol.* **2009,** 47, 336-342.
[58] Mao, L.; Yang, J.; Xu, D.; Yuan, F. Gao, Y. Effects of homogenization models and emulsifiers on the physicochemical properties of β-carotene nanoemulsions. *J. Disper. Sci. Technol.* **2010,** 31. 986-993.
[59] Yuan, Y.; Gao, Y.; Zhao, J. Mao, L. Characterization and stability evaluation of β-carotene nanoemulsions prepared by high pressure homogenization under various emulsifying conditions. *Food Res. Int.* **2008,** 41, 61-68.
[60] Yuan, Y.; Gao, Y.; Mao, L.; Zhao, J. Optimization of conditions for the preparation of β-carotene nanoemulsions using response surface methodology. *Food Chem.* **2008,** 107, 1300-1306.
[61] Kourniatis, L.R.; Spinelli, L.S.; Piombini, R.; Mansur, R.E. Formation of orange oil-in-water nanoemulsions using nonionic surfactant mixtures by high pressure homogenizer. *Colloid J.* **2010,** 72, 396-402.
[62] Donsi, F.; Wang Y.; Li J.; Huang, Q. Preparation of curcumin sub-micrometer dispersions by high-pressure homogenization. *J. Agric. Food Chem.* **2010,** 58, 2848-2853.
[63] Lamprecht, A.; Ubrich, N.; Perez, M.H. Biodegradable monodispersed nanoparticles prepared by pressure homogenization-emulsification. *Int. J. Pharm.* **1999,** 184, 97-105.
[64] Maa, Y.F.; Hsu, C.C. Performance of sonication and microfludization for liquid-liquid emulsification. *Pharm. Dev. Technol.* **1999,** 4, 233-240.
[65] Thompson, A.K.; Singh, H. Preparation of liposomes from milk fat globule membrane phospholipids using a Microfluidizer. *J. Dairy Sci.* **2006,** 89, 410-419.
[66] Morgan, D.; Hosken, B.; Davis, C. Microfluidised ice-cream emulsions. *Aust. J. Dairy Technol.* **2000,** 55, 93-93.
[67] Dalgleish, D.G.; West, S.J.; Hallett, F.R. The characterization of small emulsion droplets made from milk proteins and triglyceride oil. *Colloid Surface A.* **1997,** 123, 145-153.

[68] Panagiotou, T. Microfludizer processors: technology and applications. Online presentation from www. microfluidicscorp.com.
[69] Jafari, S.M.; He, Y.; Bhandari, B. Optimization of nano-emulsions production by microfluidization. *Eur. Food Res. Technol.* **2007,** 225, 733-741.
[70] Olson, D.W.; White, C.H.; Richter, R.L. Effect of pressure and fat content on particle sizes in microfluidized milk. *J. Dairy Sci.* **2004,** 87, 3217-3223.
[71] Dalgleish, D.G.; Tosh, S.M.; West, S. Beyond homogenization: the formation of very small emulsion droplets during the processing of milk by a microfludizer. *Netherlands Milk Dairy J.* **1996,** 50, 135-148.
[72] Tunick, M.H.; Hekken, D.L.; Cooke, P.H.; Smith, P.W.; Malin, E.L. Effect of high pressure microfluidization on microstructure of mozzarella cheese. *Food Sci. Technol.-LEB.* **2000,** 33, 538-544.
[73] Strawbridge, K.B.; Ray, E.; Hallett, F.R.; Tosh, S.M. Dalgleish, D.G. Measurement of particle size distributions in milk homogenized by a microfluidizer: estimation of populations of particles with radii less than 100 nm. *J. Colloid Interface Sci.* **1995,** 171, 392-398.
[74] Mason, T.; Graves, S.; Wilking, J.; and Lin, M. Extreme emulsification: formation and structure of nanoemulsionss. *Condens. Matter Phys.* **2006,** 9, 193-199.
[75] Hasenhuettle, G.L.; Hartel, R.W. Food emulsifiers and their applications. New York: *Springer,* **2008,** 2nd ed.
[76] Floury, J.; Desrumaux, A.; Axelos, M.; Legrand, J. Effect of high pressure homogenization on methylcellulose as food emulsifier. *J. Food Eng.* **2003,** 58, 227-238.
[77] Danov, K.D.; Kralchevsky, P.A.; Ivanov, I.B. Dynamic processes in surfactant stabilized emulsions. In *Encyclopedic Handbook of Emulsion Technology*. J. Sjoblom. New York: *Marcel Dekker,* **2001.** Ed. pp. 621-659.
[78] Hasenhuettl, G.L.; Hartel, R.W. Food emulsifiers and their applications. New York: *Springer*. **2008.** 2nd Ed.

[79] Vladisavljevic, G.T.; Surh, J.; McClements, J.D. Effect of emulsifier type on droplet disruption in repeated shirasu porous glass membrane homogenization. *Langmuir,* **2006,** 22, 4526-4533.

[80] Narsimhan, G.; Goel, P. Drop coalescence during emulsion formation in a high-pressue homogenizer for tetradecane-in-water emulsion stabilized by sodium dodecyl sulfate. *J. Coll. Interf. Sci.* **2001,** 238, 420-432.

[81] Hakansson, A.; Tragardh, C.; Bergenstahl, B. Studying the effects of adsorption, recoalescence and fragmentation in a high pressure homogenizer using a dynamic simulation model. *Food Hydrocolloid,* **2009,** 23, 1177-1183.

[82] Hakansson, A.; Tragardh, C.; Bergenstahl, B. Dynamic simulation of emulsion formation in a high pressure homogenizer. *Chemical Eng. Sci.* **2009,** 64, 2915-2925.

[83] Walstra, P. Physical chemistry of foods. New York: *Marcel-Dekker,* **2003.**

[84] Meleson, K.; Graves, S.; Mason, T.G. Formation of concentrated nanoemulsions by extreme shear. *Soft Materials.* **2004,** 2, 109-123.

[85] P. Walstra. Disperse system: basic considerations: In: O. H. Fennema, editor. Food Chemistry. New York: CRC Press. **1996,** 3rd ed. pp95-155.

[86] R. Chanamai and D. J. McClements. Impact of weighting agents and sucrose on gravitational separation of beverage emulsions. *J. Agric. Food Chem.* **2000,** 48: 5561-5565.

[87] Dickinson, E.; Golding, M.; Povey, J.W. Creaming and flocculation of oil-in-water emulsions containing sodium caseinate. *J. Colloid and interf. Sci.* **1997,** 185, 515-529.

[88] Robins M.M. Emulsions-creaming phenomena. *Curr. Opin. Colloid Interface Sci.* **2000,** 5, 265-272.

[89] Sagalowicz, L.; Leser, M.E. Delivery systems for liquid food products. *Curr. Opin. Colloid Interface Sci.* **2010,** 15, 61-72.

[90] Tadros, T.; Izquierdo, P.; Esquena, J.; Solans, C. Formation and stability of nano-emulsions. *Adv. Colloid Interface Sci.* **2004,** 108-109, 303-318.

[91] Dickinson, E. Introduction to food colloids. Oxford: *Oxford University Press*, **1992.**

[92] Akoh, C.; Min, D. Food lipids: chemistry, nutrition, and biochemistry. New York: *Marcel Dekker*, **2002,** 2nd Ed.

[93] Tadros, T.F. Applied surfactants: principles and applications. Weinheim: *Wiley-VCH*, **2005.**

[94] Chiesa, M.; Garg, J.; Kang, Y.T.; Chen, G. Thermal conductivity and viscosity of water-in-oil nanoemulsions. *Colloids Surf., A* **2008,** 326, 1-2, 67-72.

[95] Taylor, P. Ostwald ripening in emulsions. *Colloids Surf., A* **1995,** 99, 2-3, 175-185.

[96] Kabalnov, A.S.; Pertzov, A.V.; Shchukin, E.D. Ostwald ripening in emulsions: I. Direct observations of Ostwald ripening in emulsions. *J. Colloid Interface Sci.* **1987,** 118, 2, 590-597.

[97] Weiss J.; Herrmann, N.; McClements, D.J. Ostwald ripening of hydrocarbon emulsion droplets in surfactant solutions. *Langmuir.* **1999,** 15, 6652-57.

[98] Izquierdo, P.; Esquena, J.; Tadros, Th.F.; Dederen, C.; Garcia, M.J. Azemar, N.; Solan, C. Formation and stability of nano-emulsions prepared using the phase inversion temperature method. *Langmuir.* **2002,** 18, 26-30.

[99] Meinders, M.B.; Vliet, T.V. The role of interfacial rheological properties on Ostwald ripening in emulsions. *Adv. Colloid Interface Sci.* **2004,** 108-109, 119-126.

[100] Smet, Y.; Deriemaeker, L.; Finsy, R. Ostwald ripening of alkane emulsions in the presence of surfactant micelles. *Langmuir.* **1999,** 15, 6745-54.

[101] Meinders, M.; Kloek, W.; Vliet, T.V. Effect of surface elasticity on Ostwald ripening in emulsions. *Langmuir.* **2001,** 17, 3923-3929.

[102] Kabainov, A.S.; Makarov, K.N.; Shcherbakova, O.V.; Nesmeyanov, A.N. Solubility of fluorocarbons in water as a key parameter determining fluorocarbon emulsion stability. *J. Fluorine Chem*. **1990,** 50, 271-284.

[103] Taylor, P. Ostwald ripening in emulsions. *Adv Colloid Interface Sci.* **1998,** 75, 107-163.

[104] Capek, I. Degradation of kinetically-stable o/w emulsions. *Adv Colloid Interface Sci.* **2004,** 107, 125-155.

[105] Soma. J. Papadopoulos, K.D. Ostwald ripening in sodium dodecyl sulfate-stabilized decane-in-water emulsion. *J Colloid Interface Sci.* **1996,** 181, 225-231.
[106] Weiss, J. Cancelliere, C.; McClements D.J. Mass transport phenomena in oil-in-water emulsions containing surfactant micelles: Ostwald ripening. *Langmuir.* **2000,** 6833-6838.
[107] Kabalnov, A.S. Can micelles mediate a mass transfer between oil droplets? *Langmuir.* **1994,** 680-684.
[108] Sadtler, V.M.; Imbert, P.; Dellacherie, E. Ostwald ripening of oil-in-water emulsions stabilized by phenoxy-substituted dextrans. *J Colloid Interface Sci.* **2002,** 254, 355-361.
[109] Gregory, J. Particles in water. Boca Raton, FL: *CRC Press.* **2006.**
[110] Xu R. Particle characterization: light scattering methods. New York: *Kluwer Academic Publishers*. **2002.**
[111] Hernandez, E.; Baker, R.A. Turbidity of beverages with citrus oil clouding agent. *JFS.* **1991,** 56, 1024-1026.
[112] Duvoix, A., Blasius, R., Delhalle, S., Schnekenburger, M., Morceau, F.; Henry, E. Chemopreventive and therapeutic effects of curcumin. *Cancer Lett.* **2005,** 223, 181–190.
[113] Huang, M. T.; Lou, Y. R.; Ma, W.; Newmark, H. L.; Reuhl, K. R.; Conney, A. H. Inhibitory effects of dietary curcumin in forestomach, duodenal, and colon carcinogenesis in mice. *Cancer Res.* **1994,** 54, 5841–5847.
[114] Shah, P.; Bhalodia, D.; Shelat, P. Nanoemulsion: A pharmaceutical review. *Sys. Rev. Pharm.* **2010,** 1, 24-32.
[115] Shafiq, S.; Shakeel, F.; Talegaonkar, S.; Ahmad, F.; Khar, R.; Ali, M. Development and bioavailability assessment of ramipril nanoemulsion formulation. *Eur. J. Pharm. Biopharm.* **2007,** 66, 227-243.
[116] Skiff, R.; Baaklini, J.; Vlad, F. Clear flavor microemulsions comprising sugar esters of fatty acids. Patent issued to Firmenich with International Publication Number: **WO 2007/026271 A1.**

[117] Chanamai, R. Microemulsions for use in food and beverage products. Patent issued to Frost Brown Todd LLC with International publication number: **WO 2007/047237 A1.**
[118] Huang, Q.; Yu, H.; Ru, Q. Bioavailability and delivery of nutraceuticals using nanotechnology. *JFS.* **2010,** 75, R50-57.
[119] Weder, H.G.; Mutsch, M. Process for the production of a nanoemulsion of oil particles in an aqueous phase. **1992,** US Pat. 5,152,923.
[120] Jean-Thierry, S.; Sonneville, O.; Legret, S. Nanoemulsion based on oxyethylenated or non-oxyethylenated sorbitan fatty esters, and its uses in the cosmetics, dermatological and/or ophthalmological fields. **2002,** US Pat. 6,335,022.
[121] Baker, J.R.; Hamouda, T. Nanoemulsion vaccines. **2008,** US Pat. 7,314,624.
[122] Baker, J.R.; Hamouda, T.; Shih, A.; Myc, A. Antimicrobial compositions and methods of use. **2010,** US Pat. 7,767,216.
[123] Valdivia, F.; Dachs, A.; Perdiguer, N. Nanoemulsion of the oil water type, useful as an ophthalmic vehicle and process for the preparation therefore. **1997,** US Pat. 5,698,219.
[124] Sonneville, O.; Simonnet, J-T.; Legret, S. Nanoemulsion based on mixed esters of a fatty acid or of a fatty alcohol, of a carboxylic acid and of a glycerol and its uses in the cosmetics, dermatological and/or ophthalmological fields. **2002,** US Pat. 6,419,946.
[125] Monsalve-Gonzalez, A.; Ochomogo, M. Natural flavor enhancement compositions for food emulsions. US Pat. Pub. **20090196972.**
[126] Wooster, T.J.; Andrews, H.F.; Sanguansri, P. Nanoemulsions. US Pat. Pub. **20100305218.**
[127] Halbert, W.G. Method of recovering hydrocarbons with highly aqueous soluble oils using phosphate ester surfactants. **1971,** US Pat. 3,596,715.
[128] Reed, R.L; Healy, R.N.; Stenmark, D.; Gale, W.W. Recovery of oil using microemulsions. **1975,** US Pat. 3,885,628.
[129] Healy, R.N. Oil recovery method using microemulsion. **1976,** US Pat. 3,981,361.
[130] Thir, B.; Dexheimer, E.M. Microemulsions. **1986,** US Pat. 4,568,480.

[131] Wolf, P.A.; Havekotte, M.J. Microemulsions of oil in water and alcohol. **1989,** US Pat. 4,835,002.
[132] Chung, S.L.; Tan, C.T.; Tuhill, I.M.; Scharpf, L.G. Transparent oil-in-water microemulsion flavor concentrate. **1994,** US Pat. 5,320,863.
[133] Chung, S.L.; Tan, C.T.; Tuhill, I.M.; Scharpf, L.G. Transparent oil-in-water microemulsion flavor or fragrance concentrate, process for preparing same, mouthwash or perfume composition containing said transparent microemulsion concentrate, and process for preparing same. **1994,** US Pat. 5,283,056.
[134] Guenin, E.P.; Trotzinka, K.A.; Smith, L.C.; Warren, C.B.; Munteanu, M.A.; Chung, S.L.; Tan, C.T. Alcohol free perfume. **1995,** US Pat. 5,468,725.
[135] Skiff, R.H.; Baaklini, J.; Vlad, F.J. Clear flavor microemulsions comprising sugar esters of fatty acids. Int. Pub. No. **WO2007026271.**
[136] Chanamai, R. Microemulsions for use in food and beverage products. US Pat. Pub. No. **20070087104.**
[137] Garti, N.; Aserin, A.; Spernath, A.; Amar, I. Nano-sized self-assembled liquid dilutable vehicles. **2007,** US Pat. 7,182,950.

Chapter 2

Formation and Characterization of Nanoemulsions Stabilized by Food Biopolymers Using Microfluidization

Nanoemulsions were prepared using four different food grade biopolymers (different concentrations) and high pressure homogenization (Microfluidizer®, different pressures, temperature and number of passes) and then characterized using dynamic light scattering (DLS), cryogenic scanning electron microscopy (Cryo-SEM), and cryogenic transmission electron microscopy (Cryo-TEM). The biopolymers chosen for study were Gum Arabic Spray Dry FCC Powder (GA), chemically modified gum arabic (MGA), whey protein isolate (WPI), and modified starch (Purity Gum 2000, PG). The nanoemulsions used 5% w/w weighted orange oil terpenes (OT) or medium chain triglycerides (MCT) as the dispersed phase. Except for the WPI stabilized nanoemulsion, higher homogenization pressures (up to 22,000 psi) and a greater number of passes (up to 6) through the Microfluidizer produced nanoemulsions with smaller mean droplet diameters (MDD, d_V). PG showed the best performance of the food biopolymers resulting in a MDD of 77.3 nm, while GA produced nanoemulsions with the largest MDD. The MDD of PG stabilized nanoemulsions decreased with increasing PG concentrations (from 5 to 25% w/w). No significant changes in MDD were observed with increasing concentrations of MGA from 5 to 10% w/w or WPI from 2 to 4% w/w.

It was found that increasing number of passes through the Microfluidizer led to a wider particle size distribution due to a tiny tail of large droplets. The effect of oil types on MDD was complex being dependent on the emulsifier, homogenization pressure, and number of passes. The MDD of PG stabilized nanoemulsions increased with homogenization temperature: we hypothesize that this is due to changes in viscosity ratio

between the dispersed and continuous phases (η_d/η_c) when temperature is changed. The smallest MDD of PG stabilized orange oil nanoemulsion was obtained at an optimal η_d/η_c of 0.8.

This study shows that food biopolymers can be used to produce nanoemulsions using microfluidization under high pressure and multiple passes. The results provide an understanding of how manufacturing parameters and formulation influence the formation of nanoemulsions.

2.1 Introduction

Emulsions with droplet size typically in the range 20-100 nm are typically referred to as nanoemulsions (1-3). Nanoemulsions are non-equilibrium systems and cannot form spontaneously (4-5). Consequently, energy input, generally from a mechanical device, is required.

Nanoemulsions have many interesting physical properties that are different from those of larger microscale emulsions. For instance, microscale emulsions exhibit scattering of visible light and have an appearance ranging from bluish to grey (2, 4, 6). By contrast, nanoemulsion particles are much smaller than visible wavelength, so most nanoemulsions appear optically transparent, even at high volume fractions of dispersed phase, Φ. Likewise, nanoemulsions exhibit enhanced shelf stability against gravitationally driven creaming since Brownian motion keeps the droplets suspended homogenously over long time periods (2-3).

Nanoemulsions are getting more attention in recent years in the beverage industry because they have very small droplet sizes, which improves creaming stability and may facilitate flavor release and perception due to a large specific surface area and are transparent, which is desirable for flavored clear beverages, mouthwashes and fortified beverages. However, no successful nanoemulsion-based beverages are on the market primarily because of a lack of functional edible and permissible emulsifiers.

Many of the factors that influence the formation of conventional emulsions also apply to nanoemulsions. These factors include homogenization pressure, volume fraction of dispersed phase, emulsifiers, and emulsifier concentrations (7-10). Emulsifier is one of the most important parameters in determining the ability to form and stabilize a nanoemulsion (11-13). Emulsifiers also vary considerably in cost, ease of utilization, ingredient compatibility, and environmental sensitivity (14-16). There is a growing trend in the food industry to replace synthetic emulsifiers with more natural, label-friendly ones, such as phospholipids, proteins, or polysaccharides. Proteins and phospholipids (e.g. lecithin) are good at producing small droplets but have relatively poor stability to environmental stresses, e.g., pH, salt, and heating (17-20). Polysaccharides on the other hand, provide good stability to environmental stresses but are relatively poor at producing small droplets (21-22). Therefore, it is challenging to use food biopolymers such as proteins and polysaccharides to produce stable nanoemulsions.

This study had three objectives: 1) evaluate the feasibility of manufacturing nanoemulsions using food biopolymers as emulsifiers; and 2) determine the effect of various homogenization pressures and number of passes on nanoemulsion properties.

2.2 Materials and methods

2.2.1 Materials

TIC Gums, Inc. (Belcamp, MD, USA) donated samples of prehydrated gum arabic spray dry FCC powder (GA), and OSAn modified gum arabic (Ticamulsion® A-2010, MGA). OSAn modified starch (Purity Gum 2000, PG) was donated by National Starch Corp. (Bridgewater, NJ, USA). Whey protein isolate (WPI) was provided by Davisco (*Bi*PRO® whey protein isolate, Eden Prairie, MN, USA). Orange oil terpenes were obtained from Citrus and Allied Essences Ltd. (Lake Success, NY, USA) and Miglyol®812, an MCT, was purchased from Sasol (Houston, TX, USA); ester gum was obtained from J.H. Calo Co. (Westbury, NY, USA). Miglyol 812 is a combination of triglycerides based on the following fatty acid composition: $C_{6:0}$ max. 2%, $C_{8:0}$ 50% to 65%, $C_{10:0}$ 30% to 45%, $C_{12:0}$ max. 2% and $C_{14:0}$ max. 1% (Sasol, Houston, TX, USA, data from technical sheet). The orange oil terpenes used were comprised primarily of limonene (95.6%), myrcene (2.8%), sabinene (2.8%), α-pinene (0.9%), and octanal (0.2%) as measured by gas chromatography.

2.2.2 Methods

2.2.2.1 Preparation of nanoemulsions

Solutions of PG, GA, and MGA were prepared in distilled water by mixing for 2 hrs using an overhead mixer (Carter® 1L.81, Carter Motor, IL, USA) at ambient temperature. The WPI was solubilized by mixing with a magnetic stir bar for 2 hrs. A coarse emulsion was prepared by blending 5% w/w oil phase (orange terpenes with ester gum at a 1:1 ratio, or Miglyol oil with ester gum at a 4:1 ratio) and 95% w/w of an aqueous phase

containing WPI, GA, PG, or MGA using a high shear mixer (Greerco Corp., Hudson, NH, USA) at ca. 6,000 rpm for 2 min. The resulting pre-emulsion was passed through a Microfluidizer (Model M-110Y, Microfluidics Corporation, Newton, MA, USA) at different pressures and number of passes. A cooling coil immersed in cold tap water was used to control the temperature of the emulsions exiting from the microfluidizer. Orange terpenes (OT) and Miglyol (MCT) were mixed with ester gum at different ratios to produce nanoemulsions with the same density of dispersed phases. In this chapter OT and MCT nanoemulsions stand for weighted orange oil terpenes and Miglyol nanoemulsions, respectively. All emulsions were prepared in duplicate.

2.2.2.2 Characterization of nanoemulsions

Dynamic Light Scattering (DLS)

Dynamic light scattering (BIC 90Plus, Brookhaven Instrument Corporation, NY, USA) was used to quantitatively determine the mean droplet diameter (MDD) and particle size distribution of the prepared nanoemulsions. It included a photometer equipped with an electrically heated silicon oil bath, Lexel 95-2 Ar+ laser operating at a wavelength of 488 nm, Brookhaven BI-DS photomultiplier, and Brookhaven BI-9000AT correlator. The intensity correlation function was obtained at 25 ℃ and a scattering angle of 90 º. Correlation functions were fit using the REPES model to determine average

particle size and distribution. GENDIST was used for the REPES Algorithm (23). The volume average droplet size (d_V) provided by DLS is defined as

$$d_V = \frac{\sum N_i d_i^4}{\sum N_i d_i^3}$$

Where N_i is the number of particles with a diameter d_i.

Span defines a polydispersity in mass by

$$Span = \frac{d(_{v,90}) - d(_{v,10})}{d(_{v,50})}$$

where $d(_{V,10})$, $d(_{V,50})$, and $d(_{V,90})$ are diameters at which the cumulative mass of the droplets is under 10, 50, and 90%, respectively (23). A monodisperse distribution will have a *span* of 0. A *span* of 1.0 means that 80% of the mass of all the particles lies within $d(_{V,50})$ of the mean diameter, e.g., if $d(_{V,50})$ = 80 nm and the *span* = 1.0, then 80% of the droplets could lie between 50 and 130 nm; if the *span* = 2.0, then 80% of the droplet could be between 50 and 210 nm.

Cryo-Scanning Electron Microscopy (Cryo-SEM)

Cryo-SEM (Philips CM12, Philips, Eindhoven, Netherland) was also used to qualitatively characterize the droplet size of nanoemulsions. Emulsions were diluted to 0.05% w/w dispersed phase with distilled water and then one drop of emulsion was placed on a copper grid, which was quickly transferred to a liquid nitrogen bath for solidification. The copper grid was then transferred to the SEM cold stage using a cryo-

holder. The stage was kept under -170 ℃ and vacuum for 12 min to sublime the surface water from the emulsion samples.

Cryo-Transmission Electron Microscopy (Cryo-TEM)

At high polymer concentrations, it was hard to sublime the surface water from the emulsion samples and polymers aggregated and bridged to form a network after removal of surface water. These issues resulted in low quality Cryo-SEM images making it difficult to observe individual droplets. Therefore, Cryo-TEM (FEI Tecnai G^2 F30, Hillsboro, OR, USA) was also employed to qualitatively characterize nanoemulsions. Emulsions were diluted to 0.05% w/w dispersed phase with distilled water. Samples on a carbon-coated Cu grid were automatically blotted with filter paper, and the resulting thin film was vitrified in liquid ethane by using a Vitrobot. The sample was then transferred to the cryo-TEM (Gatan 626 cryoholder and cryo-transfer system) and imaged at about -170 ℃.

2.2.2.3 Measurement of viscosity

Viscosities of dispersed and continuous phases were measured using a Brookfield rotational rheometer (Brookfield, RVIII model, Stoughton, MA, USA) with cone and plate geometry. A series of standard solutions were used to calibrate the viscometer. In preliminary experimentation, different spindles and spindle ration speeds (6 to 60 rpm)

were tested. LV#61 spindle and speed of 30 rpm were selected for all samples based on the results of preliminary experiments. A water bath was used to control specified temperature of samples. The data were acquired via a personal computer using the software of Brookfield Rheocalc. Two measurements were conducted for each sample and the average was used.

2.3 Results and discussion

2.3.1 Characterization of nanoemulsions

Droplet size and particle size distribution of nanoemulsions were measured by using DLS. Figure 2.1 shows the particle size distribution of a MCT nanoemulsion stabilized by 5% w/w PG produced at 22,000 psi with 3 passes through a Microfluidizer. DLS results showed a mono-modal distribution with a MDD of 182 nm and span of 0.62. Cryo-SEM was used to confirm the MDD and particle size distribution obtained from DLS. Figure 2.2 shows the representative cryo-SEM image of the same nanoemulsion. Some clumps were found in the cryo-SEM image, which might be the free emulsifier (modified starch) or the condensation of droplets due to incomplete sublimation of water during sample preparation. From the image, one would see most droplets are within the size range of 150~200 nm and a few big droplets have a size around 300 nm, which agree with the MDD and particle size distribution from DLS very well. This agreement

supported the use of DLS as an effective and efficient tool to characterize the MDD and particle size distribution of nanoemulsions prepared in this study.

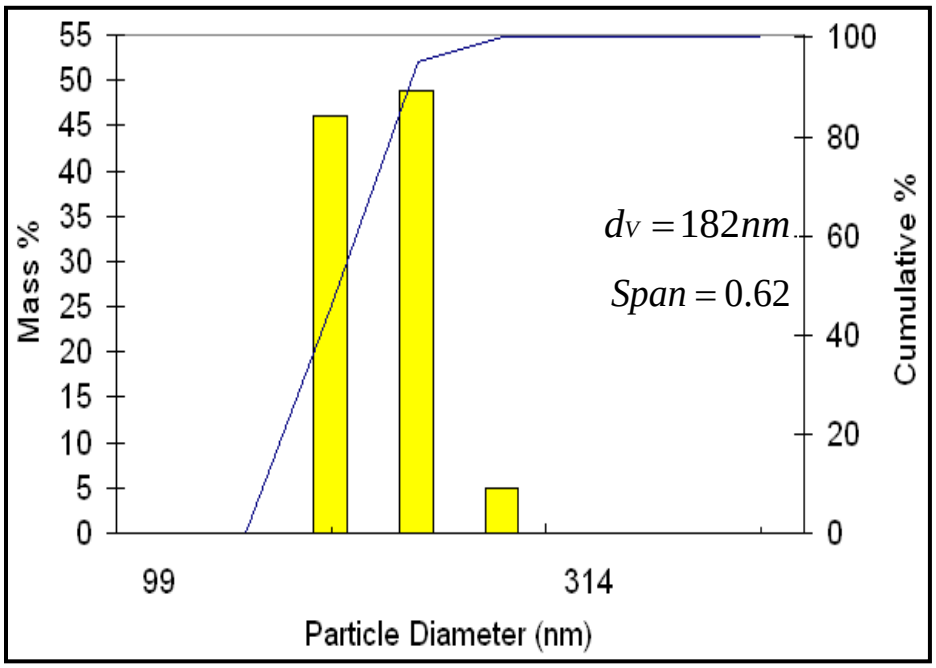

Figure 2.1 Particle size distribution of a 5% w/w PG stabilized nanoemulsions with 5% w/w MCT as dispersed phase homogenized at 22,000 psi 3 passes through microfluidizer.

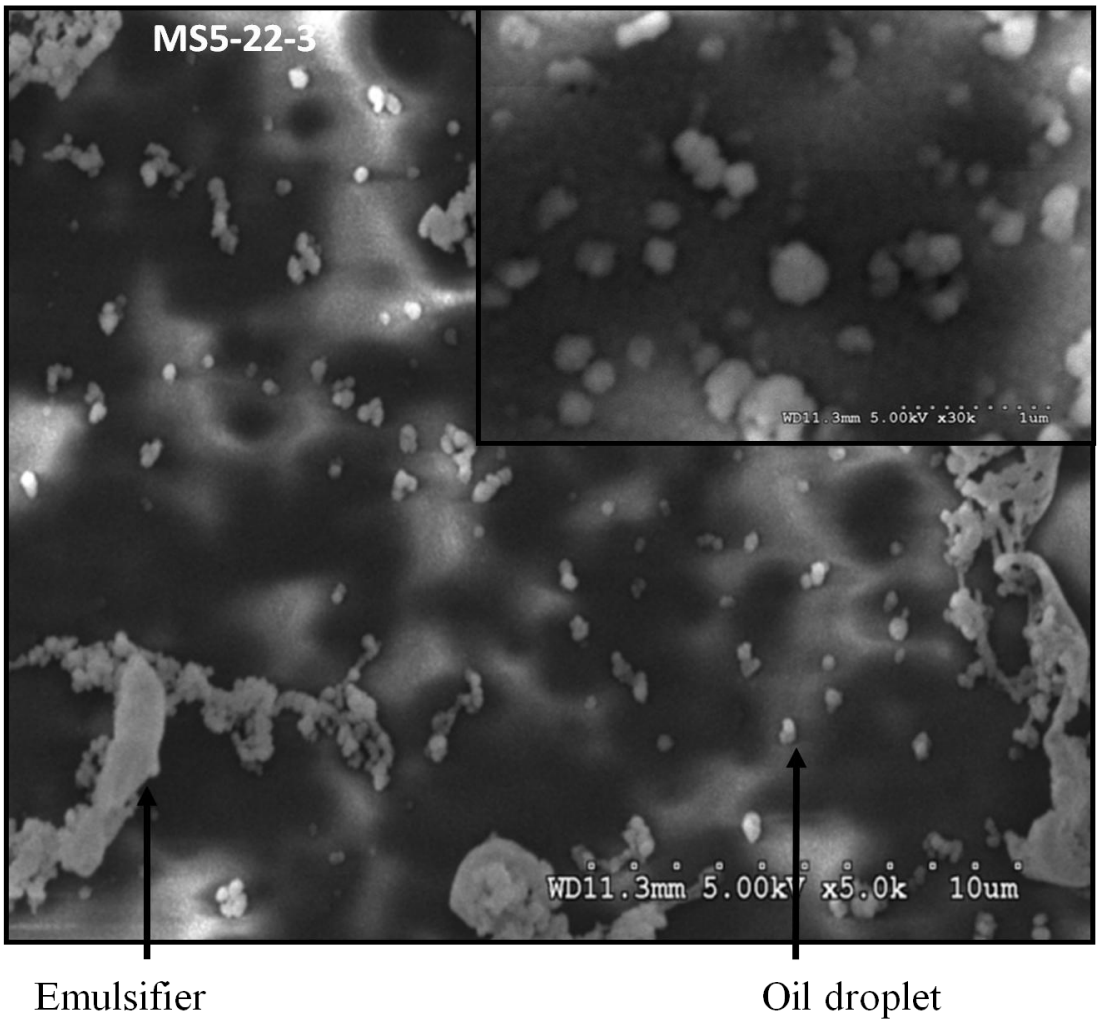

Figure 2.2 Representative cryo-SEM image of 5% w/w PG stabilized nanoemulsions with 5% w/w MCT as dispersed phase homogenized at 22,000 psi 3 passes through microfluidizer.

2.3.2 Effect of homogenization pressure on MDD

In this study, homogenization pressures ranging from 6,000 to 22,000 psi were evaluated to produce nanoemulsions stabilized by different emulsifiers. Figure 2.3 shows

effect of homogenization pressure on the MDD of GA stabilized MCT nanoemulsions. With increasing pressure from 6,000 psi to 14,000 psi, MDD decreased at 1 pass but did not change significantly at 2 and 3 passes. When the pressure was further increased to 22,000 psi, MDD decreased dramatically compared to that at lower pressures. The smallest MDD obtained was *ca.* 350 nm when homogenized at 22,000 psi and passed through the system 3 times: this is still well above the size required to be considered a nanoemulsion. This figure also shows that increasing the number of passes from 1 to 3 did not lead to great reduction in MDDs (17, 10, and 10% reduction at 6,000, 14,000 and 22,000 psi, respectively). These results suggest that GA is not a good emulsifier to produce nanoemulsions when using high pressure homogenization and using multiple passes.

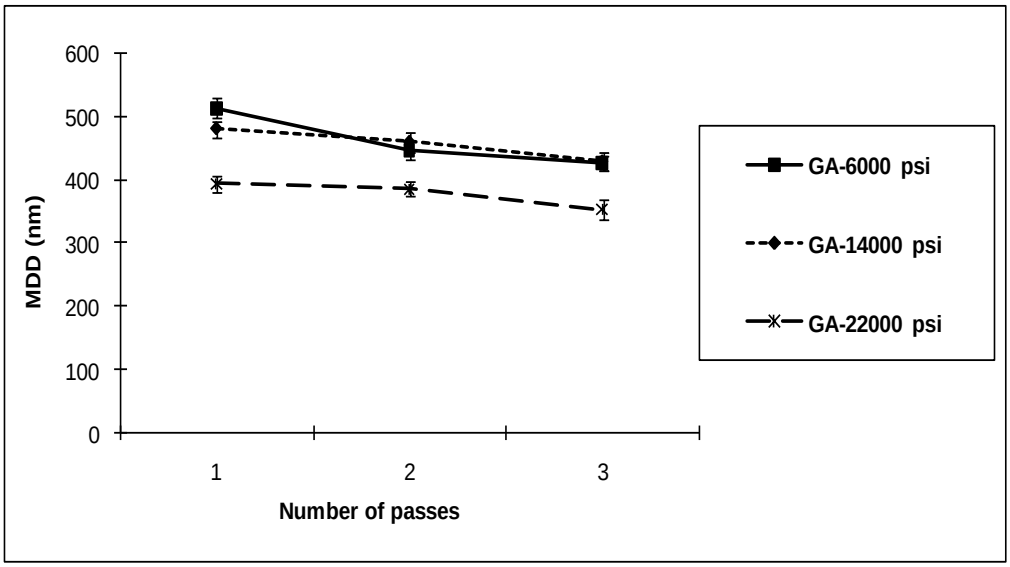

Figure 2.3 Effect of homogenization pressure and multiple passes on MDD of 10% w/w GA stabilized MCT nanoemulsions with 5% w/w dispersed phase.

The failure of producing a GA stabilized nanoemulsion could be attributed to several reasons. First, GA is less surface active than other emulsifiers due to the low proportion of surface active components, namely arabinogalactan protein (24-25). The interfacial tension of GA solutions against oil at saturation coverage is 43 mN/m, which is much higher than that of other surfactants, e.g., 26 mN/m for Tween 20 solution (26-27). According to Taylor's equation more energy input is needed to produce GA stabilized nanoemulsions. Another reason for not achieving the desired particle size is that arabinogalactan protein is a relatively large molecule which exhibits slow adsorption kinetics during homogenization. It was reported that in a 0.5% w/v GA solution, the surface tension decreased from 71 mN/m to 57.4 mN/m after 3 h of adsorption. The rate of surface tension decrease was slow and the induction time was high: the time to get 0.95 of the original surface tension was 3,041 s (28). From this point of view GA is not a good candidate for producing nanoemulsions.

The dramatic decrease in MDD when the homogenization pressure was increased from 14,000 psi to 22,000 psi was unexpected because no significant difference in MDD was found when increasing the pressure from 6,000 to 14,000 psi. There are two likely explanations for this phenomenon. First, high pressure homogenization, e.g., 22,000, changed the structure of the arabinogalactan protein, which favors emulsion formation due to conformational changes which then makes the molecule better able to accumulate at the particle interface. . While we have no direct evidence to support this hypothesis, it is a common phenomenon that high pressure processes may change protein structure and

emulsifying capability (29-31). Second, high pressure homogenization might fragment GA molecules resulting in smaller fractions of molecules and thus have higher adsorption kinetics. Floury et al. (32) reported that high pressure homogenization had an impact on molecular weight (MW) and adsorption kinetics of methylcellulose. The MW of native methylcellulose decreased from *ca.* 300,000 to 80,000 g/mol when homogenized at 300 MPa (1 pass) and the characteristic time of diffusion decreased from 14 to 4 s. Therefore, the smaller MDD of GA stabilized MCT emulsions at 22,000 psi might be attributed to modification of GA structure during homogenization.

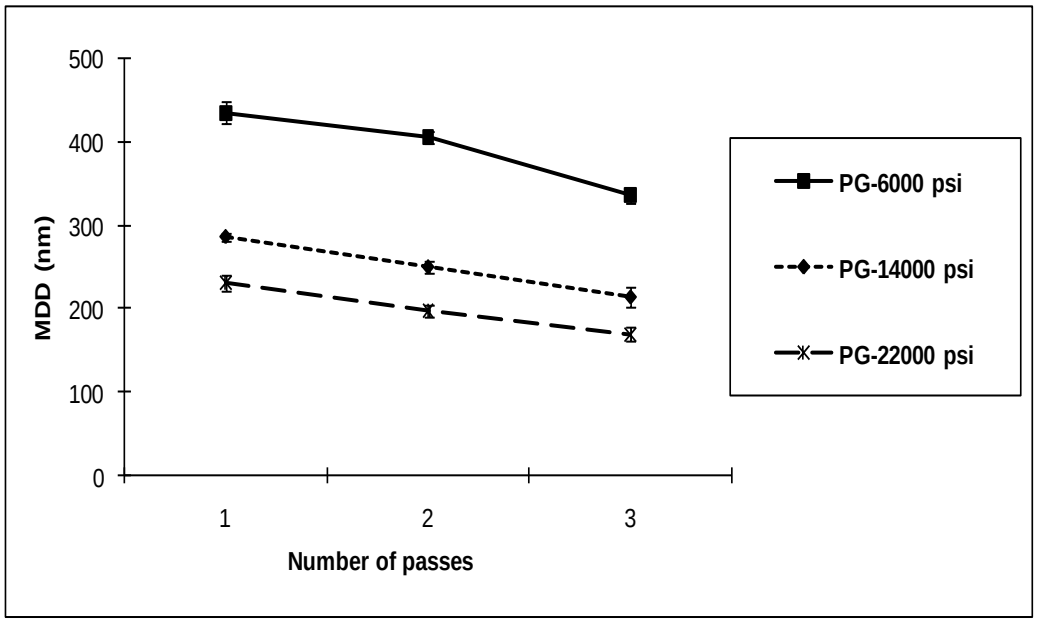

Figure 2.4 Effect of homogenization pressure and number of passes on MDD of 5% w/w PG stabilized MCT nanoemulsions with 5% w/w dispersed phase.

Figure 2.4 shows the effect of homogenization pressure and number of passes through the homogenizer on the MDD of PG stabilized emulsions. Clearly, increasing pressure and number of passes led to a decreasing MDD. The smallest MDD obtained was 169 nm at 22,000 psi (3 passes). PG is a more effective than GA in forming nanoemulsions. This may be because PG has higher adsorption kinetics to the oil/water interface than GA due to the addition of hydrophobic groups on the hydrolyzed starch molecules. Since the pressure limit of the Microfludizer used in this study is 23,000 psi, no higher pressure was examined. However, from the trend shown in figure 2.4, one would expect that the MDD will further decrease at higher pressures (> 22,000 psi) and number of passes (> 3 passes).

Chen et al. (33) reported that modified starch functioned well in producing vitamin E nanoemulsions. In the vitamin E emulsion systems, MDD decreased dramatically when pressured was increased from 2,900 to 43,500 psi. However, another study conducted by Jafari et al. (33) showed that the MDD of *d*-limonene emulsions stabilized by modified starch (Waxy corn starch modified, Hi-Cap) increased from 160 to 215 nm when pressure increased from 3,045 to 12,200 psi by using Microfludization at 1 pass. The inconsistency of results could be attributed to the differences in the modified starch and oil phase used. Modified starches with different hydrophobic groups and degree of substitution have shown variable emulsifying properties in many studies (34-37). The difference in oil phase may also cause the contradictory results, which is discussed in section of 2.3.7 of this thesis.

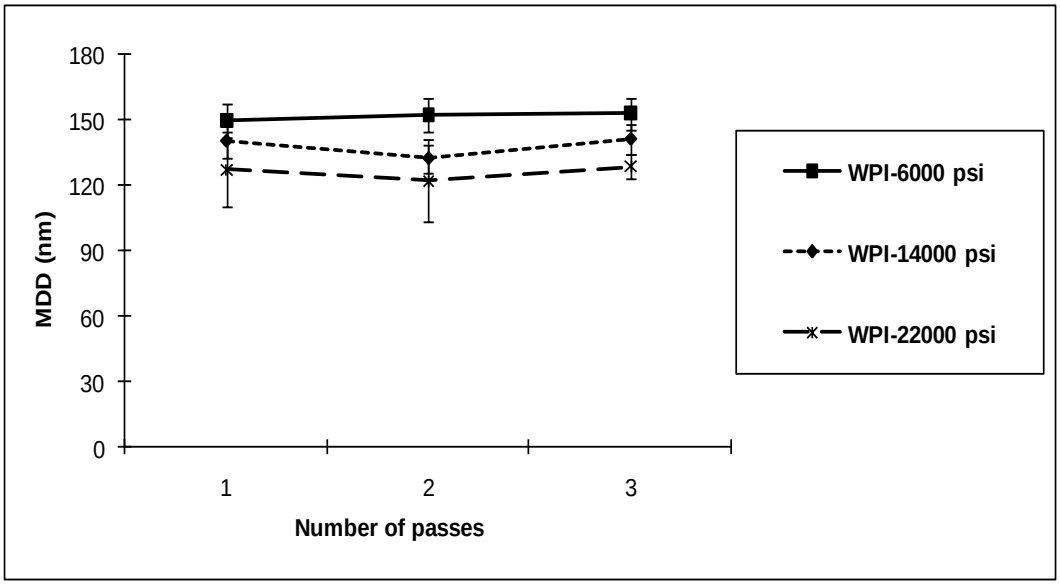

Figure 2.5 Effect of homogenization pressure and number of passes on MDD of 2% w/w WPI stabilized MCT nanoemulsions with 5% w/w dispersed phase.

Figure 2.5 shows the effect of homogenization pressure and number of passes on the MDD of WPI stabilized emulsions: increasing pressure resulted in decreasing MDD. The smallest MDD obtained was 122 nm at 22,000 psi (2 passes). A very complex relationship between pressure and MDD has been reported (38, 39) for emulsions stabilized with whey protein concentrate. Substantial size reduction was observed when the pressure was increased from 7,250 to 13,000 psi. However, when using pressures above 13,000 psi, the MDD of the sunflower oil emulsions increased with further increases in pressure and then stabilized when approaching 29,000 psi. Significant structural changes in protein conformation were observed as the homogenization pressure

was increased as indicated by microdifferential scanning calorimetry scans and polyacrylamide gel electrophoresis (40-43).

In a soy oil emulsion system stabilized with whey protein, it was found that MDD decreased with increasing pressure from 7,250 to 25,000 psi and higher pressures resulted in greater protein-protein interactions at the particle surface. Structural analysis by Fourier transform infrared showed that higher homogenization pressures led to a decrease in α-helix and an increase in β-sheet structures indicating the formation of fewer interactions with the lipid phase and more interactions between adsorbed whey proteins. In the present study, the reduction in MDD with increasing pressure suggests WPI is not "over processed" at 1 pass, but multiple passes may reduce the emulsifying properties as indicated by a slight increase in MDD above 2 passes.

2.3.3 Effect of emulsifiers on the MDD of nanoemulsions

As noted earlier, four food biopolymer emulsifiers were evaluated for their ability to facilitate the formation of nanoemulsions (GA, MGA, PG, and WPI). Comparing these emulsifiers in figure 2.6, one can see that GA is the least effective emulsifier to produce nanoemulsions, while PG shows the best performance (other than sodium docecyl sulfate (SDS) which was used as a reference). This result is quite understandable since the emulsifying properties of GA, MGA, and WPI are largely attributed to proteins and their

efficiency is significantly affected by process conditions, e.g., high pressure and temperature.

While the role of temperature has not been discussed thus far, it should be noted that an increase of 1,000 psi in homogenization pressure has been shown to increase emulsion temperature 2 to 3 ℃ depending on the composition of emulsions (38). It is possible that this increase in temperature plus the extremely high shear associated with homogenization may have a negative effect on protein structure and thus emulsification properties. High pressure homogenization may not be an effective method to produce nanoemulsions stabilized by protein emulsifiers.

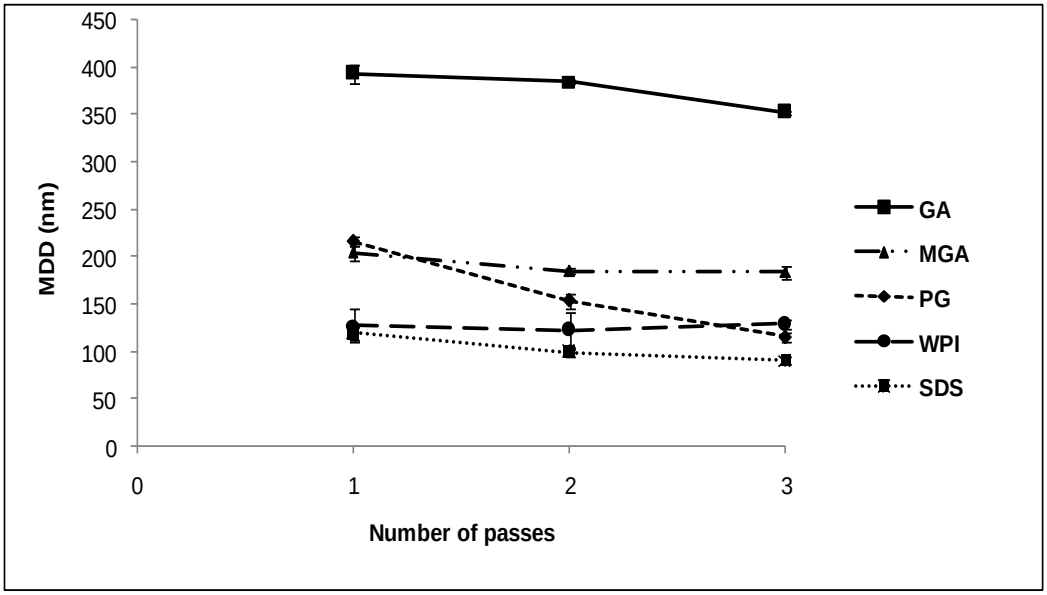

Figure 2.6 Effect of emulsifiers and number of homogenization passes on the MDD of MCT nanoemulsions with 5 wt% dispersed phase produced at 22,000. Concentrations of emulsifiers are GA 10% w/w, MGA 5% w/w, PG 20% w/w, WPI 2% w/w, and SDS 2.5% w/w.

On the contrary, PG and SDS produced nanoemulsions with MDD of ca. 100 nm at 22,000 psi (3 passes). From figure 2.6 one might expect a further reduction in MDD with additional passes through the homogenizer of the PG stabilized nanoemulsions. The high efficiency of PG in producing nanoemulsions is probably due to: 1) smaller molecular weight than MGA and WPI and thus faster adsorption; and 2) surface tension reduction due to modification of the starch hydrolysate with octenyl succinic anhydride. Some general conclusions can be made from this study: polysaccharide-based large molecule emulsifiers (GA and MGA) are not good candidates for producing nanoemulsions; Proteins are good emulsifiers to produce fine emulsions but their capability is limited by the process conditions; and small molecule emulsifiers or surfactants have better performance in producing nanoemulsions when using high pressure homogenization.

2.3.4 Effect of emulsifier concentration on MDD

Since nanoemulsions have an extremely large specific surface area (A_{sp}, surface area per unit of mass), higher concentrations of biopolymers provide better coverage of the interface and further reduces interfacial tension to facilitate droplet rupture during homogenization. Therefore, we evaluated the effects of biopolymer concentration on the MDD of nanoemulsions. Figure 2.7 shows that when WPI concentration was increased from 2 to 4% w/w, MDD decreased slightly but this was not statistically significant due to large variability. Figure 2.8 shows that when MGA was increased from 5 to 10% w/w,

MDD slight decreased but again this was not statistically significant. This confirms that the emulsifying property of WPI and MGA is determined by structure characteristics of the molecules instead of insufficient interfacial coverage of WPI or MGA during homogenization.

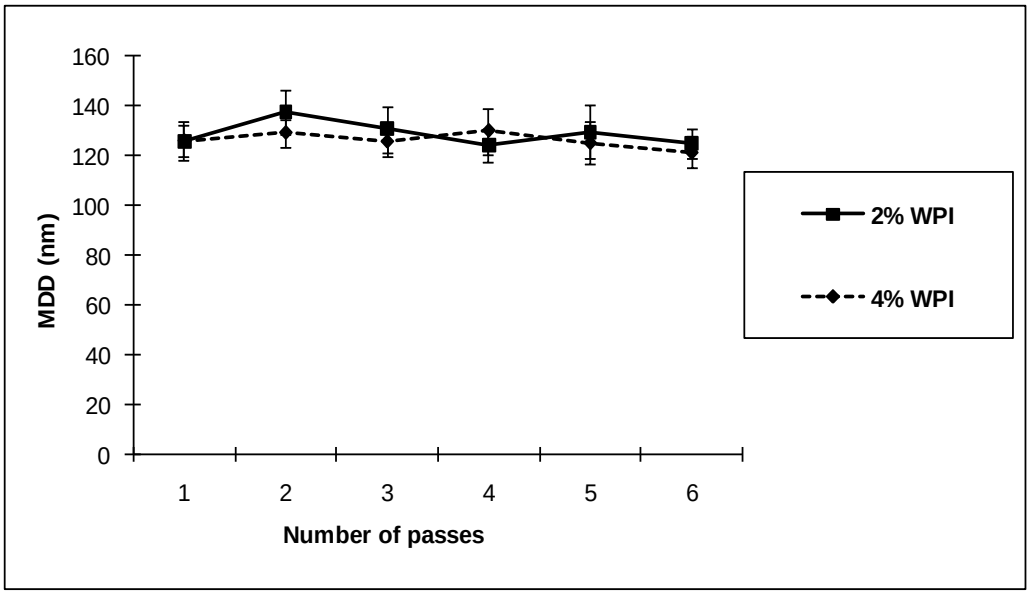

Figure 2.7 Effect of WPI concentration and number of passes on MDD of MCT nanoemulsions with 5% w/w dispersed phase produced at 22,000 psi.

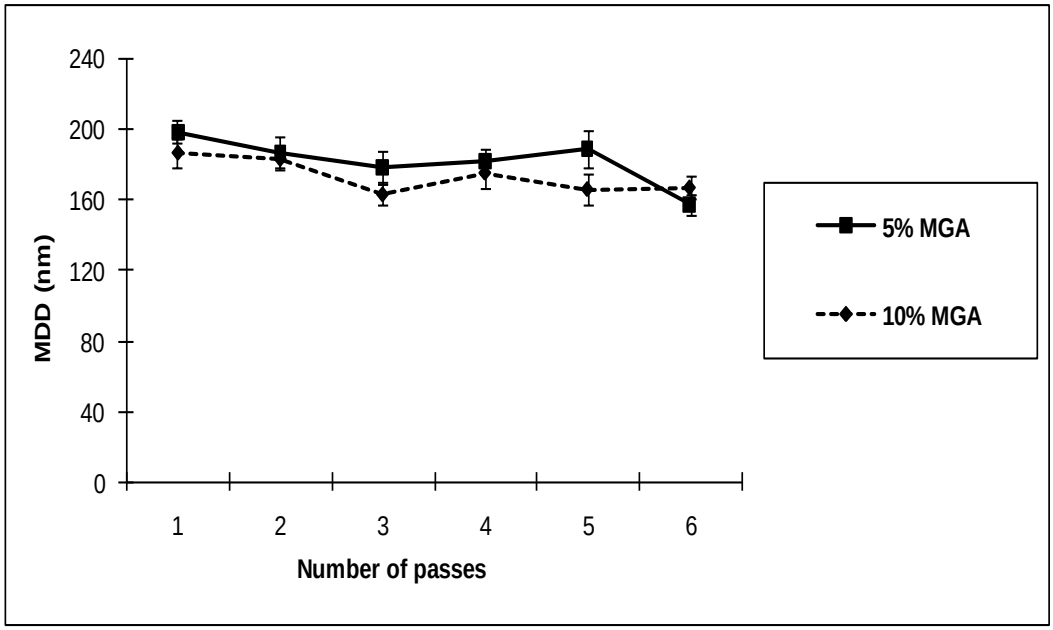

Figure 2.8 Effect of MGA concentration and number of passes on MDD of MCT nanoemulsions with 5% w/w dispersed phase produced at 22,000 psi.

Since PG showed the best performance of the emulsifiers investigated in producing nanoemulsions with small MDD, our focus of additional work was on this biopolymer. A series of PG solutions with a gradient in concentration were used to prepare nanoemulsions. Figure 2.9 shows how PG concentration affected the MDD of nanoemulsions. There is a clear trend in that MDD decreased with increasing PG concentration (from 5 to 20% w/w). No significant difference was found between samples stabilized by 20 and 25% w/w PG. The best performance was a MDD of 77.3 nm: the smallest MMD ever reported by using food biopolymers. It is not a surprise that such a high PG concentration was needed to form a good nanoemulsion. When droplet size decreases from submicron to nanoscale, the specific surface area increases

immensely. The huge interface area of nanoemulsions requires a large amount of polymer to cover and stabilize it. At optimal concentration of PG, the mass ratio of PG to oil phase is 4, which is comparable to 5.3 for vitamin E nanoemulsions stabilized by OSAn modified starch reported by Chen et al. (33).

Another factor contributing to the decrease in MDDs observed with increasing PG concentrations are the changes in phase viscosity. Figure 2.10 shows the changes in viscosities of the continuous phase with increasing concentrations of PG. Viscosity increased 20 times when PG concentration increased from 5 to 25% w/w. Dramatic changes in phase viscosity definitely affect fluid properties of emulsions and thus affect homogenization efficiency (44-46). More details about influence of phase viscosity on formation of nanoemulsions are discussed in section 2.3.8.

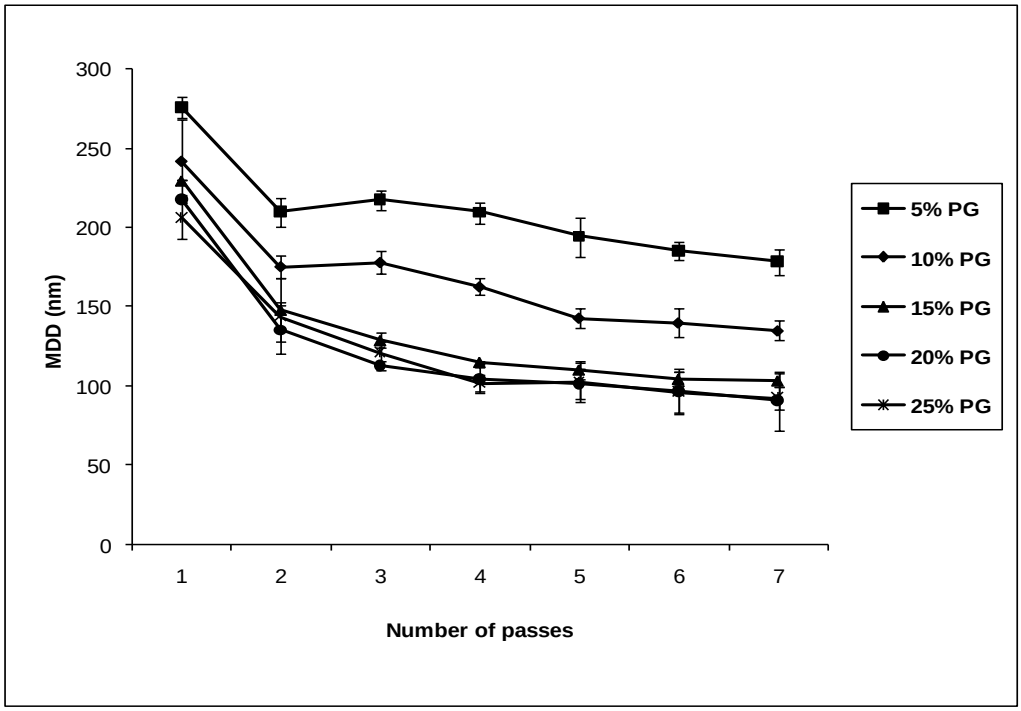

Figure 2.9 Effect of PG concentration and number of passes on MDD of MCT nanoemulsions with 5% w/w dispersed phase produced at 22,000 psi.

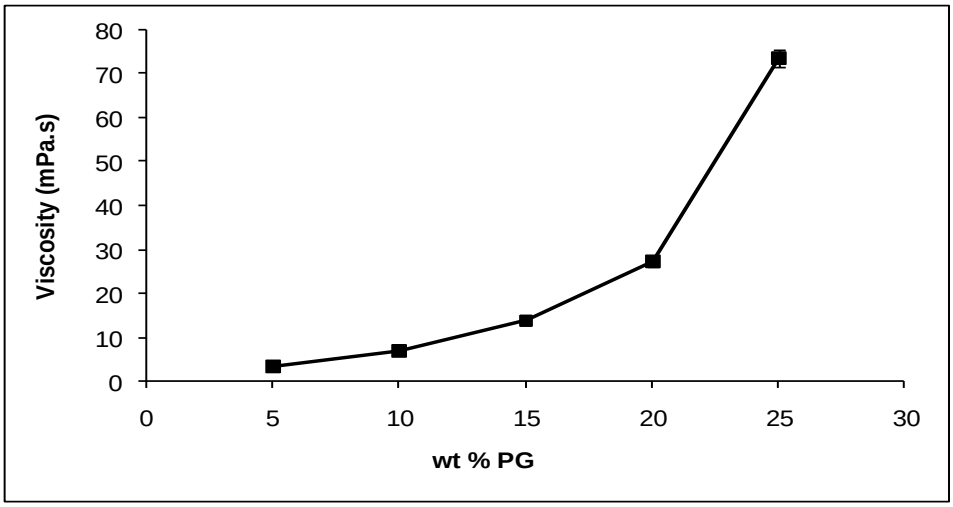

Figure 2.10 Viscosity changes with increasing concentrations of PG at room temperature.

2.3.5 Effect of number of passes on MDD

Within limits, passing an emulsion though a homogenizer additional times generally results in a decrease in MDD. Figure 2.11 shows the effect of number of passes on the MDD of nanoemulsions stabilized by different emulsifiers. Nanoemulsions stabilized by MGA, PG and SDS shows clear trends that a higher number of passes led to smaller MDD. This effect diminishes with an increasing number of passes through a Microfluidizer. Generally with one pass through homogenizer, there is certain probability that not all droplets are subjected to the same intense energy of homogenization; therefore, a portion of the coarse emulsion is not substantially reduced in size. Multiple passes increase the probability of these large droplets being reduced but the benefit of multiple pass diminishes after a certain number of passes depending on the type and conformation of the homogenization valves (47).

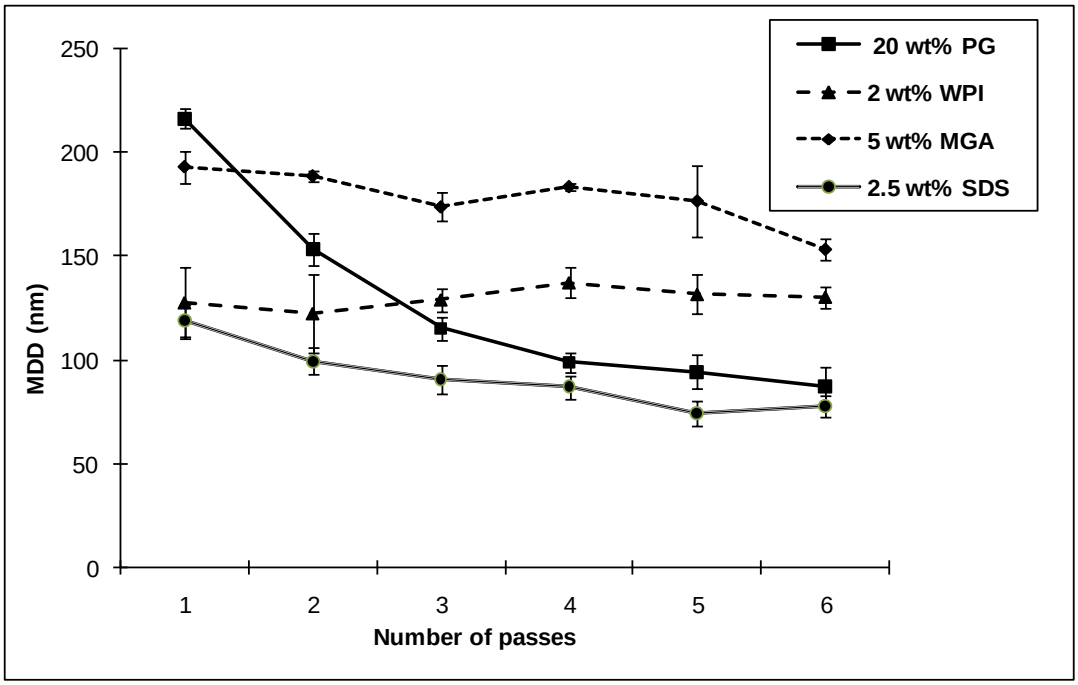

2.11 Effect of number of passes through a microfluidizer on MDD of MCT nanoemulsions with 5% w/w dispersed phase produced at 22,000 psi.

The slight increase in MDD of WPI stabilized nanoemulsions with an increasing number of passes indicates that WPI is over processed causing a loss of emulsifying properties. To the contrary, the reduction of MDD of PG stabilized nanoemulsions with multiple passes demonstrates that PG is unchanged by intense mechanic shear during homogenization. Chen et al. (33) studied effect of homogenization cycles on the MDD of vitamin E nanoemulsions stabilized with modified starch and found that MDD decreased from 210 nm to 110 nm when homogenization cycle increased from 1 to 16 at 8,990 psi. However, in another study Jafari et al. (48) reported that the MDD of modified starch stabilized *d*-limonene emulsions increased with an increasing number of passes at tested

pressures (ranging from 3,045 to 12,180 psi). The contradictory results are probably due to the difference in modified starches and oil phases used.

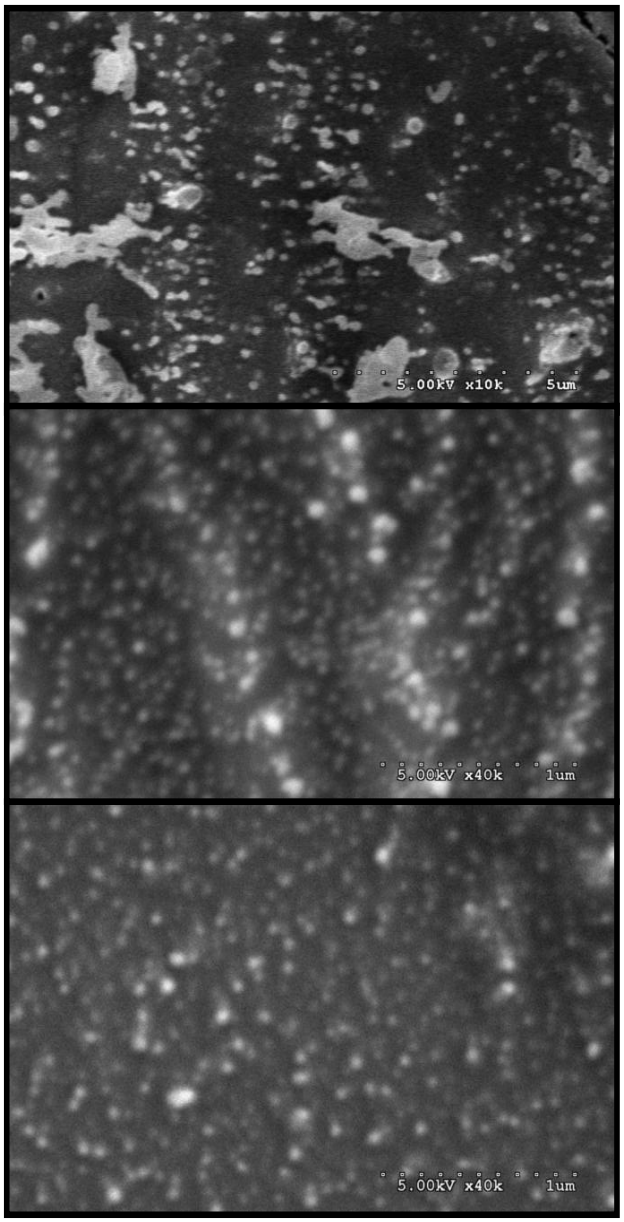

Figure 2.12 Cyro-SEM images of MCT nanoemulsions stabilized by 20% w/w PG with 5% w/w dispersed phase. Top 1 pass, middle 3 passes, and bottom 7 passes.

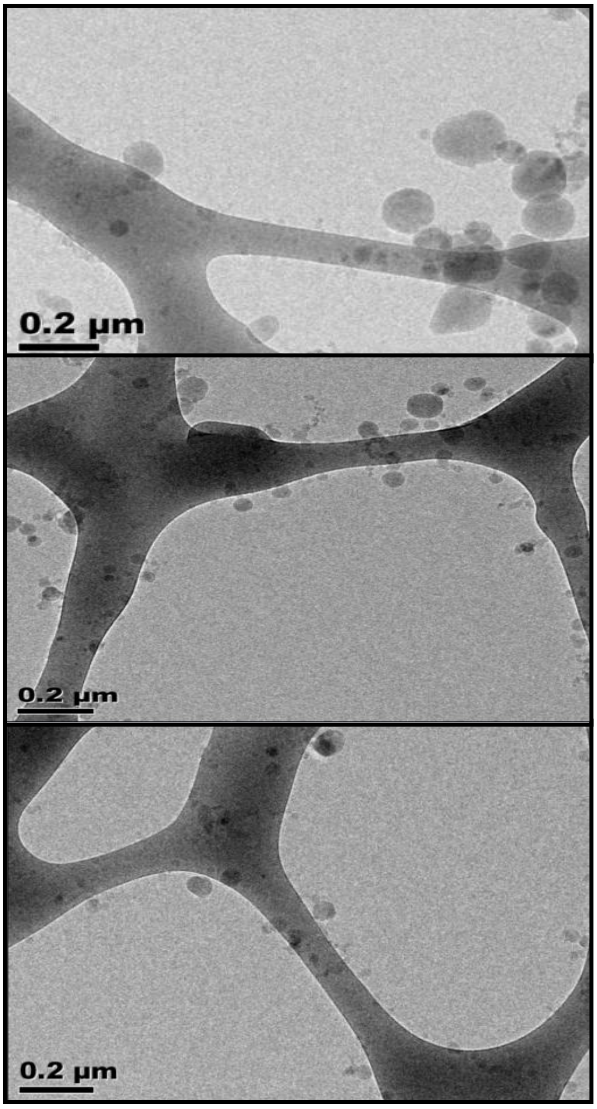

Figure 2.13 Cyro-TEM images of MCT nanoemulsions stabilized by 20% w/w PG with 5% w/w dispersed phase. Top 2 pass, middle 4 passes, and bottom 6 passes.

Figure 2.12 shows cryo-SEM images of PG stabilized MCT nanoemulsions produced by homogenization at 22,000 psi using a different number of passes through the Microfluidizer. The difference in droplet size between 1 pass and 3 passes (notice the

difference in scale) is obvious. The MDD decreased from 253 nm at 1 pass to 92 nm after 7 passes measured by DLS. The images are a little blurry probably due to condensed droplets and free polymer after removal of the water by sublimation and the residual surface water. In order to further confirm the difference in droplet size at different number of passes, cyro-TEM was used to enhance the image quality and resolution.

Figure 2.13 shows the cryo-TEM images of PG stabilized nanoemulsions. The TEM images provided better information on droplet size and size distribution due to its higher resolution and lack of interference from free emulsifier in the continuous phase and surface water. Nanoemulsions prepared by 2 passes contained a larger fraction of large droplets compared to other samples made at 4 and 6 passes. There is no significant visual difference in droplet size between the image at 4 passes and that at 6 passes, which agreed with DLS results that MDD decreased from 98 to 90 nm when the number of passes increased from 4 to 6. Overall the results suggest PG is an ideal candidate for producing nanoemulsions under multiple pass, high pressure homogenization.

2.3.6 Effect of number of passes on particle size distribution

The number of passes through a homogenizer affects not only MDD but particle size distribution. Figure 2.14 shows how droplet size distribution of PG stabilized MCT nanoemulsions changes with an increasing number of passes. MDD decreased from 142 nm at 2 passes to 90 nm at 6 passes and the mass cumulative curves of size distribution

shifted toward smaller size with an increasing number of passes through the Microfluidizer though a tiny fraction of larger particles was also observed.

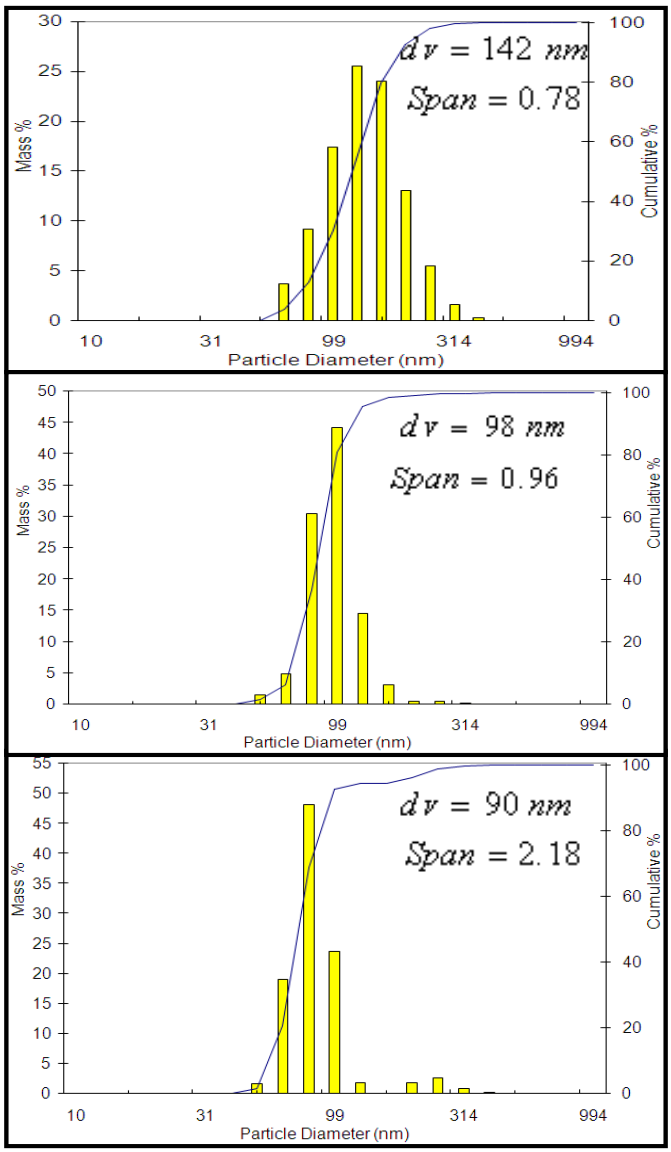

Figure 2.14 Effect of number of passes on size distribution of 20% w/w PG stabilized MCT nanoemulsions with 5% w/w dispersed phase produced at 22,000 psi. Top, middle and bottom are 2, 4, and 6 passes, respectively.

2.3.7 Effect of lipid phase on MDD

In practical applications, the oil phase composition of emulsions may vary greatly. Thus, it is necessary to evaluate the performance of different emulsifiers with different oil phases. Figures 2.15, 2.16, and 2.17 show the effects of two very different types of oil (terpene vs. triglyceride) on the MDD of nanoemulsions stabilized by different emulsifiers (PG, WPI and MGA). Interestingly the three emulsifiers behaved very differently. With PG as emulsifier, at 1 pass the MCT nanoemulsion showed a smaller MDD than the OT nanoemulsions, while with an increase in number of passes, almost no difference in MDD was observed. With WPI as emulsifier, no difference in MDD of MCT and OT nanoemulsions was observed at passes <2, but with an increasing number of passes the OT nanoemulsions showed smaller MDD than the MCT nanoemulsions. With MGA as emulsifier, OT produced nanoemulsions with smaller MDD than MCT regardless of the number of passes. These results suggest that the influence of oil type on MDD is complex depending on both emulsifier and homogenization parameters.

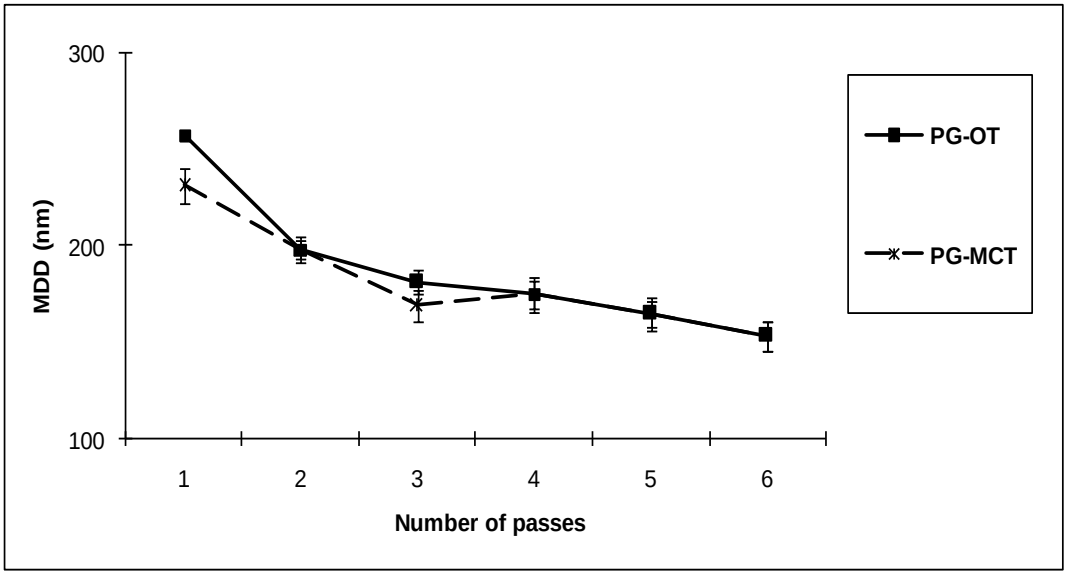

Figure 2.15 Effect of oil phase on MDD of 5% w/w PG stabilized nanoemulsions with 5% w/w dispersed phase produced at 22,000 psi.

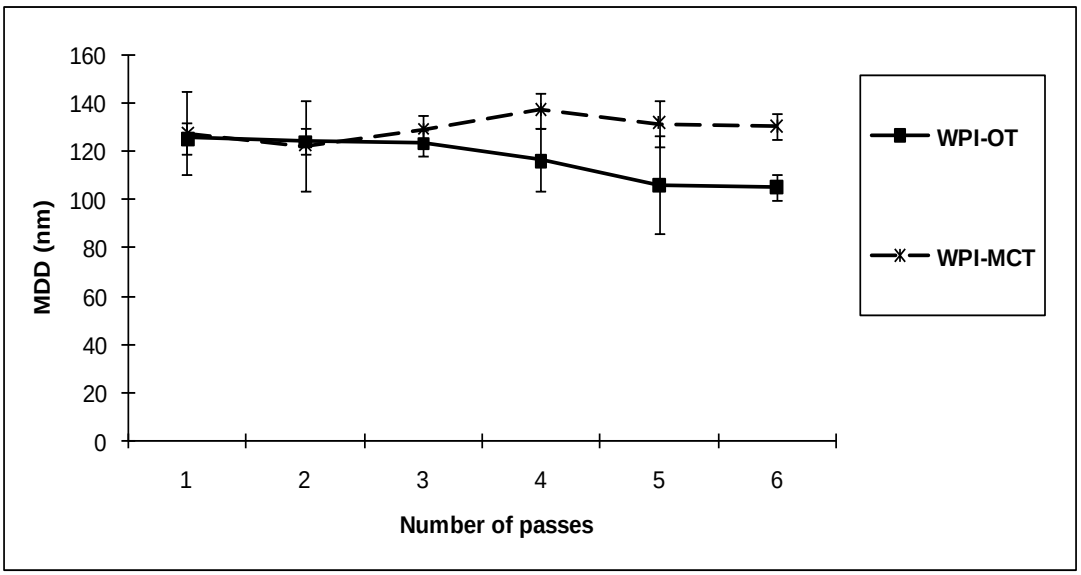

Figure 2.16 Effect of oil phase on MDD of 2% w/w WPI stabilized nanoemulsions with 5% w/w dispersed phase produced at 22,000 psi.

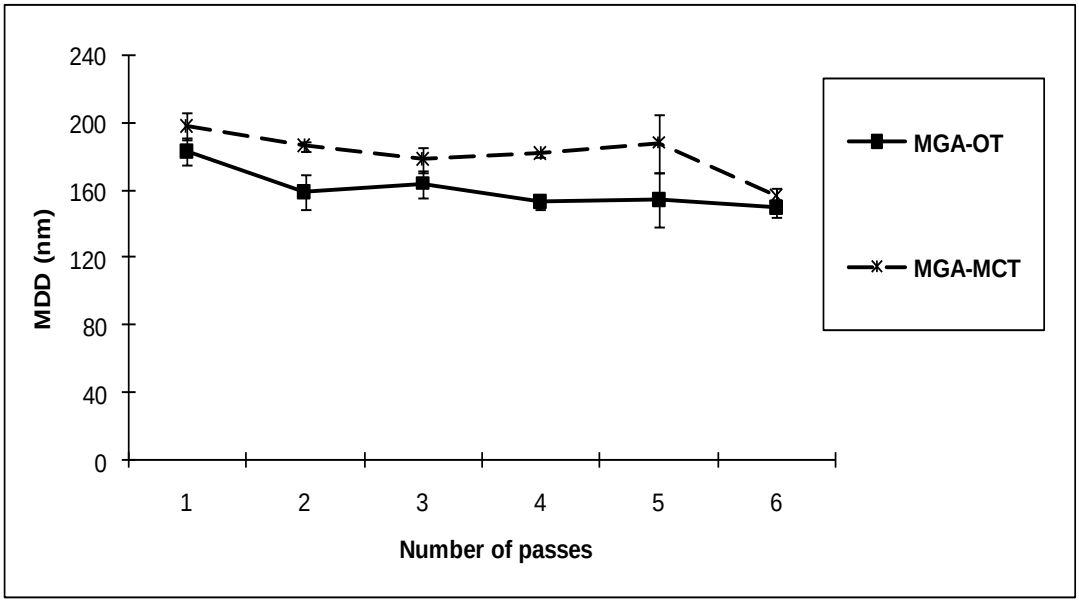

Figure 2.17 Effect of oil phase on MDD of 5% w/w MGA stabilized nanoemulsions with 5% w/w dispersed phase produced at 22,000 psi.

Reiner et al. (11) reported that OT tended to form smaller MDD than MCT in emulsions stabilized by food biopolymer emulsifiers (e.g., modified starches and gum arabic) at 13,000 psi for 1 pass. Reiner explained the results using differences in solubility, polarity and viscosity between OT and MCT. In order to further investigate the reason for the opposite observations in this present study, OT and MCT nanoemulsions stabilized by PG were produced at lower pressures, 6,000 and 14,000 psi and the results are shown in Figure 2.18. Interestingly, at 6,000 psi OT formed much smaller MDD than MCT, while at 14,000 psi no difference in MDD was observed. This clearly demonstrated that effects of oil type on emulsion formation are pressure and number of passes dependent. The literature has shown that interactions of oil phase/emulsifier and

emulsifier/emulsifier strongly influence the efficiency of emulsifiers (40-43). It is quite understandable that these interactions are influenced by homogenization conditions to a different extent depending on the nature of oils and emulsifiers.

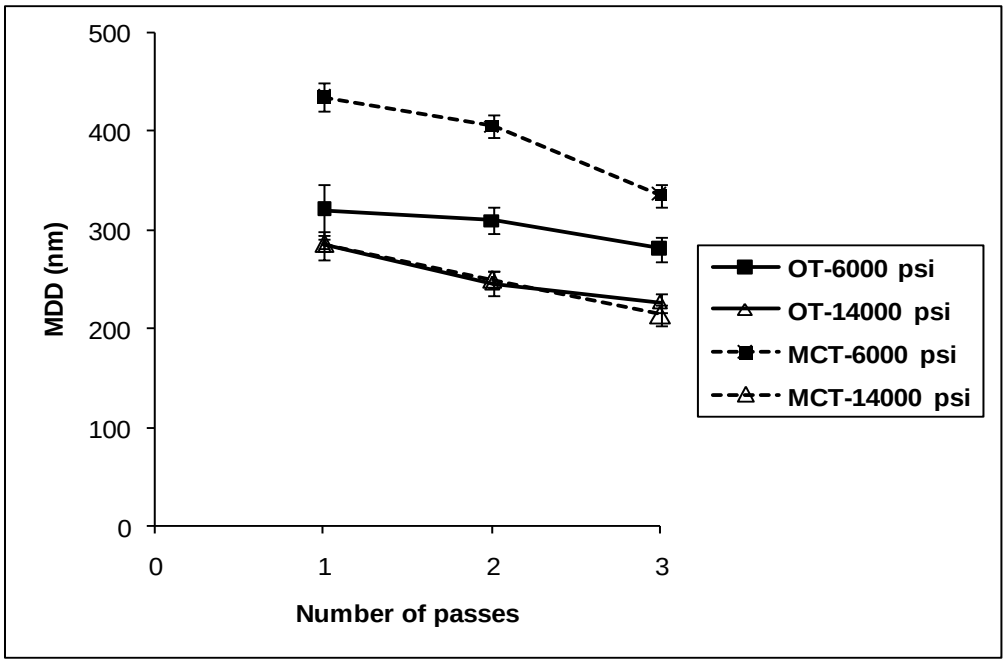

Figure 2.18 Effect of oil phase and pressure on MDD of 5% w/w PG stabilized emulsions with 5% w/w OT or MCT as dispersed phases produced at 6000 and 14000 psi.

2.3.8 Effect of phase viscosity on MDD

Initially we postulated that increasing the temperature would reduce phase viscosities and thereby further facilitate the breakdown of large droplets during homogenization. Therefore, we investigated the effects of homogenization temperature

on MDD of PG stabilized MCT nanoemulsions. Figure 2.19 shows the changes in phase viscosities with temperature. The viscosities of both the continuous and dispersed phases decreased and the ratio of phase viscosity between dispersed and continuous phase (η_d/η_c) also decreased from 1.8 to 1.3 with increasing temperature from 23 to 43 ℃. Considering increase in temperature during homogenization under high pressure, no higher temperatures were tested. The viscosity of MCT decreases more rapidly with increasing temperature than the viscosity of the PG solution, but above a certain temperature, the changes in viscosity with temperature are parallel for both phases.

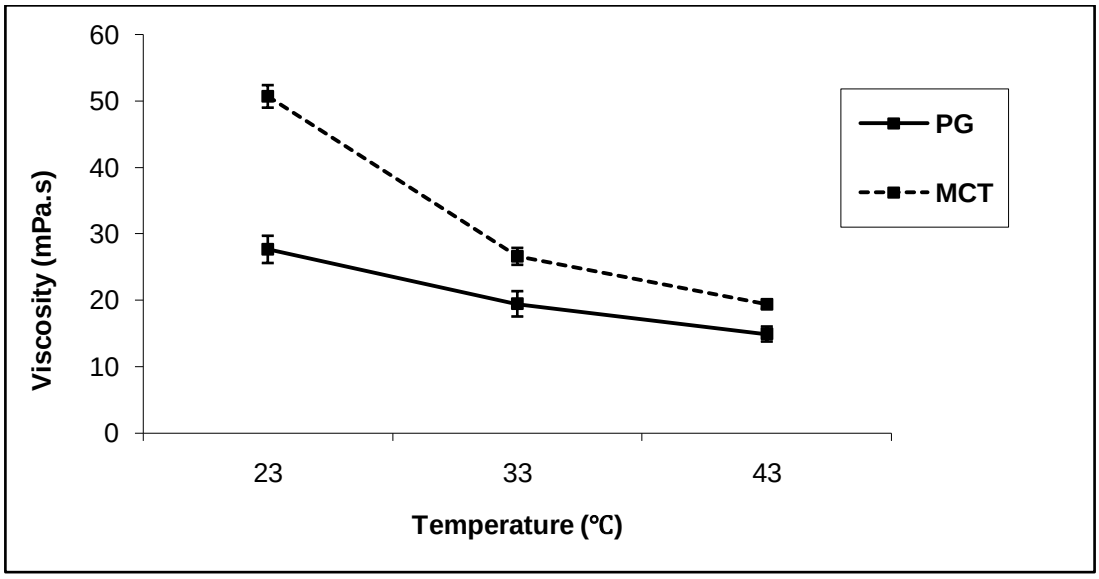

Figure 2.19 Effect of temperature on viscosity of dispersed and continuous phases of MCT nanoemulsions stabilized by 20% w/w PG.

Figure 2.20 shows the changes in MDD with increasing temperature. The results indicated that the MDD of MCT nanoemulsions increased when homogenization

temperature increased from 23 to 33 ℃. No significant changes were found when temperature was changed from 33 to 43 ℃. In order to further confirm our hypothesis, emulsions were produced with varying dispersed phase viscosities by blending orange oil and ester gum at different ratios. The result is shown in Figure 2.21. With increasing the fraction of ester gum in the dispersed phase from 0 to 60% w/w, the viscosity of the dispersed phase increased from 0.85 to 84.6 mPa.s and the ratio of η_d/η_c increased from 0.03 to 3.08. The MDD of the emulsions decreased with an increasing ratio of η_d/η_c. The MDD reached a minimum when 50 wt% ester gum was incorporated in the oil phase and η_d/η_c increased to 0.8. This may suggest that there is an optimal range of η_d/η_c to form nanoemulsions.

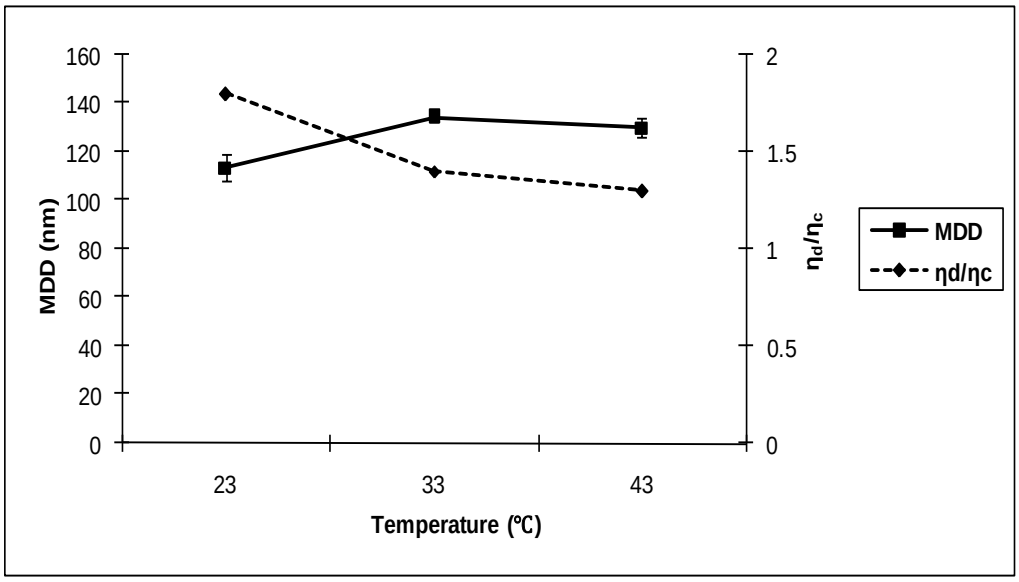

Figure 2.20 Effect of homogenization temperature on MDD of 20% w/w PG stabilized MCT nanoemulsions with 5% w/w dispersed phase produced at 22,000.

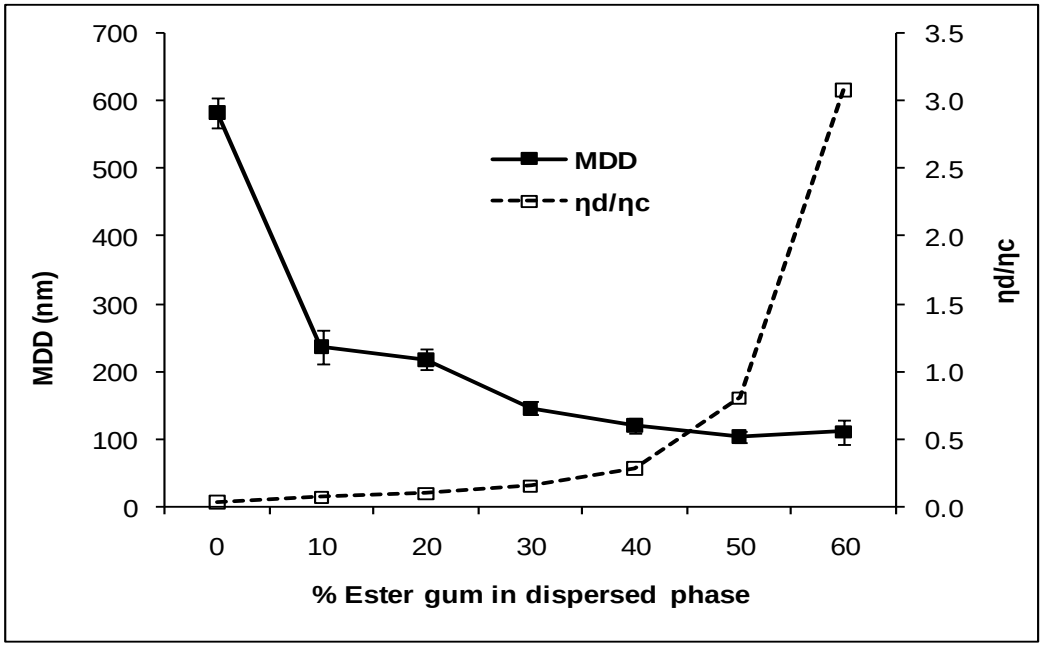

Figure 2.21 Effect of phase viscosity ratio on MDD of 20% w/w PG stabilized emulsions with a blend of orange oil and ester gum as dispersed phase (22,000 psi, 4 passes and room temperature). The viscosity of pure orange oil was obtained from Ref. (49) by Buffo et al.

Experimentation has shown that it is very important to ensure that the ratio of disperse/continuous phase viscosity (η_d/η_c) is in an optimal range to facilitate droplet disruption and form small particles (44-46). It was proposed that when η_d/η_c is too high, droplets are more resistant to disruption as there is insufficient time to deform before the flow field causes the droplets to rotate (44). This phenomenon leads to a better understanding of the role of weighting agents in manufacturing conventional flavor emulsions. Ester gum and brominated vegetable oil serve not only as a weighing agent but also to increase the dispersed phase viscosity thereby yielding emulsions with smaller

MDD. Recently Wooster et al. (50) demonstrated that droplet disruption was most efficient and the droplet size reached a minimum at a η_d/η_c between 0.5 and 5. In this study, the increase in continuous phase viscosity by adding polyethylene glycol (PEG) resulted in smaller droplet size of peanut oil nanoemulsions stabilized by SDS or Tween 80.

The better understanding of the role of phase viscosity ratio on formation of nanoemulsions may help explain why the MDD of PG stabilized MCT nanoemulsions decreased with increasing PG concentrations. Figure 2.22 shows changes in η_d/η_c and MDD of PG stabilized nanoemulsions with increasing concentrations of PG in the continuous phase. The η_d/η_c decreased from 14.5 to 0.69 mPa.s corresponding to 5 and 25 wt% PG, respectively. This decrease in η_d/η_c might enhance homogenization efficiency and thus produce smaller droplets. At the optimal PG concentration (producing the smallest MDD), the η_d/η_c was 1.8, which is within the suggested range in the literature. In the present study, changes in η_d/η_c by either altering the dispersed or continuous phase compositions led to a similar result that optimal homogenization efficiency was achieved when both phases have comparable viscosities, e.g., η_d/η_c within 0.5 ~ 2.0.

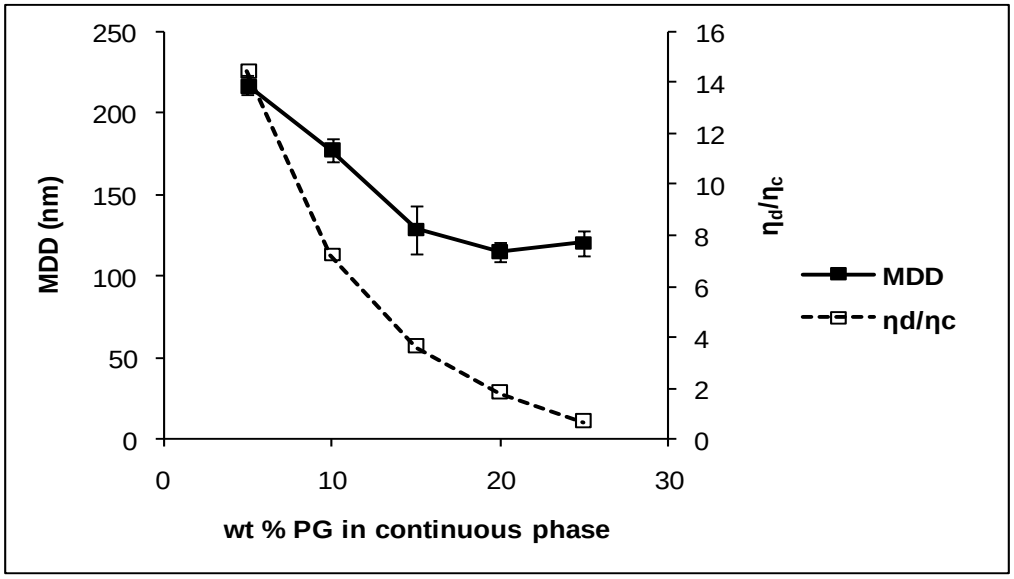

Figure 2.22 Effects of phase viscosity ratio and PG concentration on MDD of PG stabilized MCT nanoemulsions (22,000 psi, 3 passes, and room temperature).

The results of the present study demonstrated that η_d/η_c can be controlled by altering the composition of either the oil or the aqueous phase to improve homogenization efficiency. Alternatively, η_d/η_c can be tailored by controlling homogenization temperature because phase viscosities decrease rapidly with increasing temperature. This finding has the practical significance that the incorporation of viscosity modifying agents in the emulsion phases with optimal η_d/η_c could greatly facilitate the formation of nanoemulsions.

2.4 Conclusions

Overall, nanoemulsions with small MDD were successfully produced by using modified starch and other food biopolymers under multiple passes, high pressure homogenization. MCT nanoemulsions could be manufactured with a MDD as small as 77 nm. Homogenization pressure, number of passes through a microfludizer, lipid phase, emulsifier type and concentration significantly affected the MDD of nanoemulsions. The influence of these factors on MDD was complex and interactions between factors were observed. It was found that viscosity ratio between phases had a great impact on homogenization efficiency and thus the modification of the emulsion formula to produce an optimal η_d/η_c could produce nanoemulsions. This work has provided a practical understanding of the factors influencing the formation of nanoemulsions thereby providing guidance for the formulation and processing of them.

References

[1] Solans, C.; Izquierdo, P.; Nolla, J.; Azemar, N.; Garcia-Celma, M. Nano-emulsions. *Curr. Opin. Colloid Interface Sci.* **2005,** *10,* 102-110.

[2] Mason, T.; Wilking, J.; Meleson, K.; Chang, C.; Graves, S. Nanoemulsions: formation, structure, and physical properties. *J. Phys.: Condens. Matter,* **2006,** *18,* R635-R666.

[3] Tadros, T.; Izquierdo, P.; Esquena, J.; Solans, C. Formation and stability of nano-emulsions. *Adv. Colloid Interface Sci.* **2004,** *108-10,* 303-318.

[4] Gutierrez, J.; Gonzalez, C.; Maestro, A.; Sole, I.; Pey, C.; Nolla, J. Nano-emulsions: new applications and optimization of their preparation. *Curr. Opin. Colloid Interface Sci.* **2008,** *13,* 245-251.

[5] Meleson, K.; Graves, S.; Mason, T. Formation of concentrated nanoemulsions by extreme shear. *Soft Materials,* **2004,** *2,* 109-123.

[6] Wang, L.; Mutch, K.; Eastoe, J.; Heenan, R.; Dong J. Nanoemulsions prepared by a two-step low-energy process. *Langmuir.* **2008,** *24,* 6092-99.

[7] McClements, D.J. Food emulsions: principles, practice, and techniques. Boca Raton, FL: *CRC Press.* **2005.** 2nd ed.

[8] Goulden, J.D.; Phipps, L.W. Factors affecting the fat globule sizes during the homogenization of milk and cream. *J. Dairy Res.* **1964,** 31, 195-200.

[9] Mirhosseini, H.; Tan, C.P.; Hamid, N.; Yusof, S. optimization of the content of Arabic gum, xanthan gum and orange oil affecting turbidity, average particle size, polydispersity index and density in orange beverage emulsion. *Food Hydrocolloid.* **2008,** 22, 1212-1223.

[10] McClements, D.J. Emulsion design to improve the delivery of functional lipophilic components. *Annu. Rev. Food Sci. Technol.* **2010,** 1, 241-69.

[11] Reiner, S.J.; Reineccius G.A.; Peppard, T.L. A comparison of the stability of beverage cloud emulsions formulated with different gum acacia- and starch-based emulsifiers. *JFS.* **2010,** E236-E246.

[12] Mirhosseini, H.; Tan, C.P.; Hamid, N.; Yusof, S.; Chern, B.H. Characterization of the influence of main emulsion components on the physicochemical properties of orange beverage emulsion using response surface methodology. *Food Hydrocolloid.* **2009,** 23, 271-280.

[13] Mirhosseini, H.; Tan, C.P.; Taherian, A.R.; Chern, H. Modeling the physicochemical properties of orange beverage emulsion as function of main emulsion components using response surface methodology. *Carbohyd. Polym.* **2009,** 75, 512-520.

[14] Dickinson, E. Hydrocolloids as emulsifiers and emulsion stabilizers. *Food Hydrocolloid*. **2009,** 23, 1473-1482.

[15] Nakauma, M.; Funami, T.; Noda, S.; Ishihara, S.; AI-Assaf, S.; Nishinari, K.; Phillips, G. Composition of sugar beet pectin, soybean soluble polysaccharide, and gum Arabic as food emulsifiers. 1. Effect of concentration, pH, and salts on the emulsifying properties. *Food Hydrocolloid.* **2008,** 22, 1254-1267.

[16] Guzey, D.; and McClements, D.J. Formation, stability and properties of multilayer emulsions for application in the food industry, *Adv. in Colloid Interface Sci.* **2006.** 128-130, 227-248.

[17] Pallander,S.; Decker, E.A.; McClements D.J. Improvement of stability of oil-in-water emulsions containing caseinate-coated droplets by addition of sodium alginate. *JFS.* **2007,** 72, E518-E524.

[18] Klinkesorn, U., Sophanodora, P., Chinachoti, P., Decker, E.A., and Mcclements, D.J. Encapsulation of emulsified tuna oil in two-layered interfacial membranes prepared using electrostatic layer-by-layer deposition, *Food Hydrocolloid.* **2005,** 19, 1044-1053.

[19] Aoki, T., Decker, E.A., Mcclements, D.J. Influence of environmental stresses on stability of O/W emulsions containing droplets stabilized by multilayered membranes

produced by a layer-by-layer electrostatic deposition technique, *Food Hydrocolloid.* ***2005,*** 19, 209-220.

[20] Surh, J., Yeun, S.G., Decker, E.A., Mcclements, D.J. Influence of Environmental stresses on stability of O/W emulsions containing cationic droplets stabilized by SDS-Fish gelatin membrances, *J. Agric. Food Chem. 2005,* **53**, 4236–4244.

[21] Hasenhuettl, G.L.; Hartel, R.W. Food emulsifiers and their applications. New York: *Springer.* **2008.** 2nd Ed.

[22] Castellani, O.; AI-Assaf, S.; Axelos, M.; Phillips, G.O.; Anton, M. Hydrocolloids with emulsifying capacity. Part 2-Adsorption properties at the n-hexadecane-water interface. *Food Hydrocolloid.* **2010,** 24, 121-130.

[23] Zhu, Z. X.; Anacker, J. L.; Ji, S. X.; Hoye, T. R.; Macosko, C. W.; Prudhomme, R. K. Formation of block copolymer-protected nanoparticles via reactive impingement mixing. *Langmuir* **2007**, *23*, 10499-10506.

[24] Dickinson, E.; Murray, B.; Stainsby, G.; Anderson, D. Surface activity and emulsifying behavior of some Acacia gums. *Food Hydrocolloid.* **1988,** 2, 477-490.

[25] Randall, R.; Williams, P. The role of the proteinaceous component on the emulsifying properties of gum Arabic. *Food Hydrocolloid*, **1988,** 2, 131-140.

[26] Jonsson, B.; Lindman, B.; Holmberg, B. Surfactants and polymers in aqueous solution. Chichester, UK: *John Wiley & Sons*, **1998.**

[27] Walstra, P. Studying food colloids: past, present and future, in Food Colloids, Biopolymers and Materials, Cambridge, UK: *Royal Society of Chemistry,* **2003b.**

[28] Castellani, O.; Guibert, D.; AI-Assaf, S.; Axelos, M; Phillips, G.O.; Anton, M. Hydrocolloids with emulsifying capacity. Part 1- Emulsifying properties and interfacial characteristics of conventional (*Acacia Senegal* (L.) Willd. Var. *senegal*) and matured (Acacia (*sen*) SUPER GUM™) *Acacia senegal*. *Food Hydrocolloid.* **2010,** 24, 193-199.

[29] Mozhaev, W.; Heremans, K.; Frank, J.; Masson, P.; Balny, C. High pressure effects on protein structure and function. *Proteins.* **1996.** 24, 81-91.

[30] Silva, J.L.; Foguel, D.; Royer, C.A. Pressure provides new insights into protein folding, dynamics and structure. *Trends Biochem. Sci.* **2001.** 26, 612-618.
[31] Messens, W.; Camp, J.; Huyghebaert, A. The use of high pressure to modify the functionality of food proteins. *Trends Food Sci. and Technol.* **1997,** 8, 107-112.
[32] Floury, J.; Desrumaux, A.; Axelos, M.; Legrand, J. Effect of high pressure homogenization on methylcellulose as food emulsifier. *J. Food Eng.* **2003,** 58, 227-238.
[33] Chen, C.; Wagner, G. Vitamin E nanoparticle for beverage applications. *Chem. Eng. Res. Des.* **2004,** 82, 1432-1437.
[34] Nilsson, L.; Bergenstahl, B. Emulsification and adsorption properties of hydrophobically modified potato and barley starch. *J. Agri. Food Chem.* **2007,** 55, 1469-1474.
[35] Nilsson, L.; Bergenstahl, B. Adsorption of hydrophobically modified starch at oil/water interfaces during emulsification. *Langmuir,* **2006,** 22, 8770-8776.
[36] Tesch, S.; Gerhards, Ch.; Schubert, H. Stabilization of emulsions by OSA starches. *J. Food Eng.* **2002,** 54, 167-174.
[37] Prochaska, K.; Kedziora, P.; Thanh, J.L.; Lewandowicz, G. Surface activity of commercial food grade modified starches. *Colloids Surf., B.* **2007,** 60, 187-194.
[38] Desrumaux, A.; Marcand, J. Formation of sunflower oil emulsions stabilized by whey proteins with high pressure homogenization (up to 350 MPa): effect of pressure on emulsion characteristics. *Int. J. Food Sci. Technol.* **2002,** 27, 263-269.
[39] Robin, O.; Blanchot, V.; Vuillemard, J.C.; Paquin, P. Microfludization of dairy model emulsions. I. Preparation of emulsions and influence of processing on the size distribution of milk fat globules. *Lait,* **1992,** 72, 511-550.
[40] Lee, S.; Lefevre, T.; Subirade, M.; Paquin, P. Effects of ultra-high pressure homogenization on the properties and structure of interfacial protein layer in whey protein-stabilized emulsion. *Food Chem.* **2009,** 113, 191-195.

[41] Lee, S.; Lefevre, T.; Subirade, M.; Paquin, P. Changes and role of secondary structure of whey protein for the formation of protein membrane at soy oil/water interface under high-pressure homogenization. *J. Agric. Food Chem.* **2007,** 55, 10924-10931.
[42] Hinrichs, J.; Rademacher, B. High pressure thermal denaturation kinetics of whey proteins. *J. Dairy Res.* **2004,** 71, 480-488.
[43] Bouaouina, Hakim, Desrumaux, A.; Loisel, C.; Legrand, J. Functional properties of whey proteins as affected by dynamic high-pressure treatment. *Int. dairy J.* **2006,** 16, 275-284.
[44] McClements, D.J. Food emulsions: principles, practice, and techniques. Boca Raton, FL: *CRC Press.* **2005.** 2nd ed.
[45] P. Walstra. Disperse system: basic considerations: In: O. H. Fennema, editor. Food Chemistry. New York: *CRC Press.* **1996,** 3rd ed. pp95-155.
[46] R. Chanamai and D. J. McClements. Impact of weighting agents and sucrose on gravitational separation of beverage emulsions. *J. Agric. Food Chem.* **2000,** 48: 5561-5565.
[47] Pandolfe, W.D. Processing of emulsions and dispersions by homogenization. In *APV homogenizer handbook*. **2003.**
[48] Jafari, S.M.; He, Y.; Bhandari, B. Optimization of nano-emulsions production by microfluidization. *Eur. Food Res. Technol.* **2007,** 225, 733-741.
[49] Buffo, R.A.; Reineccius, G.A. Modeling the rheology of concentrated beverage emulsions. *J. Food Eng.* **2002,** 51, 267-272.
[50] Wooster, T.J.; Golding, M.; Sanguansri, P. Impact of oil type on nanoemulsion formation and Ostwald ripening stability. *Langmir.* **2008,** 24, 12758-12765.

Chapter 3

Optical Properties and Stability of Nanoemulsions Stabilized by Food Biopolymers

Factors influencing the optical properties and physical stability of nanoemulsions were examined. It was found that interface composition, relative refractive index, volume fraction of dispersed phase and droplet size influenced the turbidity. A polynomial relationship was found between mean droplet diameter (MDD) and turbidity within the MDD range of 80 to 400 nm. The effects of lipid phase and interface composition on turbidity were droplet size dependent. At larger MDD (>150 nm), the lipid phase and interfaces with higher refractive indices imparted higher turbidity to the prepared nanoemulsions. This effect disappeared as the MDD decreased to *ca.* 150 nm. At smaller MDDs (<150 nm), the turbidity of nanoemulsions seems to be independent on lipid phase and particle interface. A linear relationship between volume fraction of dispersed phase and turbidity was established. Experiment results demonstrated that matching refractive indices between phases led to clear emulsions. Finally the primary destabilization mechanism of MCT nanoemulsions emulsified with modified starch was identified as coalescence from a two-week shelf life study.

This study provides an understanding of how the physicochemical properties of nanoemulsions influence their turbidity and stability. The results demonstrated that modified starch stabilized nanoemulsions could provide a transparent appearance at low volume fraction of dispersed phase but that the stability against coalescence has to be improved for potential applications.

3.1 Introduction

Emulsions are widely used in beverage products since one is generally incorporating water-insoluble flavors, colors, and actives into an aqueous beverage. Beverages containing conventional emulsions tend to be cloudy due to significant light scattering. There is a market need for producing emulsion-based beverages that are optically clear (1-5). The flavor and nutraceutical industries have been looking for new technologies (e.g., micelles, nanoemulsions, and microemulsions) to solve this problem (6-9), but this challenge is largely unmet because of the difficulties in formulating such emulsions using edible and legally permissible ingredients. Nanoemulsions would seem to be promising candidates for addressing this problem. Nanoemulsions with oil droplet sizes below 100 nm have the potential to deliver insoluble flavoring materials and yet provide a transparent appearance (9-13). Therefore, the unique optical properties of nanoemulsions have received more attention recently in the flavor and nutraceutical industries.

When droplets are much smaller than the wavelength of the incident light, Reyleigh scattering occurs (14). Rayleigh scattering explains the blue sky when looking away from the sun during the day and the red sky when looking toward the sun. Nanoemulsions appear transparent, yet a bit bluish due to the dominance of low-wavelength light scattered from them. When looking nanoemulsions towards a white

light source, they appear transparent with a reddish tinge since the blue light is scattered away (15).

The optical properties of emulsions are characterized by turbidity which is correlated to the emulsion particle size. The relationship between particle size and turbidity indicates strong oscillatory behavior, particularly at low wavelengths (16-18). The maximum turbidity increases as wavelength decreases. The turbidity at light wavelengths similar to the radius of particles reaches a maximum (15, 19). For nanoemulsions, the dimension of lipid droplets is much smaller than the wavelength of light ($r << \lambda$), causing weak light scattering and hence low turbidity (15).

Most research on nanoemulsions has centered on particle size reduction using small molecule surfactants (20-22) or biological activity in *in-vitro* studies (23, 24): little information is available on the optical properties of real nanoemulsions. The only guidance for the present study is the report by Chen et al. (25) on vitamin E nanoparticles in a clear beverage application. Chen established a linear relationship between the mean droplet diameter (MDD) of vitamin E nanoparticles and turbidity at 62.5 ppm of the dispersed phase. However, the relationship that was established was based on a narrow particle size range (80 ~ 200 nm) and only a few data points were included.

Although turbidity can be predicted through theoretical modeling, the prediction has limits in real emulsion systems because a number of assumptions must be made (14, 16). Hernandez et al. (26) modeled the turbidity of clouding agents in beverages using uniform latex particles at different concentrations and particle sizes ranging from 0.1 to

5.85 μm. The results showed that for a given particle concentration, turbidity increased as wavelength of the scattered light decreased and maximum turbidity was obtained for particle size between 0.2 and 0.3 μm.

In the current study the factors influencing the turbidity of nanoemulsions were studied systematically for the first time. These factors include type of lipid phase, droplet size, interface composition, relative refractive index (particulate to continuous phase), and droplet concentration. The stability of nanoemulsions stabilized by food biopolymers was also evaluated. This study had three objectives: 1) identify the critical factors determining the optical properties of nanoemulsions; 2) establish a quantitative relationship between the droplet size and turbidity of nanoemulsions; and 3) identify destabilization mechanisms of nanoemulsions.

3.2 Materials and methods

3.2.1 Materials

TIC Gums, Inc. (Belcamp, MD, USA) donated samples of prehydrated gum acacia spray dry FCC powder (GA), and OSAn modified gum arabic (Ticamulsion® A-2010, MGA). OSAn modified starch (Purity Gum 2000, PG) was donated by National Starch Corp. (Bridgewater, NJ, USA). Whey protein isolate (WPI) was provided by Davisco (*Bi*PRO® whey protein isolate, Eden Prairie, MN, USA). Orange oil terpenes and cold

pressed Valencia orange oil were obtained from Citrus and Allied Essences Ltd. (Lake Success, NY, USA) and Miglyol®812, an MCT, was purchased from Sasol (Houston, TX, USA); ester gum was obtained from J.H. Calo Co. (Westbury, NY, USA). Miglyol 812 is a combination of triglycerides based on the following fatty acid composition: $C_{6:0}$ max. 2%; $C_{8:0}$ 50% to 65%; $C_{10:0}$ 30% to 45%; $C_{12:0}$ max. 2% and $C_{14:0}$ max. 1% (Sasol, Houston, TX, USA, data from technical sheet). The orange terpenes used were comprised primarily of limonene (95.6%); myrcene (2.8%); sabinene (2.8%); α-pinene (0.9%); and octanal (0.2%) as measured by gas chromatography. Citric acid, sodium citrate, sodium benzoate and sodium dodecyl sulfate (SDS) were purchased from Sigma Chemical Co. (St. Louis, MO, USA).

3.2.2 Methods

3.2.2.1 Preparation of nanoemulsions

Solutions of PG, GA, and MGA were prepared in distilled water by mixing for 2 hrs using an overhead mixer (Carter® 1L.81, Carter Motor, IL, USA) at ambient temperature. The WPI and SDS were solubilized by mixing with a magnetic stir bar for 2 hrs. A coarse emulsion was prepared by blending 5% w/w oil phase (orange terpenes with ester gum at a 1:1 ratio, or Miglyol oil with ester gum at a 4:1 ratio) and 95% w/w of an aqueous phase containing WPI, GA, PG, or MGA using a high shear mixer (Greerco

Corp., Hudson, NH, USA) at ca. 6,000 rpm for 2 min. The resulting pre-emulsion was passed through a microfluidizer (Model M-110Y, Microfluidics Corporation, Newton, MA, USA) at different pressures and number of passes. A cooling coil immersed in cold tap water was used to control the temperature of the emulsions exiting from the microfluidizer. Orange terpenes (OT) and Miglyol (MCT) were mixed with ester gum at different ratios to produce nanoemulsions with the same density of dispersed phases. In this chapter OT and MCT nanoemulsions stand for weighted orange oil terpenes and Miglyol nanoemulsions, respectively. All emulsions were prepared in duplicate.

3.2.2.2 Measurement of refractive index

Refractive indices of dispersed phase were measured at 589 nm using an Abbe refractometer (Carl Zeiss, Jena, Germnay) at room temperature. Distilled water was used as a standard assuming it had a refractive index of 1.333.

3.2.2.3 Measurement of droplet size of nanoemulsions

Dynamic light scattering (BIC 90Plus, Brookhaven Instrument Corporation, NY, USA) was used to quantitatively determine the mean droplet diameter (MDD) and particle size distribution of the prepared nanoemulsions. It included a photometer equipped with an electrically heated silicon oil bath, Lexel 95-2 Ar+ laser operating at a

wavelength of 488 nm, Brookhaven BI-DS photomultiplier, and Brookhaven BI-9000AT correlator. The intensity correlation function was obtained at 25 ℃ and a scattering angle of 90 º. Correlation functions were fit using the REPES model to determine average particle sizes and distribution. GENDIST was used for the REPES Algorithm (23). The volume average droplet size (d_V) provided by DLS is defined as

$$d_V = \frac{\sum N_i d_i^4}{\sum N_i d_i^3}$$

Where N_i is the number of particles with a diameter d_i. The polydispersity index (PDI) is defined as below to describe the size distribution of emulsions (28)

$$PDI = \frac{(D^2 - D^{*2})}{q^4 \Gamma^2}$$

Where D is diffusion coefficient, D^* is the average diffusion coefficient of droplet, q is the amplitude of scattering vector, and Γ is decay rate. Generally, PDI < 0.08 indicates nearly monodisperse samples, 0.08 < PDI < 0.3 indicate a narrow size distribution, and PDI > 0.3 means broad size distribution (29).

3.2.2.4 Measurement of ζ-potential

The electrical charge on the oil droplets in the emulsions was determined using a particle electrophoresis instrument (ZetaPALS, Brookhaven Instruments, Holtsville, NY, USA). The ζ-potential is determined by measuring the velocity of the droplet when in an

applied electrical field. Emulsions were diluted in a 10 mM, pH 3.6 citric buffer and then placed in a standard four-sided, 1 cm polystyrene cuvette. A parallel plate electrode (0.45 cm^2 square platinum plates with a 0.4 cm gap) was inserted and the cuvette was placed in a temperature-controlled holder at 25 ℃. Each measurement was set as 90 seconds with 4 replicates. The ζ-potential was calculated from the electrophoretic mobility using the Smoulokowski model.

3.2.2.5 Measurement of turbidity

A Turbidimeter (Hach 2100AN, Geotech Environmental Equipment, Denver, CO) with a range of 0-8000 NTU (Nephelometric Turbidity Units) was used to determine the turbidity of the nanoemulsions prepared in this study. The turbidimeter consists of a color filter module for 455 nm wavelength and a 90 ℃ angle detector. The turbidimeter was calibrated using a series of turbidity standards ranging from 0 to 2,000 NTU. All prepared emulsions were diluted to 0.05% w/w dispersed phase for turbidity measurement. Two measurements were taken for each sample.

3.2.2.6 Shelf life study

According to the methods described in section 3.2.2.1, MCT nanoemulsions stabilized by 20% w/w PG or 2.5% w/w SDS were prepared using 22,000 psi (3 passes).

The continuous phase was prepared using pH 3.6, 10 mM citric buffer instead of distilled water. Prepared nanoemulsions were stored at room temperature until droplet size and turbidity measurements were made. Both emulsions were prepared in duplicate.

3.3 Results and discussion

3.3.1 Effect of lipid phase on turbidity

Since the ratio of refractive indices (RI) between the emulsion phases is a main parameter related to the intensity of light scattering, it was of interest to investigate how this parameter influences nanoemulsion turbidity. Figure 3.1 shows the relationship between the MDD and turbidity of nanoemulsions based on OT or MCT as the dispersed phase. Although the same trend is evident, i.e. turbidity increased with MDD, the two types of nanoemulsions demonstrated very different patterns of light scattering with the changes in MDD. When the MDD was large (> 150 nm), the turbidity difference between MCT and OT nanoemulsions increased with MDD. However, when droplets were on a nano-scale (<150 nm), MCT and OT nanoemulsions showed almost the same turbidity. The refractive indices of weighted OT and MCT were measured as 1.5045 and 1.4619, respectively. The higher turbidity of the OT emulsions is attributed to its higher RI.

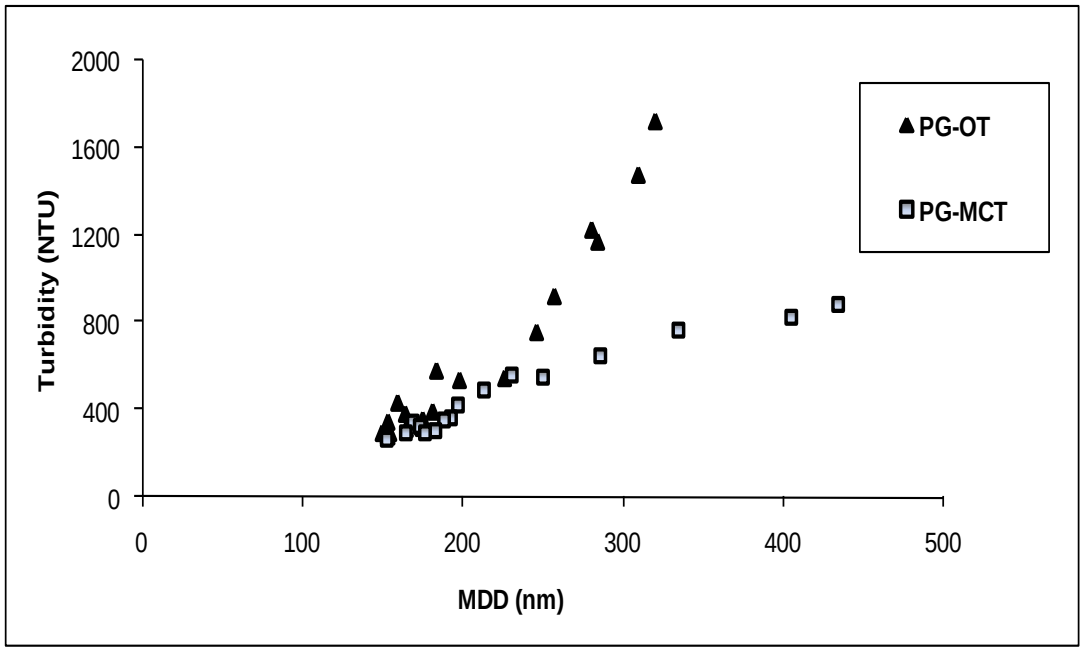

Figure 3.1 Relationship between MDD and turbidity of 5% w/w PG stabilized emulsions with OT or MCT as the dispersed phase. Emulsions were produced using different pressures (6,000 to 22,000 psi) and a different number of passes through the microfluidizer).

It should be noted that influence of size distribution was ignored in this experiment because of the difficulty of incorporating particle size distribution data for real emulsion systems. Figure 3.2 shows particle size distribution of OT and MCT emulsions expressed as polydispersity index (PDI). All PDIs are smaller than 0.2 which means they have narrow size distributions. Moreover, the PDIs of OT and MCT emulsions were not related to the dispersed phase but the manufacturing parameters and thus, the PDIs varied similarly across the two materials. This result rules out the possibility that difference in

size distribution caused the difference in turbidity of OT and MCT emulsions shown in Figure 3.1.

The effect of particulate phase RI on turbidity can be explained by Rayleigh and Mie scattering theories (16, 18). Small droplets (i.e., below 100 nm) follow Rayleigh scattering and thus the relative refractive index of the dispersed phase to continuous phase has a small impact on light scattering intensity (16). Whereas large droplets (i.e., from 100 nm to several microns) follow Mie scattering and the light scattering intensity is largely dependent on the relative RI.

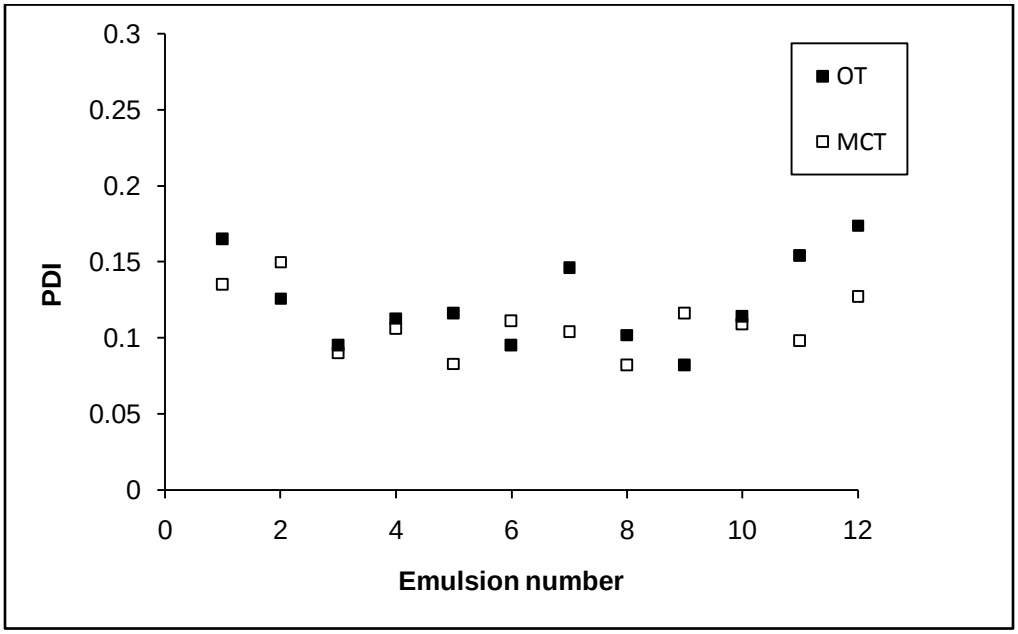

Figure 3.2 PDI of 5% w/w PG stabilized emulsions produced at different pressures (6,000 to 22,000 psi and different numbers of passes through the microfluidizer). The data are presented such that each comparison (emulsion number) is between particulate phase types using the same homogenization parameters.

A general conclusion is that the effects of particulate phase material on emulsion turbidity are size dependent. When the droplets are within the submicron size range (100 ~ 500 nm), particulate phases with higher RIs imparted higher turbidity and the difference in turbidity is exaggerated with increasing MDD. When droplets are within nano-scale range (< 100 nm), turbidity seems to be independent of the RI of the particulate phase. This finding provided us with a better understanding of the effects of particulate phase RI on light scattering and approaches to manufacturing cloudy or clear emulsions. Orange oil terpenes, MCT, beeswax, and ester gum are the primary materials used to formulate cloud emulsions (30, 31). Considering RI effects, ester gum (RI *ca.* 1.52) and orange oil terpenes (RI *ca.* 1.47) are the most effective clouding agents while beeswax and vegetable oil with RIs *ca.* 1.44 have less capability to impart cloudiness. This explains why emulsions formulated with higher levels of ester gum are more turbid. If one wishes to make a clear emulsion, particulate phases with lower RIs are preferred, e.g., vegetable oils, beeswax, or a lipid phase without ester gum.

3.3.2 Effect of particle interface on turbidity

It is understandable that the interface composition and droplet conformation will influence turbidity since they affect light scattering. However, no information was found on how this interface affects the turbidity on nanoemulsions. Thus, we chose to investigate this relationship. Figure 3.3 shows the relationship between the MDD and

turbidity of MCT nanoemulsions stabilized by different food polymers and a small surfactant. We are assuming that if we compare two emulsions that have the same MDD but were made with different emulsifiers, any observed difference in turbidity would be due to the particle interface composition. Since the turbidity was measured at 500 ppm of particulate phase, changes in RI of the continuous phase with different emulsifiers is negligible. The results are interesting because nanoemulsions stabilized by different molecules clustered at different locations in the plot. The protein interface (WPI) imparted higher turbidity than that of a polysaccharide interfaces (PG and MGA) for equivalent MDD. The MGA stabilized emulsions clustered between WPI and PG (5% w/w) stabilized emulsions, which may be attributed to its special polysaccharide-peptide coupled structure. However, the distribution of SDS and PG (20% w/w) stabilized nanoemulsions overlapped within the nano-scale range of droplet size, which suggested that the two interfaces have the same pattern of light scattering even though they are totally different in composition. This finding may suggest that the effects of interface on turbidity are also droplet size dependent. Within a submicron size range, the interface greatly affects light scattering; while within nano-scale range, turbidity is less dependent on interface composition and conformation. In order to validate this finding, further studies were conducted to explore the effect of particle interface on emulsion clarity

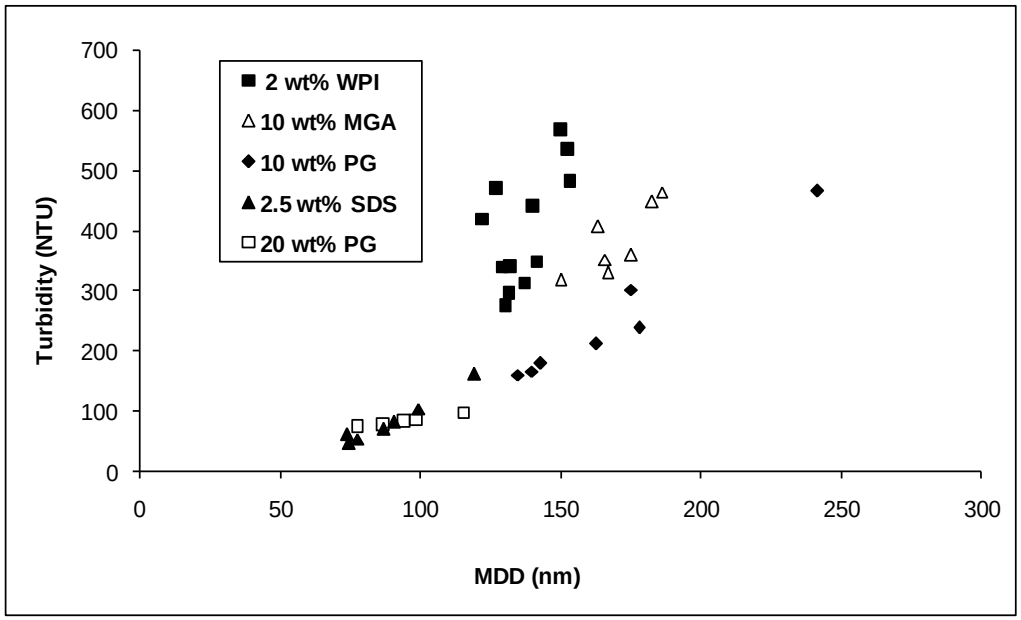

Figure 3.3 Effect of interface composition on turbidity. (MGA, PG, and SDS emulsions were produced at 22,000 psi, variable number of passes; WPI emulsions were produced at pressures of 6,000, 14,000, and 22,000 psi, variable number of passes).

An observation from Figure 3.3 was that WPI emulsions clustered in a large range of turbidity (280 to 550 NTU) but a small range of MDD (125 to 150 nm). Based on the small range in MDD for these emulsions, one would not have expected to see such a large difference in turbidity. We postulated that size distribution might have contributed to this result (samples may have had a similar MDD but wider particle size distributions). Figure 3.4 shows the relationship between turbidity and PDI of 2% w/w WPI stabilized MCT emulsions. However, this plot indicates that the size distribution (PDI) was not necessarily associated with turbidity in this case. Therefore, it appears that WPI at the particle interface imparts more turbidity to an emulsion than the other emulsifiers and the

turbidity of WPI stabilized emulsions increased faster with MDD than those stabilized by the other emulsifiers tested.

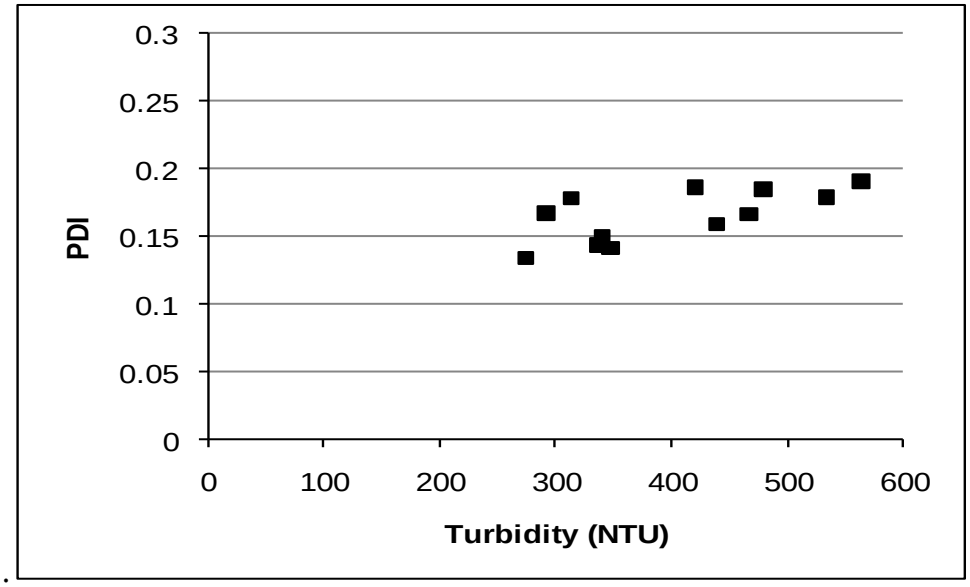

Figure 3.4 Relationship between turbidity and PDI of 2% w/w WPI stabilized MCT emulsions (produced at 6,000, 14,000, and 22,000 psi, multiple passes).

The effect of interface on emulsion turbidity has not been reported yet. This effect was also found in MGA stabilized MCT emulsions. Figure 3.6 shows effects of number of passes and MGA concentration on MDD and turbidity of MGA stabilized MCT emulsions. When the concentration of MGA was increased from 5 to 10% w/w, the MDD showed a slight decrease but this was not statistically significant due to large variability in the data. However, the turbidity increased greatly with increasing MGA concentration. The turbidity of the 10% w/w MGA solution (prepared under the same processing

conditions but without MCT) was 1.42 NTU, which excluded the possibility that the turbidity increase was associated with the MGA itself. Figure 3.7 shows the particle size distribution of MGA stabilized emulsions. The PDIs of all emulsions fell between 0.1~ 0.2 indicating a very narrow size distributions. Therefore, the difference in turbidity is not likely due to differences in MDD or size distribution but due to the changes in interface composition.

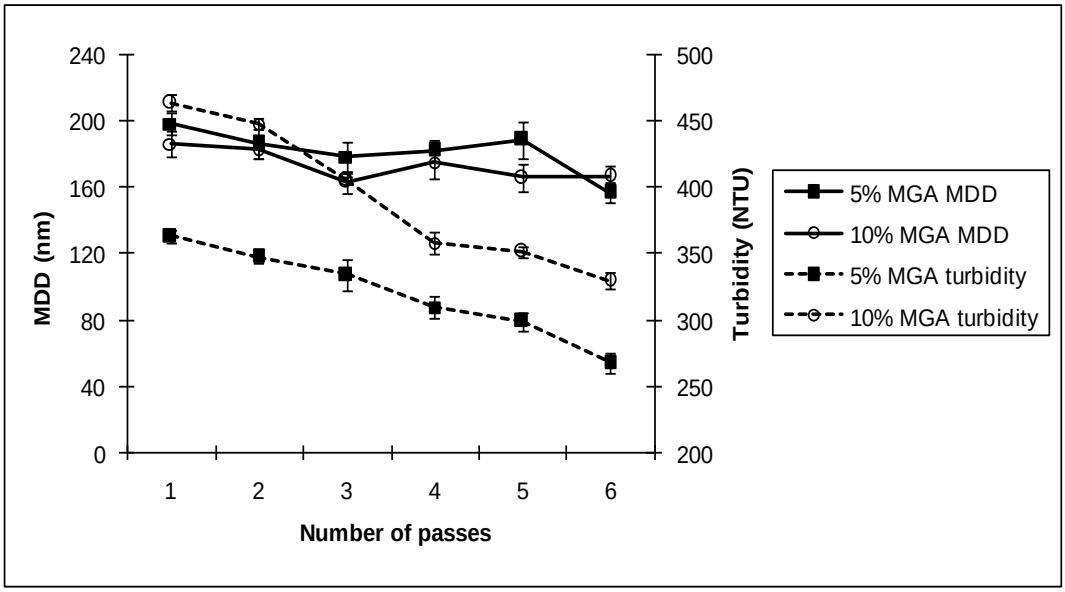

Figure 3.6 Effect of number of passes and MGA concentration on turbidity of MGA stabilized MCT emulsions (22,000 psi).

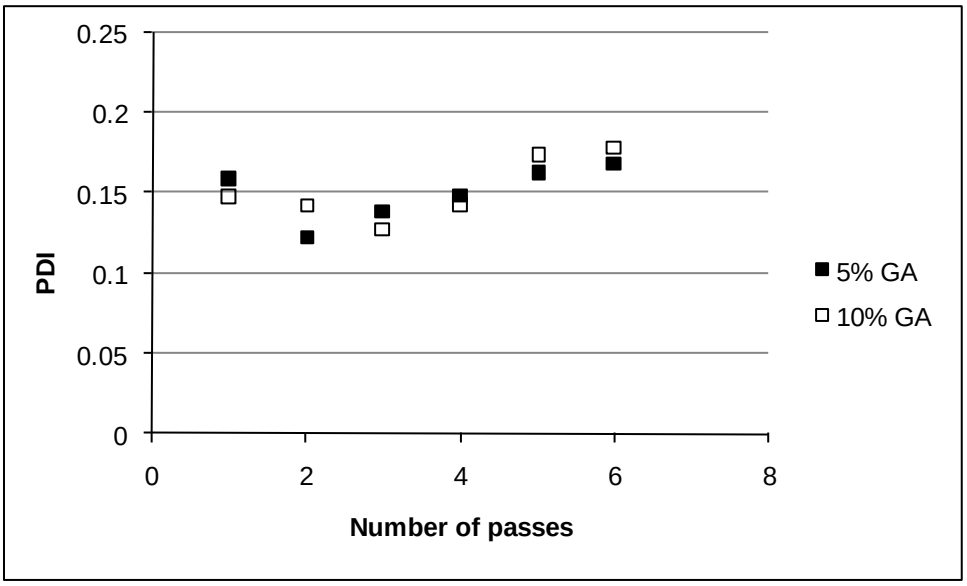

Figure 3.7 Relationship between number of passes through the homogenizer and the PDIs of 2% w/w WPI stabilized MCT emulsions.

Further investigation on zeta potential of MGA stabilized emulsions provided further evidence that interfacial conformation and composition had an impact on the turbidity of emulsions. Figure 3.8 shows that emulsions with 10% w/w GA had a much lower interfacial charge than those stabilized with 5% w/w GA. The interfacial charge is directly associated with charged molecules on the particle interface. Higher surface charges of the 10% w/w MGA stabilized emulsions suggest a higher interfacial load of MGA due to denser packing of the MGA molecules on the interface causing greater light scattering. It is well known that gum arabic tends to accumulate at the particle interface due to its unique polysaccharide-peptide coupled structure. The change in MGA load and packing pattern at the interface leads to changes in interface composition and

conformation. It appears that the formation of a thick interfacial membrane of MGA strongly affects the scattering of incident light and thus generates higher turbidity of the prepared emulsions.

The results of this study provide direct evidence that the particle interface has substantial impact on the turbidity of emulsions. Generally proteins impart higher turbidity to emulsions while polysaccharides impart lower turbidity and polysaccharide-peptide results in turbidity between the two. This phenomenon can be attributed to both the RIs of biopolymers (proteins have higher RIs than polysaccharides) and also the conformation/orientation of emulsifier molecules at the interface. However, the impact of particle interface on turbidity seems to be droplet size dependent and disappears as droplets approach nano-scale. In the present study, we have no information for MDD < 70 nm due to our inability to create smaller MDD using the emulsifiers we have chosen. It would be interesting to validate our conclusions for particles in the range of 20 ~ 70 nm.

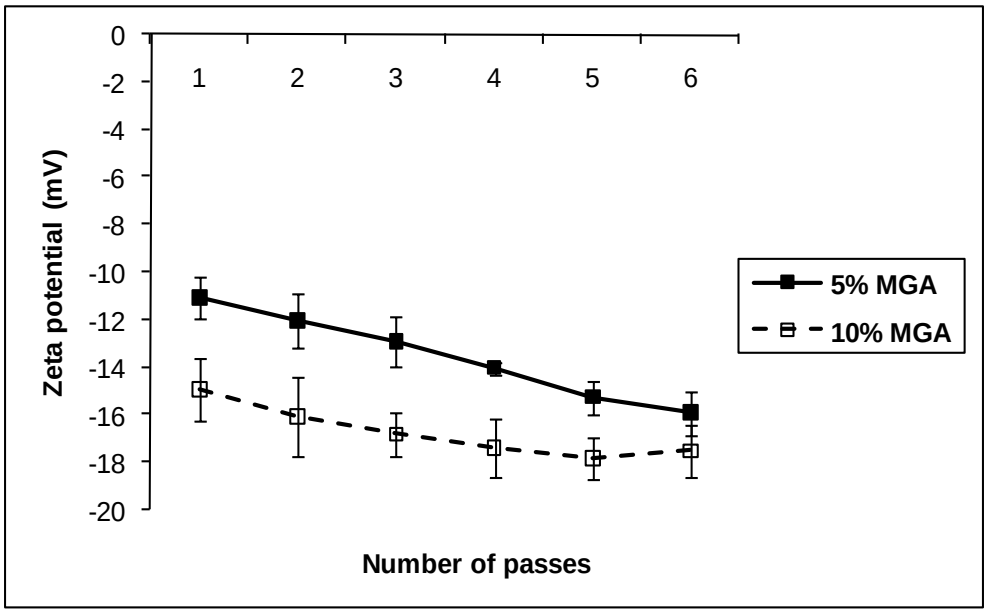

Figure 3.8 Effect of number of passes and MGA concentration on zeta potential of MGA stabilized MCT emulsions (22,000 psi).

3.3.3 Effect of MDD on emulsion turbidity

It is desirable to establish the relationship between MDD and turbidity since this provides valuable information on the need to control droplet size in manufacturing to achieve products of the desired turbidity. Theoretically, specific turbidity is proportional to the $(MDD)^3$ assuming all droplets are mono-dispersed and droplet size is smaller than a tenth of the wavelength of incident light (16). But within a larger range of droplet sizes there is a polynomial relationship between MDD and turbidity (19, 26). Figure 3.9 shows the plot of MDD vs. turbidity of PG stabilized nanoemulsions. The regression of MDD and turbidity showed a good polynomial curve within the droplet size range of 80 to 400

nm. Since this curve was based on nanoemulsions with the same lipid phase and biopolymer emulsifier, and more than 45 points were included, this line reflects the true relationship between MDD and turbidity of emulsions in a practical case. This provides us information on the MDDs needed to manufacture emulsions of the desired turbidities.

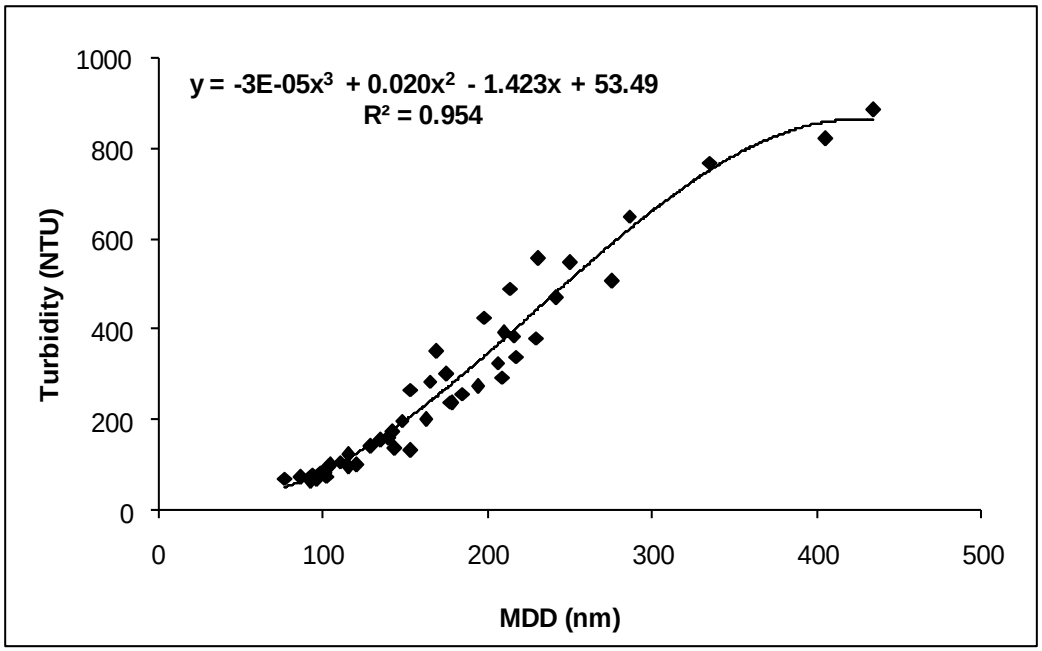

Figure 3.9 Relationship between MDD and turbidity of PG stabilized MCT nanoemulsions.

Interestingly, the curve flattens at about 400~500 nm, which suggests that the turbidity reaches a maximum and will decrease with further increases in MDD. This observed relationship agreed with the theoretical prediction very well. Based on theoretic calculations, turbidity at light wavelengths similar to the radius of particles reaches a

maximum (16). In the present study the incident light wavelength is 455 nm, therefore, one would expect the MDD with maximum turbidity is within 400 ~ 500 nm. This finding provides a better understanding of how to produce cloudy and clear emulsions. If one wishes to produce cloudy emulsions, one would want the majority of droplets to fall within the flatten area to create the desired turbidity with minimum usage levels. For producing clear emulsions, one would want the majority of droplets fall below 100 nm to create minimum turbidity. For nanoemulsions, the dimensions of the particulate phase are much smaller than the wavelength of light ($r << \lambda$), causing weak light scattering and hence low turbidity. Therefore, nanoemulsions tend to be transparent in appearance.

3.3.4 Effect of dispersed phase concentration on turbidity

Considering that in practice lipophilic materials are used at different concentrations, e.g., 10 ~ 500 ppm for flavor oils, the relationship between turbidity and dispersed phase concentration is of interest. Figure 3.10 shows the correlation between turbidity of MCT emulsions and dispersed phase concentrations. A good linear relationship was obtained in the range of 100 ~ 1000 ppm of MCT as the dispersed phase. Figure 3.11 shows images of emulsion appearance at different concentrations of dispersed phase. At 100 ppm of MCT, the emulsion had a turbidity of *ca.* 50 NTU, which is visually close to water. Therefore, biopolymer stabilized nanoemulsions have potential

commercial applications for potent flavors, i.e. those that can be used at low concentrations.

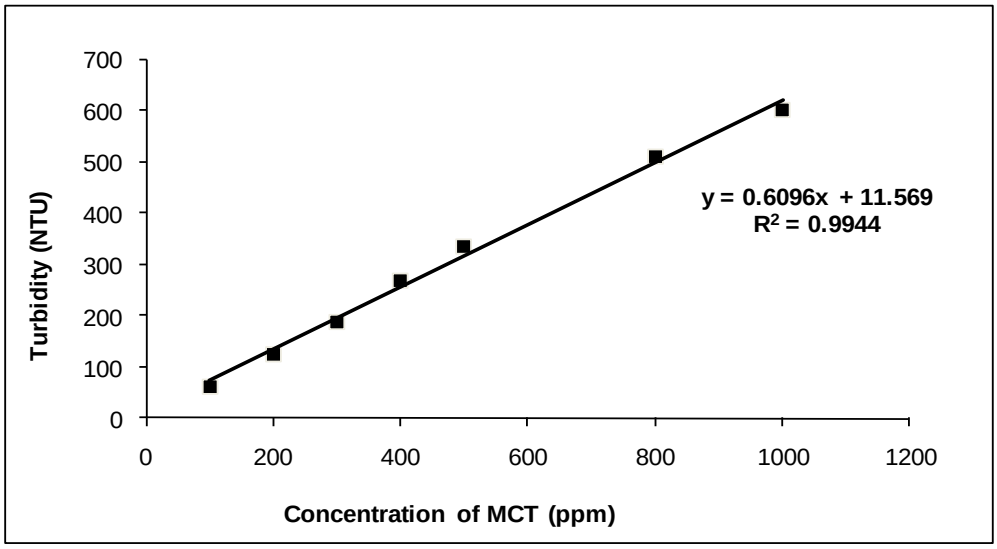

Figure 3.10 Relationship between turbidity and dispersed phase concentration of 5% w/w PG stabilized emulsions (22,000 psi, 4 passes).

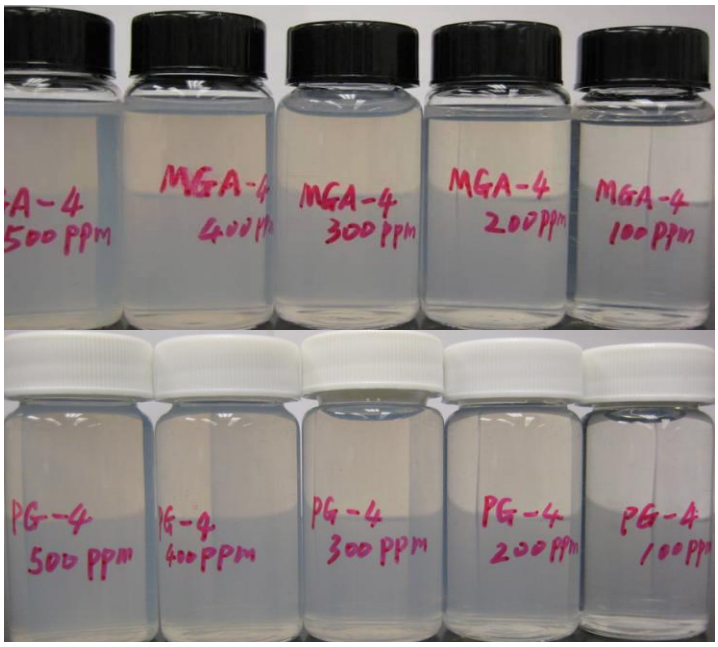

Figure 3.11 Images of MCT emulsions containing different concentrations of dispersed phase. Emulsions were stabilized by 5% w/w MGA (top) or PG (bottom) produced at 22,000 psi (4 passes). From left to right: 500, 400, 300, 200, 100 ppm of MCT in the continuous phase.

3.3.5 Effect of continuous phase type on turbidity

According to light scattering theories, refractive indices of the phases have a substantial impact on the turbidity of emulsions. In order to investigate this effect, a nanoemulsion concentrate was diluted in sucrose solutions differing in concentrations from 0 to 60% w/w. The dispersed phase refractive index (RI) was measured as 1.4619 and continuous phase refractive indices varied from 1.333 (without sucrose) to 1.4418

(60% w/w sucrose). Figure 3.12 shows the correlation between turbidity and RI of the continuous phase. A relatively good polynomial correlation was obtained. As expected, turbidity drops to zero when the RI of the continuous phase equals the RI of the dispersed phase.

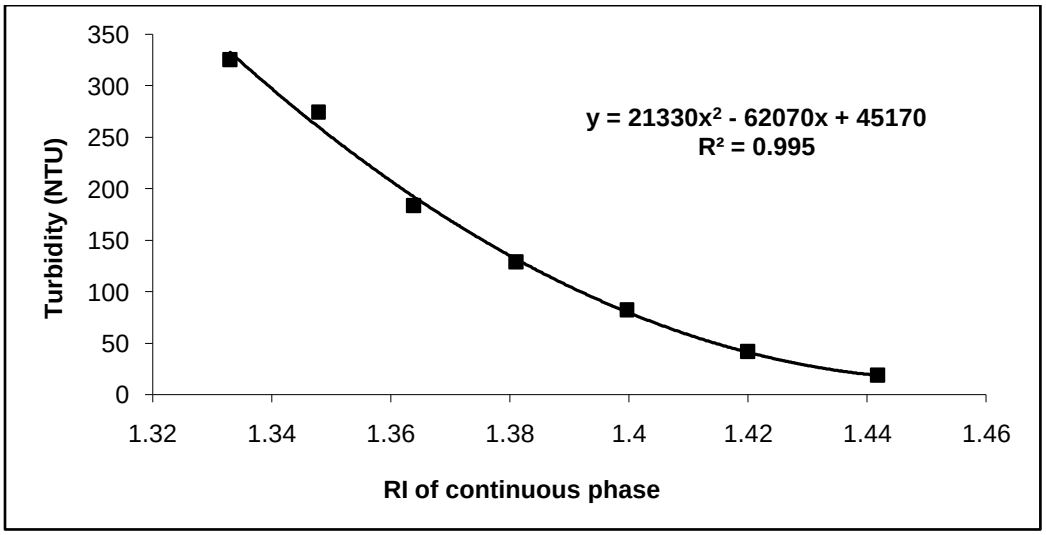

Figure 3.12 Relationship between turbidity of MCT emulsions and the RI of the continuous phase. Emulsions were stabilized with 5% w/w PG, produced at 22,000 psi (4 passes) and diluted to 500 ppm of dispersed phase.

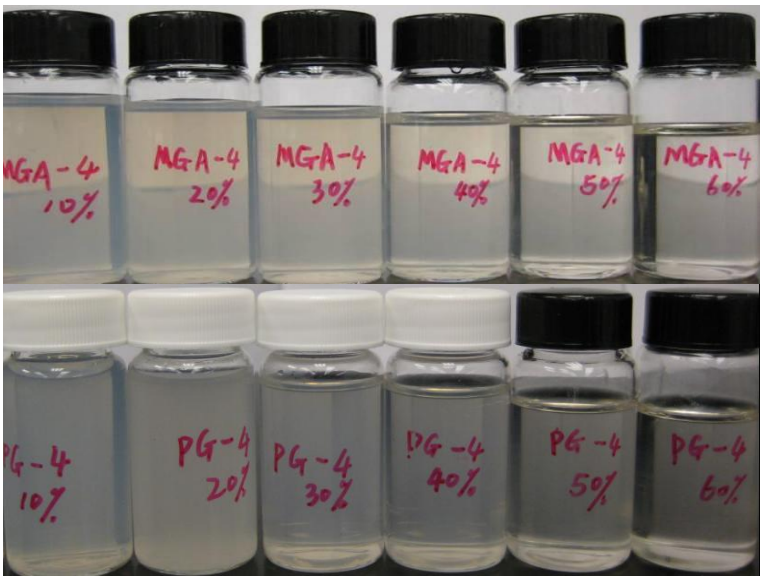

Figure 3.13 Images of MCT emulsions containing 500 ppm of dispersed phase and different concentrations of sucrose in the continuous phase. Emulsions were stabilized by 5% w/w MGA (top) or PG (bottom) produced at 22,000 psi (4 passes). From left to right: 10, 20, 30, 40, 50, and 60% w/w of sucrose in the continuous phase.

Figure 3.13 shows the appearance of nanoemulsions as a function of sucrose concentrations in the continuous phase. Clarity of the diluted nanoemulsions increased with sucrose concentration and was clear at 60% w/w of sucrose. Theoretically, if the RI of the dispersed phase matches that of the continuous phase, the turbidity is zero. In turn, the RI of the dispersed phase can be determined by extrapolating the curve of turbidity vs. RI to zero turbidity where the RI of the continuous phase must equal that of dispersed phase. The physics behind this phenomenon is well known but it is not well recognized in emulsion formulation. A particular application of this phenomenon is clear beverage

syrups, e.g., coffee syrups which have sugar content more than 50% w/w, tend to be clear.

From Figure 3.12, the RI of the dispersed phase is calculated as 1.481 by extrapolating the regression line to zero turbidity, which is larger than the RI of oil phase measured as 1.4619. It was postulated that adsorption of emulsifiers at the interface increases the RI of the oil globules thus influences light scattering (turbidity) since starch has a much higher RI of 1.54 (32) than the oil phase.

3.3.6 Destabilization mechanism of MCT nanoemulsions

Emulsion stability is a major concern in nearly all applications. The main destabilization mechanism of nanoemulsions is suggested to be Ostwald ripening. Ostwald ripening is the transport of dispersed phase molecules from small droplets to larger droplets through the continuous phase, which is driven by free energy differences (33). Analytically one can determine if Ostwald ripening is the main destabilization mechanism by plotting the cube of emulsion radius vs. time since manufacture. This process is based on the Lifshita-Slesov-Wagner (LSW) theory as described by the equation below (34).

$$r3 = \frac{8c(\infty)\gamma vD}{9\rho RT}t$$

Where D is diffusion coefficient of the dispersed phase in the continuous phase, ρ is the density of dispersed phase, γ is the interfacial tension, C(∞) reprsents the solubility of the oil phase in the bulk phase, *V* is the molar volume of the oil phase, R is gas constant and T is the absolute temperature.

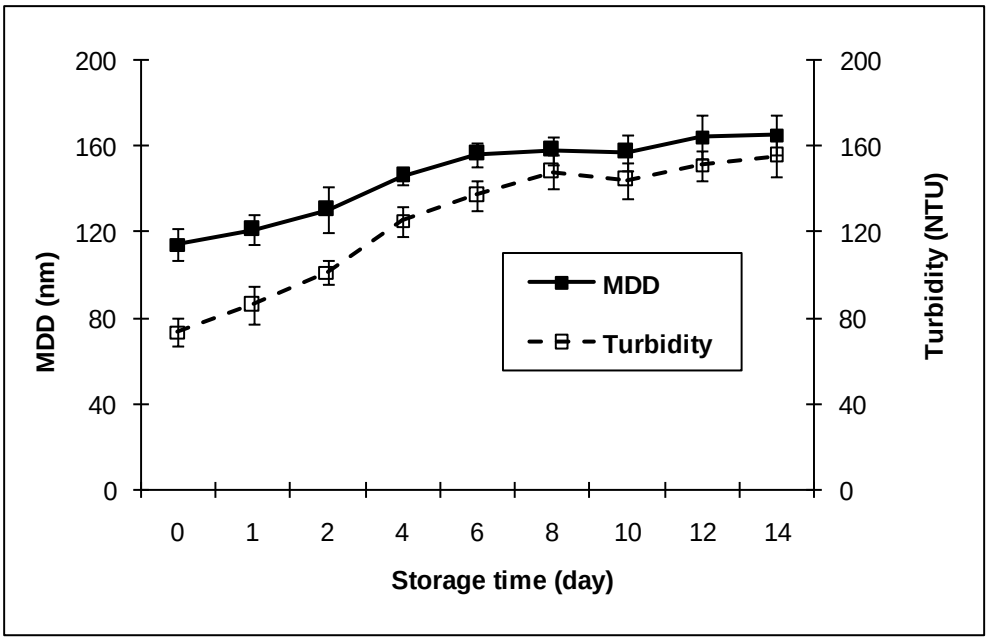

Figure 3.14 Changes in the MDD and turbidity of 20% w/w PG stabilized nanoemulsions during storage at room temperature.

Figure 3.14 shows the effect of storage time on both the turbidity and the MDD of MCT nanoemulsion concentrates. Both MDD and turbidity increased substantially in the first week and then increased slowly. This could have been caused by Ostwald ripening or coalescence. On plotting the MDD vs. storage time, a linear relationship between

MDD^3 and storage time was not found (data not shown) which excludes Ostwald ripening as the primary destabilization mechanism. It is proposed that coalescence is the main destabilization mechanism of MCT nanoemulsions considering that MCT is very insoluble in water; however, there is no direct way to prove this hypothesis. However, more information was gathered on failure mechanisms by studying SDS emulsified MCT nanoemulsions.

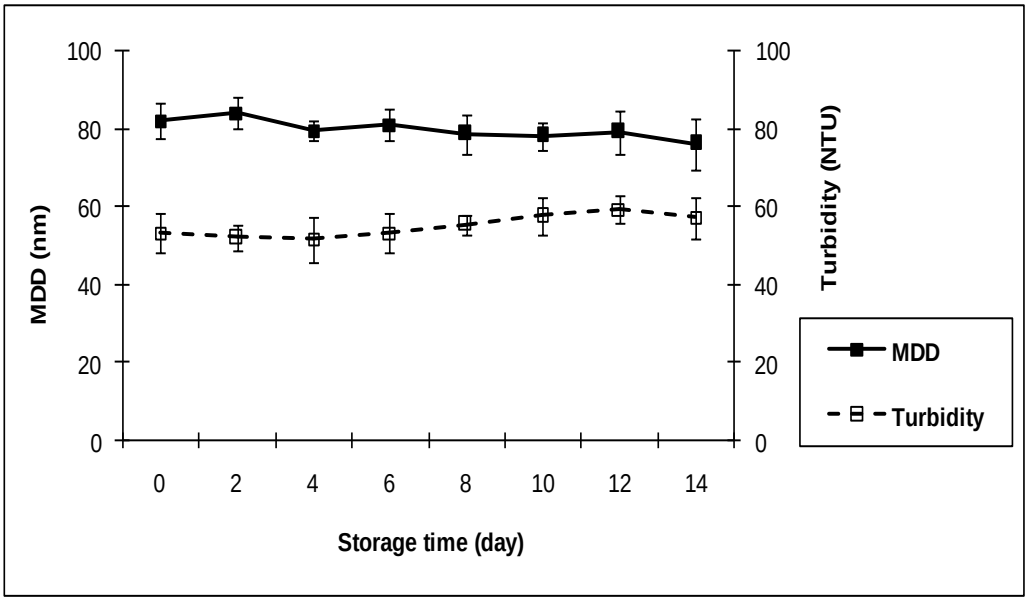

Figure 3.15 Changes in MDD and turbidity of 2.5% w/w SDS stabilized MCT nanoemulsions during storage at room temperature.

Figure 3.15 presents the MDD and turbidity of SDS emulsified MCT nanoemulsion concentrates during storage. Both MDD and turbidity were stable over time which indicates that no Ostwald ripening occurred. For SDS and PG stabilized nanoemulsions,

the relevant differences are interfacial tension and diffusion coefficient of droplets due to bulk phase viscosity differences. If Ostwald ripening occurs, the MDDs of both nanoemulsions will increase during storage but with different rates of increase in MDDs. Since Ostwald ripening was not observed in the SDS emulsified nanoemulsions, we suggest that the primary destabilization mechanism of PG stabilized MCT nanoemulsion is coalescence. This conclusion is consistent with Wooster's finding (34) that vegetable oils such as peanut oil, are stable against Ostwald ripening due to their low solubility in water.

Assuming then that coalescence is the relevant mechanism for particle size changes in PG stabilized nanoemulsions, the difference in interfacial charge between PG and SDS nanoemulsions may be relevant. PG stabilized nanoemulsions showed a low interfacial charge of -3.72 mV, which is not high enough to protect the nanoemulsion from coalescence. For emulsions with low electrolyte content in the aqueous phase, a zeta potential of 30 mV is found to be sufficient to establish an energy barrier to ensure emulsion stability (35-37). It was reported (38) that modified starches (Purity Gum 17773 and Purity Gum 2000) showed poorer performance in stabilizing beverage clouding emulsions (pH 3.6) compared to gum acacia and modified gum acacia. Considering substantially larger interfacial area of nanoemulsions than that of cloud emulsions, it is not surprising that PG stabilized nanoemulsions is instable against coalescence.

3.4 Conclusions

Overall, we have prepared nanoemulsions with small MDD and low turbidity by using modified starch and other food biopolymers. MCT-based nanoemulsions could be manufactured with a MDD as small as 77 nm and turbidity as low as 71 NTU at 500 ppm of dispersed phase. Factors influencing nanoemulsion turbidity were identified as droplet size, dispersed phase concentration, particulate phase RI, and interface composition. More specifically, the effects of particulate phase RI and interface composition on turbidity were size dependent. The relationship between the MDD and turbidity of nanoemulsions was established providing us valuable information on optical properties of nanoemulsions. The destabilization mechanism of MCT-based nanoemulsions was identified as coalescence instead of Ostwald ripening.

This study has provided a practical understanding of the factors influencing the optical properties of nanoemulsions thereby providing guidance for the formulation of them. However, several issues have to be addressed before practical application is possible. More research is needed on stabilizing nanoemulsions to prevent either coalescence or Ostwald ripening. Since some flavorings have relatively high solubility in water compared to that of vegetable oils, Oswald ripening is likely to be an important mechanism. Regarding coalescence, currently there is no obvious way to inhibit it when using PG alone since it has a low charge density, insufficient to stabilize the interface.

References

[1] Given, P.S. Encapsulation of flavors in emulsion for beverages. *Curr. Opin. Colloid In.* **2009,** 14, 43-47.

[2] Sekikawa, K.; Watanabe, M. Transparent emulsified composition for use in beverage. *US patent application:* **US2009/0285952.**

[3] Garti, N.; Jacobs, L.G.; Lane, B.; Zakharia, I. Isotropic transparent structured fluids. *US patent application:* **US2003/0228395.**

[4] Skiff, R.H.; Baaklini, J.; Vlad, F.J. Clear flavor microemulsions comprising sugar esters of fatty acids. *US patent application:* **US2010/0136175.**

[5] Chanamai, R. Microemulsions for use in food and beverage products. *US patent application:* **US2007/0087104.**

[6] Garti, N.; Yaghmur, A.; Leser, M.E.; Clement, V.; Watzke, H.J. Improved oil solubilization in oil/water food grade microemulsions in the presence of polyols and ethanol. *J. Agric. Food Chem.* **2001,** 49, 2552-2562.

[7] Spernath, A.; Yaghmur, A.; Aserin, A.; Hoffman, R.; Garti, N. Food-grade microemulsions based on nonionic emulsifiers: media to enhance lycopene solubilization. *J. Agric. Food Chem.* **2002,** 50, 6917-6922.

[8] Spernath, A.; Aserin, A. Microemulsions as carriers for drug and nutraceuticals. *Adv. Colloid Interface. Sci.* **2006,** 128-130, 47-64.

[9] Garti, N.; Aserin, A.; Spernath, A.; Amar, I. nano-sized self-assembled liquid dilutable vehicles. **US patent 7182950**.

[10] Wooster, T.J.; Golding, M.; Sanguansri, P. Impact of oil type on nanoemulsion formation and Ostwald ripening stability. *Langmir.* **2008,** 24, 12758-12765.

[11] Gutierrez, J.; Gonzalez, C.; Maestro, A.; Sole, I.; Pey, C.; Nolla, J. Nano-emulsions: new applications and optimization of their preparation. *Curr. Opin. Colloid Interface Sci.* **2008,** *13*, 245-251.

[12] Nicolosi, R.; Wilson, T. Compositions and methods for making and using nanoemulsions. *US patent application:* **US2008/0274195.**

[13] Solans, C.; Izquierdo, P.; Nolla, J.; Azemar, N.; Garcia-Celma, M. Nano-emulsions. *Curr. Opin. Colloid Interface Sci.* **2005,** *10*, 102-110.

[14] Xu R. Particle characterization: light scattering methods. Norwell, MA: *Kluwer Academic Pulishers.* **2000**.

[15] Mason, T.; Wilking, J.; Meleson, K.; Chang, C.; Graves, S. Nanoemulsions: formation, structure, and physical properties. *J. Phys.: Condens. Matter,* **2006,** *18,* R635-R666.

[16] Gregory, J. Particles in water, principles and processes. Boca Raton, FL: *CRC Press.* **2006.**

[17] Kleizen, H.H.; Putter, A.B.; Beek, M.; Huynink, S.J. Particle concentration, size and turbidity. *Filtration and Separation.* **1995,** 32, 897-901.

[18] Syvitski, J. Principles, methods and applications of particle size analysis. New York: *Cambridge University Press.* **1991.**

[19] Hernandez, E.; Baker, R.A. Turbidity of beverages with citrus oil clouding agent. *JFS.* **1991,** 56, 1024-1026.

[20] Mao, L.; Xu, D.; Yang, J.; Yuan, F.; Gao, Y.; Zhao, J. Effects of small and large molecule emulsifiers on the characteristics of β-carotene nanoemulsions prepared by high pressure homogenization. *Food Technol. Biotechnol.* **2009,** 47, 336-342.

[21] Cheong, J.N.; Tan, C.P. Palm-based functional lipid nanodispersions: preparation, characterization and stability evaluation. *Eur. J. Lipid Sci. Technol.* **2010,** 112, 557-564.

[22] Donsi, F.; Wang Y.; Li J.; Huang, Q. Preparation of curcumin sub-micrometer dispersions by high-pressure homogenization. *J. Agric. Food Chem.* **2010,** 58, 2848-2853.

[23] Shafiq, S.; Shakeel, F.; Talegaonkar, S.; Ahmad, F.; Khar, R.; Ali, M. Development and bioavailability assessment of ramipril nanoemulsion formulation. *Eur. J. Pharm. Biopharm.* **2007,** 66, 227-243.

[24] Wang, X.Y.; Wang, Y.W; Huang, R. Enhancing stability and oral bioavailability of polyphenols using nanoemulsions. In: *Micro/Nanoencapsulation of Active Food Ingredients.* Q. R. Huang, P. Given and M. Qian (Editors). **2009.** ACS Symposium Series 1007. Washington, DC.

[25] Chen, C.; Wagner, G. Vitamin E nanoparticle for beverage applications. *Chem. Eng. Res. Des.* **2004,** 82, 1432-1437.

[26] Hernandez, E.; Baker, R.A.; Crandall, P.G. Model for evaluating turbidity in cloudy beverages. *JFS.* **1991,** 56, 747-750.

[27] Zhu, Z. X.; Anacker, J. L.; Ji, S. X.; Hoye, T. R.; Macosko, C. W.; Prudhomme, R. K. Formation of block copolymer-protected nanoparticles via reactive impingement mixing. *Langmuir* **2007**, *23*, 10499.

[28] Wang, X.; Jiang, Y.W.; Wang, Y.; Huang, M.T.; Ho, C.T.; Huang, Q. Enhancing anti-inflammation activity of curcumin through O/W nanoemulsions. *Food Chem.* **2008,** 108, 419-424.

[29] Instrumental manual of BIC 90Plus, Brookhaven Instrument Corporation.

[30] Buffo, R.A.; Reineccius, G.A. Shelf-life and mechanism of destabilization in dilute beverage emulsions. *Flavour Frag. J.* **2001,** 16, 7-12.

[31] Reineccius, G. Flavor chemistry and technology. Boca Raton, FL: *CRC Press.* **2006.** 2nd Ed.

[32] Karppinen, T.; Kassamakov, I.; Heggstrom, E.; Stor-Pellinen, J. Measuring paper wetting processes with laser transmission. *Meas. Sci. Technol.* **2004,** 15, 1223-1229.

[33] Gutierrez, J.; Gonzalez, C.; Maestro, A.; Sole, I.; Pey, C.; Nolla, J. Nano-emulsions: new applications and optimization of their preparation. *Curr. Opin. Colloid Interface Sci.* **2008,** *13*, 245-251.

[34] Wooster, T. J.; Golding, M.; Sanguansri, P. Impact of oil type on nanoemulsion formation and Ostwald ripening stability. *Langmir*, **2008,** 24, 12758-12765.

[35] Stachurski, J.; Michalek, M. The Effect of the ζ Potential on the Stability of a Non-Polar Oil-in-Water Emulsion. *J. Colloid Interface Sci.* **1996,** 184, 433-436.

[36] Friberg, S.E.; Goldsmith, L.B.; Hilton, M.L. Theory of emulsion in Pharmaceutical dosage forms: dispersion systems. Lieberman, H.A.; Reiger, M.M.; Banker, G.S., Eds.; New York: Marcel Dekker, Inc. **1988.**

[37] Li, L.C.; Tian, Y. Zeta Potential in Encyclopedia of pharmaceutical technology. Swarbrick, J.; Ed.; Informa Healthcare USA, Inc. **2007.**

[38] Reiner, S.J.; Reineccius G.A.; Peppard, T.L. A comparison of the stability of beverage cloud emulsions formulated with different gum acacia- and starch-based emulsifiers. *JFS.* **2010,** E236-E246.

Chapter 4

Multilayer emulsions as beverage clouding agents

The ability to prepare secondary and tertiary beverage clouding emulsions using a layer-by-layer deposition technique was developed. Proteins, β-lactoglobulin (L) and sodium caseinate (S), were selected to stabilize the primary emulsions. Biopolymers of sodium alginate (S), ι-carrageenan (C), gum Arabic (G), pectin (P), chitosan (Ch), and gelatin (Ge) were evaluated as secondary and tertiary layers. Biopolymer concentration was optimized based on droplet size and ζ-potential. Finally, the performance of multilayered emulsions in beverage cloud applications was evaluated.

Biopolymer concentration and pH were found critical to the formation of stable multilayered emulsions. Protein and polysaccharide type also impacted droplet size and ζ-potential of multilayer emulsions. Interestingly, β-lactoglobulin was found better than sodium caseinate in forming protein-polysaccharide interfacial complexes as demonstrated by smaller mean droplet diameters (MDD) of LA, LP and LC than those of SA, SP and SC. It was also found biopolymer concentration has to be above a critical value (0.2 ~ 0.5% w/w depending on the type of proteins and polysaccharides) to prevent multilayer emulsions from bridging flocculation. Our data showed that both secondary (LA, LC, LG) and tertiary (LGC) emulsions formed by electrostatic deposition could provide the same performance as traditional emulsifiers of gum Arabic (G) and modified starch (M). After four weeks of storage at room temperature, beverage clouds stabilized with G, M, LA, LC, LG and LGCh showed MDDs of 0.68, 0.67, 0.90, 0.82, 0.65 and 2.2 μm, respectively, and turbidity losses of 18, 28, 22, 19, 25 and 17%, respectively.

Overall, multilayered emulsions as beverage clouding agent show significant commercial values.

4.1 Introduction

Beverage emulsions are oil-in-water emulsions that are prepared in a concentrated form and diluted to the desired levels prior to consumption (1-2). A typical formula always contains vegetable oil, flavor oil, weighting agents and fat soluble antioxidants as the oil phase, whereas the aqueous phase consists of water, emulsifier, stabilizer, sweetener, preservatives, dye and acids (3-5). Beverage emulsions are thermodynamically unstable systems and thus tend to undergo phase separation during storage. Historically, beverage emulsion stability is problematic due to creaming, flocculation, coalescence or Ostwald ripening (5-8). In the beverage and flavor industries, the ring test is commonly used to predict the stability of beverage emulsions which is based on the observation of a ring (separated oil) at the neck of the beverage bottle (6, 10).

Gum arabic is traditionally the hydrocolloid used for emulsifying and stabilizing beverage emulsions. The stability of beverage emulsions heavily relies on the quality of the gum arabic: This is reflected by the large amount of research focused on correlating the characteristics of gum arabic and its emulsifying performance (11-14). A disadvantage of gum arabic as an emulsifier is that it has to be used at relatively high concentrations, e.g., 20% w/w for stabilizing 10% w/w flavor oils (10,15). In addition, though considered as the industry "gold standard" in stabilizing beverage emulsions, there are often problems associated with gum arabic such as consistent quality,

availability and cost (10, 14). Consequently, there is a constant interest in finding alternatives to gum arabic, such as modified starch and proteins (10, 16-20).

Globular proteins, such as those from milk, are good emulsifiers even at low usage levels, e.g., < 1% whey proteins for stabilizing 12.5% w/w oil-in-water emulsions (10, 20). However, globular protein stabilized emulsions are sensitive to pH, ionic strength and thermal treatment (15). Therefore, ideally it would be desirable to have a natural emulsifier that can provide good emulsion stability against environment stress but used at low levels.

Recently considerable research has been done by McClements' group on multilayered food emulsions (21-25). Their results showed that the formation of protein-polysaccharide double layers at the oil/water interface significantly improves emulsion stability. This technique involves the formation of multiple layers of biopolymers at the interface using a layer-by-layer (LBL) electrostatic deposition technique. Figure 4.1 shows the principle of the LBL technique. In this approach, sequential multi-layers of oppositely charged polymers are added to form a thick droplet shell. The first step in creating this structure is homogenization followed by the addition of a primary emulsifier, then an oppositely charged polymer is added with pH adjustment, and finally a third polymer is added to form a thick shell around the emulsion droplets. Based on biopolymer electrostatic interactions, various combinations of proteins and polysaccharides can be used to form stable O/W emulsions.

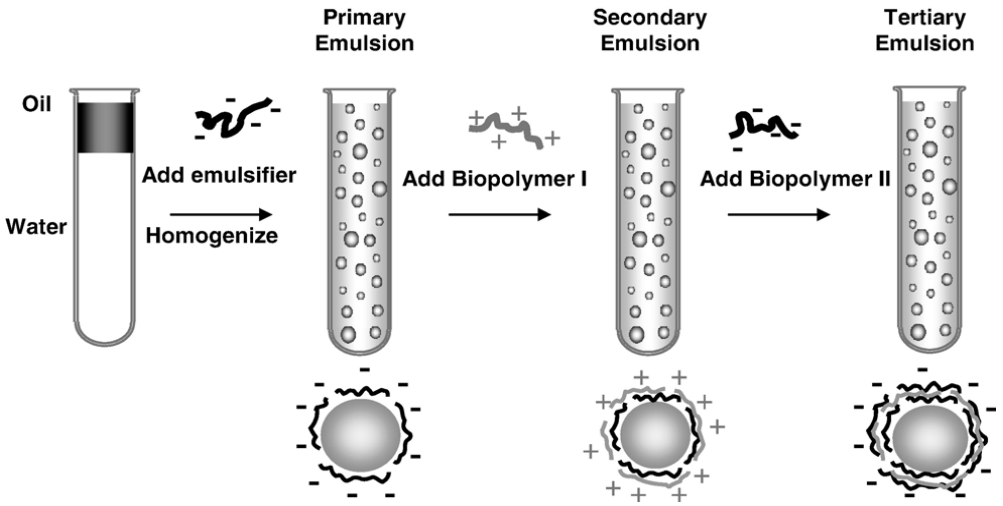

Figure 4.1 Principle of preparation of multilayered emulsions; reprinted from Ref. 26.

One of the most important factors determining the formation and properties of multilayered emulsions is the solution pH. The pH determines the ionization of surface groups and therefore, the final surface charge density (26, 27). Many of the biopolymers used in food industry have ionizable groups that are relatively weak acids or bases. The negative charges of biopolymers can be from sulfate, phosphate ($pKa \approx$ 1-2) or carboxyl groups ($pKa \approx$ 4-5), whereas the positive charges come from amino groups ($pKa \approx$ 7-11) (27, 28). At a certain pH, the adsorption of one biopolymer to the oil droplets coated with primary emulsifier (e.g., proteins) occurs, and this process largely depends on the magnitude and sign of the charges on the two types of biopolymer molecules.

Research has shown that multilayer emulsions offer better physical stability against environmental stresses, such as pH, salt, thermal processing, chilling and freezing (23-25, 29, 30). Guzey and McClements (26) presented a thorough review of multilayered

emulsions for applications in the food industry. Interestingly, the LBL structures on oil droplets also provide additional protection from oxidation and degradation of labile compounds with the proposed mechanism that net positive charges of emulsion droplets repel iron ions (pro-oxidants) in the continuous phase (21, 22). This effect was demonstrated using combinations of sodium dodecyl sulfate (SDS) and chitosan to form an interfacial complex. This bi-layer system resulted in reduced *p*-cymene formation from citral over time compared to a gum arabic-based conventional emulsion. However, there is little information in the literature on the long term stability of multilayered emulsions and their applications in beverages. Therefore, in the present study the performance of multilayered emulsions in a beverage cloud application was evaluated.

This study has two objectives: 1) to establish the major factors that influence interfacial adsorption onto the droplet surface in primary emulsions to form stable secondary and tertiary emulsions; and 2) to evaluate the storage stability of secondary and tertiary emulsions in beverage cloud applications. In present study, β-lactoglobulin and sodium caseinate were selected as emulsifiers to prepare primary emulsions due to their high emulsifying efficacy. Sodium alginate, ι-carrageenan, pectin, chitosan, and gelatin were selected as secondary or tertiary layer materials because they are used in the food industry and offer the desired electrical charge.

4.2 Materials and methods

4.2.1 Materials

Orange oil terpenes were obtained from Citrus and Allied Essences Ltd. (Lake Success, NY, USA); orange oil terpenes used were comprised primarily of limonene (95.6%); myrcene (2.8%); sabinene (2.8%); α-pinene (0.9%); and octanal (0.2%) as measured by gas chromatography. Ester gum was obtained from J.H. Calo Co. (Westbury, NY, USA); modified starch (Purity Gum^{TM} 2000, M) was obtained from National Starch (Bridgewater, NJ, USA); sodium caseinate (S) was obtained from American Casein Company (Burlington, NJ, USA). TIC$^{®}$FCC gum arabic (*A senegal*, G*)* and sodium alginate (A) were donated by TIC gums (Belcamp, MD, USA). Granulated FD&C Yellow #6 was purchased from Sensient Colors (Milwaukee, WI, USA); sodium hydroxide, hydrochloric acid, sodium phosphate, and citric acid were from Fisher Scientific (Fair Lawn, NJ, USA); β-lactoglobulin (L) was provided by Davisco (Eden Prairie, MN, USA); ι-carrageenan (C) was obtained from FMC BioPolymer (Piladelphia, PA, USA); citrus pectin (P) with a degree of esterification 60%; medium molecular weight chitosan (Ch) and sodium benzoate were purchase from Sigma Chemical Co. (St. Louis, MO, USA). Type A gelatin (275 bloom/20 mesh, Ge) was purchased from PB Leiner (Jericho, NY, USA).

4.2.2 Methods

4.2.2.1 Preparation of solutions

Individual dispersions of 16% w/w gum Arabic (G), 12% w/w modified starch (M), 1% w/w sodium caseinate (S), 1% w/w ι-carrageenan (C), 1% w/w sodium alginate (A), 1% w/w chitosan (Ch), 1% w/w type A gelatin (Ge) and 1% w/w pectin (P) were prepared with complete hydration and dispersion by stirring with an overhead mixer (Carter® 1L.81, Carter Motor, IL, USA) for two hours. Type A gelatin was heated to 40 ℃ during mixing. The β-lactoglobulin solution (L) (0.5% w/w) was prepared by stirring for 30 min using a stir bar.

4.2.2.2 Preparation of multilayered emulsions

Orange oil terpene-in-water multilayered emulsions were prepared based on the electrostatic LBL deposition technique. Figure 4.2 shows the preparation diagram for a secondary (double layered) and tertiary (three layered) emulsions. The primary emulsion was prepared by premixing 10% w/w oil phase (orange oil terpenes and ester gum at a 1:1 ratio) and 90% w/w aqueous phase containing 0.5% w/w β-lactoglobulin, 1% w/w sodium caseinate, 16% w/w gum arabic or 12% w/w modified starch using a high shear mixer (Greerco Corp., Hudson, N.H., USA) at *ca.* 6,000 rpm for 2 min. The resultant coarse emulsion was passed through a Microfluidizer® (Model M-110Y, Microfluidics Corporation, Newton, MA, USA) at 13,000 psi, 1 pass. The fine primary emulsion was

then diluted with biopolymer solutions and distilled water at appropriate ratios. The pH of the resultant emulsions was adjusted to 3.6 to form the double layer at the oil droplet surface. Solutions of 0.1M HCl or NaOH were used to adjust pH. Then the resultant secondary emulsions were sonicated (FS110H, Fisher Scientific, Fairlawn, NJ, USA) for 5 min (output 42 kHz) to break flocs. The secondary emulsion was further diluted with another biopolymer solution to form a tertiary emulsion followed by sonication (secondary and tertiary emulsions for stability testing were passed through a microfludizer at 3,000 psi for 1 pass to break flocs). The pH of prepared tertiary emulsions was adjusted to 3.6.

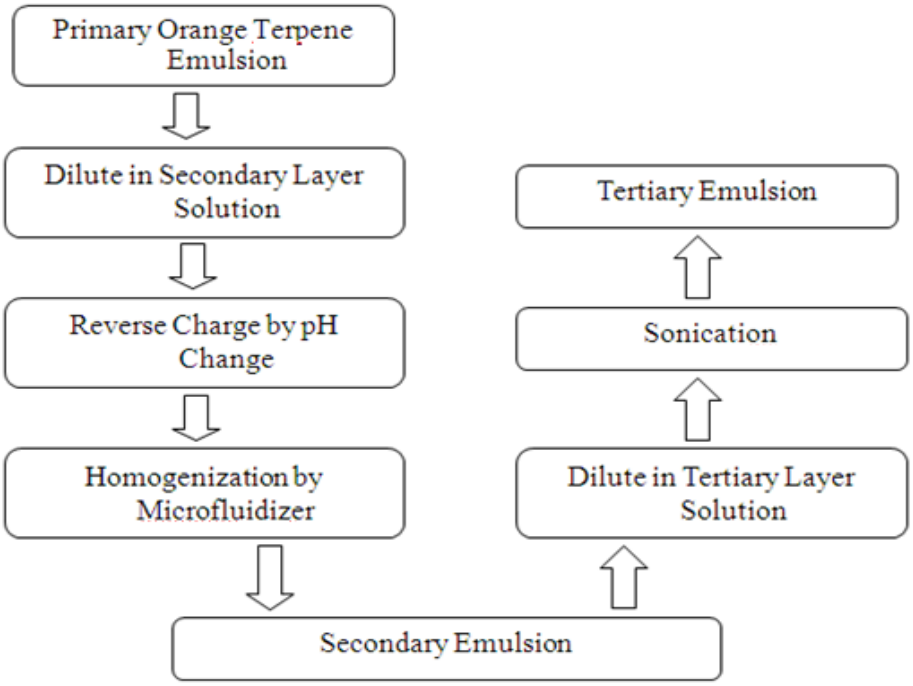

Figure 4.2 Schematic diagram of producing multilayered emulsions.

Figure 4.3 shows the combinations of different biopolymers used in this study to produce secondary and tertiary emulsions. It should be noted that the oil phase fraction was kept at 5% w/w in both the secondary and tertiary emulsions by changing the ratios of emulsion, biopolymer and distilled water. For secondary emulsions, the primary emulsion was diluted with biopolymer solution and distilled water to form secondary emulsions with 5% w/w oil phase. For tertiary emulsions, the primary emulsion was diluted to form secondary emulsions with 7.5% w/w oil phase and the resultant secondary emulsion was then diluted with another biopolymer solution and distilled water to form tertiary emulsion with 5% w/w oil phase. The oil phase fraction was intentionally kept the same to compare their shelf life stability during storage.

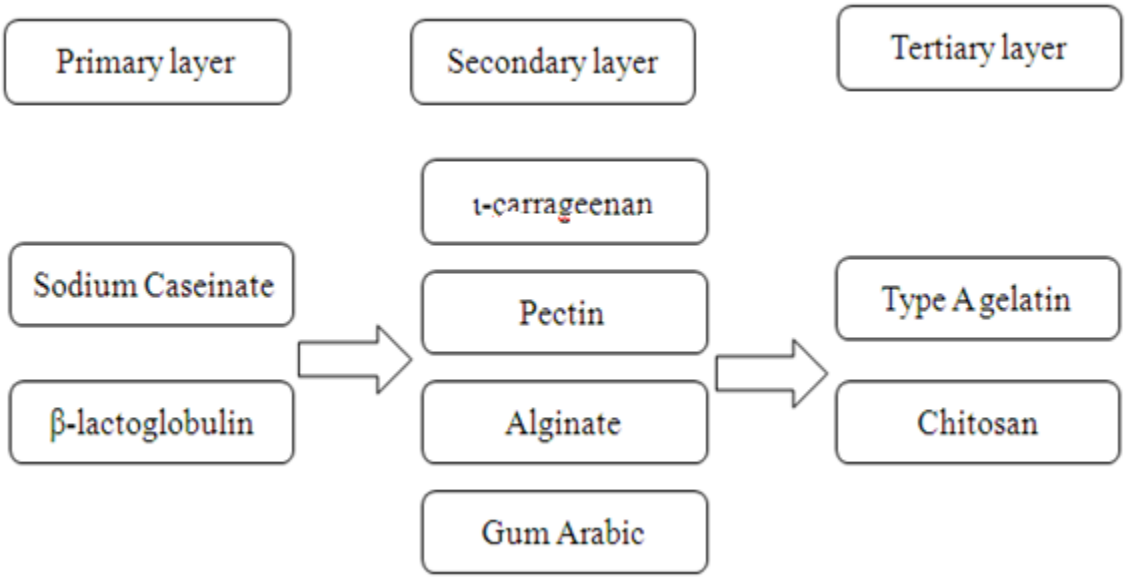

Figure 4.3 Schematic diagram of combinations of different proteins and polysaccharides for producing secondary and tertiary emulsions.

4.2.2.3 Measurement of ζ-potential

The electrical charge on the oil droplets in the emulsions was determined using a particle electrophoresis instrument (ZetaPALS, Brookhaven Instruments, Holtsville, NY, USA). The ζ-potential is determined by measuring the velocity of the droplet when placed in an applied electrical field. Emulsions were diluted in10 mM citric buffer (with the same pH as the emulsion concentrates) and then placed in a standard four-sided, 1 cm polystyrene cuvette. A parallel plate electrode (0.45 cm^2 square platinum plates with a 0.4 cm gap) was inserted and the cuvette was placed in a temperature-controlled holder at 25 ℃. Each measurement was set as 90 sec with 3 replicates. The ζ-potential was calculated from the electrophoretic mobility using the Smoulokowski model.

4.2.2.4 Droplet size measurement

The mean droplet diameter (MDD) of emulsions was determined using a Mastersizer S (Malvern Instruments, Southborough, MA) at an obscuration between 20 and 25%. Measurements of volume/mass-based MDD were recorded. The lower size limit for this instrument is 0.50 μm and the upper size limit is 900 μm. To determine the MDD of emulsion concentrates, emulsion was added dropwise to the sample collector containing buffer solution with the same pH as the emulsion concentrates until the required obscuration was reached. All emulsions were prepared in duplicate except that emulsions

for stability testing were prepared in triplicate. To measure the MDD of beverages, samples were gently mixed (by turning bottles upside-down) and then poured into the sample collector containing pH 3.6, 10 mM citric buffer until the required obscuration was reached. All samples were analyzed in duplicate. The results were subjected to a one-way analysis of variance (ANOVA). Individual treatments were compared using Fisher's least significant difference (LSD) test. All statistical analysis was performed using Statgraphics Centurion XV statistical software (Herndon, VA, USA) at a significance level of $\alpha = 0.05$.

4.2.2.5 Beverage preparation

The beverage formula used to evaluate beverage cloud stability is presented in Table 4.1. Beverages were made three days after preparation of the emulsion concentrates. Seven 8 oz. clear plastic bottles were prepared from each emulsion. One bottle was used for monitoring appearance (visual), one bottle for the turbidity testing, and other five bottles for weekly MDD measurements. Beverages were stored at room temperature and analyzed weekly for four weeks.

Table 4.1 Beverage formulations.

Ingredient	Sucrose	Citric acid	Sodium benzoate	Emulsion concentrate	Yellow #6 1% solution	Distilled water
Concentration % w/w	10	0.3	0.05	2	0.3	q.s. 100

4.2.2.6 Measurement of beverage turbidity

Changes in turbidity over time were determined using a spectrophotometer (Spectronic 20, Spectronic Instrument, Inc., Rochester, NY, USA) at a wavelength of 400 nm. Since the added dye increased the absorbance tremendously, all samples had to be diluted in order to be able to read the absorbance. To prepare the dilution, 1 mL of beverage was carefully pipetted from the bottom of each bottle so as not to disturb the sample and then diluted 10 times with pH 3.6, 10 mM citric buffer. Distilled water served as the blank.

4.2.2.7 Ringing test

A white ring appears in the neck of a bottle when sufficient creaming has occurred in a beverage. Any beverage that formed a visible ring on storage was considered unstable. Both the beverage concentrates and the resulting beverages were checked for signs of ringing during storage, respectively, daily for 3 d and once per week over 4 wk.

Rings that formed were easily identified since they were white in contrast to the dyed solution.

4.3 Results and Discussions

4.3.1 Effect of pH on the formation of secondary emulsions

The pH is critical in the formation of the multilayers because it affects the sign and density of charges of biopolymers (e.g. proteins and polysaccharides). When system pH is below the *pI*, proteins take a net positive charge and otherwise they are neutral (at *pI*) or take a net negative charge. Except for chitosan, all polysaccharides used as second or third layers had a negative charge. The charge density on a biopolymer depends on its *pKa* and the pH of the continuous phase. Table 4.2 presents the *pI* or *pK*a of all biopolymers used in the present study.

Table 4.2 *pI* and *pKa* of biopolymers.

Proteins	Sodium caseinate	β-lactoglobulin	Type A gelatin
pI	4.6	4.7～5.2	7～9

Polysaccharides	Sodium alginate	Chitosan	ι-carrageenan	Pectin
pKa	3.3～3.6	6.3～7.0	2.0	3.5～4.5

Figure 4.4 shows the charge reversal of β-lactoglobulin-carrageenan (LC) secondary emulsions when changing pH (3.6 vs. 6.2) or upon the addition of negatively charged carrageenan. At pH 3.6, the primary emulsion had a ζ-potential of *ca*. + 52.9 mV imparted by β-lactoglobulin due to the net positive charge below its *pI*, whereas at pH 6.2, the primary emulsion had a ζ-potential of *ca*. -29.1 mV due to the net negative charge of β-lactoglobulin above its *pI*. At both pHs, the ζ-potential of emulsions decreased with increasing carrageenan concentrations. In the system at pH 3.6, there was a reversal of ζ-potential upon the addition of carrageenan indicating interactions between β-lactoglobulin and carrageenan – essentially the neutralization of the positive protein charge and dominance of the carrageenan negative charge. Further addition of carrageenan led to a negative ζ-potential introduced by sulfate groups of the carrageenan.

In the system at pH 6.2, the ζ-potential of the emulsions also decreased with increasing carrageenan concentrations. This phenomenon could be explained by the attractive forces between β-lactoglobulin and carrageenan, e.g., hydrogen bonding, hydrophobic interactions and electrostatic interactions between sulfate and amine groups. These interactions are weaker compared to the strong electrostatic interactions in the system at pH 3.6. Interestingly at both pHs the ζ-potential slightly increased when the carrageenan concentration increased from 0.2 to 0.4% w/w. These data clearly show that anionic carrageenan molecules adsorbed to the surface of the cationic protein-coated droplets until a critical carrageenan concentration was reached. It is quite understandable that when the droplet surfaces were completely coated with carrageenan molecules,

further adsorption was prevented due to saturation of all the available cationic sites, electrostatic repulsion between adsorbed and non-adsorbed carrageenan molecules, or steric hindrance (27).

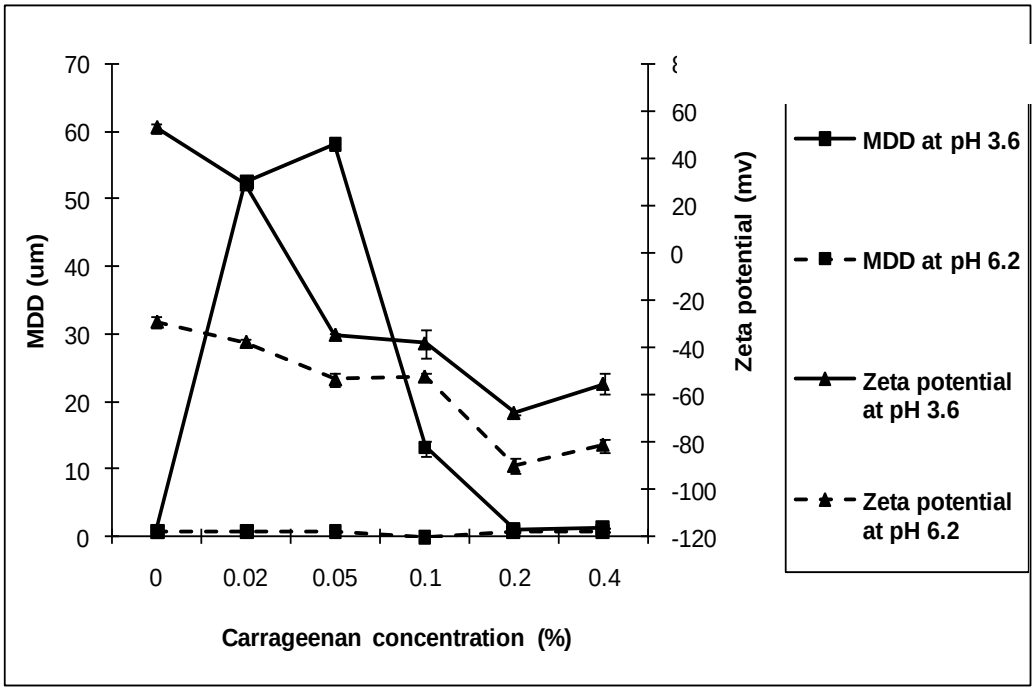

Figure 4.4 Charge reversal on pH changes; β-lactoglobulin-carrageenan multilayer emulsions with 0.25% β-lactoglobulin and 5% oil phase.

The effect of pH on β-lactoglobulin-carrageenan interactions also can be elucidated by measuring droplet size changes (Figure 4.4). At pH 6.2, emulsion MDD was relatively stable (*ca.* 0.67 μm) and is independent of carrageenan concentration, which suggests there is no strong interaction between carrageenan and the droplet surface of the primary

emulsions. In contrast, at pH 3.6 with increasing concentration of carrageenan, the emulsion MDD increased first and then decreased to a plateau value (*ca.* 1.18 μm). The concentration of carrageenan corresponding to the plateau value agreed with that where emulsions reached the lowest ζ-potential. The changes in both MDD and ζ-potential suggest that an interfacial complex of β-lactoglobulin-carrageenan (LC) was formed. The impact of polysaccharide concentration on droplet size of secondary emulsions is discussed in detail in Section 4.3.2.

4.3.2 Effects of biopolymer concentration on the formation of secondary emulsions

Different biopolymers with variable concentrations were added to β-lactoglobulin or sodium caseinate stabilized primary emulsions in order to form secondary emulsions. Figure 4.5 shows the effects of polysaccharide concentration on ζ-potential and MMD of secondary emulsions stabilized by β-lactoglobulin-pectin (LP) and β-lactoglobulin-alginate (LA). With increasing biopolymer concentration, LP and LA emulsions have similar pattern in terms of MDD and ζ-potential. The sharp decrease of ζ-potential at low concentrations of pectin and alginate illustrated strong electrostatic interactions between β-lactoglobulin and polysaccharides. Charge reversal occurred with adding 0.02 ~ 0.05% w/w polysaccharides. Alginate imparted more negative charge to the interface than pectin due to the high degree of esterification (60%) of the pectin and thus, less carboxyl groups were available. The MDD of the LA system decreased from 136 μm at 0.1% w/w alginate

to 1.2 μm at 0.4% w/w alginate. The MDD of the LP system was quite small (*ca.* 0.65 μm) at 0.02% w/w pectin, but increased to 10 ~ 20 μm at 0.05 ~ 0.4% w/w pectin.

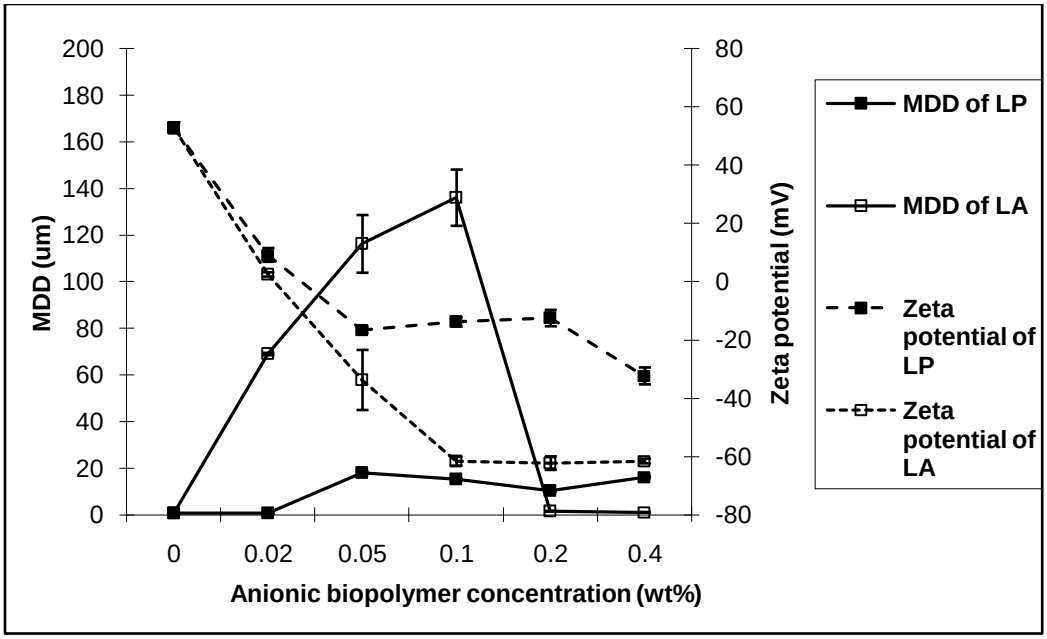

Figure 4.5 Effects of pectin and alginate concentration on MDD and Zeta-potential of LA, and LP; emulsions contained 0.25% β-lactoglobulin and 5% oil phase; β-lactoglobulin-pectin, LP, and β-lactoglobulin-alginate, LA.

Figure 4.6 shows the effects of polysaccharide concentration on the ζ-potential and MDD of secondary emulsions made of sodium caseinate-pectin (SP), sodium caseinate-alginate (SA), and sodium caseinate-carrageenan (SC). When polysaccharide concentration was above 0.2% w/w, the MDD was relatively unchanged. SP, SA, and SC multilayered emulsions showed larger MDD (2.8 ~ 5.4 μm) than LC and LA.

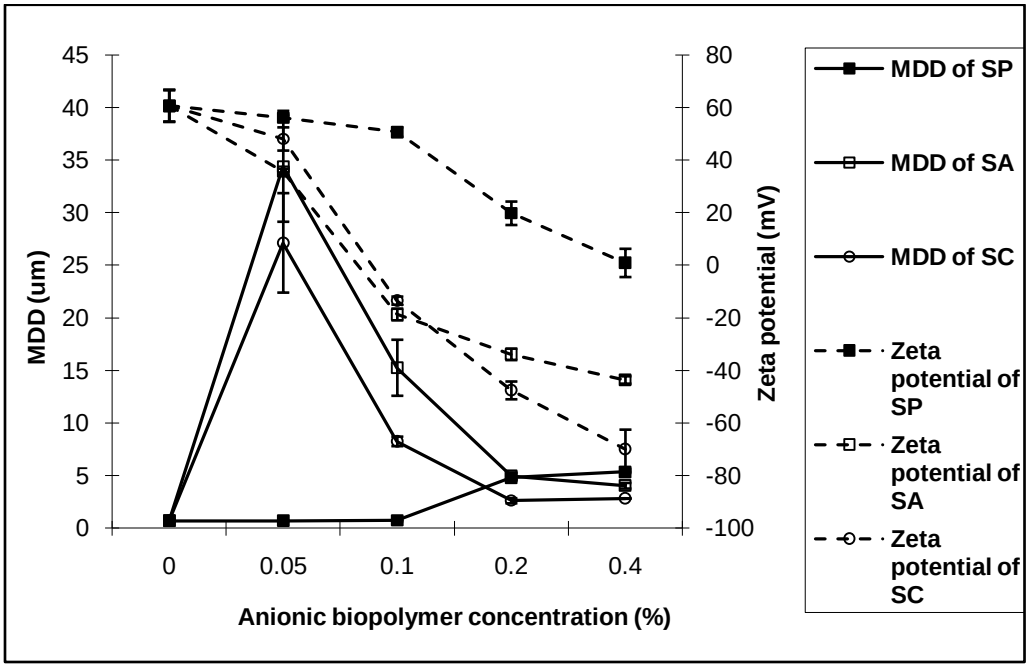

Figure 4.6 Effect of polysaccharide concentration on MDD and Zeta-potential of SP, SA and SC: emulsions contained 0.5% sodium caseinate and 5% oil phase; caseinate-pectin, SP, sodium caseinate-alginate, SA, and sodium caseinate-carrageenan, SC.

While both protein and gum arabic have good emulsification properties, they have different primary stabilization mechanisms, i.e. steric and electrostatic forces. At pH 3.6, gum arabic takes on a net negative charge and interacts with sodium caseinate or β-lactoglobulin assuming there is no competition for absorbing onto the droplet surface between these emulsifiers. Therefore, it is of interest to investigate protein-gum arabic interactions on the particle interface. Figure 4.7 shows the effect of gum arabic concentration on MDD and ζ-potential of sodium caseinate-gum arabic (SG) and β-

lactoglobulin-gum arabic (LG) multilayered emulsions. LG showed a smaller MDD and lower ζ-potential than SG at 0.5% w/w gum arabic.

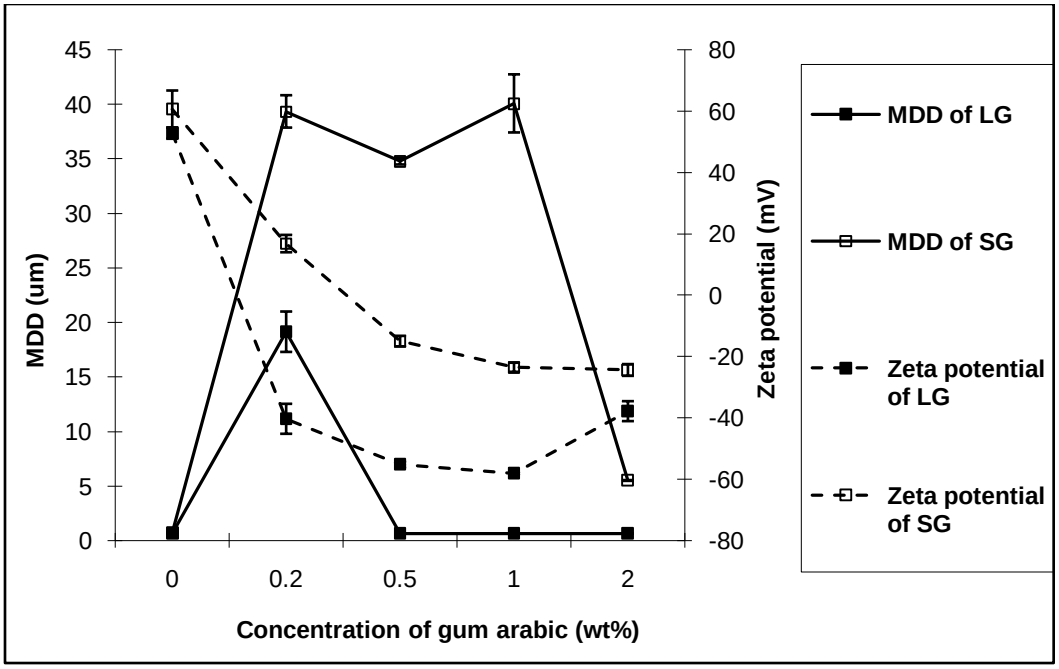

Figure 4.7 Effect of gum arabic concentration on MDD and Zeta-potential of LG and SG; emulsions contained 0.25% β-lactoglobulin or 0.5 sodium caseinate, and 5% oil phase; sodium caseinate-gum arabic, SG) and β-lactoglobulin-gum arabic, LG.

Figures 4.5, 4.6 and 4.7 demonstrated that anionic biopolymer concentration (C_{bp}) is crucial to form secondary emulsions with small MDDs. More specifically, only when C_{bp} is above a critical level, can secondary emulsions with small MDDs be created. Results show that alginate and carrageenan have a critical C_{bp} of 0.2% w/w, whereas gum arabic has a critical of C_{bp} 0.5% w/w. The concept of critical C_{bp} has been reported in

literature (26, 27) as the saturation concentration of a polysaccharide on the particle interface (C_{Sat}). When the polysaccharide concentration is insufficient to completely saturate the droplet surface, bridging flocculation occurs. Without complete coverage by a secondary polysaccharide layer, oil droplets would have both positive and negative patches on the surfaces, which promote droplet aggregation upon collision. It is also suggested that when free polysaccharide concentration in the continuous phase is high and exceeds a critical value (C_{Dep}), depletion flocculation occurs because the attractive depletion forces are strong enough to overcome the various repulsive forces (e.g., electrostatic and steric). Therefore, to produce a stable multilayered emulsion against bridging and depletion flocculation, it is necessary to ensure $C_{Sat.} < C_{bp} < C_{Dep.}$ In this present study, the polysaccharide concentrations were well below $C_{Dep,}$ so no depletion flocculation was observed.

Interestingly, pectin was not functional in this application: emulsions with large MMD were formed with both β-lactoglobulin and sodium caseinate resulting in rapid phase separation. The large MDDs of LP and SP emulsions may be attributed to the low charge density of the pectin due to its high degree of esterification of pectin (60%) and *pKa* close to that of the system (3.6). After careful examination of the ζ-potential changes with increasing polysaccharide concentration, it was found LP showed smaller and slower changes than LA or LC indicating weaker electrostatic interactions with the β-lactoglobulin. We postulate that this weak interaction might promote droplet aggregation during mixing and homogenization. To the contrary, interactions of β-lactoglobulin-

carrageenan and β-lactoglobulin-alginate were strong demonstrated by a sharp decrease in ζ-potential with increasing concentration of carageenin or alginate, which is also reported by Harnsilawat et al. (15) in a model beverage emulsion.

As one might expect, protein types also affected the formation and stability of multilayered emulsions. β-lactoglobulin showed better performance in forming protein-polysaccharide interfacial complexes as was reflected by much smaller MDDs of LA, LC and LG (0.65 ~ 1.18 μm) than those of SA, SC and SG (2.8~ 5.4 μm). Although both proteins have similar *pI*, their differences in molecular structure and conformation at the interface may account for the difference in interactions. Sodium caseinate has minimal solubility and charge density at pH 3.7 ~ 4.6 (31, 32) which is close to the system pH (3.6). This low pH reduces emulsifying efficacy of sodium caseinate (33, 34) and promotes irreversible droplet aggregation (32). This may explain the larger MDDs and poor stability of sodium caseinate-polysaccharide multilayer emulsions at acidic conditions.

4.3.3 Effects of biopolymer concentration on the formation of tertiary emulsions

Since β-lactoglobulin was more effective than sodium caseinate in forming secondary emulsions, only β-lactoglobulin was used as primary emulsifier in the study of tertiary emulsions. Chitosan and gelatin were used in forming the tertiary layer of the emulsions: β-lactoglobulin-gum arabic-chitosan (LGCh), β-lactoglobulin-gum arabic-

gelatin (LGGe), and β-lactoglobulin-carrageenan-gelatin (LCGe). Figure 4.8 shows the effects of tertiary cationic biopolymer concentration on the MDD and ζ-potential of LGCh, LGGe, and LCGe. LGGe and LCGe showed relatively large MDDs (26.6 and 110.7 μm, respectively) and small ζ-potentials. Changes in the ζ-potential of LGGe (68.9 mV) and LCGe (39.26 mV) upon adding 0.4% w/w gelatin is much smaller than that of LGCh (140 mV) upon adding 0.4% w/w chitosan. The LGCh emulsion gave the best results providing an emulsion with a MDD of 2.8 um when 0.4% w/w chitosan was used in the system. This difference between gelatin and chitosan indicates chitosan has strong interactions at the secondary emulsion interface whereas gelatin has weak interactions.

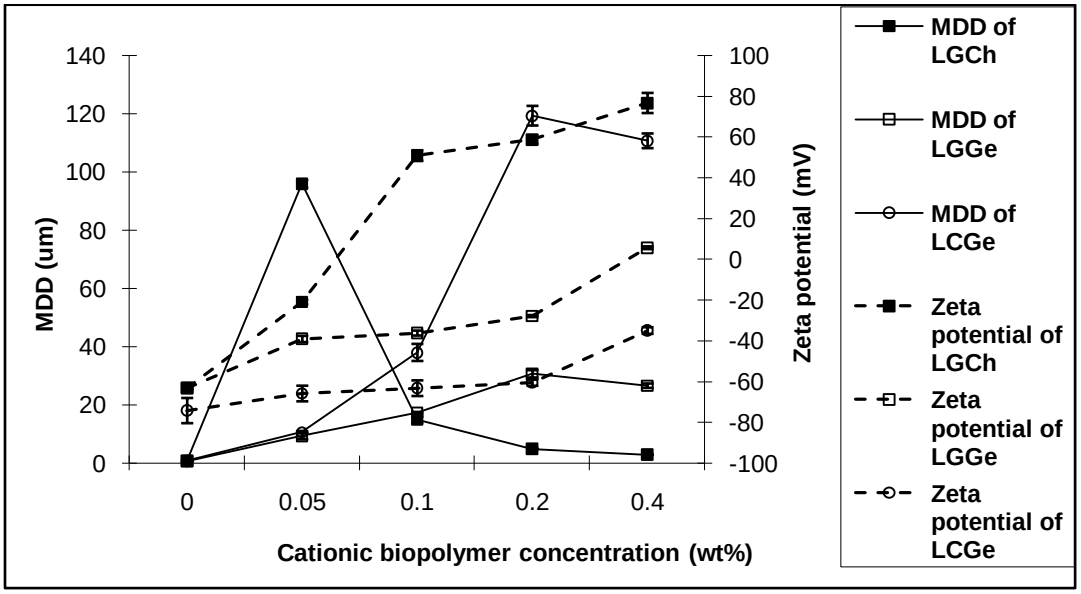

Figure 4.8 Effect of chitosan and gelatin concentration on tertiary emulsion formation; emulsions contained 0.25% β-lactoglobulin and 0.5% gum arabic or 0.2% carrageenan; β-lactoglobulin-gum arabic-chitosan, LGCh; β-lactoglobulin-gum arabic-gelatin, LGGe; and β-lactoglobulin-carrageenan-gelatin, LCGe.

Type-A Gelatin used in this study has a *pI* of 7~ 9, which suggests it should be highly charged at pH 3.6. Thus, one would expect gelatin to strongly interact at the interface of secondary emulsions and show charge reversal at low concentrations of gelatin. The fact that this was not observed is not understoodt. The use of gelatin in this study was inspired by the fact that gelatin and gum arabic are commonly used to prepare complex coacervates through electrostatic interactions at acid conditions (35, 36). However, our data on ζ-potential indicated that gelatin did not adsorb well to the surface of secondary layer. We propose that the strong repulsive electrostatic interactions between gelatin molecules prevented deposition of gelatin at the particle interface.

4.3.4 Multilayered emulsions in beverage cloud applications

As noted in this thesis, multilayered emulsions of LA, LG, LC and LGCh were successfully produced with small MDDs indicating potential in beverage clouds applications. Thus, it was of interest to compare their performance to traditional emulsifiers, i.e. gum arabic (G) and modified starch (M), in stabilizing beverage cloud emulsions. Table 4.3 shows the biopolymer compositions and concentrations of emulsions with single (G and M), double (LG, LA and LC) and tertiary (LGCh) layers of interfacial complexes.

Table 4.3 Biopolymer compositions of emulsions for stability testing.

Emulsions	Biopolymer concentration (% w/w)
G	gum arabic 16
M	modified starch 12
LG	β-lactoglobulin 0.25, gum arabic 0.5
LA	β-lactoglobulin 0.25, sodium alginate 0.4
LC	β-lactoglobulin 0.25, carrageenan 0.2
LGC	β-lactoglobulin 0.25, gum arabic 0.5, chitosan 0.4

Figure 4.9 shows changes in MDD of beverage clouds during four weeks of storage at room temperature. The MDDs of emulsions G, M, LA, LC and LG were stable during storage while the MDD of LGCh increased and exhibited excessive variation. After four-weeks of storage, LGCh had a MDD of 2.2 μm, whereas G, M, LC and LG had MDDs 0.68, 0.67, 0.82, and 0.65 μm, respectively. It is interesting that LA showed a significant decrease in MDD during storage with an initial MDD of 1.04 μm and then 0.90 μm after 4 weeks. Reiner et al (10) reported similar phenomenon in orange oil terpene-based beverages and proposed that loss of biopolymers from the surface of oil droplets in diluted solutions caused the decrease in MDD. This would most likely occur for protein-polysaccharide interfacial complexes with weak electrostatic interactions. The large variations observed in MDD for LGCh tertiary emulsions suggest that the interfacial complexes are not stable and the reproducibility of their preparation is poor.

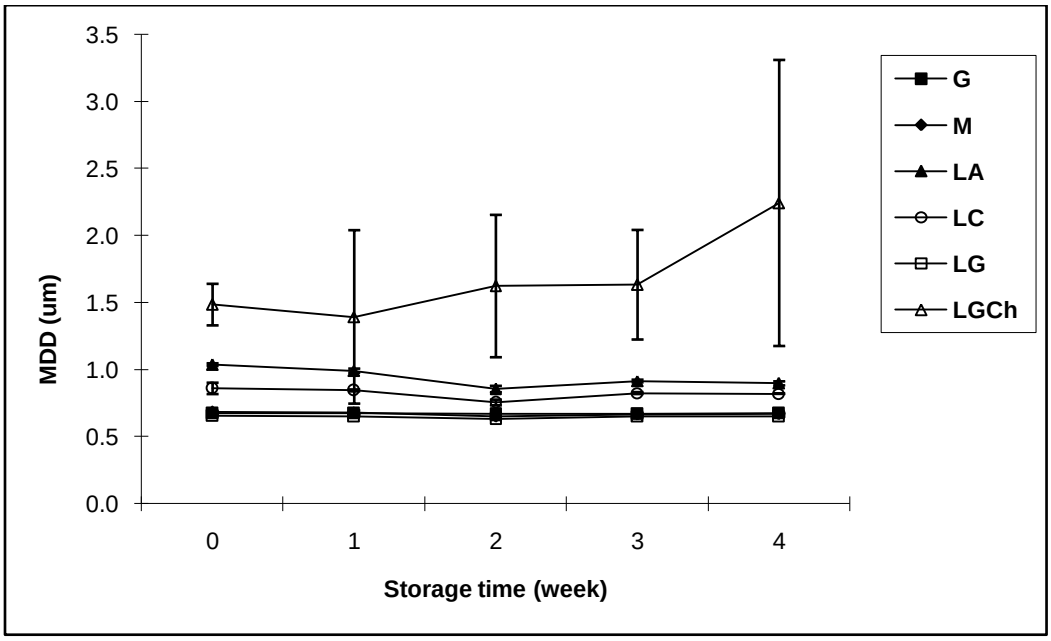

Figure 4.9 Changes in MDD of beverage clouds during storage at room temperature.

The observation of variable MDD of tertiary emulsions was also reported in other studies (23, 27). This is inherently associated with the process of producing tertiary emulsions. An issue in producing tertiary emulsions is the disruption of interfacial structure during mixing, sonication or low pressure homogenization. The orientation of biopolymer molecules on the interface may be affected by intense mechanical shear causing interfacial rearrangement of macromolecules. On the other hand, without mechanical shear, the flocs promote droplet aggregation and thus destabilize tertiary emulsions. Therefore, the process to prepare tertiary emulsions from secondary emulsions has to be optimized to obtain smaller MDD without changing interfacial structures considerably.

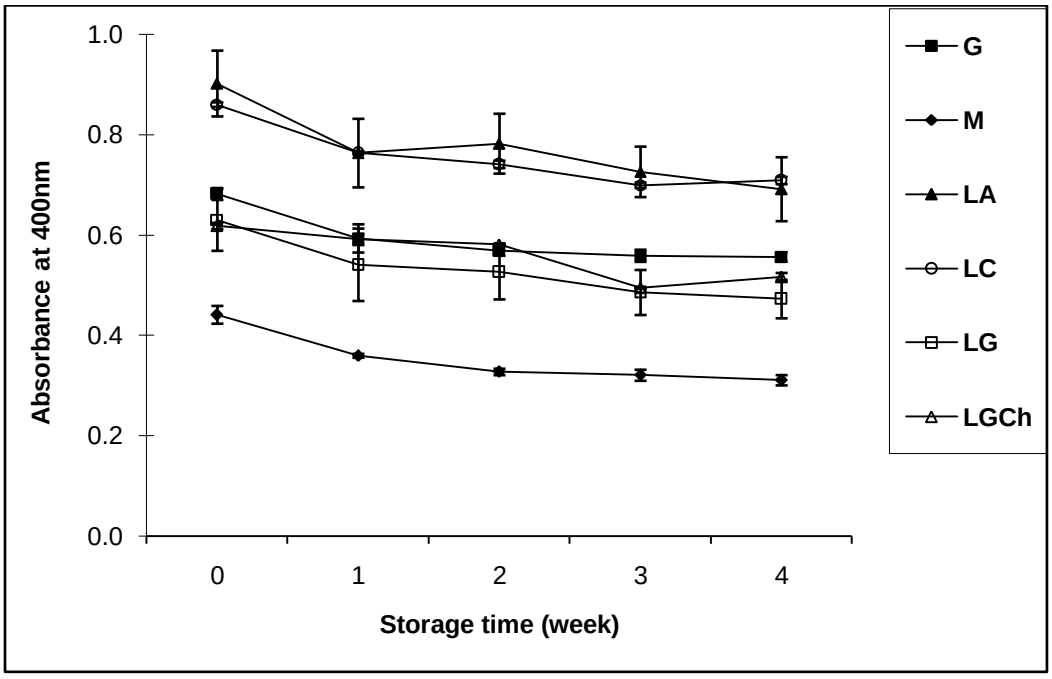

Figure 4.10 Changes in turbidity (absorbance) of beverage clouds during storage at room temperature.

During storage, all beverage clouds lost significant absorbance (turbidity, Figure 4.10). Absorbance decreased most quickly during the first week of storage and then the rate of slowed on further storage. In terms of clouding ability, initially, LA and LC have the highest absorbance, G and LG have the second highest absorbance, and M had the lowest absorbance. After four weeks of storage, GA, MS, LA, LC, LG, and LGC lost absorbances of 18.4, 27.6, 21.9, 18.7, 24.9 and 16.5%, respectively (Figure 4.11). Statistically, GA, LA, LC and LGCh showed the same loss of absorbance whereas MS

and LG had the same loss. It should be mentioned that turbidity measurements have somewhat large variability which is inherently associated with the method of sampling.

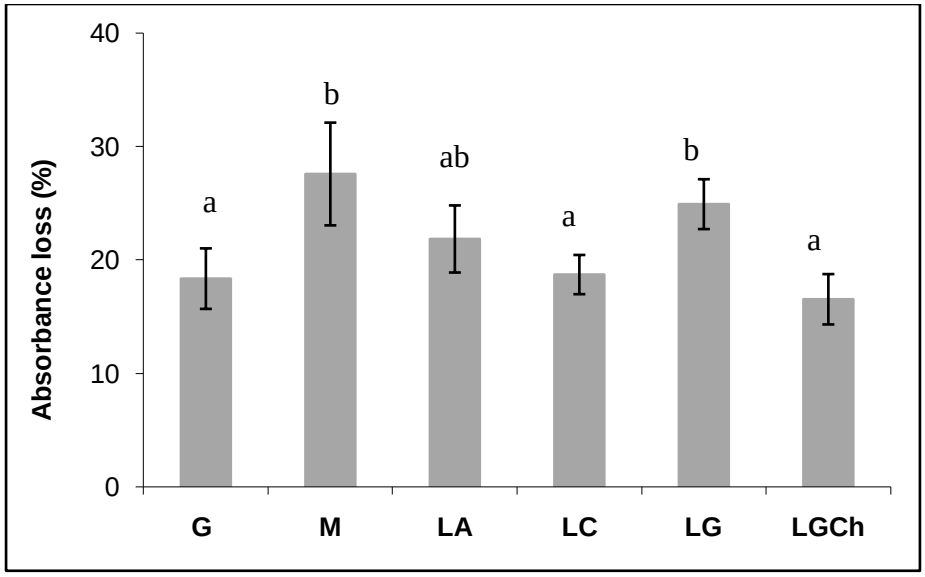

Figure 4.11 Loss of turbidity (absorbance) of beverage clouds after 4 weeks of storage at room temperature; different letters stands for significant difference in absorbance loss.

The loss of turbidity on storage is a common phenomenon in diluted beverage emulsions and has been reported in literature (5, 6, 8, 10). In the present study, this is most likely due to creaming. The rate of turbidity loss depends on the creaming velocity which is accelerated by emulsion flocculation, coalescence and Ostwald ripening. Interestingly, LGCh had the largest MDD but the lowest loss of absorbance. While this is counter intuitive, this may be attributed to the thick interfacial layer and electrostatic repulsive forces preventing droplets from destabilization by flocculation and coalescence

and thus, reducing the creaming velocity of the droplets. This observation demonstrates that particle size is not always a good predictor of emulsion stability.

Figure 4.12 shows the images of beverage clouds after 4 weeks of storage at room temperature. No ringing occurred for G, M, LA, LC, and LG, which suggests that secondary emulsions are as stable as conventional emulsions (at least within the storage period observed in this study). It was difficult to conduct the ring test in the LGCh beverage because we could not use the dye in this system due to its incompatibility with chitosan. Nevertheless, while the ring test may be less sensitive in this beverage, no ringing was observed. Our results suggest that multilayer emulsions with low biopolymer usage levels may have the potential to replace gum arabic and modified starch as stabilizers in beverage cloud emulsions. One must recognize that using a protein in this application has other impacts in terms of potential flavor interactions (Maillard reactions), allergen labeling, and pH or salt sensitivity.

Figure 4.12 Images of beverage clouds after 4 weeks of storage at room temperature; from left to right: G, M, LA, LC and LG; LGCh not shown due to incompatibility of yellow # 6 and chitosan in the beverage.

4.4 Conclusions

This study has shown that secondary and tertiary emulsions suitable for beverage cloud applications could be produced using the LBL deposition technique. The interfacial complex is formed by protein-polysaccharide electrostatic interactions. Consistent with the literature, pH and biopolymer concentrations are crucial for producing stable multilayered emulsions. Biopolymer concentration has to be within an optimal range to prevent bridging and depletion flocculation. Protein and polysaccharide types also affect the formation and stability of multilayered emulsions. Electrical characteristics of the interfacial complex are determined by the charge density of the proteins and

polysaccharides governed by solution pH and biopolymer type. Results of limited stability testing suggests that multilayer emulsions stabilized by protein-polysaccharide complexes could provide the same stability as monolayer emulsions stabilized using conventional emulsifiers in beverage applications.

While the literature suggests that multilayer emulsions are quite stable to environmental stresses, e.g., pasteurization, high mineral content, etc., these factors need to be evaluated for the specific emulsifier systems developed in this study.

References

[1] Tan C.T. Beverage emulsions. In: Friberg SE, Larsson K, editors. *Food emulsions*. 3rd ed. New York, N.Y.: Marcel Dekker, **1997.**

[2] Reineccius G.A. Flavor chemistry and technology. 2nd ed. Boca Raton, FL: CRC Press, **2006.**

[3] Tan, C. T. Beverage flavor emulsion-a form of emulsion liquid membrane encapsulation. In *Food Flavors: Formation, Analysis and Packaging Influences*; Contis, E. T., Ed.; New York: Elsevier, **1998.**

[4] Tan, C. T. Beverage emulsions. In *Food Emulsions*; Friberg, S. E., Larsson, K., Sjoblom, J., Eds.; New York: Dekker, **2004.**

[5] Buffo, R.; Reineccius, G.A. Shelf-life and mechanisms of destabilization in dilute beverage emulsions. *Flavour Frag. J.* **2001,** 16, 7-12.

[6] Tse K-Y, Reineccius G.A. In *Flayor Technology* (ACS Symposium Series No. 610), Ho C-T, Tan C-T, Hsiang C-H (eds). American Chemical Society: Washington, DC, **1995,** 172–182.

[7] Chanamai, R.; McClements, D. J. Impact of weighting agents and sucrose on gravitational separation of beverage emulsions. *J. Agric. Food Chem.* **2000**, *48*, 5561-5565.

[8] Tse, K. Y.; Reineccius, G. A. Methods to predict the physical stability of flavorscloud emulsion. *Flavor Technol.* **1995**, *610*, 172-182.

[9] Given, P. Encapsulation of flavors in emulsions for beverages. *Curr. Opinion Colloid Interface. Sci.* **2009,** 14, 43-47.

[10] Reiner, S.; Reineccius G.A; Peppard, T. A comparison of the stability of beverage cloud emulsions formulated with different gum Arabic- and Starch-based emulsifiers. *JFS.* **2010,** 75, E236-246.

[11] Anderson, D. M. W.; Howlett, J. F.; McNab, C. G. A. The amino acid composition of the proteinaceous of Acacia senegal gum. *Carbohydr. Res.* **1985,** 2, 104-114.

[12] Jayme, M. L.; Dunstan, D. E.; Gee, M. L. Zeta potential of gum arabic stabilized oil-in-water emulsions. *Food Hydrocolloid.* **1999,** 13, 459-465.

[13] Goodrum, L. J.; Patel, A.; Leykam, J. F.; Kieliszewski, M. J. Gum arabic glycoprotein contains glycomodules of both extension and arabinogalactan-glycoproteins. *Phytochemistry*, **2000,** 54, 99-106.

[14] Buffo, R.; Reineccius, G.A.; Oehlert G. Factors affecting the emulsifying and rheological properties of gum acacia in beverage emulsions. *Food Hydrocolloid*. **2001,** 15, 53-66.

[15] Harnsilawat, T.; Pongsawatmanit, R.; McClements D.J. Stabilization of model beverage cloud emulsions using protein-polysaccharide electrostatic complexes formed at the oil-water interface. *J Agric. Food Chem.* **2006,** 54, 5540-5547.

[16] Trubiano, P. C. The role of specialty food starches in flavor emulsions. *Flavor Technol.* **1995,** 610, 199-209.

[17] Kim, Y. D.; Morr, C. V.; Schenz, T. W. Microencapsulation properties of gum arabic and several food proteins: liquid orange oil emulsion particles. *J. Agric. Food Chem.* **1996,** 44, 1308-1313.

[19] McNamee, B.; O'Ridrdan, E.; O'Sullivan, M. Effect of partial replacement of gum Arabic with carbohydrates on its microencapsulation properties. *J. Agric. Food Chem.* **2001,** 49, 3385-3388.

[20] Chanamai, R.; McClements, D. J. Comparison of gum arabic, modified starch, and whey protein isolate as emulsifiers: influence of pH, CaCl2 and temperature. *JFS*, **2002,** 67, 120-125.

[21] Djordjevic, D.; Cercaci, L.; Alamed, J.; McClements, D.J., and Decker, E.A. Chemical and physical stability of citral and limonene in sodium dodecyl sulfate-chitosan and gum Arabic-stabilized oil-in-water emulsions, *J. Agric. Food Chem.* **2007,** 55, 3585-3591.

[22] Klinkesorn, U.; Sophanodora, P.; Chinachoti, P.; Decker, E.A.; and Mcclements, D.J. Encapsulation of emulsified tuna oil in two-layered interfacial membranes prepared using electrostatic layer-by-layer deposition. *Food Hydrocolloid.* **2005,** 19, 1044-1053.
[23] Aoki, T.; Decker, E.A; Mcclements, D.J. Influence of environmental stresses on stability of O/W emulsions containing droplets stabilized by multilayered membranes produced by a layer-by-layer electrostatic deposition technique, *Food Hydrocolloid.* **2005,** 19, 209-220.
[24] Thanasukarn, P., Pongsawatmanit, R., Mcclements, D.J. Interfacial deposition technique to improve freeze-thaw stability of oil-in-water emulsions, *Food Res. Int.* **2006,** 39, 721-729.
[25] Surh, J.; Yeun, S.G.; Decker, E.A.; Mcclements, D.J. Influence of Environmental stresses on stability of O/W emulsions containing cationic droplets stabilized by SDS-Fish gelatin membrances, *J. Agric. Food Chem.* **2005,** 53, 4236–4244.
[26] Guzey, D.; McClements, D.J. Formation, stability and properties of multilayer emulsions for application in the food industry. *Adv. Colloid Interface Sci.* **2006,** 128-130, 227-248.
[27] Guzey, D. Utilization of interfacial engineering to improve food emulsion properties. Ph.D. thesis. Department of Food Science, University of Massachusetts, **2006.**
[28] Ai, H.; Jones, A.; Lvov, Y. Biomedical applications of electrostatic layer-by-layer nano-assembly of polymers, enzymes, and nanoparticles. *Cell Biochem. Biophys.* **2003,** 39, 23-43.
[29] Ogawa, S.; Decker, E.A.; McClements, D.J. Influence of environmental conditions on stability of O/W emulsions containing droplets stabilized by lecithin–chitosan membranes. *J. Agric. Food Chem.* **2003,** 51, 5522–5527.
[30] Gu, Y.S.; Decker, E.A.; and Mcclements, D.J. Application of multi-component biopolymer layers to improve the freeze-thaw stability of oil-in-water emulsions: β-lactoglobulin-ι-carrageenan-gelatin. *J. Food Eng.* **2007,** 80, 1246-1254.

[31] Jahaniaval, F.; Kakuda, Y.; Abraham, V.; Marcone, M. Soluble protein fractions from pH and heat treated sodium caseinate: physicochemical and functional properties. *Food Res. Int.* **2000,** 33, 637-647.

[32] Surh, J.; Decker, E.; McClements, D. Influence of pH and pectin type on properties and stability of sodium caseinate stabilized oil-in-water emulsions. *Food Hydrocolloid.* **2006,** 20, 607-618.

[33] AI-Hakkak, J.; Kavale, S. Improvement of emulsification properties of sodium caseinate by conjugating to pectin through the Maillard reaction. In: *The Maillard reaction in food chemistry and medical science*. International Congress Series, **2002,** 1245, 491-499.

[34] Lee, S.; Morr, C.; Ha, E. Structural and functional-properties of caseinate and whey-protein isolate as affected by temperature and pH. *JFS.* **1992,** 57, 1210-1214.

[35] Leclercq, S.; Milo, C.; Reineccius, G. Effects of cross-linking, capsule wall thickness, and compound hydrophobicity on aroma release from complex coacervate microcapsules. *J. Agric. Food Chem.* **2009,** 57, 1426-1432.

[36] Paetznick, D.; Reineccius, G. Shelf life and flavor release of coacervated orange oil. In: *Micro/Nanoencapsulation of active food ingredient*. Huang, Q.; Given, P.; Qian, M.; Eds. ACS Symposium Series, **2009,** 1007, 272-286.

Chapter 5

Preparation, Characterization and Beverage Cloud Applications of Water/Oil/Water Emulsions

The objective of this study was to use a concentrated sucrose solution as a natural weighing agent to increase the density of the oil phase by forming water-in-oil-in-water (W/O/W) double emulsions (also called multiple emulsions). Double emulsions were characterized by transmission electron microscopy, confocal microscopy and a particle size analyzer. Lipophilic and hydrophilic emulsifiers, process parameters and the stability of double emulsion concentrates and dilutes were evaluated.

The results indicated that mean droplet diameter (MDD) of W/O emulsions decreased with increasing emulsifier (polyglycerol polyricinoleate, PGPR) concentration. Homogenization pressure and number of passes through a microfluidizer affected MDD, size distribution and encapsulation efficiency (EE) of yellow #6 (included in the water phase as a marker of encapsulation efficiency). The hydrophilic emulsifier type and oil phase type had a large effect on EE and stability of the W/O/W emulsion concentrates and diluted emulsions. A high EE (>85%) was achieved in gum acacia (GA) stabilized double emulsions whereas Tween 20 and modified starch (MS) stabilized double emulsions showed low EE (< 50%) demonstrating that the type of hydrophilic emulsifier is a critical factor governing stability of double emulsions. Gelling the inner aqueous phase proved to be ineffective in improving EE and stabilizing the double emulsion in this present study. In contrast, double emulsions containing gelled water droplets tended to have wider size distributions and lower stability compared to those without gelatin.

Results on beverage cloud applications of double emulsions indicated that GA stabilized emulsions are more stable to turbidity loss and ring formation than those

stabilized by MS. Beverage clouds containing OT-based W/O/W emulsions without gelling the inner phase showed low turbidity loss during shelf-life without ring formation demonstrating potential commercial value of these emulsions. However, more research is needed to better understand the destabilization of double emulsions and improve their stability during long-term storage.

5.1 Introduction

Double emulsions, also called multiple phase emulsions, are a complex dispersion system in which the droplets of one dispersed phase are further dispersed in another phase (1, 2). Water-in-oil-in-water (W/O/W) emulsions (Figure 5.1) are the most common double emulsions. They are created using conventional homogenization in a two-step process. First, a W/O primary emulsion is prepared by homogenizing an oil phase and an aqueous phase in the presence of a lipophilic emulsifier; second, a W/O/W secondary emulsion is prepared by homogenizing the W/O emulsion with another aqueous phase in the presence of a hydrophilic emulsifier (3-5). Lipophilic and hydrophilic emulsifiers absorb at the interfaces of W/O and O/W, respectively, and form thick films which govern the stability of the double emulsions.

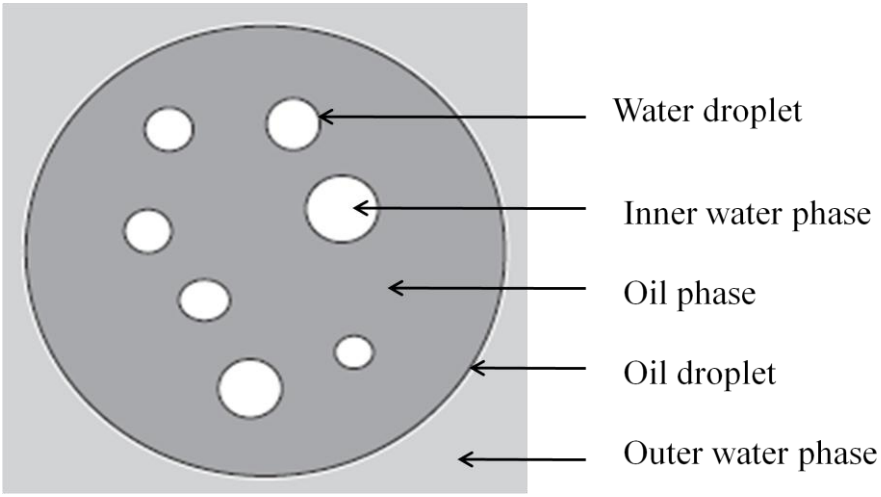

Figure 5.1 Schematic representative of W/O/W emulsions.

Increasing attention has been devoted to W/O/W emulsions due to their unique multiple compartment structure and potential applications (6, 7). W/O/W emulsions show potential applications for the controlled release of chemical substances initially entrapped in the internal droplets. They are mostly investigated as vehicles for various hydrophilic drugs (vaccines, vitamins, enzymes, hormones, etc.) that would be slowly released from inner to outer aqueous phase (5, 8-10). W/O/W emulsions are also promising in food applications mainly with relation to their capability to encapsulate water-soluble actives in the inner compartment (7, 11, 12). Several new food products based on W/O/W emulsions have been patented, such as reduced fat mayonnaise (partial replacement of fat with the aqueous compartments) and salted creams (encapsulation of salt) (13-15).

The stability of W/O/W emulsions is a major concern in practical applications (2, 12) and several methods have been proposed to improve their stability. The methods can be summarized as three categories: stabilizing the W/O interface (16-18), modifying the oil phase (19-21), and stabilizing the O/W interface (22-25). It has also been proposed that stability might be increased by thickening or gelling the inner, aqueous phase, especially if a network is formed through the inner water droplets (3). Muschiolik et al. (26) reported significant droplet size reduction of double emulsions by incorporating gelatin in the inner aqueous phase. Surh et al. (3) also reported a slight increase in encapsulation efficiency of selected marker compounds in the water droplets by gelling

the inner aqueous phase with whey protein isolated after heat treatment. However, studies on long-term stability and encapsulation efficiency of W/O/W emulsions are rare.

The overall objective of present study was to investigate the stability of W/O/W emulsions containing sucrose and gelatin in the inner phase and their applications as beverage clouding agents. This type of emulsion potentially can offer two advantages: 1) potentially eliminate weighing agents (e.g., ester gum) from the product label; and 2) produce more stable emulsions since a saturated sucrose solution has a density of 1.32 g/mL: this is considerably more dense than the traditional weighting agent – ester gum (1.08 g/mL). In this study, a concentrated sucrose solution was used as the inner aqueous phase with and without gelatin to prepare W/O/W emulsions. Adding gelatin to the inner phase provided the opportunity to evaluate the effect of gelling the inner phase on the stability of double emulsions. Both orange oil terpenes (OT) and medium chain triglycerides (MCT) were investigated as the oil phase. Different hydrophilic emulsifiers including Tween 20, modified starch (MS), and gum arabic (GA) were compared in terms of producing stabilize double emulsions. The primary process parameters for preparing secondary emulsions, i.e. process pressure and number of passes through homogenizer (critical parameters controlling particle size and encapsulation efficiency of double emulsions) were investigated. Finally, the stability of both W/O/W emulsion concentrates and diluted forms were evaluated to determine commercial feasibility as beverage clouding agents.

5.2 Materials and Methods

5.2.1 Materials

Orange oil terpenes were obtained from Citrus and Allied Essences Ltd. (Lake Success, NY, USA) and Miglyol®812, a medium chain triglyceride (MCT), was purchased from Sasol (Houston, TX, USA); Miglyol 812 is a combination of triglycerides based on the following fatty acid composition: $C_{6:0}$ max. 2%; $C_{8:0}$ 50% to 65%; $C_{10:0}$ 30% to 45%; $C_{12:0}$ max. 2% and $C_{14:0}$ max. 1% (Sasol, Houston, TX, USA, data from technical sheet). The orange oil terpenes used were comprised primarily of limonene (95.6%); myrcene (2.8%); sabinene (2.8%); α-pinene (0.9%); and octanal (0.2%) as measured by gas chromatography. TIC Gums, Inc. (Belcamp, MD, USA) donated samples of prehydrated gum acacia spray dry FCC powder (GA). Modified starch (Purity Gum™ 1773, MS) was donated by National Starch Corp. (Bridgewater, NJ, USA). Polyglycerol polyricinoleate (PGPR) was purchased from Danisco (New Century, KS, USA). Granulated FD&C Yellow #6 was purchased from Sensient Colors (Milwaukee, WI, USA). Sodium hydroxide, Sodium benzoate and hydrochloric acid were purchased from Sigma Chemical Co. (St. Louis, MO, USA). Tween 20, citric acid and sodium citrate were purchased from Fisher Scientific (Fair Lawn, NJ, USA). Type A gelatin (275 Bloom strength, 20 mesh) was provided by PB-Leiner (Davenport, IA, USA).

5.2.2 Methods

5.2.2.1 Preparation of solutions

PGPR was dispersed in OT or MCT at different concentrations and stirred using a stir bar at 50 ℃ for 30 min. A 10mM citric acid/ sodium citrate buffer (pH 3.6) was used to prepare inner and outer aqueous phase. Inner aqueous phase was prepared as follows: a 60% (w/w) sucrose solution was first prepared using pH 3.6 buffer at 50 ℃, and then 4% (w/w, based on water content) gelatin was slowly added to the sucrose solution at 75 – 80 ℃ stirring for about 1 hr until gelatin totally dissolved, and finally 0.13% (w/w) FD&C Yellow #6 was added. The inner phase was transferred to a 50 ℃ water bath to keep it from gelling. Gum arabic and modified starch were completely hydrated using an overhead mixer (Carter® 1L.81, Carter Motor, IL, USA) stirred for 2 hrs at room temperature and then stored overnight at 4 ℃. A Tween 20 solution was prepared by adding it to the aforementioned aqueous solution and then stirring for 30 min at room temperature with a stir bar. The pH of outer aqueous phase was adjusted to pH 3.6 using hydrochloric acid or sodium hydroxide as required.

5.2.2.2 Determination of oil phase fraction

The viscosity of a sucrose solution increases exponentially with concentration while the density increases almost linearly (27). A saturated sucrose solution has *ca.* 67.8 wt% solids with a density of 1.32 g/mL at 20℃. In preliminary experiments, it was found

difficult to completely dissolve gelatin in extremely viscous sucrose solutions, therefore, a 60% w/w sucrose solution (density of 1.28 g/mL and viscosity of 44.2 mPa.s at 20℃) was chosen to prepare the inner aqueous phase. The goal of this study was to weigh the oil phase with a 60% w/w sucrose solution making the oil phase of the same density as the outer aqueous phase (i.e. a dietetic beverage, density *ca.* 1.0 g/mL). The effect of gelatin on phase density was ignored in this study. By using the Pearson's Square, the ratio of inner aqueous phase to oil phase was calculated as 45/55 for OT and 22/78 for MCT.

5.2.2.3 Preparation of W/O primary emulsions

Figure 5.2 shows the process used to prepare the w/o primary emulsions. First, the inner aqueous phase and oil phase were prepared. Yellow #6 was added to the inner aqueous phase as a marker compound to measure encapsulation efficiency (EE) of W/O/W emulsions. Emulsions without yellow #6 were also prepared as a control for color measurement. A coarse primary emulsion was prepared by premixing 45% w/w inner aqueous phase with 55% w/w OT, or 22 wt% inner aqueous phase with 78% w/w MCT using a high shear mixer (Greerco Corp., Hudson, NH, USA) at *ca*. 6,000 rpm for 2 min, and the resulting coarse emulsion was passed through a Microfluidizer (Model M-110Y, Microfluidics Corporation, Newton, MA, USA) at 12,000 psi for 1 pass.

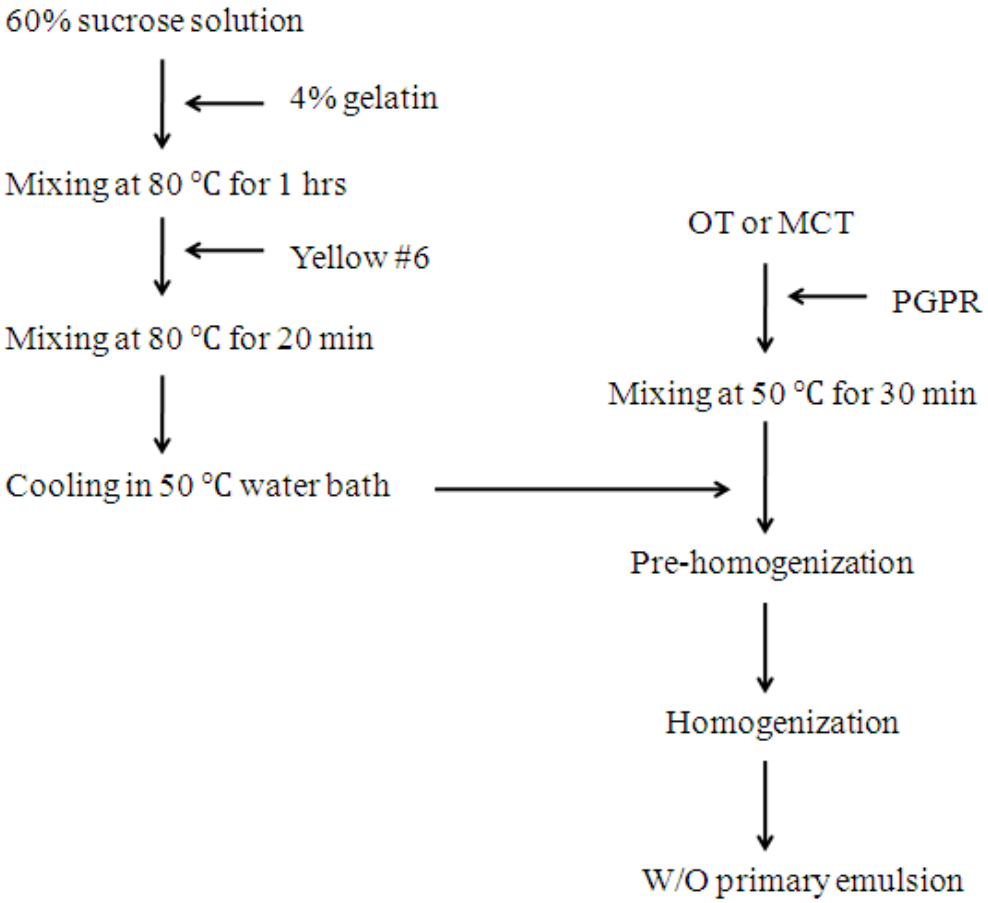

Figure 5.2 Flow diagram for preparing W/O primary emulsions**.**

In total, four different W/O emulsions were prepared: emulsion 1 (CNG - control) is without gelatin or yellow #6; emulsion 2 (NG) is without gelatin but with yellow 6; emulsion 3 (CG) is with gelatin but without yellow #6; emulsion 4 (G) is with both gelatin and yellow #6. All emulsions are prepared in duplicate.

5.2.2.4 Preparation of W/O/W secondary emulsions

W/O/W emulsions were prepared using a two-stage emulsification method. First, a primary emulsion was prepared as described above. Second, 10% w/w of the primary emulsion was mixed with 90% w/w of an emulsified hydrophilic solution (i.e. containing GA, MS or Tween 20) using an overhead mixer (Carter® 1L.81, Carter Motor, IL, USA) for 2 min at *ca.* 2000 rpm at room temperature. The resultant coarse emulsions were homogenized using a microfluidizer at low pressure. In the first part of present study (Sections of 5.3.1, 5.3.2, 5.3.3 and 5.3.5), 1% w/w Tween 20, 10% w/w MS or GA were used to stabilize the secondary emulsions (produced at 3,000 psi for 2 passes through the microfluidizer). In Sections 5.3.4 and 5.3.6, 12% w/w MS and 16% w/w GA were used because these concentrations were reported to have better performance on stabilizing conventional beverage clouding emulsions (28). All emulsions were prepared in duplicate.

5.2.2.5 Electron microscopy

W/O/W emulsions were characterized by cryogenic scanning electron microscope (Cryo-SEM, Hitachi S3500N**,** Hitachi Science Systems, Tokyo, Japan). Samples were placed into a small vessel and frozen in liquid nitrogen slush, and then quickly transferred

to SEM cold stage using a cryo-holder. The sample vessel was cut in cold stage and the cross-section of sample was imaged. This sample preparation technique was employed with the intention of seeing the microstructure of W/O/W emulsions by imaging the cross-section of droplets.

5.2.2.6 Confocal microscopy

Confocal microscopy of W/O/W emulsions prepared containing dyes in both phases is a powerful tool to characterize emulsion microstructure. A Nikon C1si laser scanning confocal microscope (Nikon, Melville, NY, USA) was used to verify if W/O/W emulsions were formed. Inner and outer aqueous phases contained 20 ug/mL riboflavin and nile red, respectively. The laser wavelengths were set at 458 and 561 nm which is close to the optimum exciting wavelengths of riboflavin and nile red, respectively.

5.2.2.7 Particle size measurement

Dynamic light scattering (Nicomp submicron particle sizer, model 370, Pacific Scientific Hiac/Royco Instruments Division, Santa Barbara, CA, USA) was used to measure the mean droplet diameter (MDD) of W/O primary emulsions. Samples were diluted 100 ~ 200 times with the continuous phase before measurement. Mean droplet diameter (MDDs) of W/O/W emulsions were measured by laser diffraction (Mastersizer

S, Malvern Instruments, Southborough, MA, USA) at an obscuration between 20% and 25%. For all samples, measurements of volume/mass based MDD were recorded.

5.2.2.8 Measurement of encapsulation efficiency by spectrophotometry

Yellow #6 was chosen as marker compound to determine encapsulation efficiency of an active in the inner aqueous phase and release properties of W/O/W emulsions (again from the inner aqueous phase). Through full scanning from 200 – 700 nm, the maximum absorbance of yellow #6 was found to be 480 nm, which agrees with the literature (29). A standard curve for determining the migration of yellow #5 from the inner phase to the bulk continuous phase was developed by measuring the absorbance of a serial dilution of yellow #6 (absorbance of each solution was within 0.2 – 0.8 absorbance units). W/O/W emulsions were centrifuged (model J2-21, Beckman Instruments, Spinco Division, Palo Alto, CA, USA) at 18,000 rpm (39,800 x g) for 2 hr to separate them into a top creaming layer and a bottom serum layer. The serum layer was collected by a syringe with a long, thin needle, and then passed through a syringe filter (0.45μm). The clear serum solution was subject to color measurement at 480 nm without dilution. Any Yellow #6 found in this serum layer had to originate from the inner aqueous phase of the primary emulsion because if the inner phase did not leak into the serum collected, this serum should have been colorless. During color measurement,

W/O/W emulsions without Yellow #6 (CNG or CG) served as blanks. Encapsulation efficiency was calculated by the following formula:

$$EE = (M_i - M_e)/M_i$$

Where M_i is the mass of dye initially present in the water droplets of the W/O emulsion and M_e is the mass of dye present in the external water phase of the W/O/W emulsion.

5.2.2.9 Beverage preparation

The beverage formula used to evaluate beverage cloud stability is presented in Table 5.1. Beverages were made three days after preparation of emulsion concentrates. Seven 8 oz. clear plastic bottles of beverages were prepared from each emulsion. One bottle was used for monitoring appearance (visual), one bottle for the turbidity test, and other bottles for weekly droplet size measurements. Beverages were stored at room temperature and analyzed weekly for four weeks.

Table 5.1 Composition of beverage clouds for storage study.

Ingredient	Yellow #6 1% solution	Citric acid	Sodium benzoate	W/O/W emulsion	Distilled water	pH
Concentration % (w/w)	0.3	0.3	0.05	1	q.s. 100	3.6

5.2.2.10 Measurement of beverage turbidity

Changes in turbidity of W/O/W beverage clouds were measured during storage using a spectrophotometer (Spectronic 20, Spectronic Instrument, Inc., Rochester, NY, USA) at a wavelength of 400 nm. All beverages were diluted 2 times with pH 3.6, 10 mM citric buffer prior to measurement. The buffer solution served as blank.

5.2.2.11 Ringing test

All beverage clouds were visually assessed for ringing. A white ring appears at the neck of the bottle when sufficient creaming has occurred in a beverage. Any beverage that formed a ring on storage was considered unstable. Rings that formed were easily identified since they were white in contrast to the dyed solution.

5.3 Results and Discussion

5.3.1 Effect of PGPR concentration on W/O emulsions

In preliminary studies not reported herein, 3, 4, and 5% w/w of gelatin was dispersed in a 60% w/w sucrose solution using heat and stirring and then cooled to room temperature. All sucrose solutions gelled once cooled. The sample containing 3% w/w gelatin formed a soft gel while the sample with 4% w/w gelatin formed a relatively firm

gel upon cooling. Therefore, 4% w/w gelatin was used in the present study as the gelling agent.

Also in preliminary studies, several lipophilic emulsifiers of soy lecithin (Yelkin® 1018, HLB=4.0), monoglyceride (Panalite 90-130 K, HLB=4.2), Span 80 (HLB=4.3) and polyglycerol polyricinoleate (PGPR, HLB=3.0) with low HLB values (hydrophilic-lipophilic balance) were evaluated for their ability to form small MDD, stable water in oil emulsions. The results showed that except for PGPR, all other lipophilic emulsifiers produced unstable OT-based W/O emulsions exhibiting phase separation shortly after preparation. On the contrary, PGPR formed stable W/O emulsions and the turbidity of prepared W/O emulsions decreased with increasing PGPR concentration (Figure 5.3). The semi-transparent appearance of W/O emulsions at higher concentration of PGPR is attributed to both the small MDD and small differences in phase refractive indices.

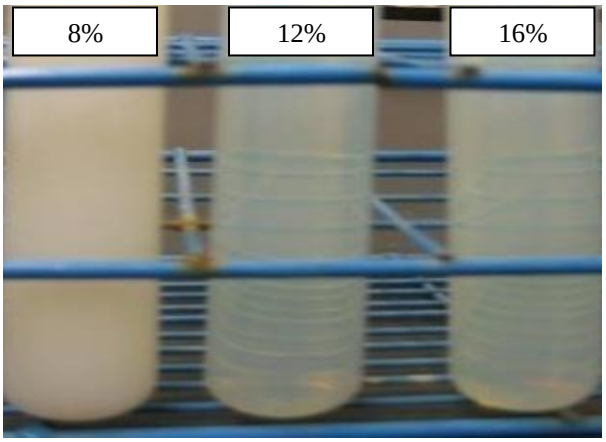

Figure 5.3 Image of OT-based W/O emulsions without gelling inner aqueous phase; emulsions stabilized by 8, 12, or 16% w/w PGPR.

Figure 5.4 shows effect of PGPR concentration on the MDD of W/O emulsions. It is clear that with increasing concentrations of PGPR, MDDs decreased. The maximum usage levels tested of 16 and 8% w/w PGPR yielded W/O emulsions with MDDs as small as 73 and 134 nm for OT and MCT-based emulsions without gelatin, respectively. The PGPR concentrations used in MCT-based primary emulsions were ca. half of those in OT-based primary emulsions because the quantity of inner aqueous phase in MCT-based emulsions was roughly half of that used for OT-based emulsions since much less sucrose solution was needed to balance the phase densities. While the decision to use different concentrations of PGPR for the two oil phase materials seems arbitrary; it does not influence our objective. The high efficiency of PGPR at high usage levels in stabilizing W/O emulsions has been reported by a number of authors (18, 23, 30). For example, Kanouni et al. (17) investigated the stabilization mechanism of lipophilic emulsifiers at the W/O interface and found that the high elasticity value of interfacial film formed by polymeric emulsifiers (e.g., PGPR) allowed the film to withstand stress without breaking and thus produced stable W/O emulsions.

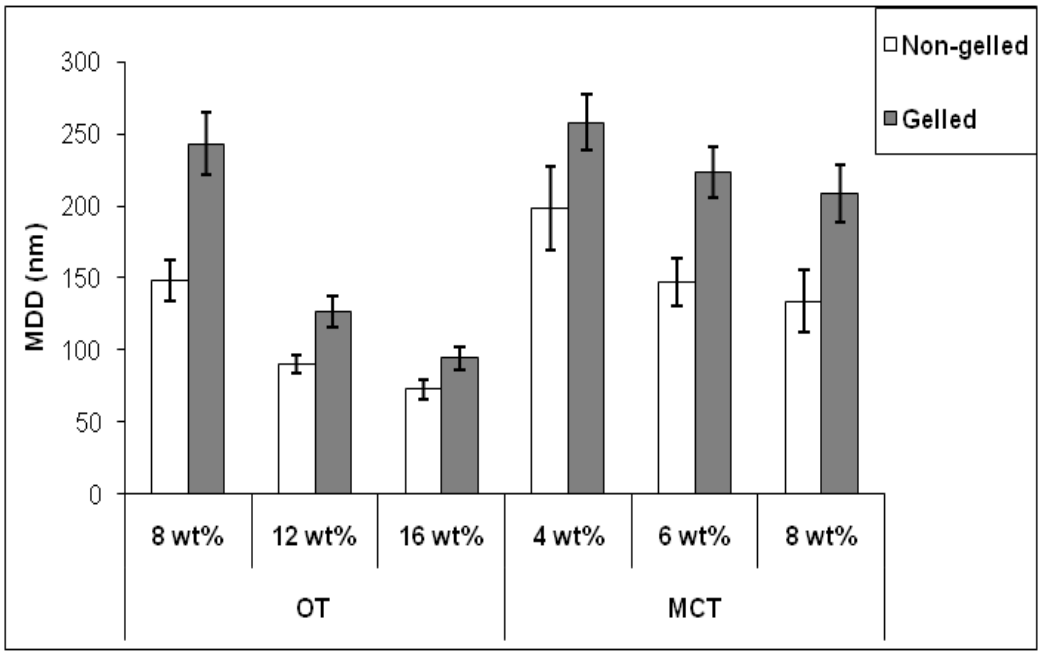

Figure 5.4 Effect of PGPR concentration on MDD of W/O emulsions (OT: orange oil terpenes based W/O primary emulsions; MCT: vegetable oil based W/O primary emulsions)

Figure 5.4 also shows MCT-based W/O emulsions have larger MDDs than OT-based emulsions. That does not necessarily mean that MCT-based emulsions must yield larger MDD than OT-based emulsions because the formulations were quite different. The larger MDD might be due to the higher viscosity of MCT (27 mPa.s) compared to 0.8 mPa.s for OT and a lower concentration of PGPR. It was found that gelling the inner aqueous phase had a negative effect on the MDD of prepared W/O emulsions at all concentrations of PGPR. That might be attributed to the extremely high viscosity of the inner aqueous phase incorporated with gelatin. Research (31, 32) has shown that the ratio of disperse/continuous phase viscosity must be kept within an optimal range in order to

facilitate droplet disruption and form small particles. Figure 5.5 shows the particle size distribution of prepared W/O emulsions. All emulsions had a narrow particle size distribution except that a small fraction of larger droplets was found in OT-based W/O emulsions without gelatin. The small MDD and narrow size distribution enabled the preparation of stable W/O/W emulsions.

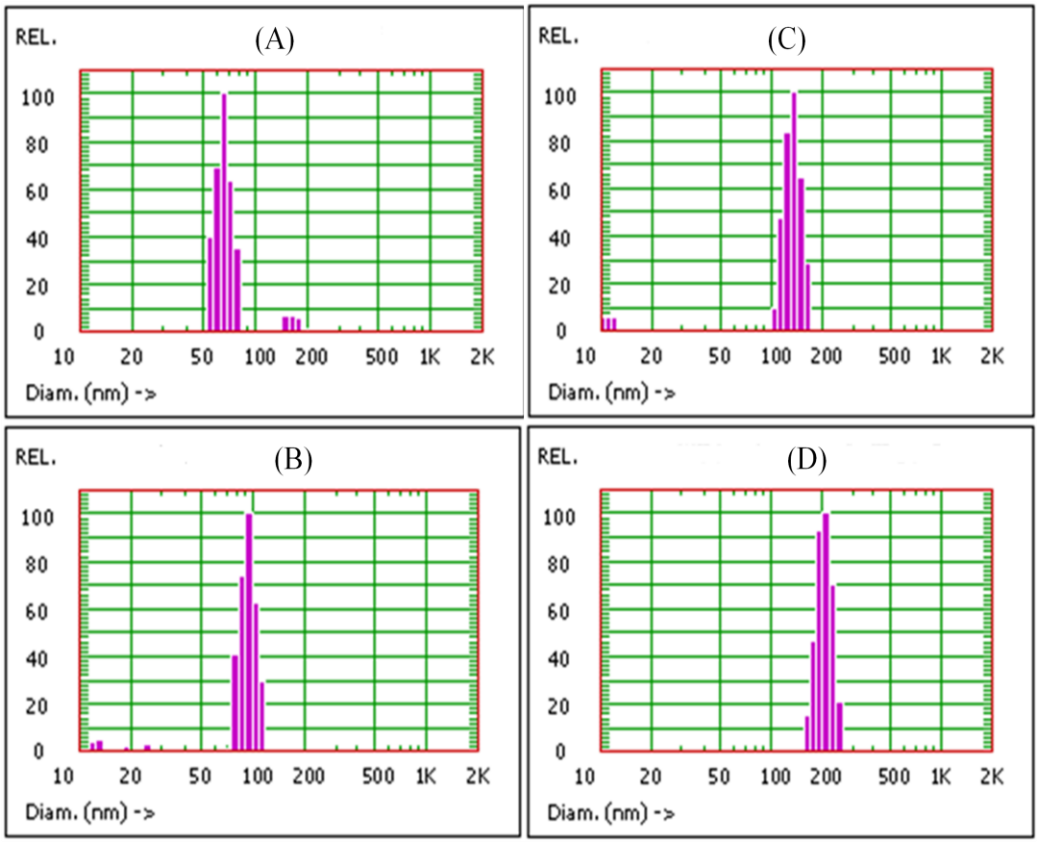

Figure 5.5 Droplet size distribution of W/O primary emulsions. (A) and (B): non-gelled and gelled OT-based W/O emulsions stabilized by 16% w/w PGPR; (C) and (D): non-gelled and gelled MCT-based W/O emulsions stabilized by 8 wt% PGPR.

5.3.2 Characterization of W/O/W emulsions

The intrinsic instability of W/O/W emulsions led us to further examine the emulsion particle structure: confocal microscopy was used for this purpose. Figure 5.6 shows confocal microscopy images of Tween 20 stabilized W/O/W emulsions. One can see that the blue water droplets (riboflavin fluorescence) are encapsulated in red oil droplets (Nile red fluorescence), which clearly confirms that the prepared emulsions are double emulsions. Although this method proves that double emulsions were formed, it does not provide quantitative information on the emulsions, e.g. how much of the primary aqueous phase is truly encapsulated in a secondary emulsion or how much of the system exists as a single vs. double emulsion. In order to get more information on the microstructure of double emulsions, SEM was chosen as a complementary approach.

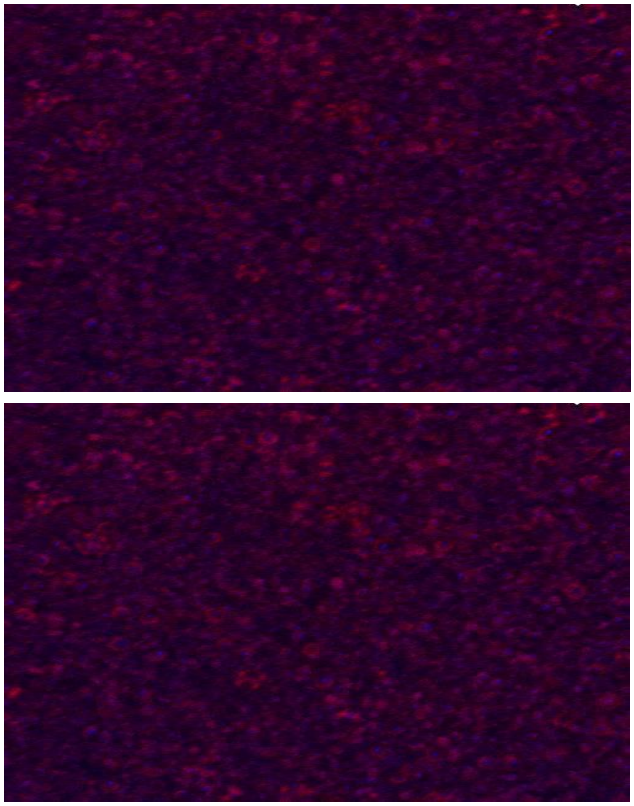

Figure 5.6 Confocal microscopy images of W/O/W emulsions stabilized by 1% w/w Tween 20. Top and bottom: non-gelled and gelled inner aqueous phase, respectively.

Unfortunately, SEM was not as successful as expected. A representative cross-section of a W/O/W emulsion was not obtained due to the intermolecular binding forces. However, Figure 5.7 provides some information on droplet size and indicates some coalescence. The observed droplet size of a single droplet is in the range of 0.5 to 1μm, which agrees with the measurement by Mastersizer (Figure 5.8). Also, from the image one can see coalescence or flocculation (the long shaped droplets) by the merging of several single droplets, which suggests that 1% w/w Tween 20 is poor at preventing

flocculation or coalescence. However, we must temper that conclusion recognizing that we may have induced coalescence in preparing the sample for microscopy. The emulsion must be frozen and even if frozen in liquid nitrogen, this may have induced coalescence.

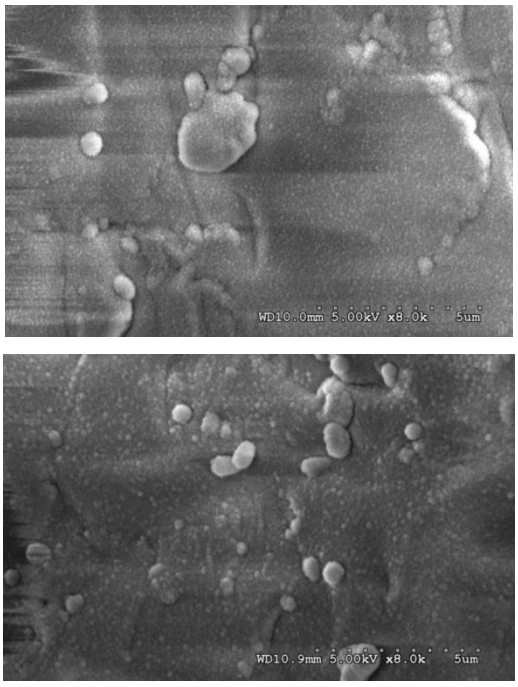

Figure 5.7 Cryo-SEM images of W/O/W emulsions stabilized by 1% Tween 20. Top and bottom, non-gelled and gelled inner aqueous phase, respectively.

5.3.3 Effects of hydrophilic emulsifiers on W/O/W emulsions

Figures 5.8 and 5.9 show the effects of hydrophilic emulsifier type on the MDD and encapsulation efficiency (EE) of W/O/W emulsions. One can see that MCT-based double emulsions have smaller MDD than those of OT-based emulsions. This result is opposite to that found in W/O primary emulsions where MCT-based W/O emulsions had

larger MDDs. This could be attributed to the difference in phase viscosity between OT and MCT. In W/O primary emulsions, OT and MCT are in the continuous phase while in W/O/W emulsions they are dispersed phase. Therefore, oil type has a different impact on the MDDs of W/O and W/O/W emulsions.

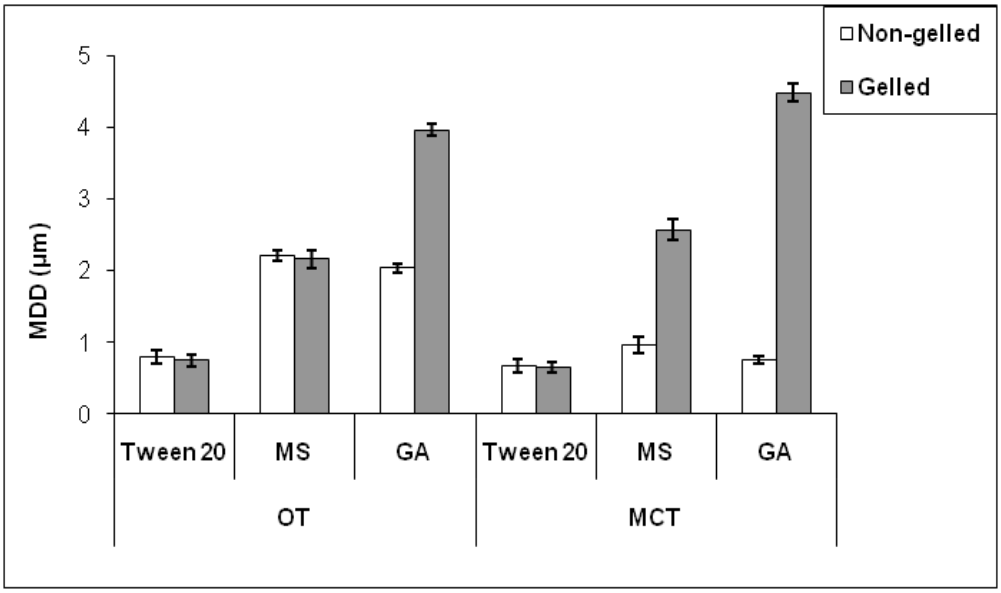

Figure 5.8 Effect of hydrophilic emulsifier type and gelatin on the MDD of W/O/W emulsions.

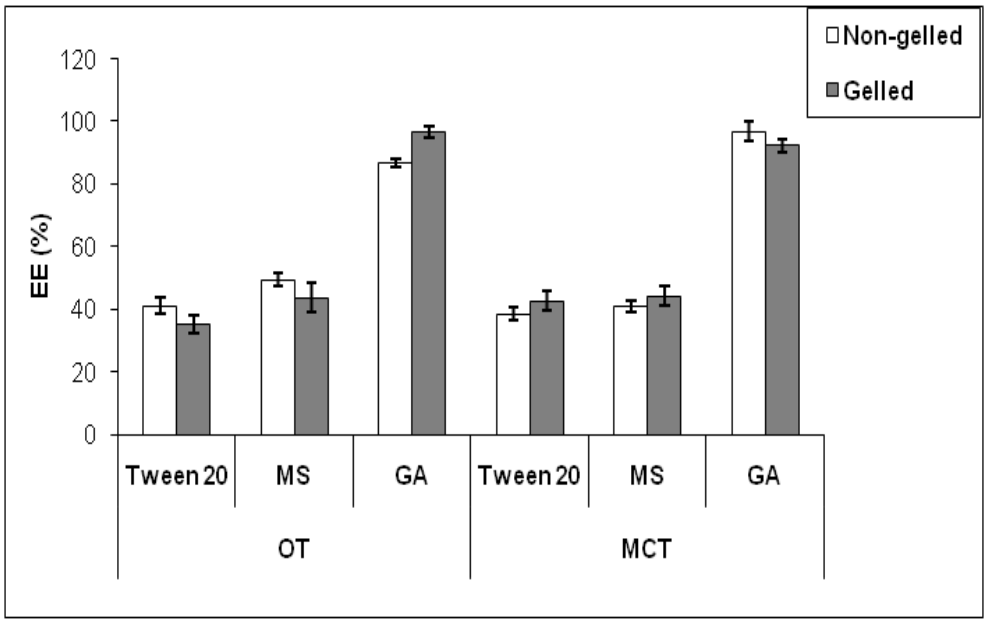

Figure 5.9 Effect of hydrophilic emulsifier type and gelatin on the EE of W/O/W emulsions.

The effect of gelatin on the MDD of W/O/W emulsions is complex depending on both type of oil phase and the hydrophilic emulsifier chosen. With OT as oil phase, gelatin did not show a significant effect on the MDD of double emulsions stabilized by Tween 20 or MS while gelling the inner phase increased the MDD of GA stabilized double emulsions. With MCT as the oil phase, the incorporation of gelatin led to larger MDDs of double emulsions stabilized by MS or GA. Figure 5.10 shows an example of how gelatin and oil type influence the size distribution of GA stabilized double emulsions. Obviously wider particle size distributions were obtained in double emulsions with gelatin in the inner phase or MCT as oil phase.

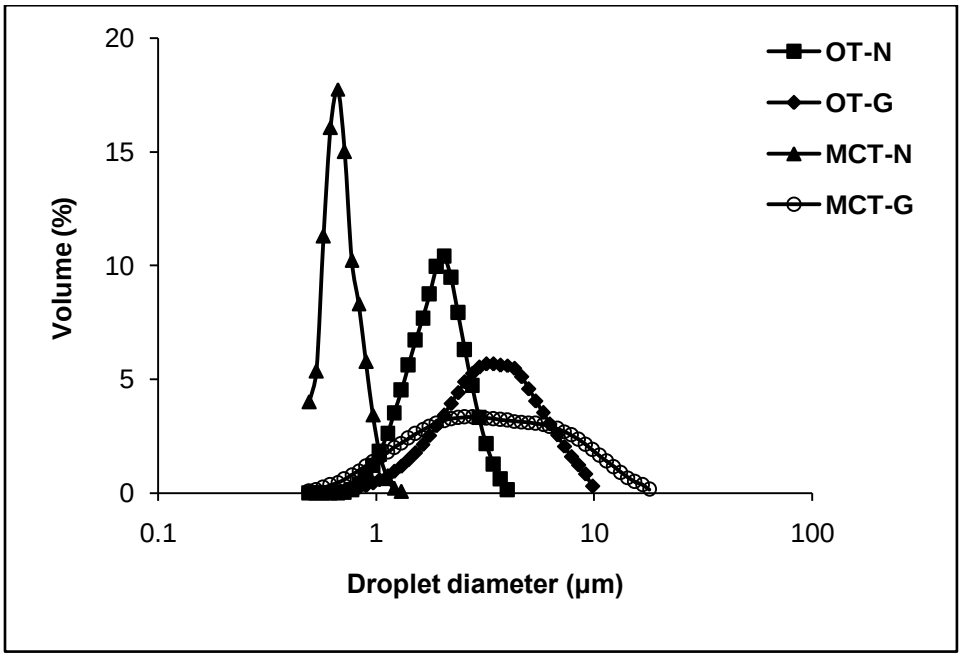

Figure 5.10 Particle size distribution of W/O/W emulsions stabilized by GA. N, non-gelled inner aqueous phase; G, gelled inner phase; OT-N, orange terpene-based W/O/W emulsions with non-gelled inner phase; MCT-N, MCT-based W/O/W emulsions with non-gelled inner phase.

The influence of gelatin on the MDD might be due to the interactions between gelatin and PGPR or hydrophilic emulsifiers. Muschiolik et al. (26) reported that the addition of gelatin to the inner phase did not affect the MDD of fresh W/O/W emulsions stabilized by whey protein isolate, but the MDD of double emulsions with gelatin increased during storage at a slower rate compared to that of emulsions made without gelatin. The pH of the prepared emulsions in the reference above is not available and probably would be the natural pH. The inconsistent results between Muschiolik' s and the present study might be due to the difference in hydrophilic emulsifiers and the pH of the

double emulsions. In the present study, emulsions were prepared at acidic conditions, therefore, gelatin takes on a strong positive charge while MS and GA takes on a negative charge. During mixing and homogenization, gelatin may leak into the external aqueous phase and interact with MS or GA. The effect of gelatin on the MDD of the Tween 20 stabilized double emulsions is minimal probably because Tween 20 is a nonionic surfactant.

The interaction between PGPR and gelatin may partially account for the difference in MDD of emulsions with gelatin and those without gelatin. It has been reported that PGPR and sodium caseinate incorporated in the inner aqueous phase had a synergistic effect on stabilizing soybean oil double emulsions, but the interaction mechanism was not understood (30). That may explain the similar MDDs of Tween 20 stabilized secondary emulsions regardless of the addition of gelatin even though the W/O primary emulsions with gelatin had larger MDDs than those without gelatin (shown in section of 5.3.2).

Figures 5.8 and 5.9 also show that gelling the inner aqueous phase is not necessarily associated with improved EE. No direct connection was found between EE and MDDs either. Our results suggest that gelling the inner phase is not effective at preventing the diffusion of the dye from inner to the external aqueous phase probably because the dye still can move through the gel network. A similar finding was reported by Surh et al. (3), i.e. W/O/W emulsions showed similar EE (>95%) regardless of gelling the inner phase by heat treated WPI. However, as one can see from Figure 5.9 the choice of hydrophilic emulsifier plays a critical role in determining the EE of W/O/W emulsions.

GA showed the best performance in encapsulating the dye which is consistent with its high efficiency in stabilizing conventional emulsions (28, 33). The high EE (>90%) of W/O/W emulsions stabilized by macromolecules has been reported by a number of authors (23, 34, 35). Tween 20 stabilized W/O/W emulsions showed smallest MDDs but the lowest EEs. This could be due to the rupture of oil droplets during mixing and homogenization (3000 psi for 2 passes) of the secondary emulsions since the interfacial film formed by Tween 20 is less resistance to the intense shear. Therefore, polymeric amphiphilic emulsifier and macromolecules are always recommended to stabilize the secondary emulsions in literature (1, 7, 36, 37).

5.3.4 Effect of process parameters on W/O/W emulsions

Literature (3, 26, 38, 39) suggests that low pressure and membrane homogenization are effective methods to prepare stable secondary emulsions with high EE. Generally, a higher homogenization pressure reduces the MDD, but it may also reduce EE due to rupture of inner water droplets. A greater number of passes through the Microfluidizer generally narrows the droplet distribution; however, it may also decrease EE due to more chances to disrupt the inner water droplet. In the present study, the effect of homogenization pressure and number of passes through the homogenizer, which are easily controlled parameters, were evaluated for effect on EE and MDD.

Figures 5.11 and 5.12 show effects of homogenization pressure and number of passes on MDD of GA stabilized W/O/W emulsions. Interestingly the results are different for gelled and non-gelled emulsions. For double emulsions without gelatin, increasing the number of passes from 1 to 2 resulted in smaller MDD at all homogenization pressures. But no significant changes in MDD were found in emulsions with 2 and 3 passes except those produced at 10,000 psi. For double emulsions with gelatin, at 3,000 psi multiple passes resulted in larger MDD while at 7,000 and 10,000 psi multiple passes led to smaller MDD of double emulsions. The results demonstrate that the addition of gelatin to the inner aqueous phase has a large impact on the effectiveness of homogenization.

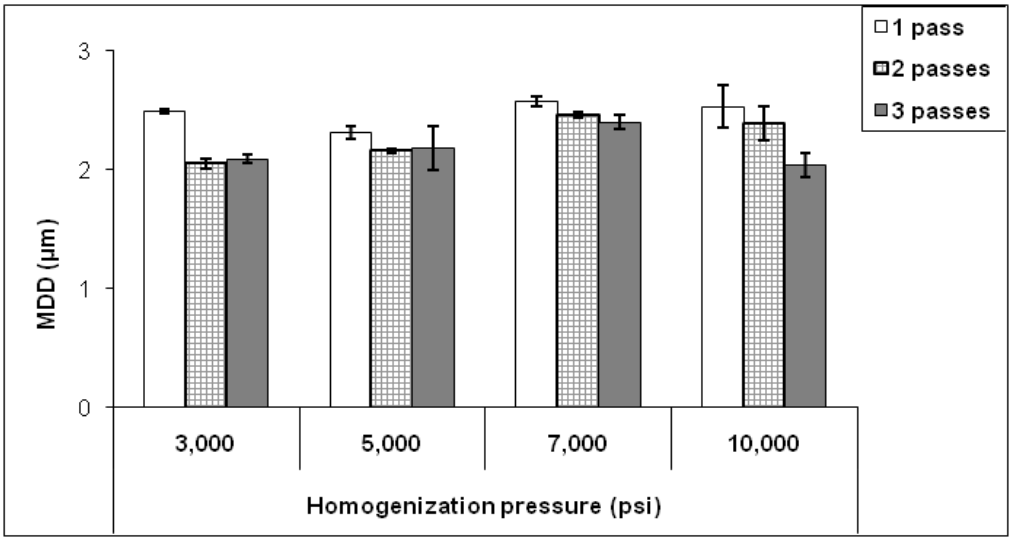

Figure 5.11 Effects of homogenization pressure and number of passes on MDD of GA stabilized W/O/W emulsions with OT as oil phase and without gelatin in the inner aqueous phase.

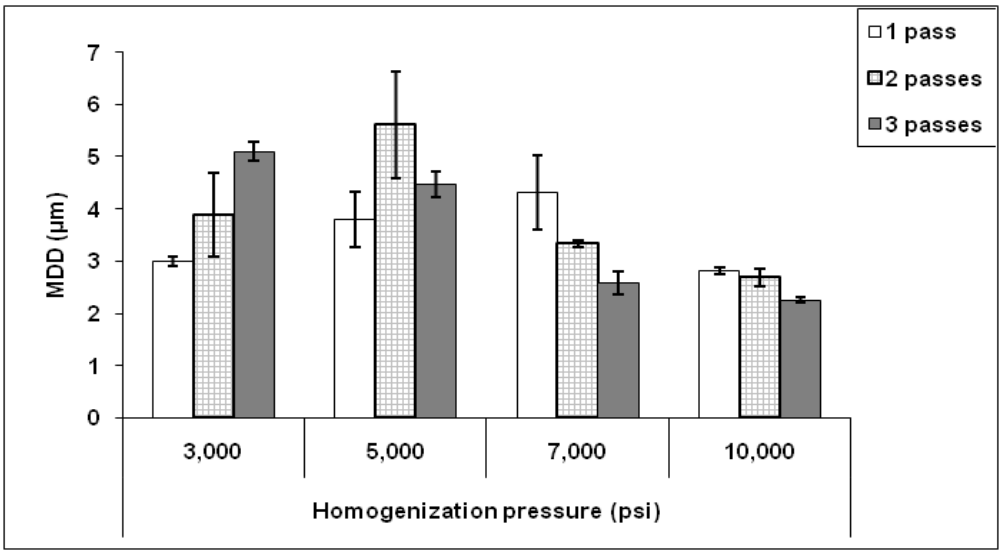

Figure 5.12 Effects of homogenization pressure and number of passes on MDD of GA stabilized W/O/W emulsions with OT as oil phase and gelatin in the inner aqueous phase.

Figure 5.13 shows effect of number of homogenization passes on size distribution of GA stabilized double emulsions produced at 3,000 psi. Increasing the number of passes resulted in a narrower size distribution of double emulsions without gelatin but a wider particle size distribution of those with gelatin. Figure 5.14 shows the effect of homogenization pressure on size distribution of GA stabilized double emulsions with 1 pass through a Microfludizer. Adding gelatin to the inner phase led to a wider size distribution of emulsions produced at all pressures. Therefore, it can be concluded that gelling inner phase has a negative effect on MDD and size distribution of GA stabilized double emulsions regardless of the process pressure and number of homogenization passes.

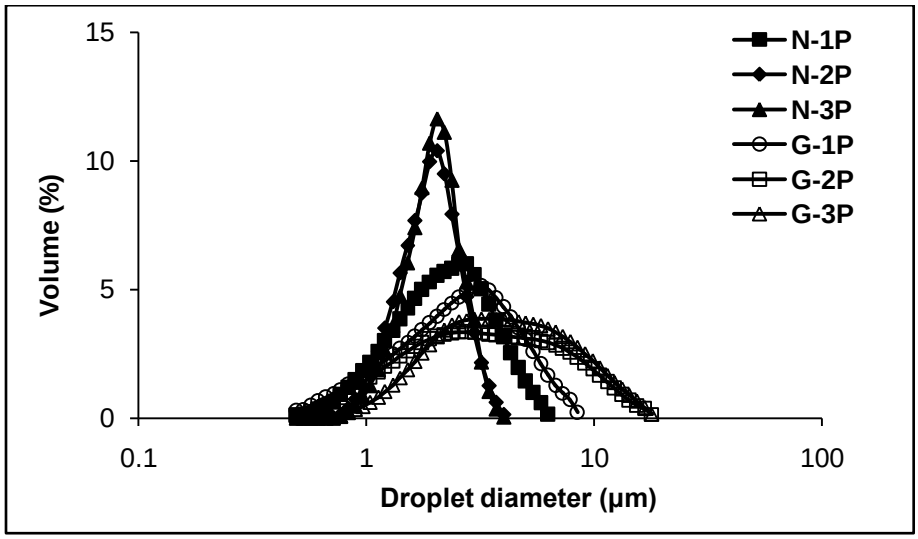

Figure 5.13 Droplet size distribution of OT-based W/O/W emulsions stabilized by GA and produced at 3000 psi for different passes. N, non-gelled inner aqueous phase; G, gelled inner phase; 1P, 2P and 3P stand for 1, 2, and 3 passes, respectively, through Microfludizer.

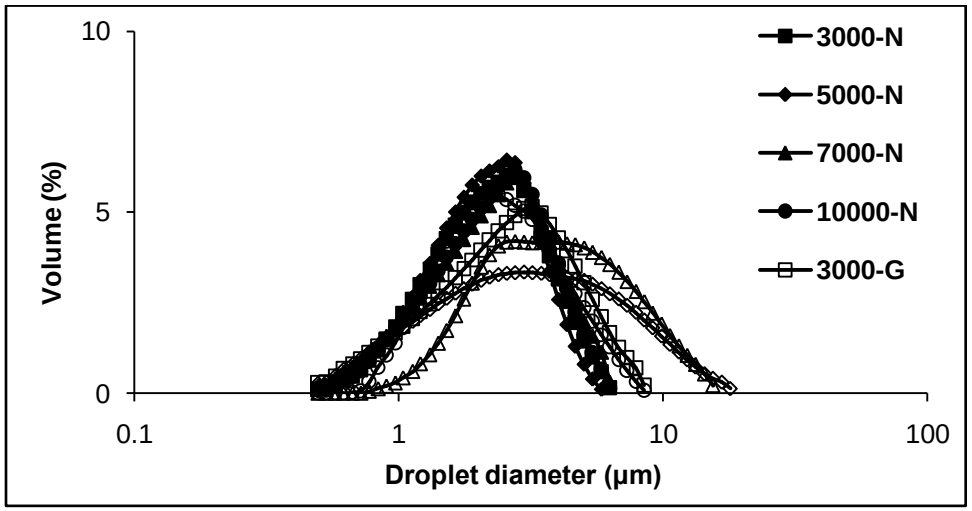

Figure 5.14 Droplet size distribution of OT-based W/O/W emulsions stabilized by GA and produced at different pressures for1 pass through Microfludizer. N, non-gelled inner aqueous phase; G, gelled inner phase.

Figures 5.15 and 5.16 show the effects of homogenization pressure and number of passes through a microfludizer on the EE of GA stabilized W/O/W emulsions. One general observation is that the EE decreased when the number of passes increased from 1 to 2 at all homogenization pressures regardless of gelling the inner phase and this effect is more significant at lower homogenization pressures than higher pressures. It was also observed that lower pressures led to higher EE when homogenized for 1 pass: 95.77 ± 2.25 at 3,000 psi vs. 91.77 ± 1.11 at 10,000 psi for non-gelled emulsions and 95.79 ± 0.93 at 3,000 psi vs. 87.4 ± 0.8 at 10,000 psi for gelled emulsions. In the present study, high EEs were achieved even at high homogenization pressures (7,000 and 10,000 psi) suggesting that a Microfludizer is good at producing W/O/W emulsions with small MDD and high EE.

Muschiolik et al. (26) reported that the type of homogenization device has a large impact on the EE of double emulsions. In a model system of soybean oil W/O/W emulsion stabilized by whey protein isolate-dextrin conjugates, almost 100% EE was achieved by using membrane emulsification while 97 and 57% EE were achieved by using a combi-valve and ball-valve homogenizer, respectively. In contrast, 80% EE was obtained with an EmulsiFlex C5 homogenizer. Based on our results, a Microfludizer could serve as an alternative to membrane emulsification in order to achieve high EE of W/O/W emulsions.

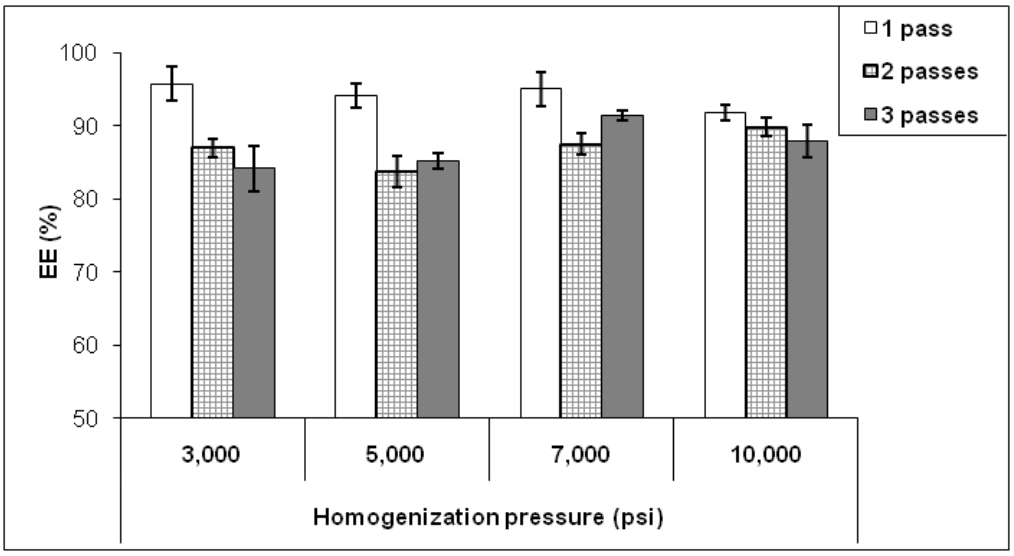

Figure 5.15 Effects of homogenization pressure and number of passes on EE of GA stabilized W/O/W emulsions without gelatin.

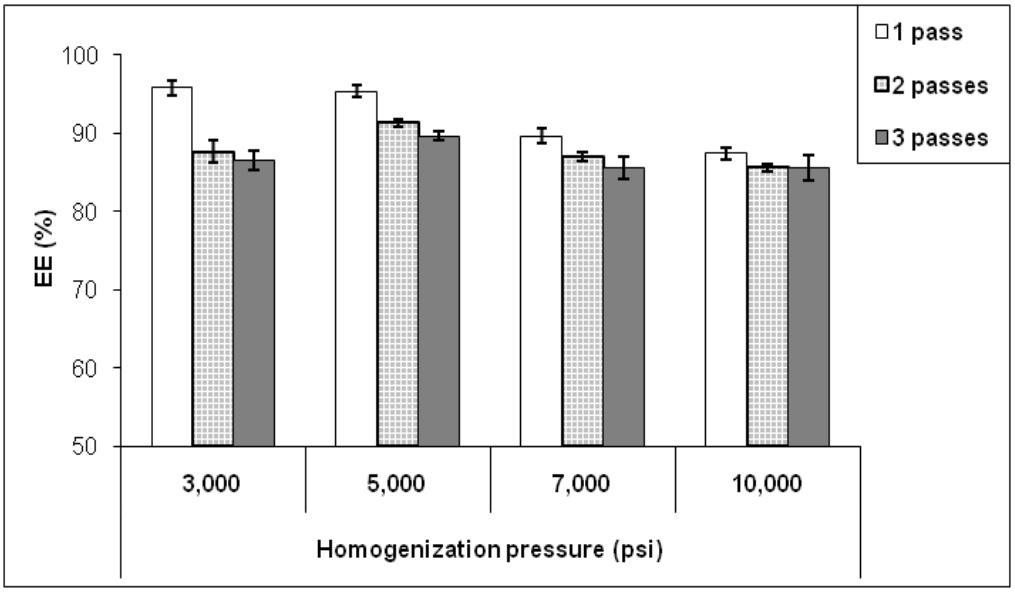

Figure 5.16 Effects of homogenization pressure and number of passes on EE of GA stabilized W/O/W emulsions with gelatin.

5.3.5 Stability of W/O/W emulsion concentrates

In this experiment, the stability of double emulsion concentrates was studied and provides a basis for the later work on evaluating their stability in dilute systems. Figures 5.17 and 5.18 show changes in MDD and EE of OT and MCT-based W/O/W emulsion stabilized by Tween20. The MDD of non-gelled emulsions is relatively small and quite stable, whereas the MDD of the emulsion containing a gelled inner phase increased slightly during the first two weeks storage and then increased rapidly. After four weeks storage, droplets of gelled emulsions have a bimodal or multimodal size distribution (Figure 5.19). Both the gelled and non-gelled emulsions have low encapsulation efficiency (EE), which decreased over time. A slower decrease in EE of MCT-based emulsions was observed compared to that of OT-based emulsions. This could be explained by the higher viscosity of MCT than that of OT (27 vs. 0.8 mPa.s at room temperature) and thus slower diffusion rate of yellow #6 from inner to outer aqueous phase.

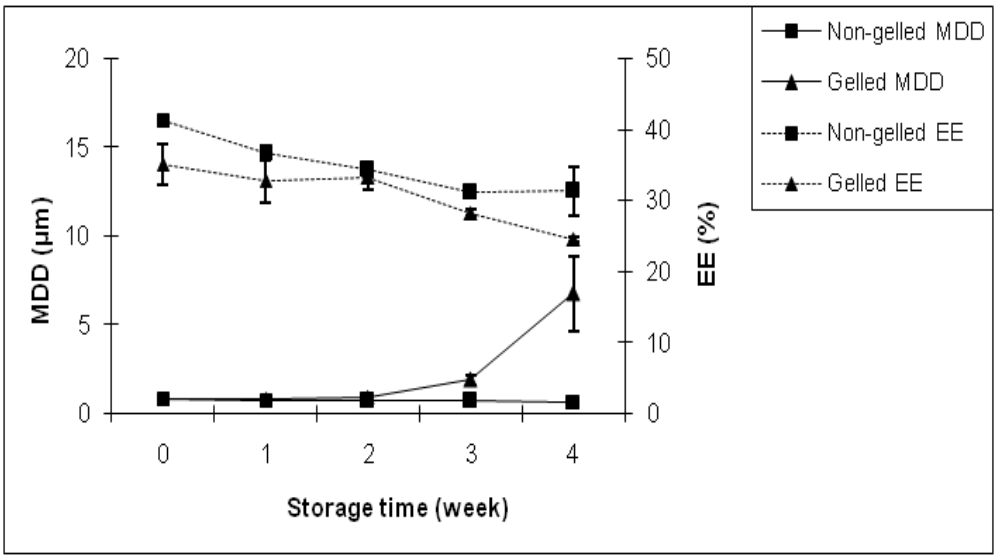

Figure 5.17 Changes in MDD and EE of OT-based double emulsion concentrates stabilized by Tween 20 during storage at room temperature.

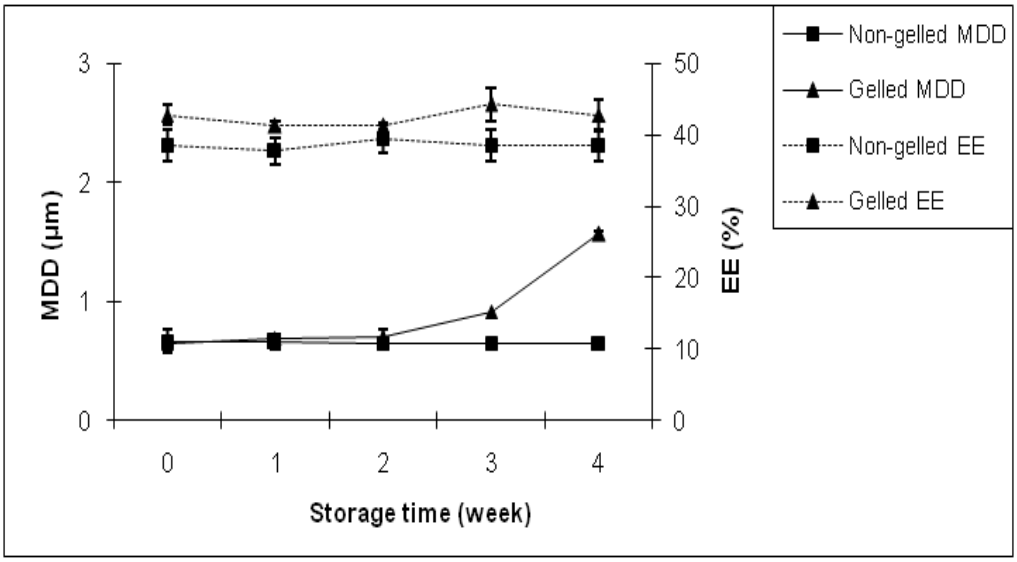

Figure 5.18 Changes in MDD and EE of MCT-based double emulsion concentrates stabilized by Tween 20 during storage at room temperature.

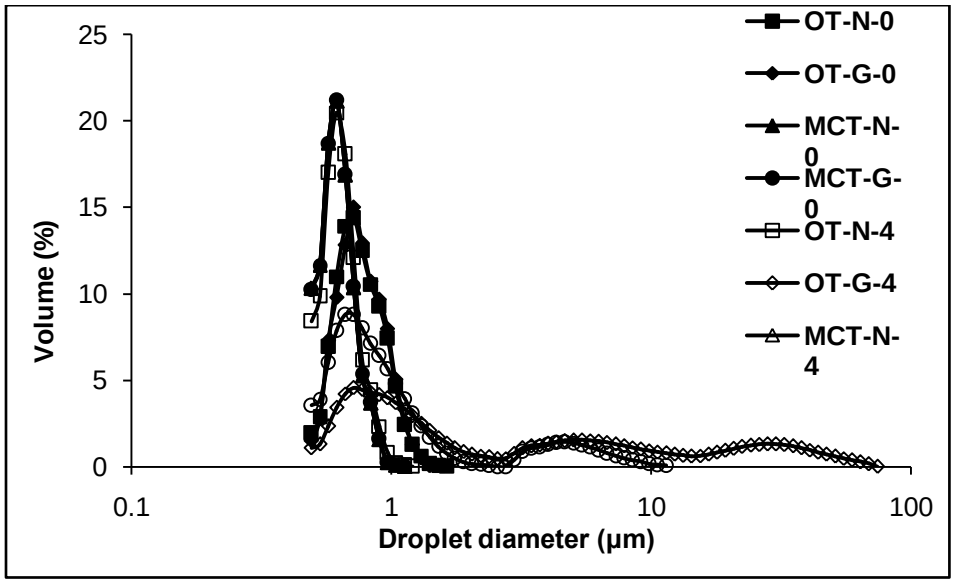

Figure 5.19 Size distribution of Tween 20 stabilized W/O/W emulsions. N, non-gelled inner phase; G, gelled inner phase; the number followed N or G stands for weeks of storage, e.g., OT-N-0 means OT-based double emulsions with gelatin at time zero.

Figures 5.20 and 5.21 show changes in MDD and EE of OT and MCT-based W/O/W emulsions stabilized by MS. For OT-based emulsions, the MDD of non-gelled emulsion increased rapidly over time whereas the MDD of gelled emulsions increased slowly. For MCT-based emulsions, the MDD of both non-gelled and gelled emulsions increased rapidly during the first week of storage and then increased slowly thereafter. After 4 weeks storage all emulsions showed wider size distributions than were originally made (Figure 5.22) and particularly, OT-based emulsions with a gelled inner phase showed bimodal size distributions suggesting MCT-based double emulsions stabilized by MS are more stable than OT-based emulsions.

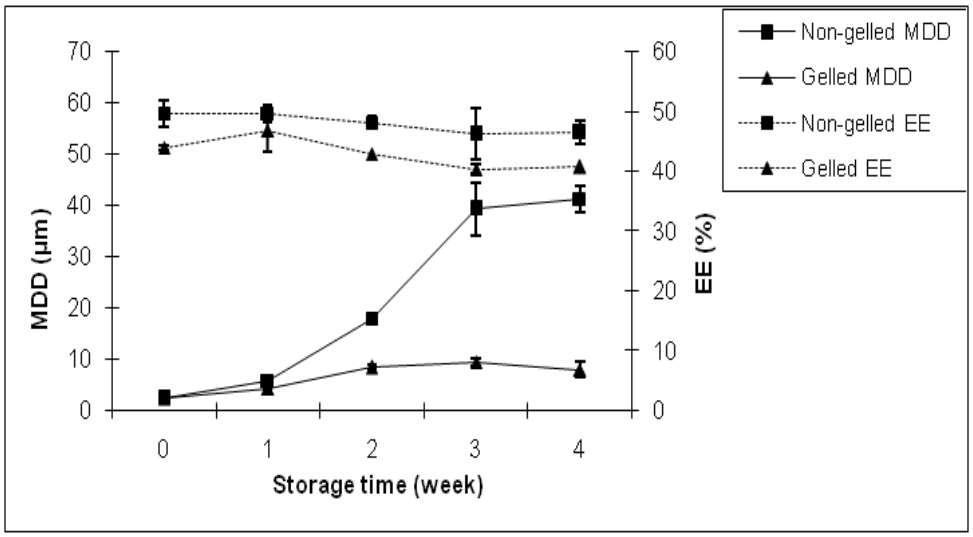

Figure 5.20 Changes in MDD and EE of OT-based double emulsion concentrates stabilized by MS during storage at room temperature.

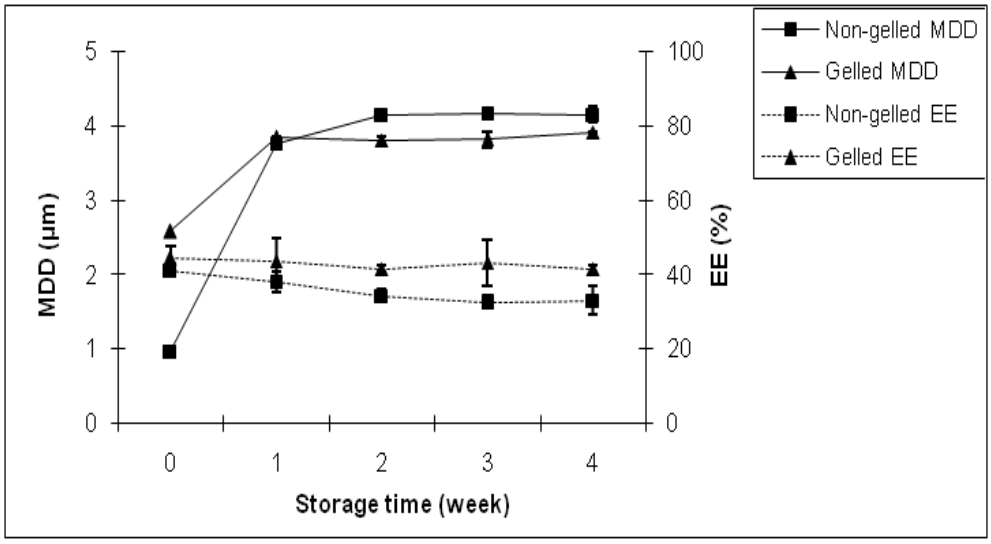

Figure 5.21 Changes in MDD and EE of MCT-based double emulsion concentrates stabilized by MS during storage at room temperature.

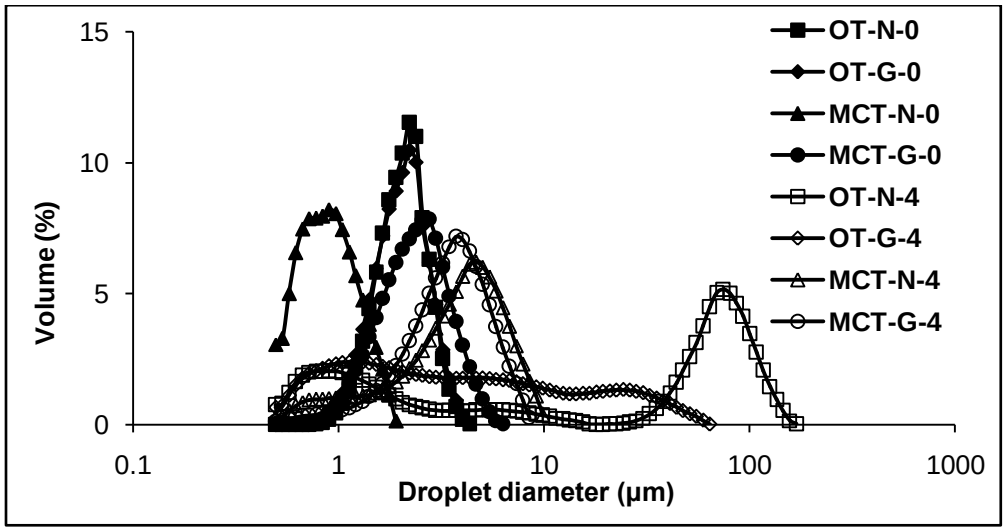

Figure 5.22 Size distribution of MS stabilized W/O/W emulsions. N, non-gelled inner phase; G, gelled inner phase; the number followed N or G stands for weeks of storage, e.g., OT-N-0 means OT-based double emulsions with gelatin at time zero.

All emulsions stabilized with MS showed a slow decrease in EE over time regardless of the oil phase type. One may argue that OT-based emulsions should have a faster release of the dye considering Yellow #6 has a faster diffusion coefficient in OT than MCT as demonstrated in the Tween 20 stabilized double emulsions. We postulated that for MS stabilized double emulsions, the factor limiting diffusion is the O/W interfacial film instead of the lipid barrier. On the contrary, for Tween 20 stabilized double emulsions, the factor limiting diffusion is the lipid barrier instead of the O/W interfacial film. The differences originate from the differences in interfacial films formed by Tween 20 and MS and also from the large impact of interfacial film on diffusion of the dye from the inner to the outer aqueous phase. The above explanation is supported by

previous findings in the literature (1, 7, 40) noting that the release of water-soluble substance from the inner to the outer aqueous phase of double emulsions largely depends on phase composition (e.g., solid content of the aqueous phase, salt concentration, and oil type) and interfacial films (e.g., emulsifier type and concentration).

Figures 5.23 and 5.24 show changes in MDD and EE of OT and MCT-based W/O/W emulsions stabilized by GA. For all W/O/W gelled emulsions, phase separation occurred within 3 days of preparation suggesting there may be some interaction between gelatin and GA. The MDD of non-gelled emulsions increased rapidly during the first week of storage and then increased slowly thereafter. After 4 weeks storage, emulsions showed wider size distributions (Figure 5.25) regardless oil types.

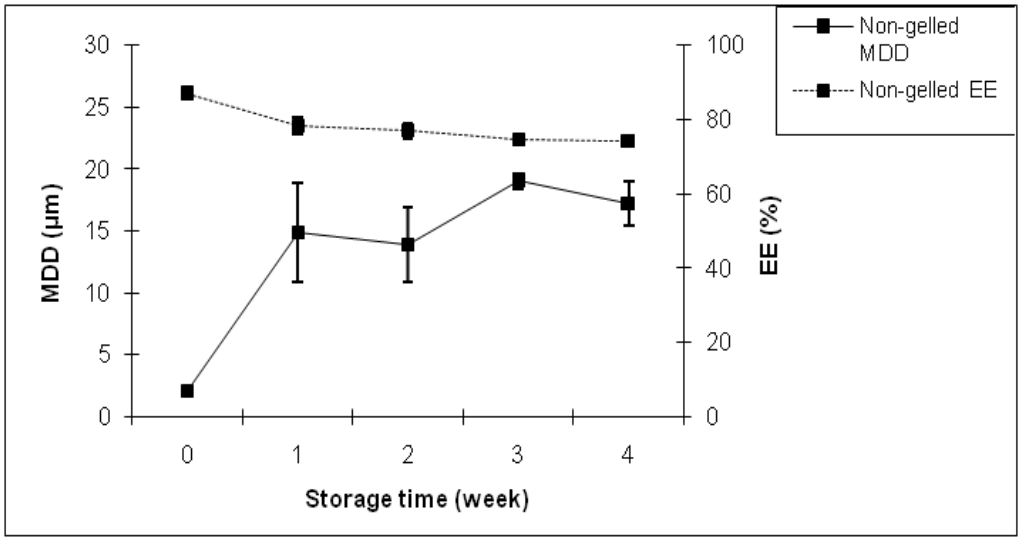

Figure 5.23 Changes in MDD and EE of OT-based double emulsion concentrates stabilized by GA during storage at room temperature.

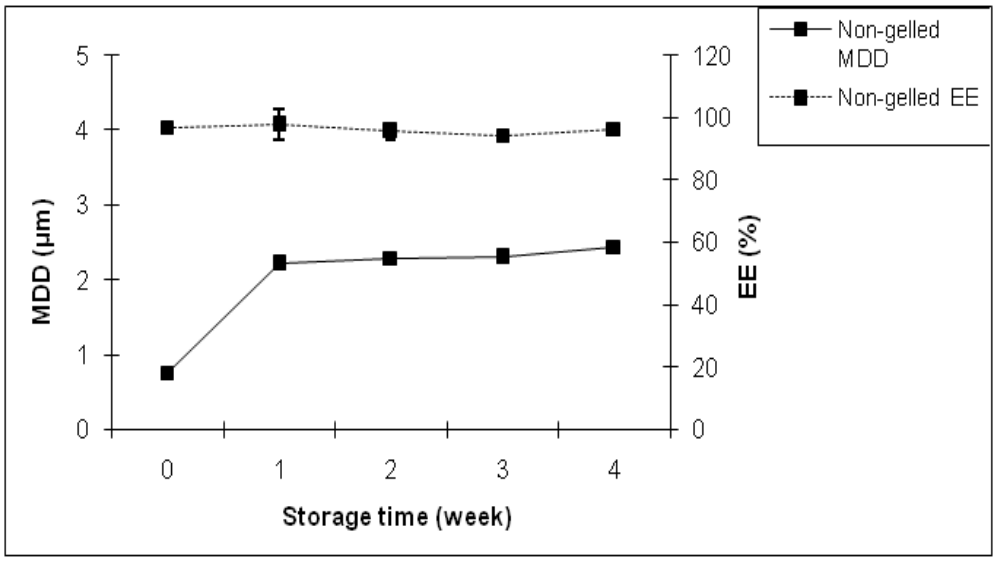

Figure 5.24 Changes in MDD and EE of MCT-based double emulsion concentrates stabilized by GA during storage at room temperature.

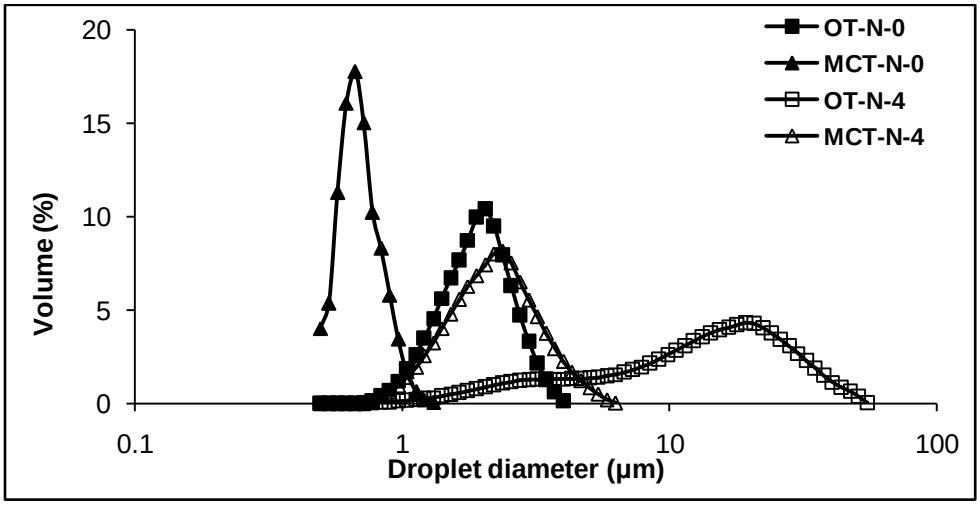

Figure 5.25 Size distribution of GA stabilized W/O/W emulsions. N, non-gelled inner phase; the number followed N stands for weeks of storage, e.g., OT-N-0 means OT-based double emulsions with gelatin at time zero.

For OT-based emulsions, EE decreased significantly during the first week of storage and then decreased slowly thereafter. After four weeks storage, EE had decreased from 86.7 to 75%. For MCT-based emulsions, EE was much higher than that of OT-based emulsions (86.7 vs. 96.7 at week zero) and they were stable over time.

Overall, Tween 20 stabilized double emulsions have small MDDs but low EEs. MS stabilized double emulsions have relatively large MDDs and low EEs. Fortunately, GA produces small MDDs and shows high EEs relative to MCT-based W/O/W emulsions. This may be attributed to GA forming thick films on the O/W interface thereby reducing diffusion and improving emulsion stability. The high efficiency of GA in stabilizing various emulsions has been reported in numerous publications (e.g. 28, 35, 41-43). During storage, MCT-based double emulsions showed a slower decrease in EE compared to OT-based double emulsions regardless of the secondary emulsifiers used suggesting an impact of oil type on EE. The size distribution of double emulsions with a gelled inner phase or OT as oil phase changed greatly during storage indicating potential stability issues associated with these emulsions in a longer term. All results suggest that gelling the inner phase of double emulsions with gelatin is not beneficial in our system and that a more viscous oil phase (e.g., MCT) would be desirable achieving a smaller MDD and higher EE.

5.3.6 Stability of W/O/W emulsion-based beverage clouds

As noted in the introduction of this study, one particular application of W/O/W emulsions is for beverage clouds with the potential benefits of eliminating the use of weighing agents and improving creaming stability by matching phase densities. In this study, two key parameters were monitored during storage: turbidity and ringing which are important criteria of beverage stability. MDDs were also measured as a predictive parameter of beverage stability. A stable beverage would have a low turbidity loss and no ring formation during storage. Two commonly used emulsifiers in beverage emulsions, MS and GA were compared in stabilizing W/O/W emulsions in beverage cloud application.

Figures 5.26 and 5.27 show changes in MDD and absorbance of W/O/W-based beverage clouds stabilized by MS. No visible ringing occurred in any beverages during storage except OT-based beverage clouds with a gelled inner aqueous phase which showed small rings after 2 weeks of storage (Figure 5.28). For OT-based emulsions, MDD increased slowly and absorbance decreased greatly over time. For MCT-based emulsions MDD started to increase after three weeks of storage and absorbance decreased at a slower rate compared to that of OT-based emulsions. The difference in stability could have originated from the oil phase composition as discussed in Section 5.3.5. The large loss (> 60% during 4 weeks of storage) in absorbance for OT-based beverage clouds is not desirable in practical applications. MCT-based beverage clouds were more stable against absorbance loss and thus are more promising in practical applications. However, a longer shelf life study is needed since MDD increased

dramatically in the fourth week of storage and size distribution (Figure 5.29) got wider during storage indicating potential stability issues upon longer term storage.

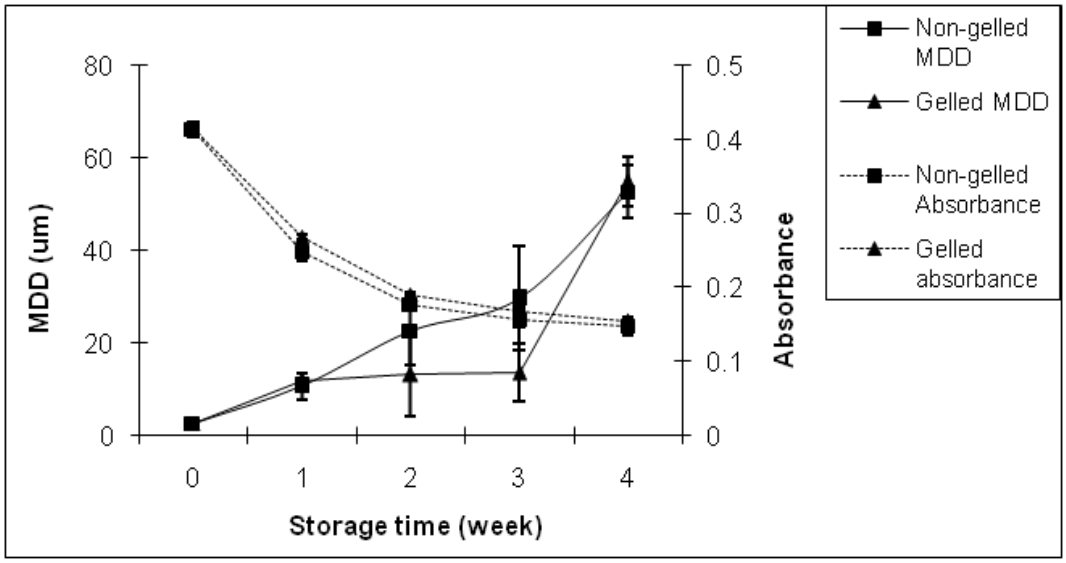

Figure 5.26 Changes in MDD and absorbance of W/O/W-based beverage clouds with OT as oil phase and MS as secondary emulsifier.

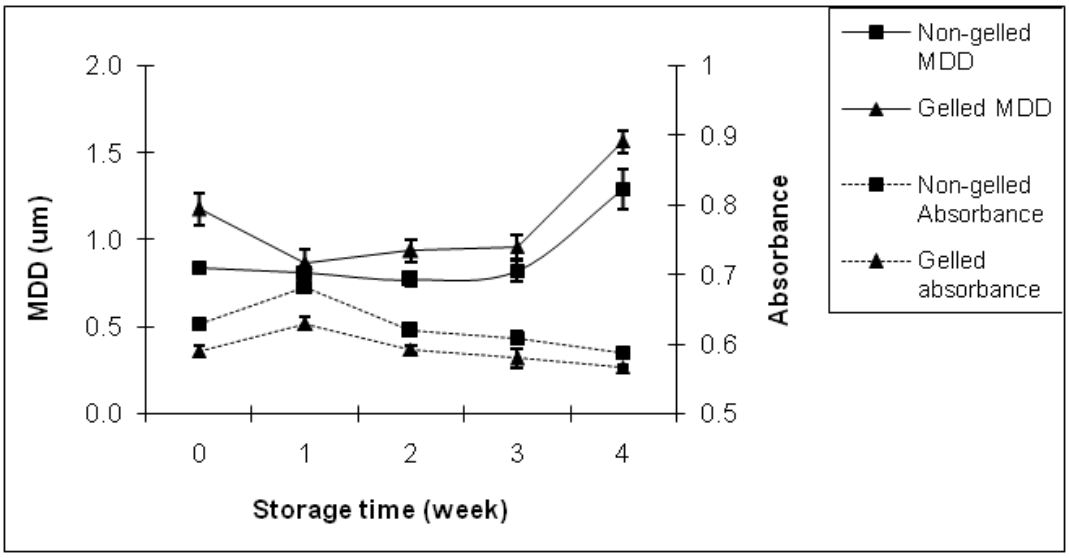

Figure 5.27 Changes in MDD and absorbance of W/O/W-based beverage clouds with MCT as oil phase and MS as secondary emulsifier.

Figure 5.28 Appearance of W/O/W emulsion-based beverage clouds stabilized by MS. All emulsions used OT as oil phase; Top, without gelled inner phase; bottom, with gelled inner phase; from left to right: 0, 1, 2 and 3 weeks of storage, respectively.

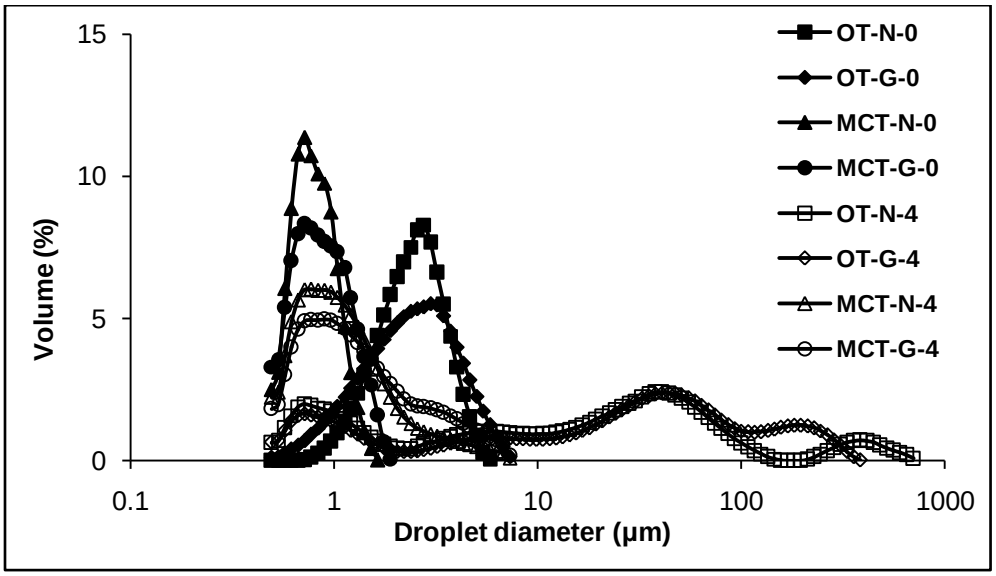

Figure 5.29 Size distribution of W/O/W-based beverage clouds stabilized by MS. N, non-gelled inner phase; G, gelled inner phase; the number following N or G stands for weeks of storage, e.g., OT-N-4 means OT-based double emulsions without gelling inner phase after 4 weeks storage.

Figures 5.30 and 5.31 show changes in MDD and absorbance of W/O/W-based beverage clouds stabilized by GA. GA stabilized beverage clouds were more stable in terms of MDD and absorbance compared to those stabilized by MS. The higher stability of double emulsions-based beverage clouds stabilized by GA agreed with the higher stability of GA stabilized double emulsion concentrates.

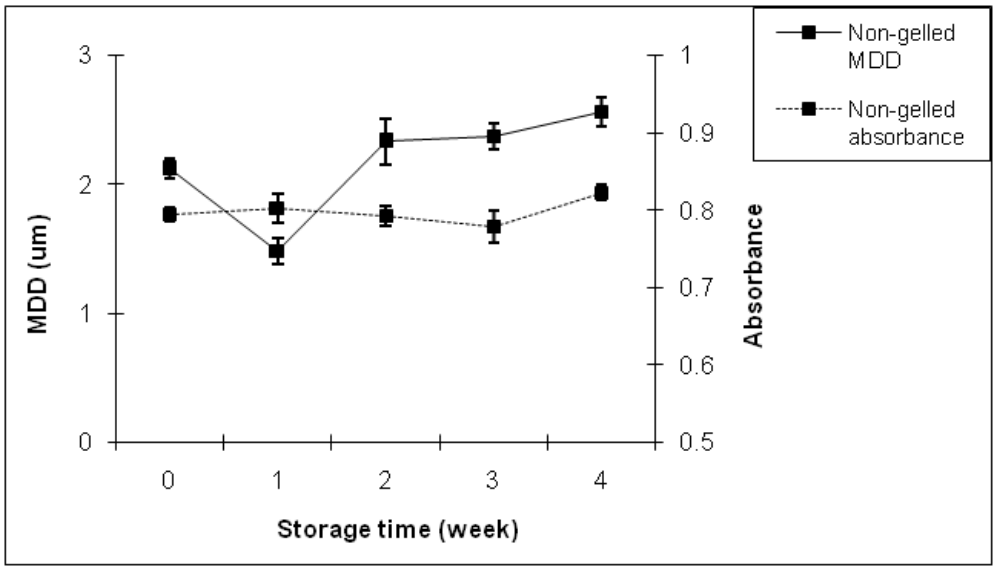

Figure 5.30 Changes in MDD and absorbance of W/O/W-based beverage clouds with OT as oil phase and GA as secondary emulsifier.

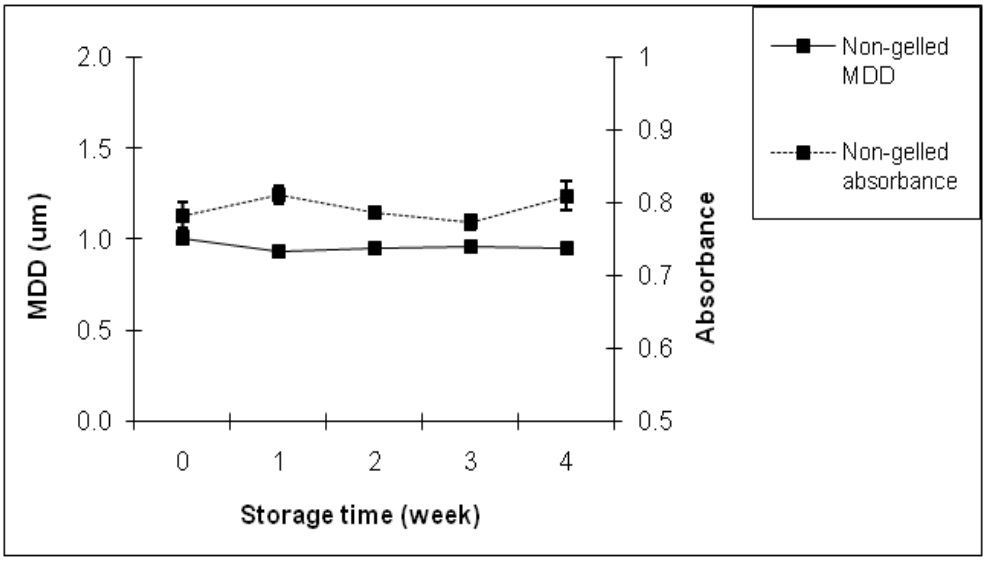

Figure 5.31 Changes in MDD and absorbance of W/O/W-based beverage clouds with MCT as oil phase and GA as secondary emulsifier.

Figure 5.32 shows W/O/W emulsion-based beverage clouds during storage. No ringing occurred in OT-based beverages while surprisingly heavy ringing occurred in MCT-based beverages after1 week of storage. Ring formation indicates significant creaming driven by density difference in phases and accelerated by large droplet size. One would expect MCT-based beverage to be more stable than OT-based beverages considering the smaller MDD and stable absorbance of the MCT-based beverages. Droplet size distributions of beverage clouds are plotted in Figure 5.33 to further investigate this unexpected observation. No significant changes in particle size distribution were found for MCT-based beverage clouds while the particle size distribution of OT-based beverage clouds showed bimodal size distributions after 4 weeks storage. The particle size distribution result does not support our observation of ring formation in MCT-based beverage clouds. Although the occurrence of ringing is not well understood, there is the possibility that reversible flocculation occurred in MCT-based beverage clouds. The flocs may be broken upon on stirring during measurement of MDD; however, droplet flocculation accelerates the rate of gravitational separation in dilute emulsions and thus promotes ringing (44, 45).

Figure 5.32 Appearance of W/O/W emulsion-based beverage clouds stabilized by GA. All W/O/W emulsions without gelling inner phase: top and bottom, OT and MCT as oil phase, respectively; from left to right: 0, 1, 2, 3 and 4 weeks of storage, respectively.

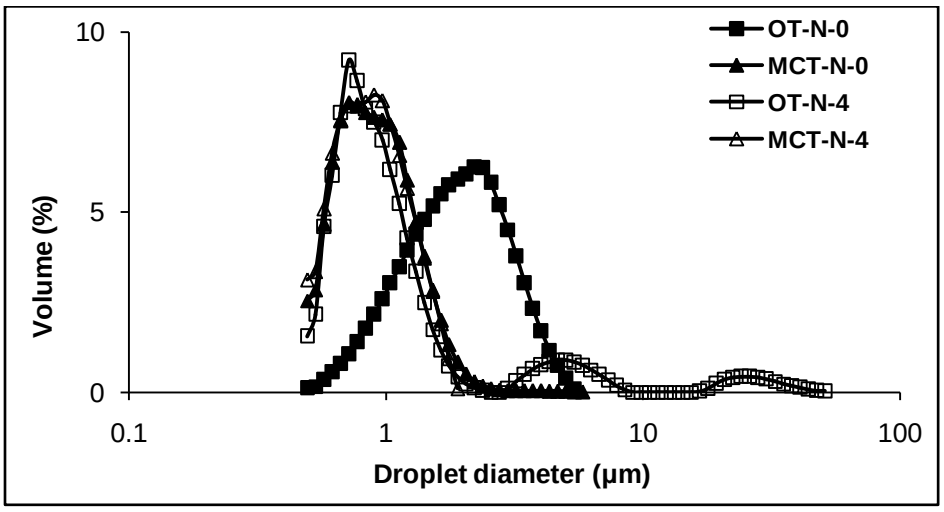

Figure 5.33 Size distribution of W/O/W-based beverage clouds stabilized by GA. N, non-gelled inner phase; G, gelled inner phase; the number following N or G stands for weeks of storage, e.g., OT-N-4 means OT-based double emulsions without gelling inner phase after 4 weeks storage.

Figure 5.33 also shows an interesting phenomenon in that the particle size distribution of OT-based W/O/W emulsion changed greatly although MDD only slightly increased. The size of the majority of droplets shifted to the left suggesting that droplets shrank during storage. This observation is different from that found in GA stabilized double emulsion concentrates (Figure 5.25) indicating different destabilization mechanisms in concentrated and diluted double emulsions. In double emulsion concentrates, swelling of the inner water droplets due to osmotic difference between inner and outer aqueous phase, as well as coalescence caused wider size distribution of emulsions during storage. In diluted double emulsions, extreme swelling of inner water droplets might occur resulting in bursting of the oil droplets and formation of single emulsions with a smaller droplet size.

The difference in swelling of the inner water droplets in concentrated and diluted double emulsions could originate from the composition difference in the aqueous phase (e.g., emulsifiers). In the present study, incorporation of sucrose and gelatin in the inner aqueous phase created higher osmotic pressure in the internal than in the external aqueous phase driving water through the oil phase from outer to inner phase and thus swelling the water droplets. However, this high osmotic pressure is partly counterbalanced by the huge Laplace pressure in the nano-sized water droplets. The high concentrations of GA and MS in continuous phase also contribute to balancing the osmotic difference, as well as high viscosity of double emulsions, all of which are beneficial to stabilizing double emulsions. Many materials (e.g., electrolytes, sugar,

protein, and drugs) in the aqueous phase of double emulsions were found to effect osmotic pressure (46-48) and it was reported that double emulsions with a balance of osmotic and Laplace pressure have maximum stability (49-51). In the present study the effect of osmotic pressure was not considered but it would be helpful in the future to investigate this effect by incorporating electrolyte (e.g., sodium chloride) in the aqueous phase and find out how stability changes with electrolyte concentration.

Overall, diluted double emulsions stabilized by GA showed better stability against ringing and turbidity loss compared to those stabilized by MS. However, more research is needed to investigate the destabilization mechanisms of double emulsion concentrates and dilutes and thus to improve their long-term stability in beverage cloud applications.

5.4 Conclusions

In the present study, PGPR concentration, hydrophilic emulsifier, oil type, and processing parameters were found to affect the MDD, EE and stability of double emulsions. GA stabilized double emulsions and the equivalent diluted double emulsions showed relatively good turbidity and stability in storage. However, longer term stability needs to be evaluated in beverage cloud applications. Based on our data, we have no evidence that gelling the inner aqueous phase contributes to the stability of double emulsions in our system. On the contrary, it seems that emulsions containing gelled water droplets showed lower stability compared to those without a gelled inner phase. The

chemistry behind this phenomenon is not understood yet. The effects of osmotic pressure and interactions between components need to be investigated in the future to better understand the destabilization of double emulsions.

References

[1] Pays K, Giermanska-Kahn J, Pouligny B, Bibette J, Leal-Calderon F. Double emulsions: how does release occur? *J. Control Release*. **2002,** 79, 193-205.

[2] Garti N, Bisperink C. Double emulsions: progress and applications. *Curr. Opin. Colloid Interface Sci.* **1998,** 3, 657-667.

[3] Surh, J. Vladisavljevic, G. T., Mun, S., McClements D. J. Preparation and characterization of water/oil and water/oil/water emulsions containing biopolymer-gelled water droplets. *J. Agric. Food Chem.* **2007,** 55: 175-184.

[4] Garti, N. and Aserin, A. Double emulsions stabilized by macromolecular surfactants. *Adv. Colloid Interface*, **1996,** 65: 37-69.

[5] Ficheux, M. F., Bonakdar, L., Leal-Calderon, F., Bibette, J. Some stability criteria for double emulsions. *Langmuir*, **1998,** 14: 2702-2706.

[6] Muschiolik, G. Multiple emulsions for food use. *Curr. Opin. Colloid Interface Sci.* **2007,** 12, 213-220.

[7] Garti, N. Progress in stabilization and transport phenomena of double emulsions in food applications. *Lebensm.-Wiss. u.-Technol.*, **1997,** 30: 222-235.

[8] Nakhare, S.; Vyas, S. P. Preparation and characterization of multiple emulsion based systems for controlled diclofenac sodium release. *J. Microencapsul.* **1996,** 13, 281-292.

[9] Meng, F. T.; Ma, G. H.; Liu Y. D.; Qiu, W.; Su, Z. G. Microencapsulation of bovine hemoglobin with high bio-activity and high entrapment efficiency using a W/O/W double emulsion technique. *Colloids Surf., B.* **2004,** 33, 177-183.

[10] Garti, N.; Aserin, A.; Cohen, Y. Mechanistic considerations on the release of electrolytes from multiple emulsions stabilized by BSA and nonionic surfactants. *J. Control Release.* **1994,** 29, 41-51.

[11] Matsumoto, S.; Kohda, M. Rheological properties of water-in-oil-in-water type multiple-phase systems. In: Sherman, P. Ed. *Food Texture and Rheology*. London: Academic Press, **1979,** 437-452.

[12] De Cindio, B.; Grasso, G.; Cacace, D. Water-in-oil-in-water emulsions for food applications. *Food Hydrocolloid.* **1991,** 4, 339-353.

[13] Folmer, B.; Michel, M.; Gehin-Delval, C.; Acquistapace, S.; Leser, M.; Syrbe, A.; Marze, S. Stable double emulsions. **US Patent Application 20100233221.**

[14] Bams, G. W.; Megen, W. H. Edible water-in-oil-in-water emulsions. **US Patent 4,650,690.**

[15] Gaonkar, A. G. Stable multiple emulsions comprising interfacial gelatinous layer, flavor-encapsulating multiple emulsions and low/no-fat food products comprising the same. **US Patent 5,332,595.**

[16] Jager-Lezer, N.; Terrisse, I.; Bruneau, F.; Tokgoz, S.; Ferreira, L.; Clausse, D.; Seiller, M.; Grossiord, J-L. Influence of lipophilic surfactant on the release kinetics of water-soluble molecules entrapped in a W/O/W multiple emulsion. *J. Control Release.* **1997,** 45, 1-13.

[17] Kanouni, M.; Rosano, H. L.; Naouli, N. Preparation of a stable double emulsion (W1/O/W2): role of the interfacial films on the stability of the system. *Adv. Colloid Interface Sci.* **2002,** 99, 229-254.

[18] Akhtar, M.; Dickinson, E. Water-in-oil-in-water multiple emulsions stabilized by polymeric and natural emulsifiers. In: Kickinson, E.; Miller, R. Eds. *Food Colloids: fundamentals of formulation.* Cambrige: The Royal Society of Chemistry, **2001,** 133-143.

[19] Jahaniaval, F.; Kakuda, Y.; Abraham, V. Characterization of a double emulsion system (oil-in-water-in-oil emulsion) with low solid fats: microstructure. *J. Am. Oil Chem. Soc.* **2003,** 80, 25-31.

[20] Garti, N.; Aserin, A.; Tiunova, I.; Binyamin, H. Double emulsions of water-in-oil-in-water stabilized by α-form fat microcrystals. Part 1: Selection of emulsifiers and fat microcrystalline particles. *J. Am. Oil Chem. Soc.* **1999,** 76, 383-389.

[21] Garti, N.; Binyamin, H.; Aserin, A. Stabilization of water-in-oil emulsions by submicrocrystalline α-form fat particles. *J. Am. Oil Chem. Soc.* **1998,** 75, 1825-1831.

[22] Benna-Zayani, M.; Kbir-Ariguib, N.; Trabelsi-Ayadi, M.; Grossiord, J. L. Stabilization of W/O/W double emulsion by polysaccharides as week gels. *Colloid Surf., A.* **2008,** 316, 46-54.

[23] Fechner, A.; Knoth, A.; Scherze, I.; Muschiolik, G. Stability and release properties of double-emulsions stabilized by caseinate-dextran conjugates. *Food Hydrocolloid.* **2007,** 21, 943-952.

[24] Garti, N. A new approach to improved stability and controlled release in double emulsions, by the use of graft-comb polymeric amphiphiles. *Acta Polym.* **1998,** 49, 606-616.

[25] Michaut, F.; Hebraud, P.; Perrin, P. Amphiphilic polyelectrolyte for stabilization of multiple emulsions. *Polym. Int.* **2003,** 52, 594-601.

[26] Muschiolik, G.; Sherze, I.; Preissler, P.; Weiss, J.; Knoth, A.; Fechner, A. Multiple emulsions-preparation and stability. *IUFoST World Congress of Food Science and Technology*. **2006,** 123-137.

[27] http://lclane.net/text/sucrose.html. Accessed January 4, 2011.

[28] Reiner, S.; Reineccius G.A; Peppard, T. A comparison of the stability of beverage cloud emulsions formulated with different gum Arabic- and Starch-based emulsifiers. *J. Food Sci.* **2010,** 75, E236-246.

[29] McKone, H. T. Identification of FD&C dyes by visible spectroscopy. A consumer-oriented undergraduate experiment. *J. Chem. Educ.* **1977,** 54, 376-377.

[30] Su, J.; Flanagan, J.; Hemar, Y.; Singh, H. Synergistic effects of polyglycerol ester of polyricinoleic acid and sodium caseinate on the stabilization of water-oil-water emulsions. *Food Hydrocolloid.* **2006,** 20, 261-268.

[31] Walstra, P. Disperse system: basic considerations: In: O. H. Fennema, editor. *Food Chemistry.* New York: CRC Press. **1996,** 3rd ed. pp95-155.
[32] R. Chanamai and D. J. McClements. Impact of weighting agents and sucrose on gravitational separation of beverage emulsions. *J. Agric. Food Chem.* **2000,** 48: 5561-5565.
[33] Tan, C.T. Beverage flavor emulsion-A form of emulsion liquid membrane microencapsulation. *Dev. Food Sci.* **1998,** 40, 29-42.
[34] Schmidts, T.; Dobler, D.; Nissing, C.; Runkel, F. Influence of hydrophilic surfactants on the properties of multiple W/O/W emulsions. *J. Colloid Interface Sci.* **2009,** 338, 184-192.
[35] Su J.; Flanagan, J.; Singh, H. Improving encapsulation efficiency and stability of water-in-oil-in-water emulsions using a modified gum Arabic (Acacia (sen) SUPER GUM^{TM}). *Food Hydrocolloid.* **2008,** 22, 112-120.
[36] Michaut, F.; Perrin, P.; Hebraud, P. Interface composition of multiple emulsions: rheology as a probe. *Langmuir.* **2004,** 20, 8576.
[37] Dickinson, E. Double emulsions stabilized by food biopolymers. *Food Biophysics.* Published online: 18 November **2010**.
[38] Graaf, S.; Schroen, C. G. P. H.; Boom, R. M. Preparation of double emulsions by membrane emulsification-a review. *J. Membrane Sci.* **2005,** 251, 7-15.
[39] Nakashima, T.; Shimizu, M; Kukizaki, M. Particle control of emulsion by membrane emulsification and its application. *Adv. Drug Delivery Rev.* **2000,** 45, 47-56.
[40] Wen, L.; Papadopoulos, K. D. Effects of osmotic pressure on water transport in W1/O/W2 emulsions. *J. Colloid Interface Sci.* **2001,** 235, 398-404.
[41] Castellani, O.; Guibert, D.; AI-Assaf, S.; Axelos, M; Phillips, G.O.; Anton, M. Hydrocolloids with emulsifying capacity. Part 1- Emulsifying properties and interfacial characteristics of conventional (*Acacia Senegal* (L.) Willd. Var. *senegal*) and matured (Acacia (*sen*) SUPER GUM^{TM}) *Acacia senegal*. *Food Hydrocolloid.* **2010,** 24, 193-199.

[42] Chanamai, R.; McClements, D. J. Comparison of gum arabic, modified starch, and whey protein isolate as emulsifiers: influence of pH, CaCl2 and temperature. *J Food Sci,* **2002,** 67, 120-125.

[43] Buffo, R.; Reineccius, G.A.; Oehlert G. Factors affecting the emulsifying and rheological properties of gum acacia in beverage emulsions. *Food Hydrocolloid*. **2001,** 15, 53-66.

[44] Tan, C.T. Beverage emulsions, In *Food Emulsions,* 4th ed., Friberg, S.; Larsson, K.; Sjoblom, J. Eds., Marcel Dekker, New Yok, **2004**.

[45] Luyten, H.; Jonkman, M.; Kloek, W.; Vliet, T. Creaming behavior of dispersed particles in dilute xanthan solutions, in *Food colloids and polymers: stability and mechanical properties*, Dickinson; E.; Walstra, P. Eds., Royal Society of Chemistry, Cambridge, UK, **1993**.

[46] Florence, A.T.; Whitehill, D. The formulation and stability of multiple emulsions. *Int. J. Pharm.* **1982,** 11, 277-308.

[47] Cueman, G.H.; Zatz, J.L. Multiple emulsions. In: *Controlled release systems: fabrication technology*, Hsieh, D.S., ed. Boca Raton: CRC Press, **1988.**

[48] Garti, N.; Aserin, A. Emulsions and microemulsions. In: *Drug and the pharmaceutical sciences*, Benita, S., ed. New York: Dekker, **1996.**

[49] Jiao, J.; Rhodes, D.G.; Burgess, D.J. Multiple emulsion stability: pressure balance and interfacial film strength. *J. Colloid Interface Sci.* **2002,** 250, 444-450.

[50] Mezzenga, R.; Folmer, B.M.; Hughes, E. Design of double emulsions by osmotic pressure tailoring. *Langmuir,* **2004,** 20, 3574-3582.

[51] Jiao, J.; Burgess, D.J. Multiple emulsion stability: pressure balance and interfacial film strength. In: *Multiple emulsion: technology and applications,* Aserin, A., ed., New York: John Wiley & Sons, Inc., **2007.**

Literature Cited

Abismail, B.; Canselier, J.P.; Wilhelm, A.M.; Delmas, H.; Gourdon, C. Emulsification by ultrasound: droplet size distribution and stability. *Ultrason. Sonochem.* **1999,** 6, 75-83.

Ai, H.; Jones, A.; Lvov, Y. Biomedical applications of electrostatic layer-by-layer nano-assembly of polymers, enzymes, and nanoparticles. *Cell Biochem. Biophys.* **2003,** 39, 23-43.

AI-Hakkak, J.; Kavale, S. Improvement of emulsification properties of sodium caseinate by conjugating to pectin through the Maillard reaction. In: *The Maillard reaction in food chemistry and medical science*. International Congress Series, **2002,** 1245, 491-499.

Akhtar, M.; Dickinson, E. Water-in-oil-in-water multiple emulsions stabilized by polymeric and natural emulsifiers. In: Kickinson, E.; Miller, R. Eds. *Food Colloids: fundamentals of formulation.* Cambrige: The Royal Society of Chemistry, **2001,** 133-143.

Akoh, C.; Min, D. Food lipids: chemistry, nutrition, and biochemistry. New York: *Marcel Dekker,* **2002,** 2nd Ed.

Anderson, D. M. W.; Howlett, J. F.; McNab, C. G. A. The amino acid composition of the proteinaceous of Acacia senegal gum. *Carbohydr. Res.* **1985,** 2, 104-114.

Aoki, T., Decker, E.A., Mcclements, D.J. Influence of environmental stresses on stability of O/W emulsions containing droplets stabilized by multilayered membranes produced by a layer-by-layer electrostatic deposition technique, *Food Hydrocolloid.* ***2005,*** 19, 209-220.

Baker, J.R.; Hamouda, T. Nanoemulsion vaccines. **2008,** US Pat. 7,314,624.

Baker, J.R.; Hamouda, T.; Shih, A.; Myc, A. Antimicrobial compositions and methods of use. **2010,** US Pat. 7,767,216.

Bams, G. W.; Megen, W. H. Edible water-in-oil-in-water emulsions. **US Patent 4,650,690.**

Becher, P. Encyclopedia of emulsion technology-basic theory. New York: *Marcel Dekker.* **1983.**

Benna-Zayani, M.; Kbir-Ariguib, N.; Trabelsi-Ayadi, M.; Grossiord, J. L. Stabilization of W/O/W double emulsion by polysaccharides as week gels. *Colloid Surf., A.* **2008,** 316, 46-54.

Bouaouina, Hakim, Desrumaux, A.; Loisel, C.; Legrand, J. Functional properties of whey proteins as affected by dynamic high-pressure treatment. *Int. dairy J.* **2006,** 16, 275-284.

Buffo, R.A.; Reineccius, G.A. Modeling the rheology of concentrated beverage emulsions. *J. Food Eng.* **2002,** 51, 267-272.

Buffo, R.A.; Reineccius, G.A. Shelf-life and mechanism of destabilization in dilute beverage emulsions. *Flavour Frag. J.* **2001,** 16, 7-12.

Buffo, R.; Reineccius, G.A.; Oehlert G. Factors affecting the emulsifying and rheological properties of gum acacia in beverage emulsions. *Food Hydrocolloid*. **2001,** 15, 53-66.

Capek, I. Degradation of kinetically-stable o/w emulsions. *Adv Colloid Interface Sci.* **2004,** 107, 125-155.

Castellani, O.; AI-Assaf, S.; Axelos, M.; Phillips, G.O.; Anton, M. Hydrocolloids with emulsifying capacity. Part 2-Adsorption properties at the n-hexadecane-water interface. *Food Hydrocolloid.* **2010,** 24, 121-130.

Castellani, O.; Guibert, D.; AI-Assaf, S.; Axelos, M; Phillips, G.O.; Anton, M. Hydrocolloids with emulsifying capacity. Part 1- Emulsifying properties and interfacial characteristics of conventional (*Acacia Senegal* (L.) Willd. Var. *senegal*) and matured (Acacia (*sen*) SUPER GUM^{TM}) *Acacia senegal*. *Food Hydrocolloid.* **2010,** 24, 193-199.

Chanamai, R.; McClements, D. J. Impact of weighting agents and sucrose on gravitational separation of beverage emulsions. *J. Agric. Food Chem.* **2000,** 48: 5561-5565.

Chanamai, R.; McClements, D. J. Comparison of gum arabic, modified starch, and whey protein isolate as emulsifiers: influence of pH, CaCl2 and temperature. *JFS,* **2002,** 67, 120-125.

Chanamai, R. Microemulsions for use in food and beverage products. Patent issued to Frost Brown Todd LLC with International publication number: **WO 2007/047237 A1.**

Chanamai, R. Microemulsions for use in food and beverage products. US Pat. Pub. No. **20070087104.**

Chen, C.; Wagner, G. Vitamin E nanoparticle for beverage applications. *Chem. Eng. Res. Des.* **2004,** 82, 1432-1437.

Cheong, J.N.; Tan, C.P. Palm-based functional lipid nanodispersions: preparation, characterization and stability evaluation. *Eur. J. Lipid Sci. Technol.* **2010,** 112, 557-564.

Chiesa, M.; Garg, J.; Kang, Y.T.; Chen, G. Thermal conductivity and viscosity of water-in-oil nanoemulsions. *Colloids Surf., A* **2008,** 326, 1-2, 67-72.

Choi, Y.T.; El-Aasser, M.S.; Sudol, E.D.; Vanderhoff, J.W. Polymerization of styrene miniemulsions. *J. Polym. Sci. A,* **1985,** 23, 2973-81.

Chung, S.L.; Tan, C.T.; Tuhill, I.M.; Scharpf, L.G. Transparent oil-in-water microemulsion flavor concentrate. **1994,** US Pat. 5,320,863.

Chung, S.L.; Tan, C.T.; Tuhill, I.M.; Scharpf, L.G. Transparent oil-in-water microemulsion flavor or fragrance concentrate, process for preparing same, mouthwash or perfume composition containing said transparent microemulsion concentrate, and process for preparing same. **1994,** US Pat. 5,283,056.

Cueman, G.H.; Zatz, J.L. Multiple emulsions. In: *Controlled release systems: fabrication technology*, Hsieh, D.S., ed. Boca Raton: CRC Press, **1988.**

Dalgleish, D.G.; Tosh, S.M.; West, S. Beyond homogenization: the formation of very small emulsion droplets during the processing of milk by a microfludizer. *Netherlands Milk Dairy J.* **1996,** 50, 135-148.

Dalgleish, D.G.; West, S.J.; Hallett, F.R. The characterization of small emulsion droplets made from milk proteins and triglyceride oil. *Colloid Surface A.* **1997,** 123, 145-153.

Danov, K.D.; Kralchevsky, P.A.; Ivanov, I.B. Dynamic processes in surfactant stabilized emulsions. In Encyclopedic Handbook of Emulsion Technology. J. Sjoblom. New York: *Marcel Dekker,* **2001.** Ed. pp. 621-659.

De Cindio, B.; Grasso, G.; Cacace, D. Water-in-oil-in-water emulsions for food applications. *Food Hydrocolloid.* **1991,** 4, 339-353.

Desrumaux, A.; Marcand, J. Formation of sunflower oil emulsions stabilized by whey proteins with high pressure homogenization (up to 350 MPa): effect of pressure on emulsion characteristics. *Int. J. Food Sci. Technol.* **2002,** 27, 263-269.

Dickinson, E. An introduction to food colloids. Oxford, UK: Oxford Univ. Press. **1992.**

Dickinson, E. Double emulsions stabilized by food biopolymers. *Food Biophysics*. Published online: 18 November **2010**.

Dickinson, E.; Golding, M.; Povey, J.W. Creaming and flocculation of oil-in-water emulsions containing sodium caseinate. *J. Colloid and interf. Sci.* **1997,** 185, 515-529.

Dickinson, E. Hydrocolloids as emulsifiers and emulsion stabilizers. *Food Hydrocolloid*. **2009,** 23, 1473-1482.

Dickinson, E.; Murray, B.; Stainsby, G.; Anderson, D. Surface activity and emulsifying behavior of some Acacia gums. *Food Hydrocolloid.* **1988,** 2, 477-490.

Djordjevic, D., Cercaci, L.,Alamed, J., McClements, D.J., Decker, E.A. Chemical and physical stability of citral and limonene in sodium dodecyl sulfate-chitosan and gum Arabic-stabilized oil-in-water emulsions, *J. Agric. Food Chem.* **2007,** 55, 3585-3591.

Donsi, F.; Wang Y.; Li J.; Huang, Q. Preparation of curcumin sub-micrometer dispersions by high-pressure homogenization. *J. Agric. Food Chem.* **2010,** 58, 2848-2853.

Duvoix, A., Blasius, R., Delhalle, S., Schnekenburger, M., Morceau, F.; Henry, E. Chemopreventive and therapeutic effects of curcumin. *Cancer Lett.* **2005,** 223, 181–190.

EI-Jaby, U.; Cunningham, M.; McKenna, T. Comparison of emulsification devices for the production of miniemulsions. *Ind. Eng. Chem. Res.* **2009,** 48, 10147-10151.

Fanun, M. Properties of microemulsions with sugar surfactants and peppermint oil. *Colloid Polym. Sci.* **2009,** 287, 899-910.

Fechner, A.; Knoth, A.; Scherze, I.; Muschiolik, G. Stability and release properties of double-emulsions stabilized by caseinate-dextran conjugates. *Food Hydrocolloid.* **2007,** 21, 943-952.

Ficheux, M. F.; Bonakdar, L.; Leal-Calderon, F.; Bibette, J. Some stability criteria for double emulsions. *Langmuir*, **1998,** 14: 2702-2706.

Flanagan, J.; Singh, H. Microemulsions: a potential delivery systems for bioactives in food. *Crit. Rev. Food Sci. Nutr.* **2006,** 46, 221-237.

Florence, A.T.; Whitehill, D. The formulation and stability of multiple emulsions. *Int. J. Pharm.* **1982,** 11, 277-308.

Floury, J.; Desrumaux, A.; Axelos, M.; Legrand, J. Effect of high pressure homogenization on methylcellulose as food emulsifier. *J. Food Eng.* **2003,** 58, 227-238.

Folmer, B.; Michel, M.; Gehin-Delval, C.; Acquistapace, S.; Leser, M.; Syrbe, A.; Marze, S. Stable double emulsions. **US Patent Application 20100233221.**

Friberg, S.E. Food emulsions. New York, NY: *Marcel Dekker.* **1997.** 3rd ed.

Friberg, S.E.; Goldsmith, L.B.; Hilton, M.L. Theory of emulsion in Pharmaceutical dosage forms: dispersion systems. Lieberman, H.A.; Reiger, M.M.; Banker, G.S., Eds.; New York: Marcel Dekker, Inc. **1988.**

Gaonkar, A. G. Stable multiple emulsions comprising interfacial gelatinous layer, flavor-encapsulating multiple emulsions and low/no-fat food products comprising the same. **US Patent 5,332,595.**

Garti, N.; Amar, I.; Spernath, A.; Hoffman, R. Transition and loci of solubilization of nutraceuticals in U-type nonionic microemulsions studied by self-diffusion NMR. *Phys. Chem. Chem. Phys.* **2004,** 6, 2968-76.

Garti, N. A new approach to improved stability and controlled release in double emulsions, by the use of graft-comb polymeric amphiphiles. *Acta Polym.* **1998,** 49, 606-616.

Garti, N.; Aserin, A.; Cohen, Y. Mechanistic considerations on the release of electrolytes from multiple emulsions stabilized by BSA and nonionic surfactants. *J. Control Release.* **1994,** 29, 41-51.

Garti, N.; Aserin, A. Double emulsions stabilized by macromolecular surfactants. *Adv. Colloid Interface,* **1996,** 65: 37-69.

Garti, N.; Aserin, A. Emulsions and microemulsions. In: *Drug and the pharmaceutical sciences,* Benita, S., ed. New York: Dekker, **1996.**

Garti, N.; Aserin, A.; Spernath, A.; Amar, I. Nano-sized self-assembled structured liquids. U.S. Patent **20030232095.**

Garti, N.; Aserin, A.; Spernath, A.; Amar, I. Nano-sized self-assembled liquid dilutable vehicles. 2007, US Pat. **7,182,950.**

Garti, N.; Aserin, A.; Tiunova, I.; Binyamin, H. Double emulsions of water-in-oil-in-water stabilized by α-form fat microcrystals. Part 1: Selection of emulsifiers and fat microcrystalline particles. *J. Am. Oil Chem. Soc.* **1999,** 76, 383-389.

Garti, N.; Binyamin, H.; Aserin, A. Stabilization of water-in-oil emulsions by submicrocrystalline α-form fat particles. *J. Am. Oil Chem. Soc.* **1998,** 75, 1825-1831.

Garti N, Bisperink C. Double emulsions: progress and applications. *Curr. Opin. Colloid Interface Sci.* **1998,** 3, 657-667.

Garti, N.; Jacobs, L.G.; Lane, B.; Zakharia, I. Isotropic transparent structured fluids. *US patent application:* **US2003/0228395.**

Garti, N. Progress in stabilization and transport phenomena of double emulsions in food applications. *Lebensm.-Wiss. u.-Technol.*, **1997,** 30: 222-235.

Garti, N.; Yaghmur, A.; Leser, M.E.; Clement, V.; Watzke, H.J. Improved oil solubilization in oil/water food grade microemulsions in the presence of polyols and ethanol. *J. Agric. Food Chem.* **2001,** 49, 2552-2562.

Given, P.S. Encapsulation of flavors in emulsion for beverages. *Curr. Opin. Colloid In.* **2009,** 14, 43-47.

Goodrum, L. J.; Patel, A.; Leykam, J. F.; Kieliszewski, M. J. Gum arabic glycoprotein contains glycomodules of both extension and arabinogalactan-glycoproteins. *Phytochemistry*, **2000,** 54, 99-106.

Goulden, J.D.; Phipps, L.W. Factors affecting the fat globule sizes during the homogenization of milk and cream. *J. Dairy Res.* **1964,** 31, 195-200.

Graaf, S.; Schroen, C. G. P. H.; Boom, R. M. Preparation of double emulsions by membrane emulsification-a review. *J. Membrane Sci.* **2005,** 251, 7-15.

Gregory, J. Particles in water. Boca Raton, FL: *CRC Press.* **2006.**

Guenin, E.P.; Trotzinka, K.A.; Smith, L.C.; Warren, C.B.; Munteanu, M.A.; Chung, S.L.; Tan, C.T. Alcohol free perfume. **1995,** US Pat. 5,468,725.

Gutierrez, J.; Gonzalez, C.; Maestro, A.; Sole, I.; Pey, C.; Nolla, J. Nano-emulsions: new applications and optimization of their preparation. *Curr. Opin. Colloid Interface Sci.* **2008,** 13, 245-251.

Gu, Y.S.; Decker, E.A.; and Mcclements, D.J. Application of multi-component biopolymer layers to improve the freeze-thaw stability of oil-in-water emulsions: β-lactoglobulin-ι-carrageenan-gelatin. *J. Food Eng.* **2007,** 80, 1246-1254.

Guzey, D.; and McClements, D.J. Formation, stability and properties of multilayer emulsions for application in the food industry, *Adv. in Colloid Interface Sci.* **2006.** 128-130, 227-248.

Guzey, D. Utilization of interfacial engineering to improve food emulsion properties. Ph.D. thesis. Department of Food Science, University of Massachusetts, **2006.**

Hakansson, A.; Tragardh, C.; Bergenstahl, B. Studying the effects of adsorption, recoalescence and fragmentation in a high pressure homogenizer using a dynamic simulation model. *Food Hydrocolloid,* **2009,** 23, 1177-1183.

Hakansson, A.; Tragardh, C.; Bergenstahl, B. Dynamic simulation of emulsion formation in a high pressure homogenizer. *Chemical Eng. Sci.* **2009,** 64, 2915-2925.

Halbert, W.G. Method of recovering hydrocarbons with highly aqueous soluble oils using phosphate ester surfactants. **1971,** US Pat. 3,596,715.

Harnsilawat, T.; Pongsawatmanit, R.; McClements D.J. Stabilization of model beverage cloud emulsions using protein-polysaccharide electrostatic complexes formed at the oil-water interface. *J Agric. Food Chem.* **2006,** 54, 5540-5547.

Hasenhuettl, G.L.; Hartel, R.W. Food emulsifiers and their applications. New York: Springer. **2008.** 2nd Ed.

Healy, R.N. Oil recovery method using microemulsion. **1976,** US Pat. **3,981,361.**

Hernandez, E.; Baker, R.A. Turbidity of beverages with citrus oil clouding agent. *JFS.* **1991,** 56, 1024-1026.

Hernandez, E.; Baker, R.A.; Crandall, P.G. Model for evaluating turbidity in cloudy beverages. *JFS.* **1991,** 56, 747-750.

Hinrichs, J.; Rademacher, B. High pressure thermal denaturation kinetics of whey proteins. *J. Dairy Res.* **2004,** 71, 480-488.

http://lclane.net/text/sucrose.html. Accessed January 4, 2011.

Huang, M. T.; Lou, Y. R.; Ma, W.; Newmark, H. L.; Reuhl, K. R.; Conney, A. H. Inhibitory effects of dietary curcumin in forestomach, duodenal, and colon carcinogenesis in mice. *Cancer Res.* **1994,** 54, 5841–5847.

Huang, Q.; Yu, H.; Ru, Q. Bioavailability and delivery of nutraceuticals using nanotechnology. *JFS.* **2010,** 75, R50-57.

Instrumental manual of BIC 90Plus, Brookhaven Instrument Corporation.

Izquierdo, P.; Esquena, J.; Tadros, Th.F.; Dederen, C.; Garcia, M.J. Azemar, N.; Solan, C. Formation and stability of nano-emulsions prepared using the phase inversion temperature method. *Langmuir.* **2002,** 18, 26-30.

Jafari, S.; He, Y.; Bhandari, B. Nano-emulsion production by sonication and microfluidization- a comparison. *Int. J. Food Prop.* **2006,** 9, 475-485.

Jafari, S.M.; He, Y.; Bhandari, B. Optimization of nano-emulsions production by microfluidization. *Eur. Food Res. Technol.* **2007,** 225, 733-741.

Jafari, S.; He, Y.; Bhandari, B. Production of sub-micron emulsions by ultrasound and microfluidization techniques. *J. Food Eng.* **2007**, 82, 478-488.

Jager-Lezer, N.; Terrisse, I.; Bruneau, F.; Tokgoz, S.; Ferreira, L.; Clausse, D.; Seiller, M.; Grossiord, J-L. Influence of lipophilic surfactant on the release kinetics of water-soluble molecules entrapped in a W/O/W multiple emulsion. *J. Control Release.* **1997,** 45, 1-13.

Jahaniaval, F.; Kakuda, Y.; Abraham, V. Characterization of a double emulsion system (oil-in-water-in-oil emulsion) with low solid fats: microstructure. *J. Am. Oil Chem. Soc.* **2003,** 80, 25-31.

Jahaniaval, F.; Kakuda, Y.; Abraham, V.; Marcone, M. Soluble protein fractions from pH and heat treated sodium caseinate: physicochemical and functional properties. *Food Res. Int.* **2000,** 33, 637-647.

Jayme, M. L.; Dunstan, D. E.; Gee, M. L. Zeta potential of gum arabic stabilized oil-in-water emulsions. *Food Hydrocolloid.* **1999,** 13, 459-465.

Jean-Thierry, S.; Sonneville, O.; Legret, S. Nanoemulsion based on oxyethylenated or non-oxyethylenated sorbitan fatty esters, and its uses in the cosmetics, dermatological and/or ophthalmological fields. **2002,** US Pat. 6,335,022.

Jiao, J.; Burgess, D.J. Multiple emulsion stability: pressure balance and interfacial film strength. In: *Multiple emulsion: technology and applications,* Aserin, A., ed., New York: John Wiley & Sons, Inc., **2007.**

Jiao, J.; Rhodes, D.G.; Burgess, D.J. Multiple emulsion stability: pressure balance and interfacial film strength. *J. Colloid Interface Sci.* **2002,** 250, 444-450.

Jonsson, B.; Lindman, B.; Holmberg, B. Surfactants and polymers in aqueous solution. Chichester, UK: *John Wiley & Sons,* **1998.**

Kabalnov, A.S. Can micelles mediate a mass transfer between oil droplets? *Langmuir.* **1994,** 680-684.

Kabalnov, A.S.; Pertzov, A.V.; Shchukin, E.D. Ostwald ripening in emulsions: I. Direct observations of Ostwald ripening in emulsions. *J. Colloid Interface Sci.* **1987,** 118, 2, 590-597.

Kabainov, A.S.; Makarov, K.N.; Shcherbakova, O.V.; Nesmeyanov, A.N. Solubility of fluorocarbons in water as a key parameter determining fluorocarbon emulsion stability. *J. Fluorine Chem*. **1990,** 50, 271-284.

Kanouni, M.; Rosano, H. L.; Naouli, N. Preparation of a stable double emulsion (W1/O/W2): role of the interfacial films on the stability of the system. *Adv. Colloid Interface Sci.* **2002,** 99, 229-254.

Karppinen, T.; Kassamakov, I.; Heggstrom, E.; Stor-Pellinen, J. Measuring paper wetting processes with laser transmission. *Meas. Sci. Technol.* **2004,** 15, 1223-1229.

Kentish, S.; Wooster, T.; Ashokkumar, M.; Balachandran, S.; Mawson, R.; Simons, L. The use of ultrasonics for nanoemulsion preparation. *Innovat. Food Sci. Emerg. Tech.* **2008,** 9, 170-175.

Kim, Y. D.; Morr, C. V.; Schenz, T. W. Microencapsulation properties of gum arabic and several food proteins: liquid orange oil emulsion particles. *J. Agric. Food Chem.* **1996,** 44, 1308-1313.

Kleizen, H.H.; Putter, A.B.; Beek, M.; Huynink, S.J. Particle concentration, size and turbidity. *Filtration and Separation.* **1995,** 32, 897-901.

Klinkesorn, U., Sophanodora, P., Chinachoti, P., Decker, E.A., and Mcclements, D.J. Encapsulation of emulsified tuna oil in two-layered interfacial membranes prepared using electrostatic layer-by-layer deposition, *Food Hydrocolloid.* **2005,** 19, 1044-1053.

Kourniatis, L.R.; Spinelli, L.S.; Piombini, R.; Mansur, R.E. Formation of orange oil-in-water nanoemulsions using nonionic surfactant mixtures by high pressure homogenizer. *Colloid J.* **2010,** 72, 396-402.

Lamprecht, A.; Ubrich, N.; Perez, M.H. Biodegradable monodispersed nanoparticles prepared by pressure homogenization-emulsification. *Int. J. Pharm.* **1999,** 184, 97-105.

Landfester, K.; Tiarks, F.; Hentze, H.; Antonietti, M. Polyaddition inminiemulsions: a new route to polymer dispersions. *Macromol. Chem. Phys.* **2000,** 201, 1-11.

Leclercq, S.; Milo, C.; Reineccius, G. Effects of cross-linking, capsule wall thickness, and compound hydrophobicity on aroma release from complex coacervate microcapsules. *J. Agric. Food Chem.* **2009,** 57, 1426-1432.

Lee, S.; Lefevre, T.; Subirade, M.; Paquin, P. Changes and role of secondary structure of whey protein for the formation of protein membrane at soy oil/water interface under high-pressure homogenization. *J. Agric. Food Chem.* **2007,** 55, 10924-10931.

Lee, S.; Lefevre, T.; Subirade, M.; Paquin, P. Effects of ultra-high pressure homogenization on the properties and structure of interfacial protein layer in whey protein-stabilized emulsion. *Food Chem.* **2009,** 113, 191-195.

Lee, S.; Morr, C.; Ha, E. Structural and functional-properties of caseinate and whey-protein isolate as affected by temperature and pH. *JFS.* **1992,** 57, 1210-1214.

Li, L.C.; Tian, Y. Zeta Potential in Encyclopedia of pharmaceutical technology. Swarbrick, J.; Ed.; Informa Healthcare USA, Inc. **2007.**

Li, M.; Fogler, H. Acoustic emulsification. Part 1. The instability of the oil –water interface to form the initial droplets. *J. Fluid Mech.* **1978,** 88, 499-511.

Li, M. and Fogler, H. Acoustic emulsification. Part 2. Break-up of the large primary oil droplets in a water medium. *J. Fluid Mech.* **1978,** 88, 513-528.

Liu, W.; Sun, D.; Li, C.; Liu, Q.; Xu, J. Formation and stability of paraffin oil-in-water nano-emulsions prepared by the emulsion inversion point method. *J. Colloid Interface Sci.* **2006,** 303, 557-563.

Luyten, H.; Jonkman, M.; Kloek, W.; Vliet, T. Creaming behavior of dispersed particles in dilute xanthan solutions, in *Food colloids and polymers: stability and mechanical properties*, Dickinson; E.; Walstra, P. Eds., Royal Society of Chemistry, Cambridge, UK, **1993**.

Maa, Y.F.; Hsu, C.C. Performance of sonication and microfludization for liquid-liquid emulsification. *Pharm. Dev. Technol.* **1999,** 4, 233-240.

Mao, L.; Xu, D.; Yang, J.; Yuan, F.; Gao, Y.; Zhao, J. Effects of small and large molecule emulsifiers on the characteristics of β-carotene nanoemulsions prepared by high pressure homogenization. Food Technol. Biotechnol. **2009,** 47, 336-342.

Mao, L.; Yang, J.; Xu, D.; Yuan, F. Gao, Y. Effects of homogenization models and emulsifiers on the physicochemical properties of β-carotene nanoemulsions. *J. Disper. Sci. Technol.* **2010,** 31. 986-993.

Mason, T.; Graves, S.; Wilking, J.; and Lin, M. Extreme emulsification: formation and structure of nanoemulsionss. *Condens. Matter Phys.* **2006,** 9, 193-199.

Mason, T.; Wilking, J.; Meleson, K.; Chang, C.; Graves, S. Nanoemulsions: formation, structure, and physical properties. *J. Phys.: Condens. Matter*, **2006,** *18*, R635-R666.

Matsumoto, S.; Kohda, M. Rheological properties of water-in-oil-in-water type multiple-phase systems. In: Sherman, P. Ed. *Food Texture and Rheology*. London: Academic Press, **1979,** 437-452.

McClements, D.J. Food emulsions: principles, practice, and techniques. Boca Raton, FL: CRC Press. **2005.** 2nd ed.

McClements, D.J. Emulsion design to improve the delivery of functional lipophilic components. Annu. Rev. Food Sci. Technol. **2010,** 1, 241-69.

McClements, D.J. Food emulsions: principles, practice, and techniques. Boca Raton, FL: *CRC Press.* **2005.** 2nd ed.

McKone, H. T. Identification of FD&C dyes by visible spectroscopy. A consumer-oriented undergraduate experiment. *J. Chem. Educ.* **1977,** 54, 376-377.

McNamee, B.; O'Ridrdan, E.; O'Sullivan, M. Effect of partial replacement of gum Arabic with carbohydrates on its microencapsulation properties. *J. Agric. Food Chem.* **2001,** 49, 3385-3388.

Meinders, M.; Kloek, W.; Vliet, T.V. Effect of surface elasticity on Ostwald ripening in emulsions. *Langmuir.* **2001,** 17, 3923-3929.

Meinders, M.; Vliet, T.V. The role of interfacial rheological properties on Ostwald ripening in emulsions. *Adv. Colloid Interface Sci.* **2004,** 108-109, 119-126.

Meleson, K.; Graves, S.; Mason, T. Formation of concentrated nanoemulsions by extreme shear. *Soft Materials*, **2004,** 2, 109-123.

Meng, F. T.; Ma, G. H.; Liu Y. D.; Qiu, W.; Su, Z. G. Microencapsulation of bovine hemoglobin with high bio-activity and high entrapment efficiency using a W/O/W double emulsion technique. *Colloids Surf., B.* **2004,** 33, 177-183.

Messens, W.; Camp, J.; Huyghebaert, A. The use of high pressure to modify the functionality of food proteins. *Trends Food Sci. and Technol.* **1997,** 8, 107-112.

Mezzenga, R.; Folmer, B.M.; Hughes, E. Design of double emulsions by osmotic pressure tailoring. *Langmuir,* **2004,** 20, 3574-3582.

Michaut, F.; Hebraud, P.; Perrin, P. Amphiphilic polyelectrolyte for stabilization of multiple emulsions. *Polym. Int.* **2003,** 52, 594-601.

Michaut, F.; Perrin, P.; Hebraud, P. Interface composition of multiple emulsions: rheology as a probe. *Langmuir.* **2004,** 20, 8576.

Mirhosseini, H.; Tan, C.P.; Hamid, N.; Yusof, S. optimization of the content of Arabic gum, xanthan gum and orange oil affecting turbidity, average particle size, polydispersity index and density in orange beverage emulsion. *Food Hydrocolloid.* **2008,** 22, 1212-1223.

Mirhosseini, H.; Tan, C.P.; Hamid, N.; Yusof, S.; Chern, B.H. Characterization of the influence of main emulsion components on the physicochemical properties of orange beverage emulsion using response surface methodology. *Food Hydrocolloid.* **2009,** 23, 271-280.

Mirhosseini, H.; Tan, C.P.; Taherian, A.R.; Chern, H. Modeling the physicochemical properties of orange beverage emulsion as function of main emulsion components using response surface methodology. *Carbohyd. Polym.* **2009,** 75, 512-520.

Muschiolik, G.; Sherze, I.; Preissler, P.; Weiss, J.; Knoth, A.; Fechner, A. Multiple emulsions-preparation and stability. *IUFoST World Congress of Food Science and Technology*. **2006,** 123-137.

Monsalve-Gonzalez, A.; Ochomogo, M. Natural flavor enhancement compositions for food emulsions. US Pat. Pub. **20090196972.**

Morgan, D.; Hosken, B.; Davis, C. Microfluidised ice-cream emulsions. *Aust. J. Dairy Technol.* **2000,** 55, 93-93.

Moulik, S.P.; Paul, B.K. Structure, dynamics and transport properties of microemulsions. *Adv. Colloid Interface Sci.* **1998,** 78, 99-105.

Moulik, S.; Rakshit, A. Physicochemistry and applications of microemulsions. *J. Surface Sci. Technol.* **2006,** 22, 159-186.

Mozhaev, W.; Heremans, K.; Frank, J.; Masson, P.; Balny, C. High pressure effects on protein structure and function. *Proteins.* **1996.** 24, 81-91.

Muschiolik, G. Multiple emulsions for food use. *Curr. Opin. Colloid Interface Sci.* **2007,** 12, 213-220.

Nakashima, T.; Shimizu, M; Kukizaki, M. Particle control of emulsion by membrane emulsification and its application. *Adv. Drug Delivery Rev.* **2000,** 45, 47-56.

Nakauma, M.; Funami, T.; Noda, S.; Ishihara, S.; AI-Assaf, S.; Nishinari, K.; Phillips, G. Composition of sugar beet pectin, soybean soluble polysaccharide, and gum Arabic as food emulsifiers. 1. Effect of concentration, pH, and salts on the emulsifying properties. *Food Hydrocolloid*. **2008,** 22, 1254-1267.

Nakhare, S.; Vyas, S. P. Preparation and characterization of multiple emulsion based systems for controlled diclofenac sodium release. *J. Microencapsul.* **1996,** 13, 281-292.

Narsimhan, G.; Goel, P. Drop coalescence during emulsion formation in a high-pressue homogenizer for tetradecane-in-water emulsion stabilized by sodium dodecyl sulfate. *J. Coll. Interf. Sci.* **2001,** 238, 420-432.

Nicolosi, R.; Wilson, T. Compositions and methods for making and using nanoemulsions. US patent application: **US2008/0274195.**

Nilsson, L.; Bergenstahl, B. Adsorption of hydrophobically modified starch at oil/water interfaces during emulsification. *Langmuir*, **2006,** 22, 8770-8776.

Nilsson, L.; Bergenstahl, B. Emulsification and adsorption properties of hydrophobically modified potato and barley starch. *J. Agri. Food Chem.* **2007,** 55, 1469-1474.

Ogawa, S.; Decker, E.A.; McClements, D.J. Influence of environmental conditions on stability of O/W emulsions containing droplets stabilized by lecithin–chitosan membranes. *J. Agric. Food Chem.* **2003,** 51, 5522–5527.

Olson, D.W.; White, C.H.; Richter, R.L. Effect of pressure and fat content on particle sizes in microfluidized milk. *J. Dairy Sci.* **2004,** 87, 3217-3223.

Ouzineb, K.; Lord, C.; Lesauze, N.; Graillat, C.; Tanguy, P.A.; McKenna, T. Homogenization devices for the production of miniemulsions. *Chem. Eng. Sci.* **2006,** 61, 2994-3000.

Paetznick, D.; Reineccius, G. Shelf life and flavor release of coacervated orange oil. In: *Micro/Nanoencapsulation of active food ingredient*. Huang, Q.; Given, P.; Qian, M.; Eds. ACS Symposium Series, **2009,** 1007, 272-286.

Pallander,S.; Decker, E.A.; McClements D.J. Improvement of stability of oil-in-water emulsions containing caseinate-coated droplets by addition of sodium alginate. *JFS.* **2007,** 72, E518-E524.

Panagiotou, T. Microfludizer processors: technology and applications. Online presentation from www. microfluidicscorp.com.

Pandolfe, W.D. Processing of emulsions and dispersions by homogenization. In *APV homogenizer handbook*. **2003.**

Pays K, Giermanska-Kahn J, Pouligny B, Bibette J, Leal-Calderon F. Double emulsions: how does release occur? *J. Control Release*. **2002,** 79, 193-205.

Peter, G.J. Encapsulation of flavors in emulsions for beverages. *Curr. Opin. Colloid Interface Sci.* **2009,** 14, 43-47

Prochaska, K.; Kedziora, P.; Thanh, J.L.; Lewandowicz, G. Surface activity of commercial food grade modified starches. *Colloids Surf., B.* **2007,** 60, 187-194.

Randall, R.; Williams, P. The role of the proteinaceous component on the emulsifying properties of gum Arabic. *Food Hydrocolloid,* **1988,** 2, 131-140.

Reed, R.L; Healy, R.N.; Stenmark, D.; Gale, W.W. Recovery of oil using microemulsions. **1975,** US Pat. 3,885,628.

Reineccius, G. Flavor chemistry and technology. Boca Raton, FL: *CRC Press.* **2006.** 2nd Ed.

Reiner, S.J.; Reineccius G.A.; Peppard, T.L. A comparison of the stability of beverage cloud emulsions formulated with different gum acacia- and starch-based emulsifiers. *JFS.* **2010,** E236-E246.

Relkin, P.; Yung, J.M.; Kalnin, D.; Ollivon, M. Structureal behaviour of lipid droplets in protein-stabilized nano-emulsions and stability of α-tocopherol. *Food Biophys*. **2008,** 3, 163-168.

Rhoney, I.; Brown S.; Hudson, N.E.; Pethrick, A. Influence of processing method on the exfoliation process for organically modified caly systems. I. Polyurethanes. *J. Appl. Poly. Sci.* **2004,** 91, 1335-1343.

Richardson, E.S.; Pitt, W.G.; Woodbury, D.J. The role of cavitation in liposome formation. *Biophys. J.* **2007,** 93, 4100-4107.

Robins M.M. Emulsions-creaming phenomena. *Curr. Opin. Colloid Interface Sci.* **2000,** 5, 265-272.

Robin, O.; Blanchot, V.; Vuillemard, J.C.; Paquin, P. Microfludization of dairy model emulsions. I. Preparation of emulsions and influence of processing on the size distribution of milk fat globules. *Lait,* **1992,** 72, 511-550.

Sadtler, V.M.; Imbert, P.; Dellacherie, E. Ostwald ripening of oil-in-water emulsions stabilized by phenoxy-substituted dextrans. *J Colloid Interface Sci.* **2002,** 254, 355-361.

Sagalowicz, L.; Leser, M.E. Delivery systems for liquid food products. *Curr. Opin. Colloid Interface Sci.* **2010,** 15, 61-72.

Sarker, D.K. Engineering of nanoemulsions for drug delivery. *Current Drug Delivery.* **2005,** 2, 297-310.

Schmidts, T.; Dobler, D.; Nissing, C.; Runkel, F. Influence of hydrophilic surfactants on the properties of multiple W/O/W emulsions. *J. Colloid Interface Sci.* **2009,** 338, 184-192.

Schultz, S.; Wagner, G.; Urban, K.; Ulrich, J. High-pressure homogenization as a process for emulsion formation. *Chem. Eng. Technol.* **2004,** 27, 361-368.

Seikikawa, K.; Watanabe, M. Transparent emulsified composition for use in beverages. Patent application by Givaudan SA. Publication number **WO2008/055374**.

Sekikawa, K.; Watanabe, M. Transparent emulsified composition for use in beverage. *US patent application:* **US2009/0285952.**

Shafiq, S.; Shakeel, F.; Talegaonkar, S.; Ali, J.; Baboota, S.; Ahuja, A.; Khar, R.K.; Ali, M. Formulation development and optimization using nanoemulsion technique: a technical note. *Pharm. Sci. Tech.* **2007,** 8, E1-E6.

Shafiq, S.; Shakeel, F.; Talegaonkar, S.; Ahmad, F.; Khar, R.; Ali, M. Development and bioavailability assessment of ramipril nanoemulsion formulation. *Eur. J. Pharm. Biopharm.* **2007,** 66, 227-243.

Shah, P.; Bhalodia, D.; Shelat, P. Nanoemulsion: A pharmaceutical review. *Sys. Rev. Pharm.* **2010,** 1, 24-32.

Shakeel, F.; Baboota, S.; Ahuja, A.; Ali, J.; Shafiq, S. Accelerated stability testing of celecoxib nanoemulsion containing cremophor-EL. *Afr. J. Pharm. Pharacol.* **2008,** 2, 179-183.

Shefer, A.; Shefer, S.D. Multi component controlled release system for oral care, food products, nutraceutical, and beverages. U.S. Patent **20030152629.**

Silva, J.L.; Foguel, D.; Royer, C.A. Pressure provides new insights into protein folding, dynamics and structure. *Trends Biochem. Sci.* **2001.** 26, 612-618.

Sjoblom, J. Enclyopedic handbook of emulsion technology. New York: *Marcel Dekker.* **2001.**

Skiff, R.H.; Baaklini, J.; Vlad, F.J. Clear flavor microemulsions comprising sugar esters of fatty acids. Patent application by Firmenich SA. Publication number **WO2007/026271 A1.**

Skiff, R.H.; Baaklini, J.; Vlad, F.J. Clear flavor microemulsions comprising sugar esters of fatty acids. *US patent application:* **US2010/0136175.**

Smet, Y.; Deriemaeker, L.; Finsy, R. Ostwald ripening of alkane emulsions in the presence of surfactant micelles. *Langmuir.* **1999,** 15, 6745-54.

Solans, C.; Izquierdo, P.; Nolla, J.; Azemar, N.; Garcia-Celma, M. Nano-emulsions. *Curr. Opin. Colloid Interface Sci.* **2005,** 10, 102-110.

Soma, J.; Papadopoulos, K.D. Ostwald ripening in sodium dodecyl sulfate-stabilized decane-in-water emulsion. *J Colloid Interface Sci.* **1996,** 181, 225-231.

Sonneville, O.; Simonnet, J-T.; Legret, S. Nanoemulsion based on mixed esters of a fatty acid or of a fatty alcohol, of a carboxylic acid and of a glycerol and its uses in the cosmetics, dermatological and/or ophthalmological fields. **2002,** US Pat. 6,419,946.

Spernath, A.; Aserin, A. Microemulsions as carriers for drug and nutraceuticals. *Adv. Colloid Interface. Sci.* **2006,** 128-130, 47-64.

Spernath, A.; Yaghmur, A.; Aserin, A.; Hoffman, R.; Garti, N. Food-grade microemulsions based on nonionic emulsifiers: media to enhance lycopene solubilization. *J. Agric. Food Chem.* **2002,** 50, 6917-6922.

Stachurski, J.; Michalek, M. The Effect of the ζ Potential on the Stability of a Non-Polar Oil-in-Water Emulsion. *J. Colloid Interface Sci.* **1996,** 184, 433-436.

Strawbridge, K.B.; Ray, E.; Hallett, F.R.; Tosh, S.M. Dalgleish, D.G. Measurement of particle size distributions in milk homogenized by a microfluidizer: estimation of populations of particles with radii less than 100 nm. *J. Colloid Interface Sci.* **1995,** 171, 392-398.

Su, J.; Flanagan, J.; Hemar, Y.; Singh, H. Synergistic effects of polyglycerol ester of polyricinoleic acid and sodium caseinate on the stabilization of water-oil-water emulsions. *Food Hydrocolloid.* **2006,** 20, 261-268.

Su J.; Flanagan, J.; Singh, H. Improving encapsulation efficiency and stability of water-in-oil-in-water emulsions using a modified gum Arabic (Acacia (sen) SUPER GUM^{TM}). *Food Hydrocolloid.* **2008,** 22, 112-120.

Surh, J.; Decker, E.; McClements, D. Influence of pH and pectin type on properties and stability of sodium caseinate stabilized oil-in-water emulsions. *Food Hydrocolloid.* **2006,** 20, 607-618.

Surh, J. Vladisavljevic, G. T., Mun, S., McClements D. J. Preparation and characterization of water/oil and water/oil/water emulsions containing biopolymer-gelled water droplets. *J. Agric. Food Chem.* **2007,** 55: 175-184.

Surh, J., Yeun, S.G., Decker, E.A., Mcclements, D.J. Influence of Environmental stresses on stability of O/W emulsions containing cationic droplets stabilized by SDS-Fish gelatin membrances, *J. Agric. Food Chem. 2005,* **53**, 4236–4244.

Syvitski, J. Principles, methods and applications of particle size analysis. New York: *Cambridge University Press.* **1991.**

Tadros, T.F. Applied surfactants: principles and applications. Weinheim: *Wiley-VCH,* **2005.**

Tadros, T.; Izquierdo, P.; Esquena, J.; Solans, C. Formation and stability of nano-emulsions. *Adv. Colloid Interface Sci.* **2004,** 108-109, 303-318.

Tan C.T. Beverage emulsions. In *Food emulsions;* Friberg SE, Larsson K., Eds.; 3rd ed. New York, N.Y.: Marcel Dekker, **1997.**

Tan, C. T. Beverage flavor emulsion-a form of emulsion liquid membrane encapsulation. In *Food Flavors: Formation, Analysis and Packaging Influences*; Contis, E. T., Ed.; New York: Elsevier, **1998.**

Tan, C. T. Beverage emulsions. In *Food Emulsions*; Friberg, S. E., Larsson, K., Sjoblom, J., Eds.; New York, N.Y.: Dekker, **2004.**

Tang, P.L.; Sudol, E.D.; Silebi, C.A.; El-Aasser, M.S. Miniemulsion polymerization-a comparative study of preparative variables. *J. Appl. Polym. Sci.* **1991,** 43, 1059-71.

Taylor, G.I. The formation of emulsions in definable fields of flow. *Proc. R. Soc. A.* **1934,** 146, 501-507.

Taylor, P. Ostwald ripening in emulsions. *Colloids Surf., A* **1995,** 99, 2-3, 175-185.

Taylor, P. Ostwald ripening in emulsions. *Adv Colloid Interface Sci.* **1998,** 75, 107-163.

Tesch, S.; Freudig, B.; Schubert, H. Production of emulsions in high-pressure homogenizers – part I: disruption and stabilization of droplets. *Chem. Eng. Technol.* **2003,** 26, 569-573.

Tesch, S.; Gerhards, Ch.; Schubert, H. Stabilization of emulsions by OSA starches. *J. Food Eng.* **2002,** 54, 167-174.

Thanasukarn, P., Pongsawatmanit, R., Mcclements, D.J. Interfacial deposition technique to improve freeze-thaw stability of oil-in-water emulsions, *Food Res. Int.* **2006,** 39, 721-729.

Thir, B.; Dexheimer, E.M. Microemulsions. **1986,** US Pat. 4,568,480.

Thompson, A.K.; Singh, H. Preparation of liposomes from milk fat globule membrane phospholipids using a Microfluidizer. *J. Dairy Sci.* **2006,** 89, 410-419.

Trubiano, P. C. The role of specialty food starches in flavor emulsions. *Flavor Technol.* **1995,** 610, 199-209.

Tse K-Y, Reineccius G.A. In *Flayor Technology* (ACS Symposium Series No. 610), Ho C-T, Tan C-T, Hsiang C-H (eds). American Chemical Society: Washington, DC, **1995,** 172–182.

Tse, K. Y.; Reineccius, G. A. Methods to predict the physical stability of flavorscloud emulsion. *Flavor Technol.* **1995**, *610*, 172-182.

Tunick, M.H.; Hekken, D.L.; Cooke, P.H.; Smith, P.W.; Malin, E.L. Effect of high pressure microfluidization on microstructure of mozzarella cheese. *Food Sci. Technol.-LEB.* **2000,** 33, 538-544.

Valdivia, F.; Dachs, A.; Perdiguer, N. Nanoemulsion of the oil water type, useful as an ophthalmic vehicle and process for the preparation therefore. **1997,** US Pat. 5,698,219.

Vladisavljevic, G.T.; Surh, J.; McClements, J.D. Effect of emulsifier type on droplet disruption in repeated shirasu porous glass membrane homogenization. *Langmuir,* **2006,** 22, 4526-4533.

Walstra, P. Disperse system: basic considerations: In: O. H. Fennema, editor. Food Chemistry. New York: CRC Press. **1996,** 3rd ed. pp95-155.

Walstra, P. Physical chemistry of foods. New York: Marcel-Dekker, **2003.**

Walstra, P. Studying food colloids: past, present and future, in Food Colloids, Biopolymers and Materials, Cambridge, UK: *Royal Society of Chemistry,* **2003b.**

Wang, L.; Mutch, K.; Eastoe, J.; Heenan, R.; Dong J. Nanoemulsions prepared by a two-step low-energy process. *Langmuir.* **2008,** *24*, 6092-99.

Wang, X.; Jiang, Y.; Wang, Y.; Huang, M.; Ho, C.T.; Huang, Q. Enhancing anti-inflammation activity of curcumin through O/W nanoemulsions. *Food Chem.* **2008,** 108, 419-424.

Wang, X.Y.; Wang, Y.W; Huang, R. Enhancing stability and oral bioavailability of polyphenols using nanoemulsions. In: *Micro/Nanoencapsulation of Active Food Ingredients.* Q. R. Huang, P. Given and M. Qian (Editors). **2009.** ACS Symposium Series 1007. Washington, DC.

Weder, H.G.; Mutsch, M. Process for the production of a nanoemulsion of oil particles in an aqueous phase. **1992,** US Pat. 5,152,923.

Weiss, J. Cancelliere, C.; McClements D.J. Mass transport phenomena in oil-in-water emulsions containing surfactant micelles: Ostwald ripening. *Langmuir.* **2000,** 6833-6838.

Weiss J.; Herrmann, N.; McClements, D.J. Ostwald ripening of hydrocarbon emulsion droplets in surfactant solutions. *Langmuir.* **1999,** 15, 6652-57.

Wen, L.; Papadopoulos, K. D. Effects of osmotic pressure on water transport in W1/O/W2 emulsions. *J. Colloid Interface Sci.* **2001,** 235, 398-404.

Whitesides, G.M.; Grzybowski, B. Self-assembly at all scales. *Science.* **2002,** 295, 2418-26.

Wolf, P.A.; Havekotte, M.J. Microemulsions of oil in water and alcohol. **1989,** US Pat. 4,835,002.

Wooster, T.J.; Golding, M.; Sanguansri, P. Impact of oil type on nanoemulsion formation and Ostwald ripening stability. *Langmir.* **2008,** 24, 12758-12765.

Wooster, T.J.; Andrews, H.F.; Sanguansri, P. Nanoemulsions. US Pat. Pub. **20100305218.**

Xu R. Particle characterization: light scattering methods. New York: *Kluwer Academic Publishers*. **2002.**

Yuan, Y.; Gao, Y.; Mao, L.; Zhao, J. Optimization of conditions for the preparation of β-carotene nanoemulsions using response surface methodology. *Food Chem.* **2008,** 107, 1300-1306.

Yuan, Y.; Gao, Y.; Zhao, J. Mao, L. Characterization and stability evaluation of β-carotene nanoemulsions prepared by high pressure homogenization under various emulsifying conditions. *Food Res. Int.* **2008,** 41, 61-68.

Zhang, H.; Feng, F.; Li, J.; Zhan, X.; Wei, H.; Li, H.; Wang, H.; Zheng, X. Formation of food-grade microemulsions with glycerol monolaurate: effects of short-chain alcohols, polyols, salts and nonionic surfactants. *Eur. Food Res. Technol.* **2008,** 226, 613-619.

Zhu, Z. X.; Anacker, J. L.; Ji, S. X.; Hoye, T. R.; Macosko, C. W.; Prudhomme, R. K. Formation of block copolymer-protected nanoparticles via reactive impingement mixing. *Langmuir* **2007**, *23*, 10499-10506.